PD-CATALYZED ALLYLIC SUBSTITUTION FOR THE CONSTRUCTION OF QUATERNARY STEREOCENTERS

Aijie Cai

UNIVERSITAT
ROVIRA i VIRGILI

Pd-catalyzed Allylic Substitution for the Construction of Quaternary Stereocenters

Aijie Cai

DOCTORAL THESIS

2019

Pd-catalyzed Allylic Substitution for the Construction of Quaternary Stereocenters

Aijie Cai

Doctoral Thesis

Supervised by Prof. Arjan W. Kleij

Institut Català d'Investigació Química (ICIQ)

Universitat Rovira i Virgili (URV)

Department of Analytical Chemistry & Organic Chemistry

Tarragona 2019

Prof. Arjan W. Kleij, Group Leader at the Institute of Chemical Research of Catalonia (ICIQ) and Research Professor of the Catalan Institution for Research and Advanced Studies (ICREA):

I hereby state that the present work entitled "*Pd-catalyzed Allylic Substitution for the Construction of Quaternary Stereocenters*", presented by Aijie Cai for the award of the degree of Doctor, has been carried out under my supervision at the Institute of Chemical Research of Catalonia (ICIQ).

Tarragona, December 2019

Doctoral Thesis Supervisor

Prof. Arjan W. Kleij

Curriculum Vitae

After graduating with a BSc degree in Chemistry from the Xingtai University in June **2012**, Aijie began his master degree at Tianjin University, where he worked from September **2012** to July **2015** under the supervision of Prof. J.-A. Ma. During his MSc studies, his research focused on asymmetric synthesis and organofluorine chemistry. He finished his MSc studies working on *copper-triggered three-component processes involving CF$_3$CHN$_2$, nitriles, and aldehydes, resulting in highly diastereoselective routes for synthesis of CF$_3$-substituted oxazolines and vicinal amino alcohols*. His MSc thesis work was supported by the *Graduate Scholarship of Tianjin University*. Due to the success of his MSc projects, in the summer of **2015** he received his degree as an outstanding graduate. Fascinated by organometallic chemistry and regio- and enantioselective catalysis, and in search of exciting new challenges and opportunities, he decided to apply for a PhD position within the doctoral program of the Institute of Chemical Research of Catalonia (ICIQ) in Spain period during his PhD at ICIQ, he was supported by an *FPI Severo Ochoa Fellowship* from the Spanish "Ministerio de Economía y Competitividad", MINECO. During his study PhD at ICIQ as a member of the research group of Prof. Arjan W. Kleij, he worked on several challenging projects regarding the design and development of sustainable catalytic processes, and novel ligands that can be used to promote allylic substitution reactions with high regio- and enantioselectivity. The PhD thesis results have been communicated at different national and international conferences, such as the OMCOS19 in Korea (**2017**), the German-Spanish Symposium and ICIQ-Summer School in Tarragona (**2017**), and the ICIQ-RedINTECAT Schools in Tarragona (**2018** and **2019**).

List of Publications

At the time of printing, the results reported herein have been published in the following journals:

1. Lingfei Hu[+], **Aijie Cai**[+], Zhenzhen Wu, Arjan W. Kleij* and Genping Huang* "A Mechanistic Analysis of the Palladium-Catalyzed Formation of Branched Allylic Amines Reveals the Origin of the Regio- and Enantioselectivity through a Unique Inner-Sphere Pathway"
   Angew. Chem. Int. Ed. **2019**, *58*, 14694−14702.
   +: *equal contribution*

2. **Aijie Cai**, Arjan W. Kleij* "Regio- and Enantioselective Preparation of Chiral Allylic Sulfones Featuring Elusive Quaternary Stereocenters"
   Angew. Chem. Int. Ed. **2019**, *58*, 14944−14949.

3. **Aijie Cai**, Wusheng Guo*, Luis Martínez-Rodríguez, and Arjan W. Kleij* "Palladium-Catalyzed Regio- and Enantioselective Synthesis of Allylic Amines Featuring Tetrasubstituted Tertiary Carbons"
   J. Am. Chem. Soc. **2016**, *138*, 14194−14197.

4. Wusheng Guo[+], **Aijie Cai**[+], Jianing Xie, and Arjan W. Kleij* "Asymmetric Synthesis of α,α-Disubstituted Allylic Amines through Palladium-Catalyzed Allylic Substitution"
   Angew. Chem. Int. Ed. **2017**, *56*, 11797–11801.
   +: *equal contribution*

5. Jianing Xie, Wusheng Guo, **Aijie Cai**, Eduardo C. Escudero-Adán, and Arjan W. Kleij* "Pd-catalyzed Enantio- and Regioselective Formation of Allylic Aryl Ethers"
   Org. Lett. **2017**, *19*, 6388–6391.

The following publication is based on work carried out during the MSc:

6. **Aijie Cai**, Yan Zheng, Jun-An Ma* "Copper-Triggered Three-Component Reaction of CF_3CHN_2, Nitriles, and Aldehydes: Highly Diastereoselective Synthesis of CF_3-Substituted Oxazolines and Vicinal Amino Alcohols"
   Chem. Commun. **2015**, *51*, 8946–8949.

Table of Contents

Preface

The work presented in this dissertation has been carried out at the Institute of Chemical Research of Catalonia (ICIQ) during the period of February **2016** to December **2019** under the supervision of Professor Arjan W. Kleij. The thesis contains five chapters: a general introduction, four research chapters, and at the end a general conclusion of the research work. Each of the research chapters includes a brief introduction and details the aim of the respective topic, followed by a discussion of the experimental results, conclusions, and finally a comprehensive experimental section is provided. The relevant references and their numbering are independently organized by chapters.

Summary

Forging chiral quaternary stereocenters from simple and readily available starting materials under mild reaction conditions continues to be among the most challenging and attractive research goals in modern synthetic chemistry.

Since the early seminal work by Tsuji and Trost, there has been rapid progress in the development of chiral ligands and scope of the electrophilic and nucleophilic reaction partners used in Pd-catalyzed allylic substitution reactions over the past few decades. Additionally, Pd-catalyzed asymmetric allylic substitution reactions have been applied in the total synthesis of a variety of complex chiral molecules, providing solid evidence for the efficiency of such methodology in controlling both regio- and enatioselectivities. Prompted by the inherent interest of our group at ICIQ designing and developing novel catalytic processes for the preparation of valuable small molecule scaffolds, the following thesis was aimed at development of new catalytic systems for the Pd-catalyzed regio- and enantioselectivity synthesis of more sterically challenging allylic compounds. Furthermore, gaining insight into the reaction mechanism of the aforementioned, elusive Pd-catalyzed allylic amination reactions can reveal the origin of the regio- and enantioselectivity, and these aspects were also taken into account in the thesis work.

The first chapter deals with a general introduction of the historical background of transition-metal-catalyzed allylic chemistry. A particularly focus is on Pd-catalyzed asymmetric allylic substitution reactions for the construction of quaternary stereocenters. Apart from this, some pertinent mechanistic features and selected studies of Pd-catalyzed allylic amination reactions are also discussed.

The second chapter, "*Pd-catalyzed Regio- and Enantioselective Synthesis of Allylic Amines Featuring Tetrasubstituted Tertiary Carbons*", presents the first general regio- and enantioselective synthesis of α,α-disubstituted allylic *N*-**aryl** amines based on a Pd-catalyzed allylic amination protocol. This procedure utilizes readily available and modular substituted cyclic vinyl carbonates and unactivated aryl amines as reactants, and importantly can be operated without any special precautions not requiring any additives (cf. external base). Therefore, this user-friendly and efficient methodology marks a significant step forward in the challenging synthesis of these chiral allylic amine scaffolds.

The third chapter, "*Asymmetric Synthesis of α,α-Disubstituted Allylic Amines through Palladium-Catalyzed Allylic Substitution*", discusses the regio- and enantioselectivity of Pd-catalyzed allylic substitution toward the formation of α,α-disubstituted allylic *N*-**alkyl**

amines. Our contribution represents a first and important step forward in this area as no transition metal based protocol had been reported for these aliphatic amines while developing this work. By changing the use of racemic cyclic to linear tertiary allylic precursors, a series of α,α-disubstituted allylic *N*-**alkyl** amines can be obtained in good yield and with high levels of regio- and enantioselectivity. This new catalytic approach represents the only general method reported to date and should inspire other groups to further amplify this chemistry to other transition metal-mediated methodologies.

The fourth chapter, "*A Mechanistic Analysis of the Pd-catalyzed Formation of Branched Allylic Amines through a Unique Inner-Sphere Pathway*" unlocks a mechanistic manifold for the Pd-catalyzed allylic amination of vinyl cyclic carbonates using aryl amines by means of DFT calculations and various control reactions. The computations reveal that after oxidative addition/CO_2 extrusion, the nucleophilic attack leading to branched allylic amine product proceeds through a novel type of inner-sphere pathway comprising of a η^2-aryl coordination of the aromatic group of the amine reagent to the Pd center. The enantioselectivity was found to be mainly triggered by steric repulsion between the coordinated η^2-aryl and the substituted *N*-center of the phosphoramidite ligand, thus explaining the subtle interplay between the backbone chirality and the *N*-substituents. The results described in this chapter were obtained in collaboration with Prof. G. Huang from Tianjin University (China).

The fifth chapter, "*Regio- and Enantioselective Preparation of Allylic Sulfones Featuring Elusive Quaternary Stereocenters*", describes the first general regio- and enantioselective synthesis of α,α-allylic sulfones featuring quaternary stereocenters based on Pd-catalyzed allylic sulfonylation reactions. Crucial in the developed protocol is the presence of a novel and efficient phosphoramidite ligand that is able to overcome simultaneously the intrinsic challenge of achieving both high regio- and enantiocontrol, and importantly without significant catalyst deactivation. The ligand optimization studies illustrate the delicate balance between the location of the steric impediment and its influence on the reaction outcome. Finally, the formal synthesis of (−)-Agelasidine A demonstrates that these chiral allylic sulfones hold great promise as synthetic intermediates, amplifying the repertoire of nucleophiles in challenging allylic substitution reactions.

Acknowledgement

It is almost four years ago that I left China to start my PhD studies here in Tarragona. It is very important to have people around you, and with their help you can overcome and learn a lot. First and foremost, I would like to offer my sincerest gratitude to my PhD advisor, Arjan W. Kleij, for giving me the opportunity to pursue my PhD studies with him and for his tremendous support. Over the past four years, his persistent support and motivation, profound insight, wide knowledge and patience helped me to evolve into a better researcher. Arjan likes talking and sharing with us his experience, but at the same time, his curiosity drives us to think more independently and critically, this forces us to an advanced level of analyzing and understanding chemistry. Additionally, I am very grateful for the freedom and trust he gave to me over these years. I especially appreciate his patience to teach me how to solve problems that I encountered during the process of scientific research. I have learned numerous things from Arjan along the way, both in life and work, which will be beneficial in the rest my life.

Second, I would like to thank all the former and present members of the Kleij group with whom I had the pleasure to spend all these years: Carmen, Giulia, Tharun, Nicole, Moritz, Claudia, Michela, Sara, Mery, Victor, Leticia, Christian, Silvia, Sergio, Jeroen, Luis and Kike; it has been a pleasure to work around you guys, thanks for the deep conversations and the advice you have given to me. Especially Jeroen, thank you for sharing a fume hood with me and helping me with the apartment at the beginning and best wishes for your future. Thank you Luis for working with me on the first project and all the best for your future in Belgium. Rui (Prof. Huang), you have been a good lab mate and friend, you are so kind, although our ways diverted earlier than I wished, I will never forget the days we spent together, and I wish you all the best with your independent career in Dalian (China). Wusheng (Prof. Guo), you are an incredible postdoc and I had the pleasure to meet and work with you. Big thanks to you for initiating the allylic chemistry in the group. Only with your help and encouragement could I successfully finish my PhD study. Thank you for numerous discussions on the involved chemistry, and for all the constructive advice within these projects. I got to learn so much from you. Your scientific attitude, enthusiasm and persistence were paramount to me. I am sure you will be an outstanding chemist now and in the future, I hope you and your family enjoy life and prosper well in China.

Cristina, it is my great honor to have been your desk-mate, we spent so many hours sitting side by side but I still have not managed to speak many Spanish words, even though I have taught you some Chinese. Of course you are very clever, I hope you can travel to China in the near future and communicate fluently with the people in my country. My best wishes for you and your family. Àlex, it is my pleasure to have had you around, I hope you enjoy everything in Germany, even though the weather there is a little bit colder I suppose compared to Spain.

Jianing, you are very clever and hardworking, it has been a great pleasure to share a fume hood with you. Thank you for the collaboration in my second project, I could not have finished sooner if it was not for your help. I still clearly remember the days when we traveled, had dinner, played badminton and ping-pong together, and our discussion about chemistry and life. I wish you all the best with your research work and thesis. Sijing, I am glad to have met you, you are the first Chinese girl in Arjan´s group, and brought us a lot of joy, with your "Xue style" humor. I hope to have the opportunity to enjoy your cake someday. I am sure you will do a great job during your PhD. Chang, you are clever and enthusiastic, I will never forget that you organized the "Chinese Barbecue", even though Jianing and I are the "chairman". I wish all the best for your PhD. Kun you have contributed to my life and I will never forget all the hilarious moments with you. I do not want to forget, of course, the members that arrived towards the end of my PhD, but I am sure that they will have a great future as well: Alèria, Nicola, Josefine, Bart, Francesco, Alexander, Vacharaporn, Jixiang and Xuetong, very nice to have met you all, and I hope that I will have more time to know you, I hope all the best for your projects.

I have to offer my special thanks to Ingrid for all her administrative support and work throughout all these years. At ICIQ I have been fortunate to work with excellent analytical units and without them it would have been impossible to achieve the results that are described in the thesis. For UPC2 analyses, I would like to thank Simona, Marta, Maria and Meritxell, for the single crystal X-ray diffraction I want to thank Jordi, Eddy, Marta and Eduardo. For the NMR support Gabriel, Israel and Germán are kindly acknowledged, your efficient work enabled quick and solid publications of our projects.

I also would like to express my deep appreciation to many friends at ICIQ for sharing their experience and giving me support over time. The long PhD journey has been enriched by your great companion.

Last, but not the least, this thesis certainly would not have been possible with love, support and understanding from my family, especially from my parents and brothers. By

far the best thing for me was meeting my wife Yanfei. Thank you so much for all the precious encouragement, support, help and understanding through the hard times, and all the trust on every step and decisions I made. Thank you so much for bringing me such a lovely and pretty daughter during my PhD.

Aijie Cai

Abbreviations & Acronyms

In this doctoral thesis, the abbreviations and acronyms most commonly used in organic chemistry are based on the recommendations of the ACS "Guidelines for authors" which can be found at:

http://pubs.acs.org/paragonplus/submission/joceah/joceah_abbreviations.pdf

Chapter 1.

General Introduction

1.1   General Background

Organometallic chemistry represents one of the most important tools in modern organic synthesis, and especially transition-metal-catalyzed reactions continue to play a dominant role. During the last decades, a wide range of transition-metal-catalyzed coupling reactions has been developed for the synthesis of carbon−carbon and carbon−heteroatom bonds. Among these, allylic substitution reactions have gained much importance become in this area of science. In 1965, Tsuji first reported that carbon-carbon formation can be achieved by palladium-mediated allylic substitution of π−allyl-Pd complexes with carbon-based nucleophiles. Later on, Trost and co-workers developed asymmetric versions of these important C–C bond transformations. Early studies of π-allyl chemistry mainly focused on Pd catalysis[1] that typically features ample scope in both electrophilic and nucleophilic reaction partners, as well as the use of a variety of readily available chiral ligands. With time, a wider range of transition metals proved to be practical in the area. In the past few decades, complexes based on Ir, Cu, Rh, Ni, Mo, W and Ru have been explored, and each of these transition metal based catalysts were shown to have specific advantages and applicability.[1a, 2]
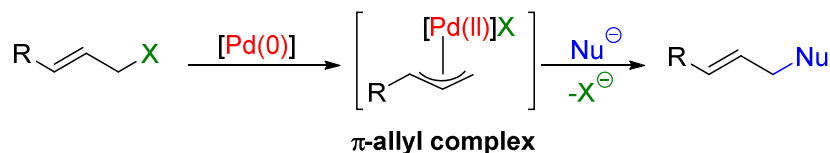
Scheme 1. Typical Pd-catalyzed allylic substitution reaction.

1.2   Pd-catalyzed Asymmetric Allylic Substitution

Pd-catalyzed allylic substitution (Scheme 1) is one of the most popular and versatile reactions in organic synthesis; it also offers a suitable transformation for testing new chiral ligands.[3] The main use of this reaction is the introduction of a new substituent in the allyl position. In 1965, Tsuji reported the first stoichiometric Pd-catalyzed allylic substitution.[4] In this seminal paper, ethyl malonate, acetoacetate and an enamine derived

---

(1) a) B. M. Trost, D. L. Van Vranken, *Chem. Rev.* **1996**, *96*, 395; b) B. M. Trost, *Chem. Pharm. Bull.* **2002**, *50*, 1; c) B. M. Trost, M. L. Crawley, *Chem. Rev.* **2003**, *103*, 2921; d) L. Milhau, P. J. Guiry, *Top. Organomet. Chem.* **2011**, *38*, 95.
(2) Z. Lu, S. Ma, *Angew. Chem., Int. Ed.* **2008**, *47*, 258.
(3) For a selective review, see: B. M. Trost, C. B. Lee, *Catalytic Asymmetric Synthesis*, 2nd ed.; Ojima, I., Ed.; Wiley-VCH: New York, **2000**; Chapter 8E, pp 503.
(4) J. Tsuji, H. Takahashi, M. Morikawa, *Tetrahedron Lett.* **1965**, *6*, 4387.

from cyclohexanone served as pro-nucleophiles together with dimeric π-allyl-Pd chloride, and these combinations smoothly afforded the desired allylic product. A catalytic version was reported in 1970,[5] and by 1977 the first Pd-catalyzed asymmetric allylic substitution was presented by Trost.[6] Since then, this reaction that now is known as the "*Tsuji-Trost reaction*" has been widely studied in terms of chemo-, regio-, and enantioselectivity.

1.2.1 Mechanistic Studies of Pd-catalyzed Allylic Substitutions

The introduction of asymmetric induction in allylic substitution reactions represented an important breakthrough to increase the application of the Tsuji-Trost reaction in organic synthesis. There are two general classes of reactions which differ in the nature of the nucleophile. The typical mechanism using "soft" nucleophiles is defined as those derived from conjugate acids whose $pK_a < 25$, and these are depicted in Scheme 2.
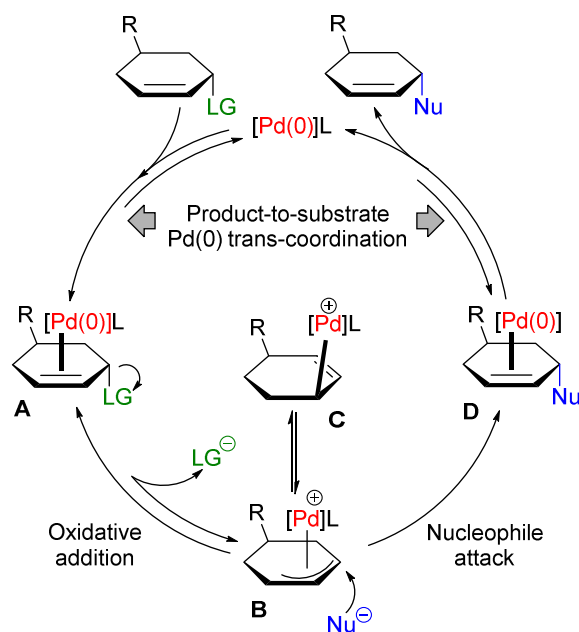
Sheme 2. Allylic substitution reactions using soft nucleophiles.

π−Coordination of the allylic precursor to the electron-rich Pd(0) precursor takes place *anti* to its leaving group (LG) and provides a Pd(0)-coordinated substrate **A**. Subsequent oxidative addition affords the π-allyl-Pd(II) complex **B**,[5a] which is in equilibrium with the isometric σ-Pd(II) intermediate **C**. Nucleophilic attack on the electrophilic complex **B** *anti* to the metal-allyl species generates (usually irreversibly) the Pd(0)-coordinated

(5) a) K. E. Atkins, W. E. Walker, R. M. Manyik, *Tetrahedron Lett*. **1970**, *11*, 3821; b) G. Hata, K. Takahashi, A. Miyake, *J. Chem. Soc. D*, **1970**, 1392.
(6) B. M. Trost, P. E. Strege, *J. Am. Chem. Soc*. **1977**, *99*, 1649.

product **D**. Finally, product-for-substrate ligand exchange releases the desired product and completes the catalytic cycle. Pertinent to this process is the fact that bond breaking and making events occur outside the coordination sphere of the metal. Thus, the nucleophile and the leaving group are segregated from the chiral environment of the ligand in the intermediate π-allyl moiety.

In this catalytic system, some specific features should be mentioned. Although the counter-anion in **B** resides outside the metal coordination sphere usually as a tight ion-pair, in complex **C** it is present in the metal coordination sphere. Donor ligands such as (di)phosphines are necessary to provide an electron-rich Pd(0) precursor thus allowing for the oxidation addition step to take place. More precisely, moderately electron-donor phosphine ligands are those that allow for the fastest turnovers. Indeed, electron-withdrawing ligands increase the electrophilicity of the allylic complex **B** toward ion-pair return (**B**→**A**) to a higher degree than exogenous nucleophilic attack (**B**→**D**).[7] Further ways to prevent ion-pair return are the addition of salts of non-coordinating anions to break up tight ion-pairs, or to use more efficient leaving groups.

On the other hand, "hard" nucleophiles ($pK_a > 25$) normally affect Tsuji-Trost reactions by coordination of the nucleophile to the metal, leading to an overall inversion of the stereochemistry followed by reductive elimination and decoordination (Scheme 3).
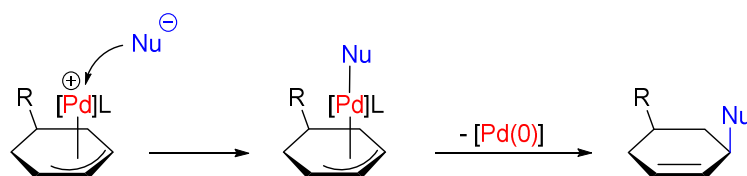
Scheme 3. Allylic substitution reactions in the presence of "hard" nucleophiles.

Oxidative addition is the enantio-discriminating step: Depending on the nature of the substrate and nucleophile and the reaction conditions, according to the classical catalytic cycle shown in Scheme 2, enantio-discrimination in asymmetric allylic substitution may occur during the olefin-to-metal coordination and subsequent oxidative addition, or the nucleophilic attack. When the nucleophilic attack is faster than the interconversion of diastereomeric π-allyl complex, oxidative addition is the enantio-discriminating step. There are two distinct manifolds:

(7) a) L. A. Evans, N. Fey, J. N. Harvey, D. Hose, G. C. Lloyd-Jones, P. Murray, A. G. Orpen, R. Osborne, G. J. J. Owen-Smith, M. Purdie, *J. Am. Chem. Soc.* **2008**, *130*, 14471; b) C. Amatore, E. Génin, A. Jutand, L. Mensah, *Organometallics* **2007**, *26*, 1875.

Slowly π-σ-π equilibrating η^3-allyl-Pd complex: As in many other catalytic asymmetric reactions, differentiation of enantiotopic olefin faces is crucial. When starting from achiral primary allylic substrates, if π-allyl interconversion is slow compared to nucleophilic attack, the chiral Pd(allyl)L* complex should distinguish between the two prochiral faces of the olefin. When the chiral catalyst is capable of selecting preferentially one of the enantiotopic faces of the alkene, the reaction can be directed toward the corresponding chiral product (Scheme 4).
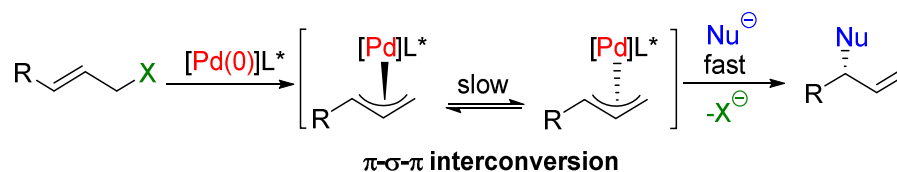
Scheme 4. Tsuji-Trost reaction with π-σ-π interconversion being slower than nucleophilic attack.

There are only limited examples known that have the enantioselective olefin complexation as the enantio-determining step in the transition-metal catalyzed allylic alkylations. In 1999, Trost and Asakawa reported an example of a Pd-catalyzed intramolecular asymmetric allylic substitution for which it was determined that oxidation addition was the enantio-determining step (Scheme 5). Various control experiments that accelerated the rate of racemization through additives or by a higher catalyst concentration decreased the asymmetric induction. Notably, limiting the interconversion of π-allyl complex by acceleration of the nucleophilic attack increased the enantioselectivity.[8]
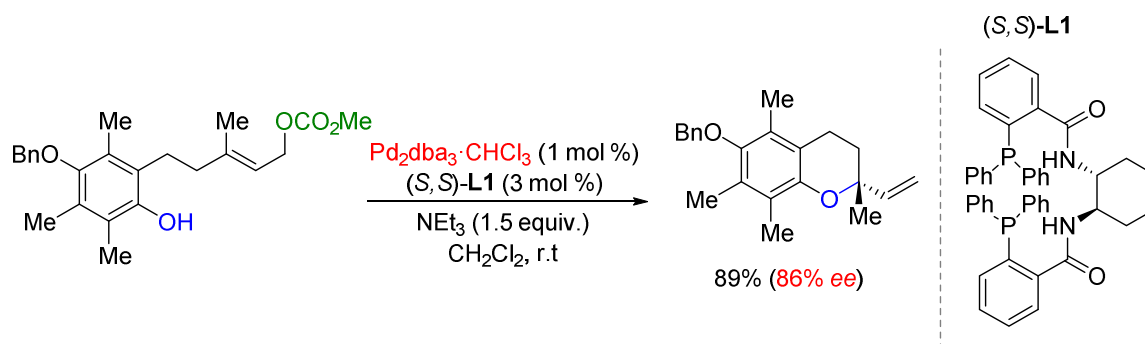
Scheme 5. Olefin complexation is the enantio-determining step in the Pd-catalyzed allylic alkylation

---

(8) B. M. Trost, N. Asakawa, *Synthesis* **1999**, 1491.

Oxidative addition of secondary allylic substrates leads to diastereomeric π-allyl complexes that not interconvert or interconvert slowly compared to nucleophilic attack. In this case, due to a double inversion process, a kinetic resolution may be observed if coordination or ionization of one enantiomer is more favored than for the other one (Scheme 6).
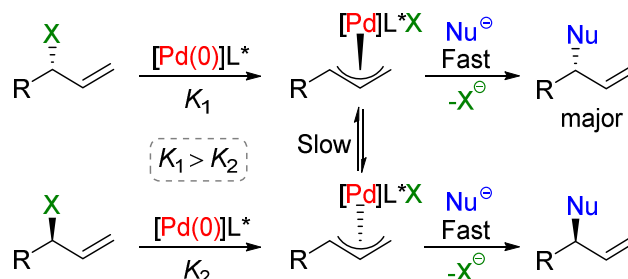
Scheme 6. Kinetic resolution of secondary allylic substrates.

In 2003, Trost and Toste developed a new Pd-catalyzed asymmetric allylic substitution for the synthesis of 4-acyloxy-2-butenodides. [9] Initially, a Pd-catalyzed kinetic asymmetric transformation using oxygen-based nucleophiles was reported (Scheme 7).
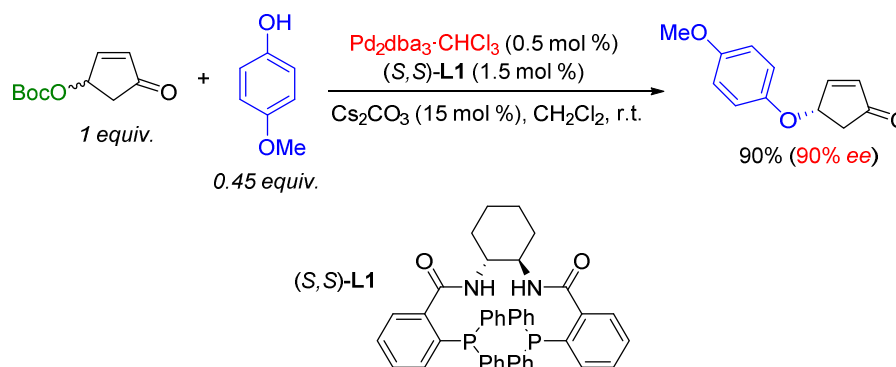
Scheme 7. Pd-catalyzed kinetic resolution in the synthesis of 4-acyloxy-2-butenodides.

Enantiotopic ionization of leaving groups: For achiral substrates with two geminal enantiotopic leaving groups or *meso*-substrates with two enantiotopic leaving groups, enantio-discrimination of the leaving groups during the coordination/oxidative addition step in the presence of a chiral ligand generates chiral π-allyl complexes. These complexes were found to react with nucleophiles following a classical double inversion process (Scheme 8).

---

(9) B. M. Trost, F. D. Toste, *J. Am. Chem. Soc*. **2003**, *125*, 3090.
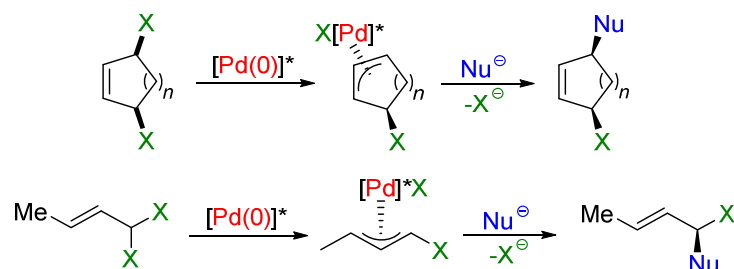
Scheme 8. Ionization of enantiotopic leaving groups

Trost and Dong presented such a Pd-catalyzed asymmetric allylic alkylation in 2006.[10] In this chemistry, by using a *meso*-diBoc-activited cyclopentene as allylic precursor, they could obtain the desired product in high yield and enantioselectivity in the presence of Trost's ligand [see (*S,S*)-**L1**, Scheme 7]. The utility of this approach was further highlighted by its application to the preparation of Agelastatin (Scheme 9).
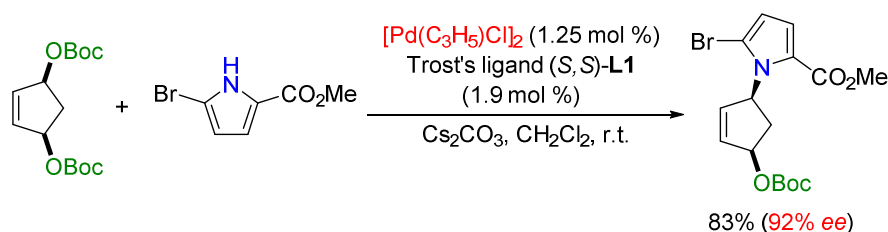
Scheme 9. Example of ionization of enantiotopic leaving groups.

Nucleophilic attack is the enantiodiscriminating step: If a chiral allylic substrate generates a *meso* π-allyl intermediate after ionization, then the two allylic termini of the Pd(allyl) complex are enantiotopic. This allows for enantioselective transformation into product which is determined by the regioselectivity of the nucleophilic attack on the allylic intermediate. Therefore, a suitable chiral ligand controls the regioselectivity of the nucleophilic attack (with both stabilized and unstabilized nucleophiles) and thus induces preferential formation of one product enantiomer over the other. In this case, a racemic allylic substrate can be converted into an enantioenriched product (Scheme 10).
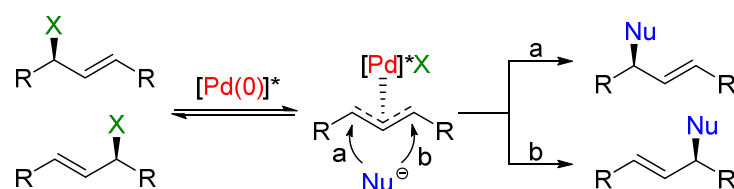
Scheme 10. Enantio-selection coinciding with regio-selection.

---

(10) B. M. Trost, G. Dong, *J. Am. Chem. Soc*. **2006**, *128*, 6054.

The most extensively studied example of such a system is 1,3-diphenylallyl acetate, which has become the benchmark substrate when exploring new ligands in cases when oxidative addition provides a *meso* intermediate. Subsequent attack by the conjugate base of dimethyl malonate at either termini (pathway **a** or **b**) affords a chiral product with high enantioselectivity (Scheme 11). [11] However, the results from this system do not necessarily translate into high enantioselectivity for other types of substrates.[1a]
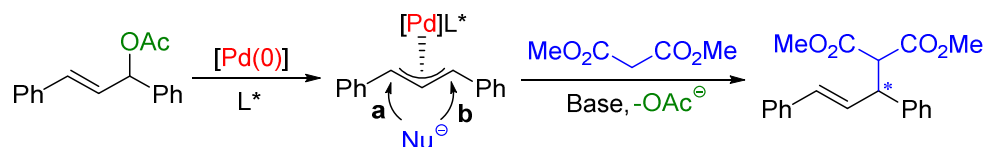
Scheme 11. Desymmetrization of a *meso*-π-allyl complex with a malonate nucleophile.

Enantiotopic olefin face coordination or enantiotopic ionization may also not the enantio-determining step in asymmetric allylic substitution reactions if the diastereomeric π-allyl metal complex interconvert faster than nucleophilic attack. A suitable chiral catalyst may allow for preferential attack of the nucleophile onto one of the two rapidly equilibrating π-allyl intermediates (Scheme 12). In this mechanistic scenario, there are several other aspects that are important apart from enantioselectivity as the regioselectivity of the nucleophilic addition should also be considered. For allylic substrates, this manifold can be grouped into two categories: the use of achiral allylic precursors, or the utilization of a racemic substrate. In the latter case, a successful reaction constitutes a dynamic kinetic asymmetric transformation (DYKAT) as both enantiomers of the starting material are converted into a single product enantiomer.
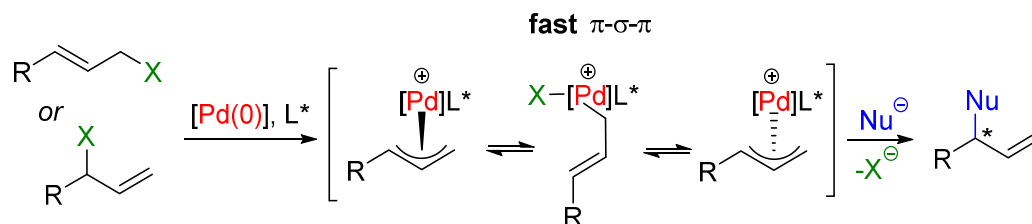
Scheme 12. Asymmetric allylic alkylation *via* enantioface exchange of a Pd(allyl) complex.

(11) a) B. M. Trost, D. J. Murphy, *Organometallics* **1985**, *4*, 1143; b) J. Sprinz, G. Helmchen, *Tetrahedron Lett.* **1993**, *34*, 1769; c) P. Wimmer, M. Widhalm, *Tetrahedron* **1995**, *6*, 657.

In the case of an achiral substrate (generally linear allylic precursors), the two diastereomeric intermediates that result from interconversion through π-σ-π equilibration on the terminal carbon of the allyl system, (the sigma complex is achiral), the initial amount of each diastereomeric complex formed may not be equal (Scheme 12). When a chiral *racemic* allylic precursor is present as substrate, a similar type of π-σ-π equilibration occurs. Initially, a 1:1 mixture of diastereomeric Pd(allyl) complexes is formed. The π-allyl intermediates must equilibrate through a terminal sigma carbon-bound complex such that the initial chirality with respect to the C-X fragment (X = leaving group) is erased or through a mechanism in which the Pd complex is temporarily coordinated by a heteroatom causing the same net effect.

Hayashi and co-workers reported the construction of chiral 4-vinyl oxazolidinones starting from symmetrical 2-butenylene dicarbamates (Scheme 13). Interestingly, both (*Z*)- and (*E*)-isomers of the substrate afford the cyclized product in essentially the same yields and enantio-selectivities, indicating that the π-σ-π interconversion of the intermediate π-allyl Pd complexes is faster than nucleophilic attack.[12]
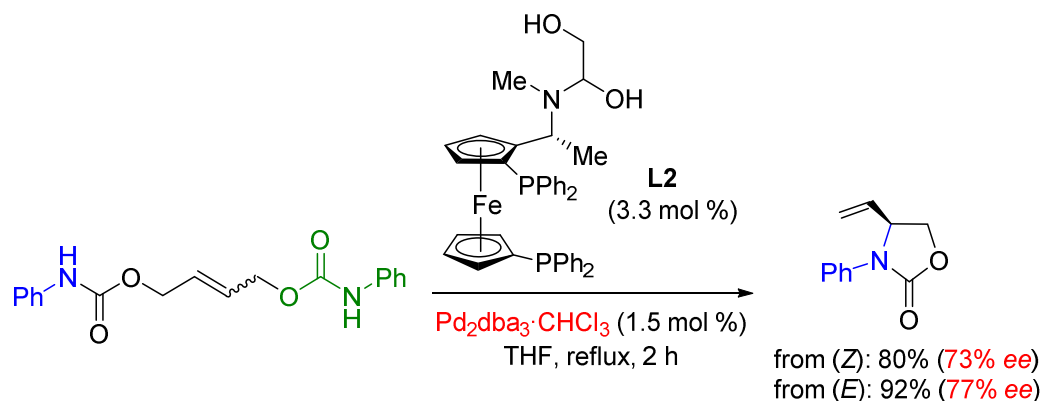
Scheme 13. Pd-catalyzed allylic substitution involving faster π-σ-π interconversion than nucleophilic attack.

Methodologies that enable concise and efficient asymmetric synthesis of tetrasubstituted stereocenters play a key role in synthetic chemistry. In this regard, dynamic kinetic asymmetric transformation in allylic substitution reactions has created wide potential for total synthesis. For example, by using racemic 3-nonyl-3,4-epoxybut-1-ene as substrate and *p*-methoxylbenzyl alcohol as nucleophile in the presence of the Trost ligand and a suitable Pd precursor, a chiral allylic ether intermediate could be

---

(12) T. Hayashi, A. Yamamoto, Y. Ito, *Tetrahedron Lett.* **1988**, *29*, 99.

produced in 74% yield and 99% *ee*. This enantioenriched compound was subsequently converted to (−)-malyngolide in 7 steps (Scheme 14).[13]
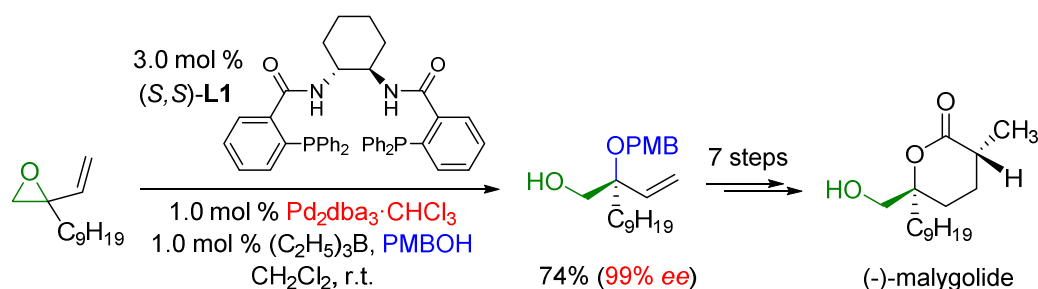
Scheme 14. A successful DYKAT approach towards (−)-malyngolide.

1.2.2 Generation of π-Allyl Complex

In the presence of Pd(0) precursor, the most common way to produce a π-allyl-Pd intermediate is through heterolytic cleavage of a C–X allylic bond (X = leaving group). This step is an oxidation addition, as the metal oxidation state is increased to +2, which normally is accompanied by the generation of a reactive, ionic η^3-allyl intermediate. Oxidative addition of a standard allylic acetate to a Pd(0) precursor was demonstrated by Yamamoto and co-workers in 1981, and they isolated and characterized the corresponding η^3-allyl(acetato) Pd complex[14] with the formation of the π-allyl-Pd intermediate being a reversible process.
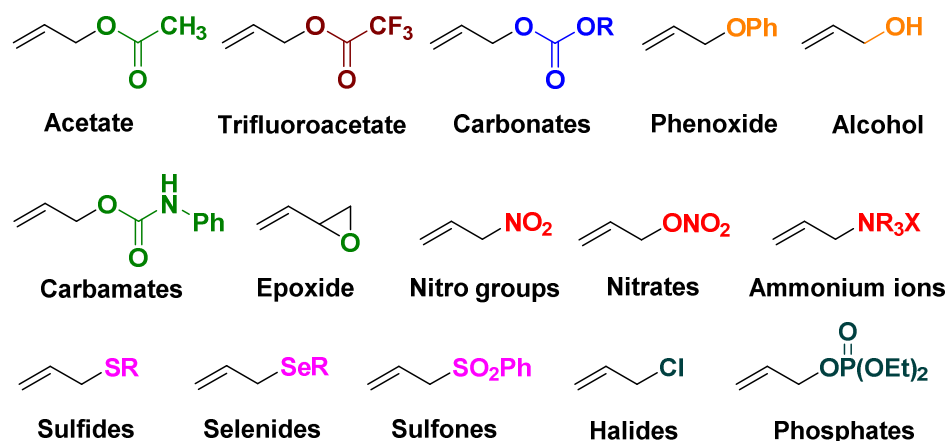
Scheme 15. Classical allylic precursors used in Pd-catalyzed allylic substitution having different leaving groups.

(13) B. M. Trost, W. Tang, J. L. Schulte, *Org. Lett.* **2000**, *2*, 4013.
(14) T. Yamamoto, O. Saito, A. Yamamoto, *J. Am. Chem. Soc.* **1981**, *103*, 5600.

11

Numerus allylic precursors have been used in this substitution reaction and some are presented in Scheme 15. Notably, the introduction of carbonate as leaving group by Tsuji in 1982 represented an important breakthrough.[15] Carbonate is a better leaving group than acetate, but its significant advantage over the latter is that it allows the reaction to occur in an almost neutral medium.

There are some other procedures that allow for the preparation of π-allyl-Pd complexes such as cleavage of a C–X benzylic bond,[16] C–H activation,[17] carbopalladation of allene substrates,[18] and nucleopalladation of 1,3-dienes.[19]

1.2.3 Synthesis of Tetrasubstituted Stereocenters

Pd-catalyzed asymmetric substitution reactions are efficient methods for the creation of new stereocenters.[20] Few transition-metal-catalyzed allylic reactions offer the ability to form carbon-carbon and carbon-heteroatom bonds while exerting asymmetric induction. However, one specific aspect of this type of reaction has significantly matured over the past 20 years, which is the synthesis of tetrasubstituted stereocenters.

1.2.3.1 Stereocontrol in Prochiral Allylic Precursors

Allylic alkylation of allyl electrophiles bearing substituents are typically easier substrates to induce asymmetric induction, however, operate via more complicated reaction mechanisms involving π-σ-π equilibration of the intermediate π-allyl complex. Additionally, the enantio-determining step of the reaction may occur during any step of the catalytic cycle depending on the substrate, catalyst, and reaction conditions. In Pd-catalyzed allylic asymmetric substitution reactions, only two possible manifolds are likely to be operative in the construction of tetrasubstituted stereocenters; one is the differentiation of enantiotopic olefin faces (Scheme 16, **a**) and the other is via π−σ−π equilibration (Scheme 16, **b**). A variety of organic products have been obtained from the various efficient approaches toward stereocontrol in allylic substitution chemistry.

(15) a) J. Tsuji, I. Shimizu, I. Minami, Y. Ohashi, *Tetrahedron Lett.* **1982**, *23*, 4809; b) J. Tsuji, I. Shimizu, I. Minami, Y. Ohashi, T. Sugiura, *J. Org. Chem.* **1985**, *50*, 1523.
(16) J.-Y. Legros, J.-C. Fiaud, *Tetrahedron Lett.* **1992**, *33*, 2509.
(17) B. M. Trost, T. J. Fullerton, *J. Am. Chem. Soc.* **1973**, *95*, 292.
(18) I. Shimizu, J. Tsuji, *Chem Lett.* **1984**, *13*, 233.
(19) S. D. Robinson, B. L. Shaw, *J. Chem. Soc.* **1963**, 4806.
(20) a) B. M. Trost, M. L. Crawley, *Chem. Rev.* **2003**, *103*, 2921; b) B. M. Trost, *J. Org. Chem.* **2004**, *69*, 5813; c) B. M. Trost, M. R. Machacek, A. Aponick, *Acc. Chem. Res.* **2006**, *39*, 747.

a: differentiation of enantiotopic olefin faces

b: π–σ–π equilibration
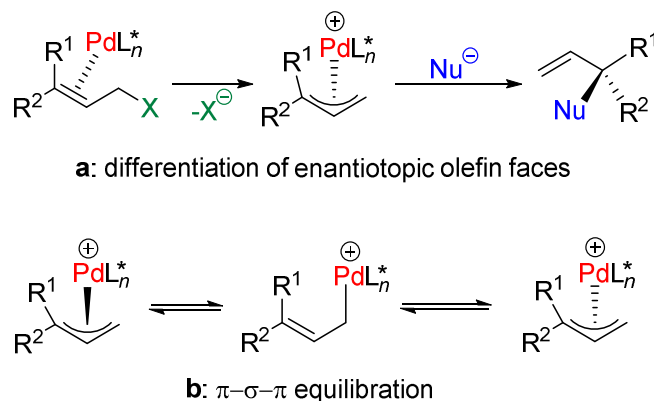
Scheme 16. Two mechanisms towards the synthesis of tetrasubstituted stereocenters.

Through the use of isoprene monoepoxide as allylic substrate, the Trost group reported branched-selective substitution for carbon-, [21] oxygen-, [22] and nitrogen-based nucleophiles, [23] affording enantioenriched building blocks featuring tetrasubstituted centers. In 1998, Trost presented a two-component catalyst system for asymmetric allylic substitutions with alcohol pro-nucleophiles (Scheme 17). The use of catalytic borane was crucial for reactivity, as the reaction proceeded with only little conversion in the absence of the borane additive. The conceptual idea of this two-component catalyst system is to active both nucleophile and electrophile which may expand these metal-catalyzed allylic alkylations to nucleophiles beyond alcohols, thereby considerably expanding the scope of this important transformation.[22a]
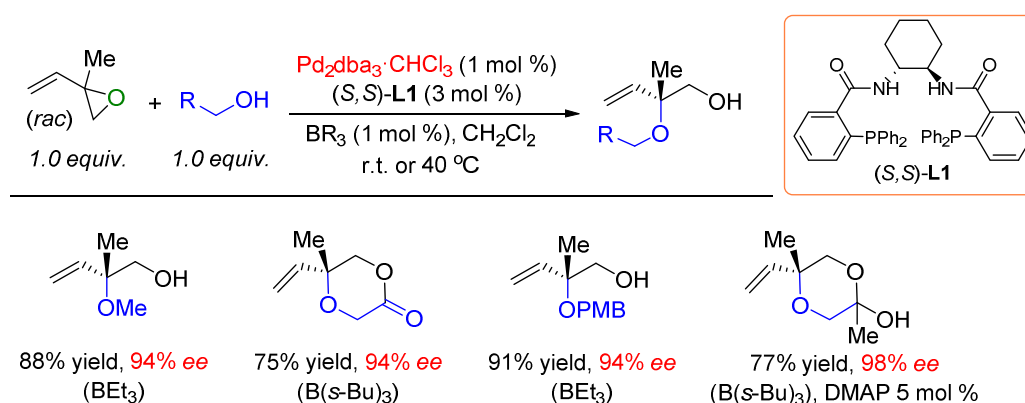
Scheme 17. The synthesis of tertiary ethers using (*rac*) isoprene monoepoxide as substrate.

(21) B. M. Trost, C. Jiang, *J. Am. Chem. Soc.* **2001**, *123*, 12907.
(22) a) B. M. Trost, E. J. McEachern, F. D. Toste, *J. Am. Chem. Soc.* **1998**, *120*, 12702; b) B. M. Trost, E. J. McEachern, *J. Am. Chem. Soc.* **1999**, *121*, 8649.
(23) a) B. M. Trost, C. Jiang, K. Hammer, *Synthesis* **2005**, 3335; b) B. M. Trost, R. C. Bunt, R. Lemoine, T. L. Calkins, *J. Am. Chem.Soc.* **2000**, *122*, 5968; c) B. M. Trost, T. L. Calkins, C. Oertelt, J. Zambrano, *Tetrahedron Lett.* **1998**, *39*, 1713.

In 1999, a net addition of "hydroxide" was discovered by the Trost group[22b] based on the reaction of the vinylepoxide and sodium hydrogen carbonate under BEt_3/Pd catalysis. In this approach, the hydrogen carbonate nucleophile is directed to the branched position with high enantioselectivity; the unstable linear carbonate intermediate then undergoes decarboxylation to provide the tertiary alcohol product (Scheme 18).
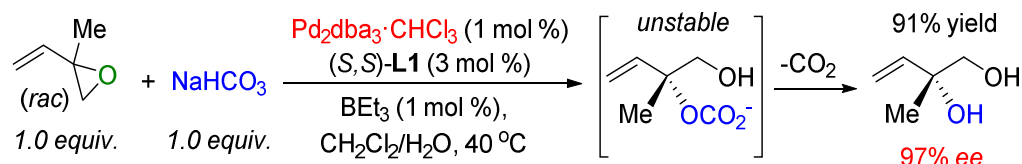
Scheme 18. The synthesis of a tertiary alcohol using sodium hydrogen carbonate.

Carbon-based nucleophiles have also been successfully applied by Trost *et al.* in this chemistry using nitromethane or β-keto esters (Scheme 19).[21] These reactions were pioneered for the Pd-catalyzed, atom-economic synthesis of acyclic all-carbon quaternary stereocenters. These chiral quaternary carbon centers comprised of three different functional groups thus allowing for easy manipulation of either one demonstrating that these molecules are useful building blocks in synthetic chemistry.
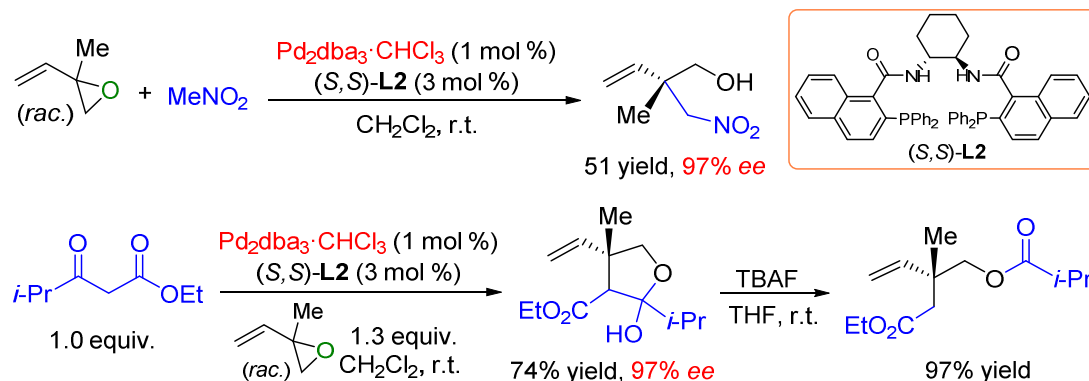
Scheme 19. Building all-carbon quaternary centers by Pd-catalyzed allylic substitution.

The Pd-catalyzed cross-coupling of racemic tertiary allylic carbonates and allyl boronates was described by Morken and co-workers in 2011.[24] This reaction generates all-carbon quaternary centers in a highly regioselective and enantioselective fashion. The outcome of these reactions is consistent with a process that proceeds by a 3,3´-reductive elimination of bis-(η^1-allyl)palladium complexes. In the reaction optimization phase it

---

(24) P. Zhang, H. Le, R. E. Kyne, J. P. Morken, *J. Am. Chem. Soc.* **2011**,*133*, 9716.

was observed that β-hydride elimination caused significant side product formation. The addition of a fluoride salt (CsF) was shown to minimize this side reaction by acceleration of the allylic transformation (Scheme 20).
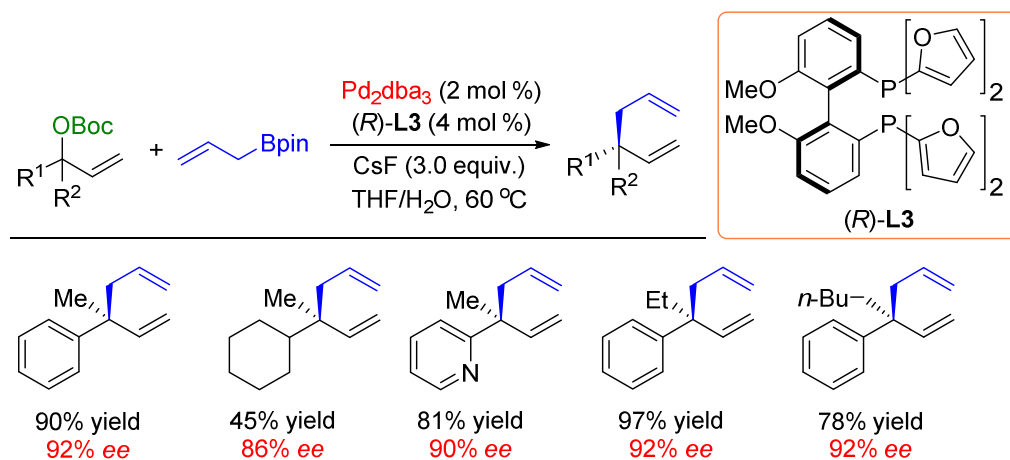
Scheme 20. Catalytic enantioselective branched-selective allyl-allyl cross-coupling.

1.2.3.2 Stereocontrol in Prochiral Nucleophiles

In Pd-catalyzed allylic asymmetric substitutions, achieving high enantioselectivity while focusing on the nucleophilic reaction partner remains much more difficult than achieving enantiocontrol that centers attention on the electrophilic partner. The main reason for this is that the nucleophilic addition has an outer-sphere character. In this allylic alkylation event, the chiral environment within the metal-ligand sphere must be successfully relayed distal from the metal in order to observe catalyst differentiation of enantiotopic faces of the (incoming) nucleophile. The first synthesis of tetrasubstituted stereocenters by reaction of prochiral nucleophiles was discovered by the Ito group in 1992. Alkylation of an acyclic 1,3-diketone by employing a point and planar chiral ferrocenyl ligand scaffold bearing an aza-crown ether produced the desired product in modest enantioselectivity.[25] In order to enhance the enantioselectivity upon nucleophilic attack of the π-allyl Pd(II) intermediate, it was envisioned that linking a crown ether to the chiral phosphine ligand would allow for recognition of the nucleophile counterion. In this case, the chiral information of the catalyst could be relayed distal to the site of the reaction, thus solving the problem of poor selectivity in the case of these prochiral nucleophiles. In both cases, significant optimization of the crown ether structure and type of counterion was necessary to obtain high enantiocontrol (Scheme 21).

---

(25) M. Sawamura, H. Nagata, H. Sakamoto, Y. Ito, *J. Am. Chem. Soc.* **1992**, *114*, 2586.
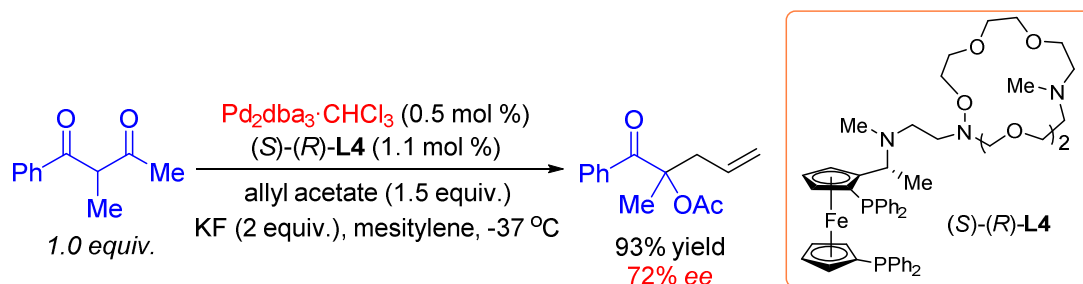
Scheme 21. Asymmetric alkylation of a 1,3-diketone by counterion recognition of a crown-ether derived chiral phosphine ligand.

In 1999, Ito and co-workers reported a highly enantioselective alkylation (up to 95% *ee*) of prochiral α-acetamido-β-ketoesters catalyzed by a chiral Pd(BINAP) complex to furnish α-allyl-α-acetamido-β-ketoesters products having a quaternary stereogenic center at the α-carbon in high yield and enantioselectivity.[26] The substitution of the prochiral nucleophiles with either (*Z*)-linear allylic precursors or the corresponding chiral racemic substrates afforded the product with nearly identical enantioselectivity (85-86% *ee*) without the formation of any undesired regio- or geometrical isomers, indicating that the nucleophilic attack may be slower than π-σ-π isomerization of the π-allyl-Pd complex initially generated (Scheme 22).
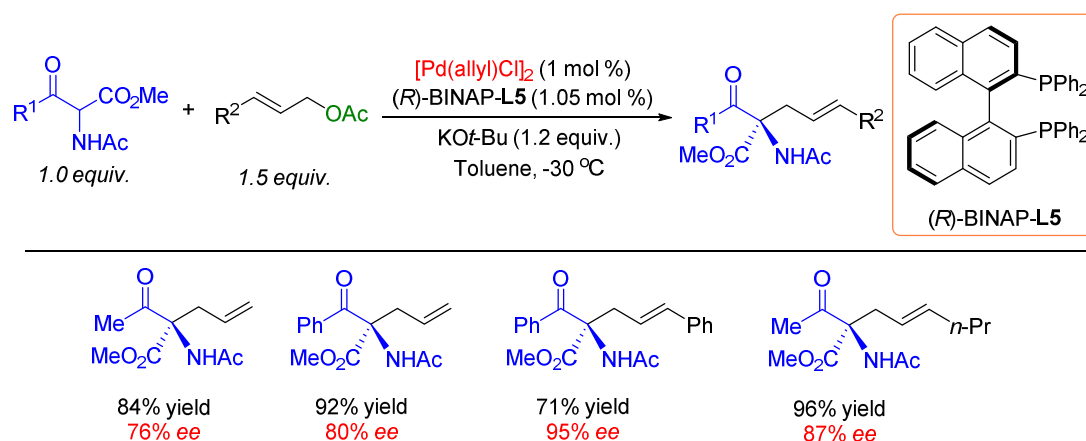
Scheme 22. Pd/BINAP-catalyzed allylation of α-acetamido-β-keto esters.

Recently, Hou and co-worker demonstrated that the Pd-catalyzed allylic substitution of acyclic amides in the presence of 1,1′-P,N-chelating ferrocene ligands provides access to the corresponding γ,δ-unsaturated amides,[27] which are important building blocks in organic synthesis. In this chemistry, they showed two examples of the enantioselective

(26) R. Kuwano, Y. Ito, *J. Am. Chem. Soc.* **1999**, *121*, 3236.
(27) K. Zhang, Q. Peng, X.-L. Hou, Y.-D. Wu, *Angew. Chem. Int. Ed.* **2008**, *47*, 1741.

synthesis of acyclic tetrasubstituted stereocenters. The *N,N*-diphenylamide substrate was found to be optimal in the initial optimization studies.
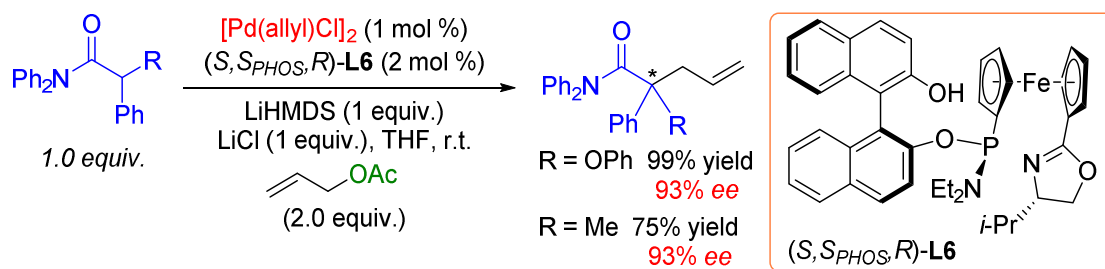
Scheme 23. Synthesis of quaternary stereocenters by α-alkylation of *N,N*-diphenylamides.

In 2011, List and Jiang developed the first highly enantioselectivity direct α-allylation of α-branched aldehydes using allylic alcohols.[28] Efficient asymmetric induction was realized through the additional presence of an achiral amine catalyst and (*S*)-TRIP **L7** (a phosphoric acid derivative) and the overall process follows an asymmetric counter-anion directed catalysis (ACDC). This reaction manifold effectively provided all-carbon quaternary stereogenic centers in a single step from readily available starting materials. However, the method was mostly limited to α-aryl-propanals as aliphatic aldehydes with longer side chains resulted in decreased enantiocontrol (Scheme 24).
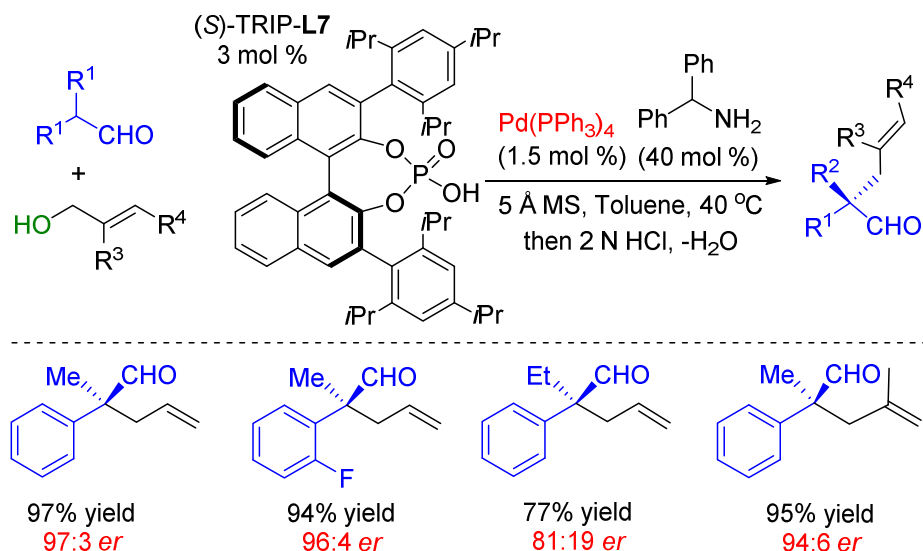
Scheme 24. The direct α-alkylation of α-arylpropanals using allylic alcohols.

---

(28) G. Jiang, B. List, *Angew. Chem. Int. Ed.* **2011**, *50*, 9471.

Another dual-catalytic approach was reported by Ooi and co-workers for the cinnamyation of α-nitro esters (Scheme 25).[29] They introduced a chiral assembly composed of an achiral quaternary ammonium-phosphine and a chiral binaphtholate anion held together through ionic interactions. This method successfully demonstrated that a remarkable ability of this ion-paired chiral ligand to induce stereocontrol in the Pd-catalyzed allylic substitution of α-nitrocarboxylates. This research provides a conceptually new approach for the design of chiral ligands for asymmetric transition-metal (TM) catalysis.
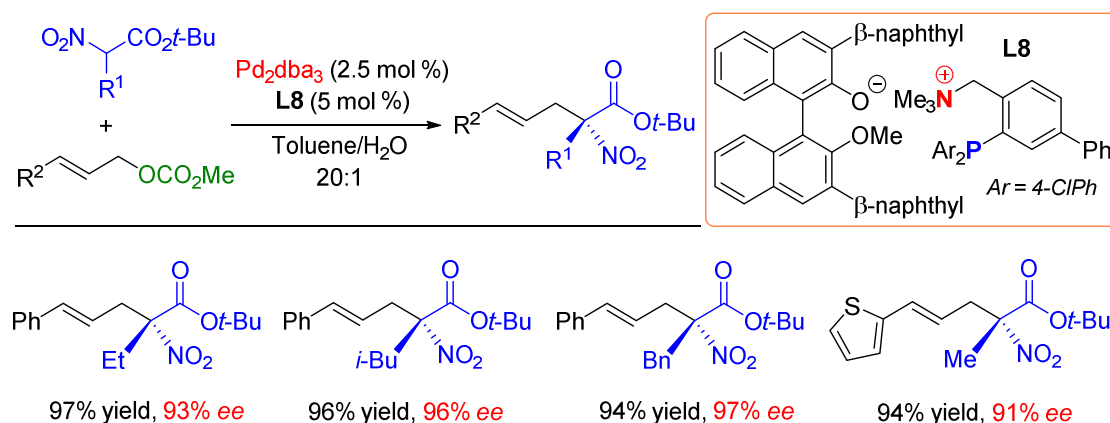
Scheme 25. Ion-paired chiral ligands for the cinnamylation of α-nitro esters.

Unlike intermolecular allylic substitution reactions, Pd-catalyzed decarboxylative allylic alkylation (DAAA) occur via a largely intramolecular reaction pathway. This strategy is based on the ionization of an allyl moiety; the π-allyl-Pd species is counterion-paired to its pro-nucleophile. Upon decarboxylation, substitution occurs via an outer-sphere attack of the nucleophile on the reactive π-allyl-Pd complex, effectively providing the desired product and regenerating the chiral Pd(0)species (Scheme 26).

(29) K. Ohmatsu, M. Ito, T. Kurieda, T. Ooi, *Nat. Chem.* **2012**, *4*, 473.
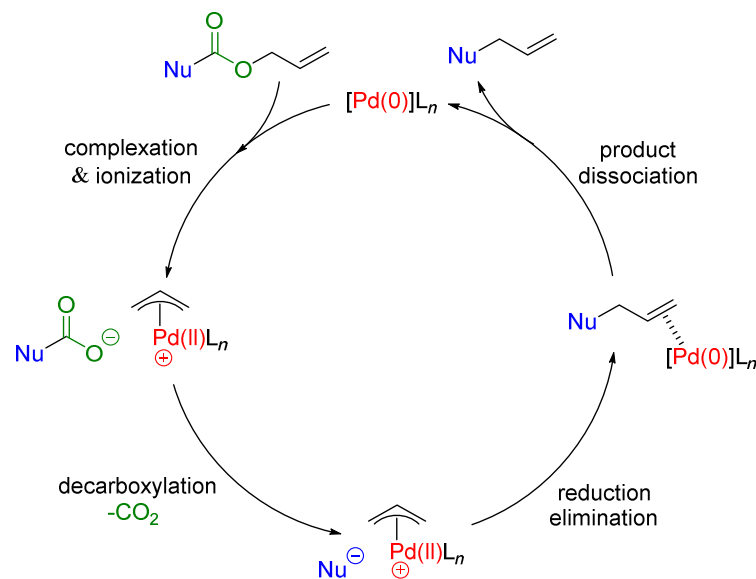
Scheme 26. Mechanism of Pd-catalyzed decarboxylative allylic substitution.

In order to investigate whether this reaction occurs via an inner- or outer-sphere mechanism, it is complicated by differences in the experimental outcomes of these reactions and the computed lowest energy pathway. [30] It is worth noting that computational work was carried out using phosphino-oxazoline (PHOX) ligands, whereas experimental evidence was gathered with the structurally different bisphosphino Trost ligands. The experimental work showed that the enol carbonate underwent Pd-catalyzed DAAA with kinetic resolution of the enantiomeric starting material. The desired alkylation product was formed with net retention of the stereochemistry, indicating an outer-sphere mechanism (Scheme 27).
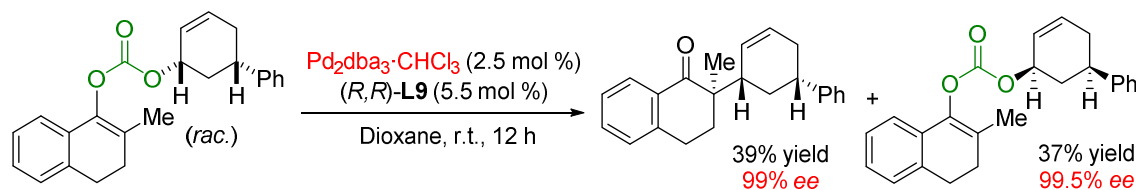
Scheme 27. Experimental evidence for an outer-sphere mechanism.

In 2007, the Trost group developed the first catalytic asymmetric synthesis of α-tertiary hydroxyaldehydes through Pd-catalyzed allylic alkylation of siloxy-enol carbonates.[31] The excellent selectivity toward aldehyde was achieved by using Trost

(30) J. A. Keith, D. C. Behenna, N. Sherden, J. T. Mohr, S. Ma, S. C. Marinescu, R. J. Nielsen, J. Oxgaard, B. M. Stoltz, W. A. Goddard, *J. Am. Chem. Soc.* **2012**, *134*, 19050.
(31) B. M. Trost, J. Xu, M. Reichle, *J. Am. Chem. Soc.* **2007**, *129*, 282.

ligand (R,R)-**L9**. These reactions proceed under very mild conditions and generate α-tetrasubstituted stereogenic centers with excellent yield and enantiomeric excess (Scheme 28).
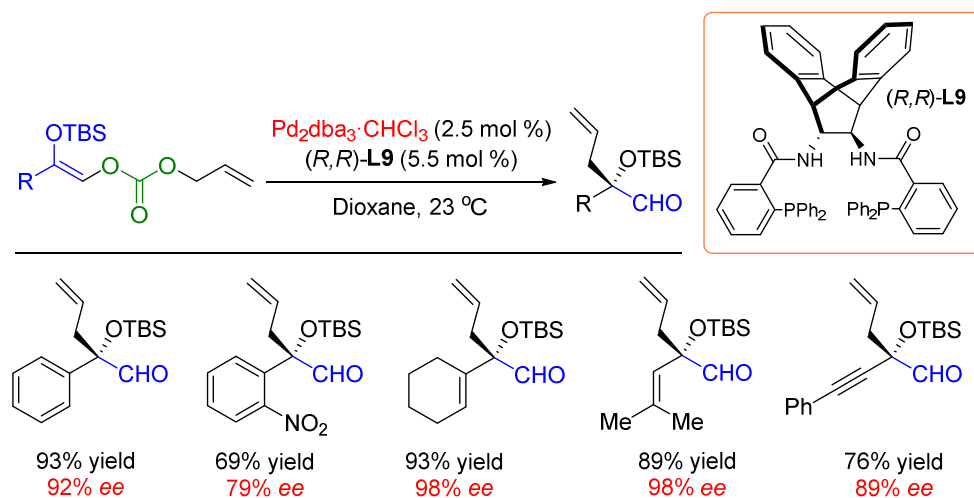
Scheme 28. Synthesis of α-tertiary hydroxyaldehydes by Pd-catalyzed DAAA.

Recently, Starkov, Marek, Stoltz, and co-workers demonstrated a divergent and modular protocol for the synthesis of acyclic molecular frameworks containing newly created quaternary carbon stereocenters. [32] This was accomplished by a unique combination of easily accessible, fully substituted stereodefined amide enolates with the
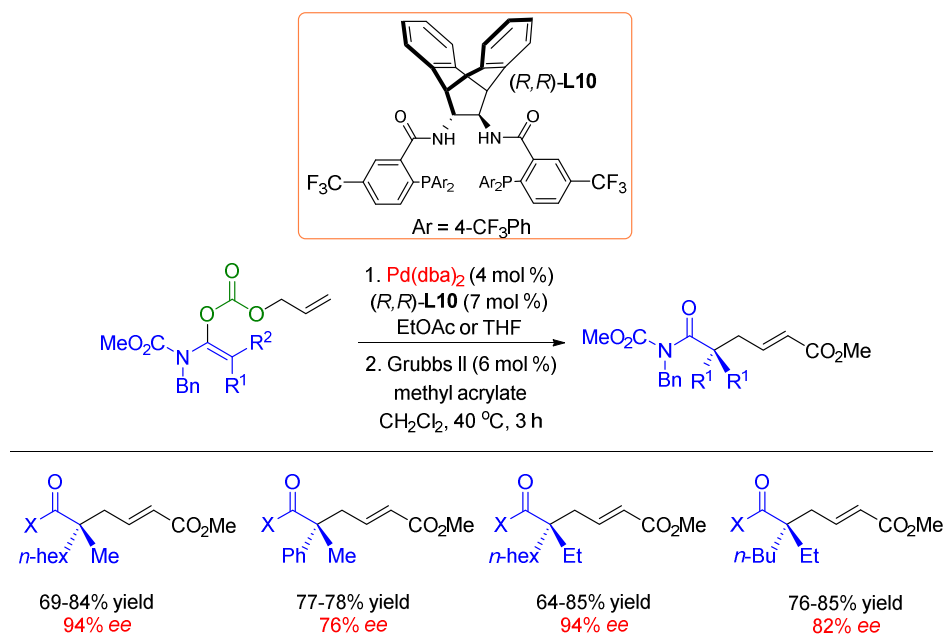
Scheme 29. Pd-catalyzed DAAA of tetrasubstituted amide enol carbonates.

---

(32) P. Starkov, J. T. Moore, D. C. Duquette, B. M. Stoltz, I. Marek, *J. Am. Chem. Soc.* **2017**, *139*, 9615.

enantioselective catalytic decarboxylative allylic alkylation reaction employing a novel electronically perturbed C_2-symmetric bisphosphine ligand [(R,R)-**L10**, Scheme 29].

The Trost group has shown a breath of Pd-catalyzed asymmetric allylic substitution reactions using azlactones and a variety of allyl electrophiles.[33] In 2012, the first palladium-catalyzed asymmetric benzylation was demonstrated using azlactones as pro-chiral nucleophiles in the presence of chiral bisphosphine ligands.[34] Benzylic electrophiles were utilized under two sets of reaction conditions to construct new tetrasubstituted stereocenters. The electron density of the phenyl ring dictates the reaction conditions, including the leaving group. The reported strategy represented a novel asymmetric carbon-carbon bond formation in an amino acid precursor (Scheme 30).
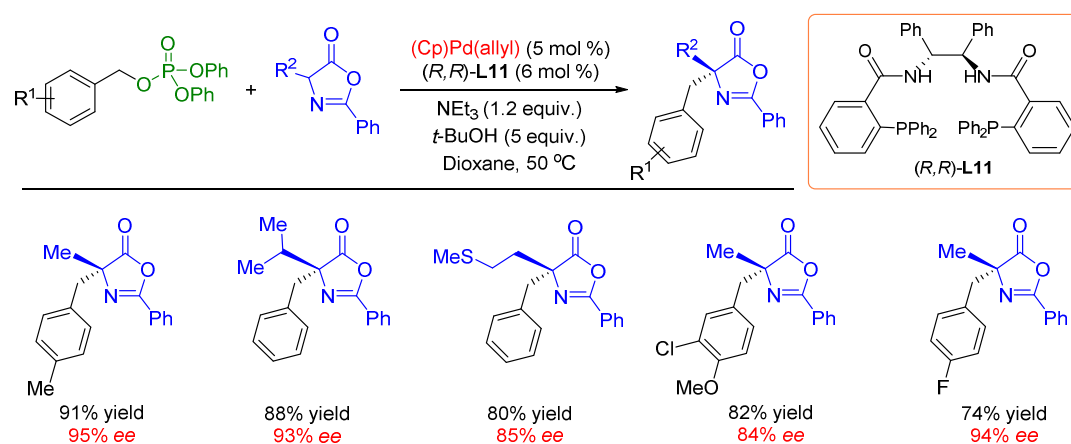
Scheme 30. Pd-catalyzed benzylation of azlactones.

1.2.3.3   Synthesis of Tetrasubstituted Stereocenters with Other Metals

The first examples within the area of asymmetric allylic alkylation (AAA) that demonstrate stereocontrol in the synthesis of acyclic stereocenters were employing Pd catalysts. However, during the last decades, major advances have been made employing other transition metals including iridium (Ir), rhodium (Rh) and molybdenum (Mo). Copper-catalyzed allylic substitution reactions nicely complement methods carried out with other metals due to the unique S_N2' pathway and the ability to employ hard

(33) a) B. M. Trost, X. Ariza, *J. Am. Chem. Soc.* **1999**, *121*, 10727; b) B. M. Trost, X. Ariza, *Angew. Chem. Int. Ed. Engl.* **1997**, *36*, 2635.

(34) a) B. M. Trost, L. C. Czabaniuk, *J. Am. Chem. Soc.* **2012**, *134*, 5778; b) B. M. Trost, L. C. Czabaniuk, *Chem. Eur. J.* **2013**, *19*, 15210.

nucleophilic precursors.[35] The selective structures of ligands used in Ir-, Rh- and Mo-catalyzed AAA are shown in (Scheme 31).

Since the first report on an Ir-catalyzed allylic substitution reaction communicated by Takeuchi and Kashio, Ir complexes were found to be efficient catalysts for allylic substitution reactions.[36] Ir catalysis has unique features compared with Pd catalysis. Particularly, allylic electrophiles with one terminal substituent usually yield achiral linear products with Pd catalysts, while Ir catalysts normally furnish branched products with excellent regio- and enantioselectivities. The most significant factor that accelerated the advancement of Ir-catalyzed asymmetric allylic substitution reactions was the discovery that chiral phosphoramidite ligands efficiently induce chirality.
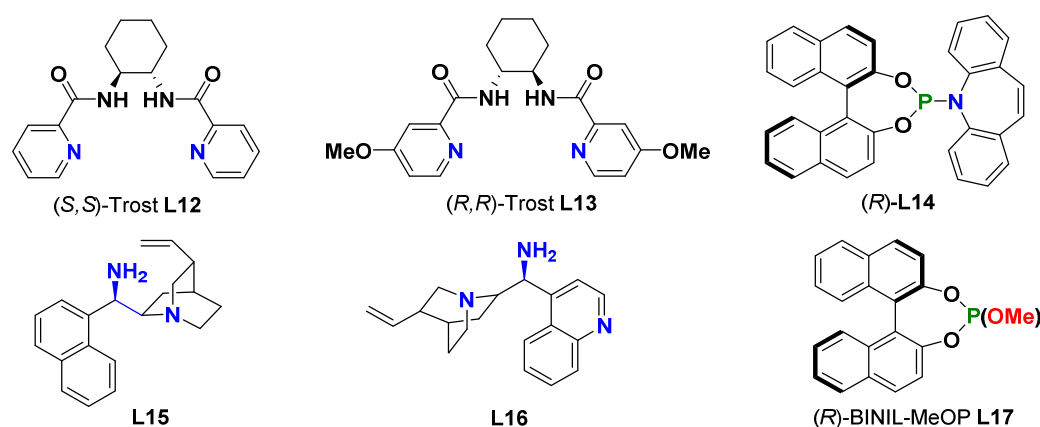
Scheme 31. Structures of ligands used in Ir, Rh and Mo-catalyzed asymmetric allylic alkylation.

In Ir-catalyzed allylic substitution, the ability to control the overall stereochemistry of the AAA reaction was first demonstrated by Takemoto and co-workers in 2003.[37] Since that first report, enantio- and diastereoselective Ir-catalyzed asymmetric allylic substitution reactions have been reported for several systems. In 2013, Catteira and co-workers described the realization of a new concept in a fully stereodivergent dual-catalytic synthesis of γ,δ-unsaturated aldehydes bearing vicinal quaternary/tertiary stereogenic centers (Scheme 32).[38] The reaction is enabled by chiral iridium and amine catalysts, which activate the allylic alcohol and aldehyde substrates, respectively.

(35) J. F. Hartwig, L. Stanley, *Copper-Catalyzed Allylic Substitution*, In *Organotransition Metal Chemistry: From Bonding to Catalysis*; J. F. Hartwig, Ed.; University Science Books: Mill Valley, **2010**, 999–1008.
(36) R. Takeuchi, M. Kashio, *Angew. Chem. Int. Ed. Engl.* **1997**, *36*, 263.
(37) T. Kanayama, D. Yoshida, H. Miyabe, K. Takemoto, *Angew. Chem. Int. Ed.* **2003**, *42*, 2054.
(38) S. Krautwald, D. Sarlah, M. A. Schafroth, E. M. Carreira, *Science* **2013**, *340*, 1065.

Furthermore, each catalyst exerts high local stereocontrol irrespective of the inherent preference of the other catalytic component.
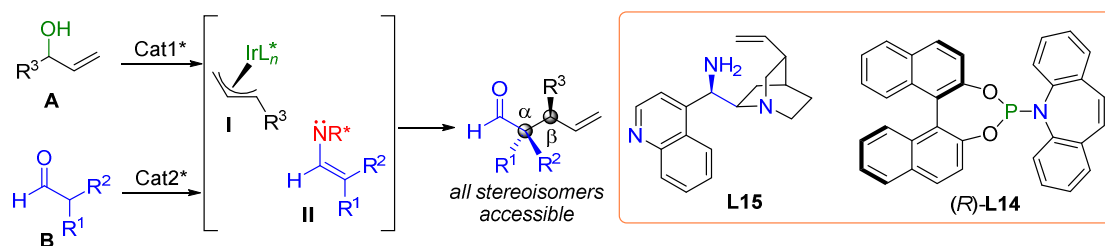
Scheme 32. Regio-, diastereo-, and enantioselective α-cinnamylation of aldehydes by a dual chiral amine/chiral Ir catalysis.

Subsequently, the branched-selective Ir-catalyzed allylic substitution of trisubstituted cinnamyl electrophiles was reported by the Stoltz group in 2017.[39] This was the first example of a highly enantioselective Ir-catalyzed allylic alkylation that provides access to products bearing allylic all-carbon quaternary stereocenters. The method utilized a masked acyl cyanide (MAC) reagent, which enabled the one-pot preparation of α-quaternary carboxylic acids, esters, and amides with a high degree of enantioselectivity (Scheme 33).
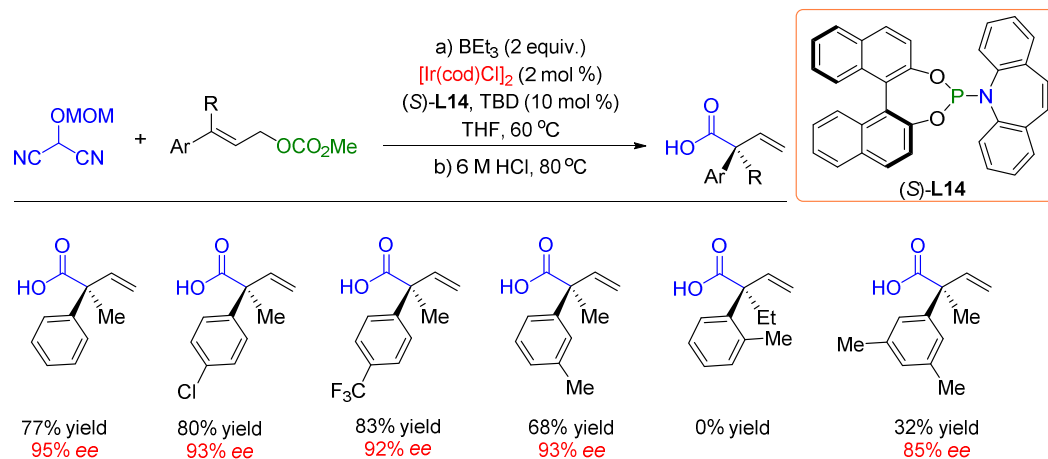
Scheme 33. Branched selective Ir-catalyzed allylic substitution of trisubstituted electrophiles by an acyl anion based nucleophile.

Exploiting the stereospecificity of the Rh-catalyzed allylic alkylation, the Evans group was able to alkylate enantiopure tertiary allylic carbonates with high regio- and stereospecificity.[40] They found that an electron-deficient phosphite ligand was able to

(39) S. E. Shockley, J. C. Hethcox, B. M. Stoltz, *Angew. Chem. Int. Ed.* **2017**, *56*, 11545.
(40) P. A. Evans, S. Oliver, J. Chae, *J. Am. Chem. Soc.* **2012**, *134*, 19314.

provide the desired product with the highest enantioselectivity compared to more electron-neutral phosphite congeners.[41] All ligands that were screened showed complete regio-specificity in this AA reaction. It was reasoned that the electron-deficient phosphite ligand facilitated a more rapid intermolecular alkylation event compared to π-σ-π equilibration.
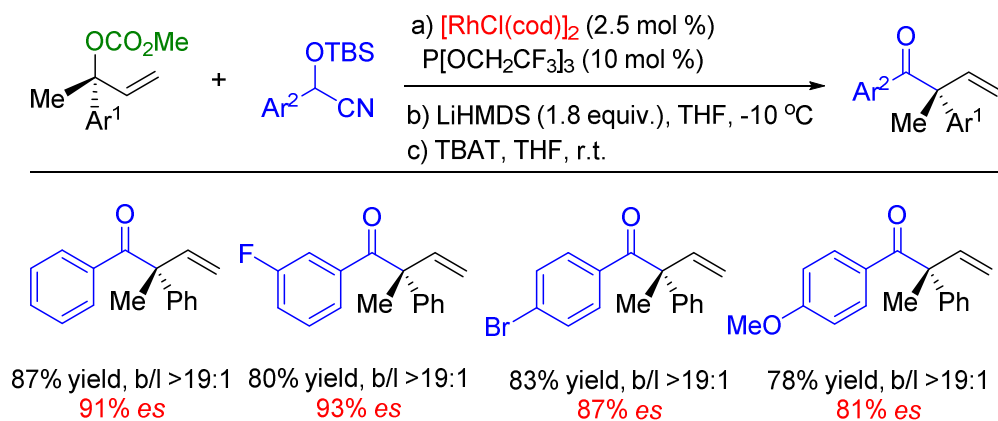
Scheme 34. Stereospecific AA reactions under Rh-catalysis.

The Evans group reported the first direct and highly enantioselective Rh-catalyzed allylic alkylation of allyl benzoate with α-substituted benzyl nitrile pro-nucleophiles. This simple and efficient protocol provided a new approach towards the synthesis of acyclic quaternary carbon stereogenic centers, and illustrates the first example of the direct asymmetric alkylation of a nitrile anion. The reaction was shown to proceed smoothly in
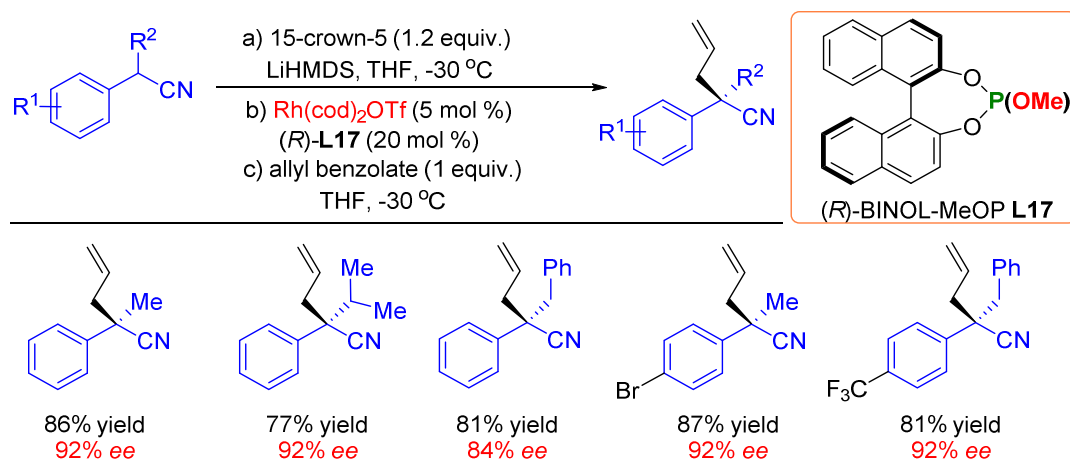
Scheme 35. Rh-catalyzed asymmetric allylic substitution of secondary benzylic nitriles.

---

(41) P. A. Evans, S. Oliver, *Org. Lett.* **2013**, *15*, 5626.

the absence of additives, however, it required the addition of a crown ether to improve the enantioselectivity. High enantio-control was demonstrated for substrates bearing methyl, isopropyl, and benzyl substituents.

The ability to selectively access branched allylic alkylation products is an attractive feature for creating stereochemistry with electrophilic partners. Among metals that typically selectively afford branched products (Mo and Ir), selectivity in the presence of nucleophilic partners was first achieved in Mo-catalyzed asymmetric allylic substitution reactions that involved azlactones[42] and oxindoles.[43] In the case of branched-selective azlactone substitutions, these transformations furnished the branched product with excellent yields as well as high diastereo- and enantioselectivity (Scheme 36). Similar levels of yield and selectivities were observed when using a carbonate or phosphate as leaving group. It is important to note that linear achiral electrophiles performed better than branched racemic allylic carbonates, presumably due to a slow π-σ-π interconversion relative to nucleophilic attack. The mode of asymmetric induction in the presence of the electrophile therefore likely results from differentiation in the enantiotopic faces of the electrophile at the stage of olefin coordination/or ionization.
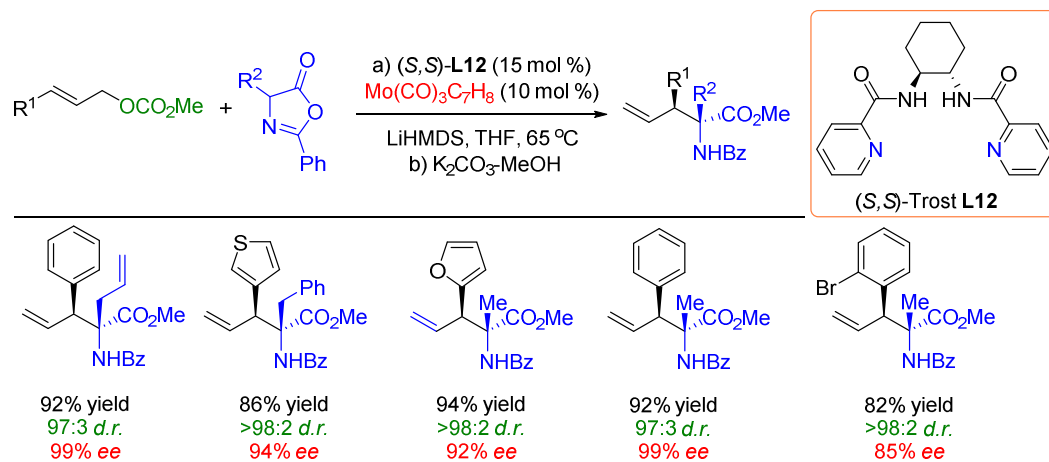
Scheme 36. Mo-catalyzed asymmetric allylic substitution of azlactones.

1.3 Summary

This chapter describes the development of Pd-catalyzed allylic substitution reactions from its inception with a partial focus on the mechanistic aspects, and the various transition-metal-catalyzed asymmetric allylic substitution strategies that have been developed for

(42) B. M. Trost, K. Dogra, *J. Am. Chem. Soc.* **2002**, *124*, 7256.
(43) a) B. M. Trost, Y. Zhang, *J. Am. Chem. Soc.* **2006**, *128*, 4590; b) B. M. Trost, Y. Zhang, *J. Am. Chem. Soc.* **2007**, *129*, 14548.

the construction of tetrasubstituted stereogenic centers. The prospective potential of these technologies uncovered during the past few decades have shown the ability to offer conceptually new manifolds to build up molecular complexity. This continues to hold promise to revolutionize approaches in synthetic chemistry. While this area has gained considerable momentum, several largely unsolved problems still need to be taken into consideration: (1) Developing reactions with other allylic precursors and nucleophiles to synthesize tetrasubstituted stereocenters which is still underdeveloped in the area of asymmetric allylic substitutions; (2) The importance to develop of robust and efficient strategies for the synthesis of more sterically encumbered stereocenters using simple, modular and readily available starting materials; (3) The Pd-catalyzed regio- and enantioselective α,α-disubstituted allylic scaffolds (up to the moment of developing this thesis work) remained rather rare and constituted a largely unexplored landscape in organic synthesis.

1.4   General Objectives of this Doctoral Thesis

Since the early seminal work by Tsuji and Trost, there has been rapid progress over the past few decades in the development of chiral ligands and reaction scope of applicable electrophiles and nucleophiles in Pd-catalyzed allylic substitution reactions. In addition, Pd-catalyzed asymmetric allylic substitution reactions have been utilized in total synthesis of a variety of complex chiral molecules,[1c] providing solid evidence of the usefulness of AAA methodology in controlling both regio- and enantio-selectivities. Despite the numerous advances already realized, forging chiral branched allylic derivatives from simple and readily available starting materials continues to be an important task in synthetic chemistry, due to the potential of these chiral allylic compounds in post-synthetic campaigns. Allylic scaffolds bearing quaternary stereocenters based on Pd-catalyzed allylic substitution reactions still remain rather underexplored. Prompted by the inherent interest of the Prof. Arjan W. Kleij group at ICIQ to design novel and concise catalytic systems for achieving valuable small molecule intermediates, this thesis is aimed at designing novel chiral ligands and their use in Pd-catalyzed regio- and enantioselective synthesis of branched allylic compounds. Furthermore, gaining insight into the details of the reaction mechanism to reveal the origin of the regio- and enantioselectivity would be much desired. In this context, the following objectives are pertinent to the content of this thesis:

- Developing a concise, efficient, regio- and enantioselective synthesis of various enantioenriched α,α-disubstituted allylic amines, including both aryl- and alkyl-substituted derivatives.

- To unlock the origin of the regio- and enantioselectivity in the asymmetric allylic alkylation by density functional theory (DFT) calculations in combination with mechanistic control experiments.

- Design new methodology that enables the regio- and enantioselective synthesis of chiral allylic sulfones featuring quaternary stereocenters, and the utilization of such methodology in the synthesis of natural compounds.

Chapter 2.

Palladium-Catalyzed Regio- and Enantioselective Synthesis of Allylic Amines Featuring Tetrasubstituted Tertiary Carbons

This chapter has been published in:

A. Cai, W. Guo, L. Martínez-Rodríguez, A. W. Kleij, *J. Am. Chem. Soc.* **2016**, *138*, 14194−14197.

2.1 Introduction

2.1.1 Allylic Amines

Nitrogen-containing compounds such as amines, enamines, and imines are valuable and commercially important as bulk chemicals, specialty chemicals, natural products, and pharmaceuticals.[1] Importantly, allylic amines are fundamental building blocks in organic chemistry, and their preparation is of high synthetic and industrial interest.[2] The versatility of allylic amines can be ascribed to the presence of two functional groups, namely the olefin and amine moieties which can be independently addressed and converted into a variety of other groups allowing to access a wide range of targets such as α-and β-amino acids, β-and γ-amino alcohols[3] alkaloid derivatives[4] and bioactive agents (Scheme 2.1).
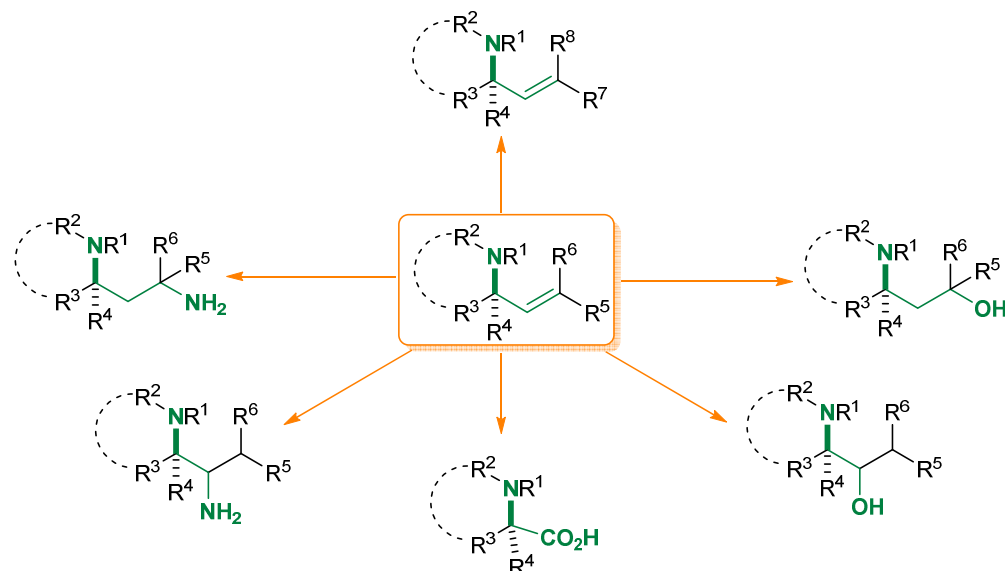
Scheme 2.1. Some representative synthetic transformations of allylic amines.

In the context of allylic amine synthesis, in 1937 the first asymmetric allylic amination reaction was reported by Levene *et al.* through the treatment of (*S*)-3-chlorohept-1-ene

(1) J. J. Brunet, D. Neibecker, *In Catalytic Heterofunctionalization from Hydroamination to Hydrozirconation*; A. Togni, H. Grützmacher, Eds. VCH, Weinheim, Germany, **2001**, pp 91-141.
(2) a) B. M. Trost, M. L. Crawley, *Chem. Rev.* **2003**, *103*, 2921; b) L. Huang, M. Arndt, K. Gooßen, H. Heydt, L. J. Gooßen, *Chem. Rev.* **2015**, *115*, 2596; c) B. M. Trost, D. L. Van Vranken, *Chem. Rev.* 1996, 96, 395; d) M. Johannsen, K. A. Jørgensen, *Chem. Rev.* **1998**, *98*, 1689.
(3) a) T. Hayashi, A. Yamamoto, Y. Ito, E. Nishioka, H. Miura, K. Yanagi, *J. Am. Chem. Soc.* **1989**, *111*, 6301; b) R. Jumnah, J. M. J. Williams, A. C. Williams, *Tetrahedron Lett.* **1993**, *34*, 6619.
(4) a) P. Magnus, J. Lacour, I. Coldham, B. Mugrage, W. B. Bauta, *Tetrahedron* **1995**, *51*, 11087; b) B. M. Trost, *Angew. Chem.* **1989**, *101*, 1199.

with ammonia to provide (*R*)-3-aminohept-1-ene in a highly enantiospecific manner (Scheme 2.2).[5] Interestingly, the term 'allylic amination' was used first by Sharpless in 1976[6] and later on the area was reviewed in detail in 1983 and 1998.[7] Since then, the focus on more sophisticated allylic aminations has increased significantly.
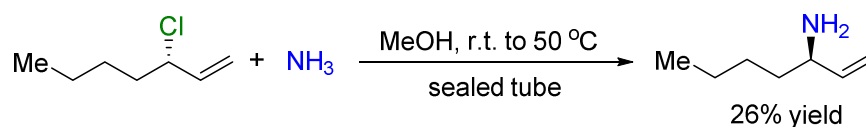
Scheme 2.2. The first asymmetric synthesis of chiral allylic amines.

2.1.2 Pd-catalyzed Asymmetric Synthesis of α-Monosubstituted Allylic Amines

The asymmetric construction of chiral allylic amines is an attractive research goal in modern synthetic chemistry, primarily due to the potential of allylic amines to act as synthetic and intermediates for bioactive agents. Transition-metal-catalyzed allylic amination up to now has been used as the most powerful and convenient method for the preparation of less sterically hindered α-monofunctionalized chiral allylic amines, a topic that is further introduced in this chapter.
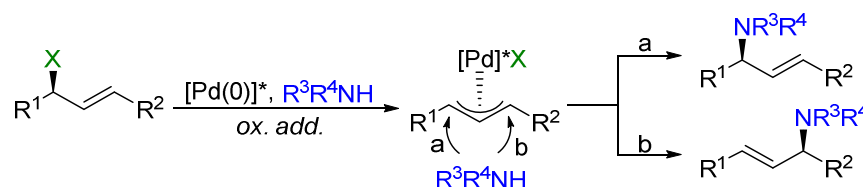
Scheme 2.3. General mechanism of the Pd-catalyzed allylic amination reaction.

Asymmetric transition-metal-catalyzed allylic substitution reactions with nitrogen-based pro-nucleophiles has evolved slowly compared to analogous processes using stabilized carbon nucleophiles.[8] A major obstacle with nitrogen-based nucleophiles is the propensity to form catalytically inactive complexes with transition metals, thereby reducing the reactivity of nucleophiles. The mechanism for the Pd-catalyzed allylic

(5) P. A. Levene, A. Rothen, M. Kuna, *J. Biol. Chem.* **1937**, *120*, 777.
(6) K. B. Sharpless, T. Hori, L. K. Truesdale, C. O. Dietrich, *J. Am. Chem. Soc.* **1976**, *98*, 269.
(7) R. B. Cheikh, R. Chaabouni, A. Laurent, P. Mison, A. Nafti, *Synthesis* **1983**, 685; b) M. Johannsen, K. A. Jørgensen, *Chem. Rev.* **1998**, *98*, 1689.
(8) a) M. Breugst, T. Tokuyasu, H. Mayr, *J. Org. Chem.* **2010**, *75*, 5250; b) T. B. Phan, C. Nolte, S. Kobayashi, A. R. Ofial, H. Mayr, *J. Am. Chem. Soc.* **2009**, *131*, 11392.

amination is generally accepted to occur via a neutral or cationic π-allyl-Pd intermediate (Scheme 2.3), which is generated by oxidation addition of the allylic precursor to the Pd(0) precursor. In the second step, the amine reagent attacks directly on the backside of the π-allyl-Pd complex finally providing the desired product with retention of configuration.

The asymmetric allylic amination of 1,3-diphenylprop-2-enol derivatives with various nitrogen pro-nucleophiles has been studied extensively ever since it was first presented by Hayashi and Ito in 1989.[9] Despite significant progress in this area, the utilization of alkyl-substituted allylic precursors in the enantio-convergent allylic amination remains extremely challenging, due to low reactivity and selectivity.[10] Nevertheless, the phosphine sulfide (*S*)-BINAP(S) **L18** and the Trost ligand (*R*, *R*)-**L1** generate high yields and enantioselectivities for the amination of allylic carbonates (Scheme 2.4).
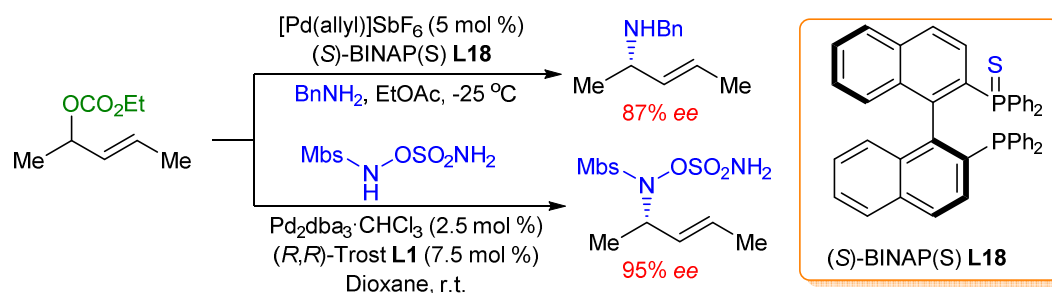
Scheme 2.4. Allylic amination of alkyl-substituted allylic carbonates.

The development of enantio-convergent allylic amination processes involving unsymmetrical π-allyl complexes is of high interest though challenging from a practical consideration. The use of unsymmetrical intermediates is considerably more challenging than symmetrical counterparts, because both regio- and enantioselectivity must be controlled simultaneously. Furthermore, isomerization of unsymmetrical intermediates through π-σ-π interconversion may occur. If this interconversion is faster than the rate of nucleophilic attack, in the presence of a suitable and efficient chiral ligand the pathways that involve the two diastereomeric complexes are kinetically sufficiently separated (Scheme 2.5). In such an event, the nucleophilic addition step determines the asymmetric induction, in which one product enantiomer is formed preferentially through a Curtin-Hammett scenario.

(9) T. Hayashi, A. Yamamoto, Y. Ito, E. Nishioka, H. Miura, K. Yanagi, *J. Am. Chem. Soc.* **1989**, *111*, 6301.

(10) H. Kodama, T. Taiji, T. Ohta, I. Furukawa, *Synlett* **2001**, 385.
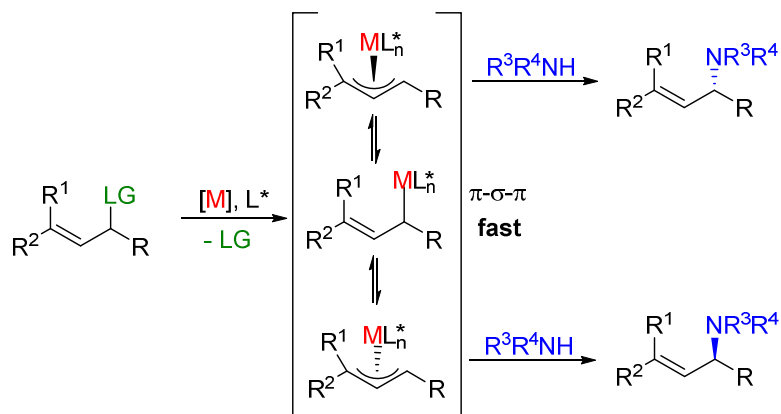
Scheme 2.5. Mechanism of allylic amination involving unsymmetrical π-allyl complexes.

In general, the nucleophilic addition of amines occurs at the least substituted carbon atom of the allyl group. The problem associated with regio- and enantioselective amination of unsymmetrically π-allyl species in the presence of a chiral Pd complex has inspired a breath of synthetic approaches. One method provides regiocontrol through steric and/or electronic differences between the terminal groups of the allylic substrate. For example, a Pd catalyst that comprises the chiral PHOX **L19** mediates the coupling of the sterically and electronically biased diphenyl-substituted allylic acetate and the allylic amine reagent in 99% yield and with 89% enantiomeric excess (Scheme 2.6).[11]
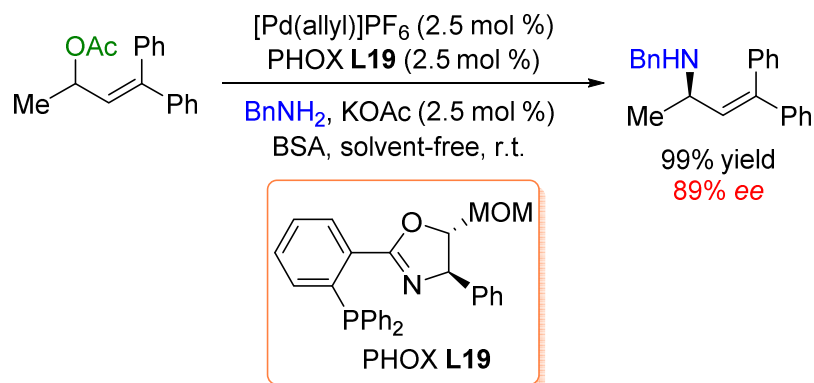
Scheme 2.6. Pd-catalyzed regio- and enantioselective synthesis of allylic amines controlled by differences in sterics/electronics between the allyl terminal groups.

Alternatively, Itoh and co-workers reported a Pd-catalyzed regio- and enantioselective allylic amination of trifluoromethyl (CF_3) substituted racemic and unsymmetrical 1,3-

---

(11) D. Popa, R. Marcos, S. Sayalero, A. Vidal-Ferran, M. A. Pericàs, *Adv. Synth. Catal.* **2009**, *351*, 1539.

disubstituted allylic esters.[12] Using Pd/(S)-BINAP/AgPF$_6$ based catalysts, the reaction proceeds through a DYKAT (dynamic kinetic asymmetric transformation) and provides a series of α-substituted allylic amines in a high yields and with a high enantioselectivity (Scheme 2.7).
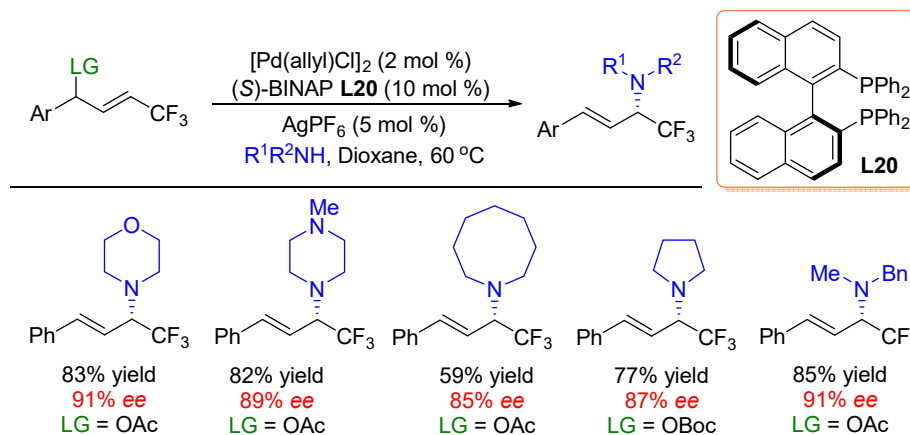
Scheme 2.7. Enantioselective allylic amination of CF$_3$-substituted allylic esters.

In asymmetric Pd-catalyzed allylic amination reactions there is a great difference in reactivity between cyclic and acyclic substrates. Usually many of the ligands developed for acyclic substrates are largely inefficient for cyclic substrates. In order to solve this problem, Trost *et al*. developed a ligand type which is very efficient for both types of substrates.[13] The ligand (known as the "Trost" ligand) is prepared from 2-(diphenylphosphino)benzoic acid (DPPBA) and a chiral C_2-synthetic diamine or diol. In 1994, the Trost group presented a Pd-catalyzed allylic substitution reaction of racemic five- to seven-membered rings with phthalimide being the nucleophile.[13] In the presence of the Trost ligand (*S,S*)-**L1** (see Chapter 1), this process resulted in the formation of allylic amines in good yield and high enantiocontrol (Scheme 2.8).
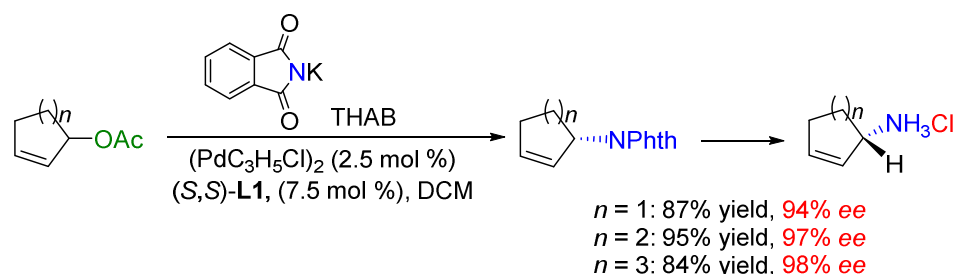
Scheme 2.8. Pd-catalyzed allylic amination of cyclic substrates.

(12) M. Kawatsura, S. Terasaki, M. Minakawa, T. Hirakawa, K. Ikeda, T. Itoh, *Org. Lett*. **2014**, *16*, 2442.
(13) B. M. Trost, R. C. Bunt, *J. Am. Chem. Soc*. **1994**, *116*, 4089.

2.1.3 Ir-catalyzed Asymmetric Synthesis of α-Monosubstituted Allylic Amines

In order to further extending allylic amination chemistry, the others transition metals have been used as powerful tool for the asymmetric construction of allylic amines, with Ir-based catalysts representing privileged systems in this domain. The first Ir-catalyzed enantioselective allylic amination was reported by the Hartwig group in 2002.[14] They developed a new catalytic process to produce branched aromatic or aliphatic secondary or tertiary allylic amines in high yield with excellent regio- and enantioselectivity from achiral allylic precursors (Scheme 2.9); the Feringa ligand **L21** proved to be particularly efficient in this reaction manifold. It was found that the solvent had an important influence on the selectivity of the reaction. THF was found to be optimal in terms of balancing both enantiocontrol and the rate of the reaction. Notably, the branched allylic amines isomerized to the thermodynamically more stable linear isomers when the reactions were allowed to proceed for a prolonged period of time. Furthermore, the terminal olefin in the branched product could be transferred to 1,3-diamines, 1,3-amino alcohols and various types of amino acids.
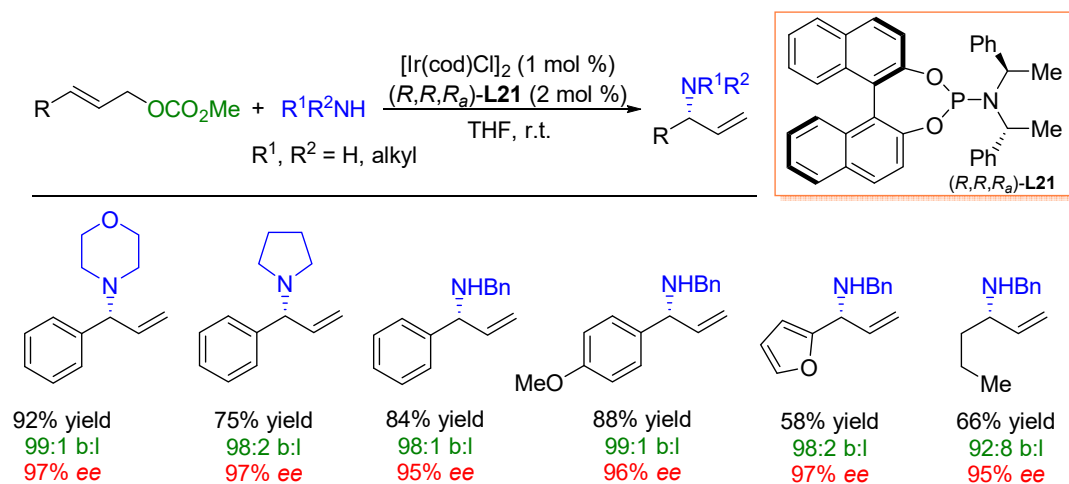
Scheme 2.9. Ir-catalyzed asymmetric allylic amination of alkyl amines.

In 2004, Helmchen and co-worker reported the highly enantioselective Ir-catalyzed allylic amination of dienyl carbonates using Feringa ligand (S,S,S_a)- **L21**.[15] For both aryl- and alkyl-substituted amine substrates very high regio-selectivities towards the desired internal substitution products were achieved (Scheme 2.10).

---

(14) T. Ohmura, J. F. Hartwig, *J. Am. Chem. Soc*. **2002**, *124*, 15164.
(15) G. Lipowsky, G. Helmchen, *Chem. Commun*. **2004**, 116.
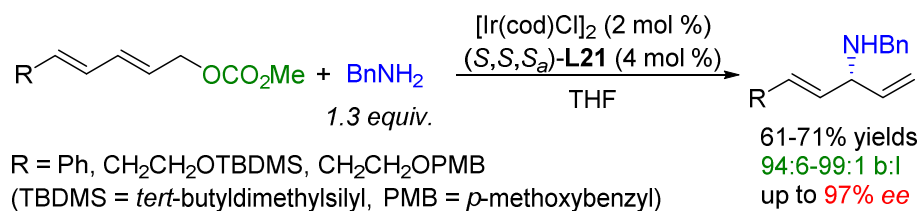
Scheme 2.10. Ir-catalyzed asymmetric amination reaction of dienyl carbonates.

Ir-catalyzed asymmetric allylic substitution reactions generally provide branched products with high enantioselectivity, in particular with a base-activated catalyst generated from [Ir(cod)Cl]$_2$ and Feringa-type ligands. However, this catalytic system is sensitive to oxygen and is also not very stable upon heating. Additionally, regiocontrol with some alkyl-substituted allylic substrates proved to be unsatisfactory. In order to overcome these problems, in 2008, the Helmchen group developed a new series of catalysts produced from [Ir(cod)Cl]$_2$ and phosphoramidite ligands. [16] In allylic substitutions, the new phosphoramidite-ligated Ir catalyst enabled an unprecedented level of regioselectivity and made it possible for the first time to run the reactions in the presence of oxygen (Scheme 2.11).
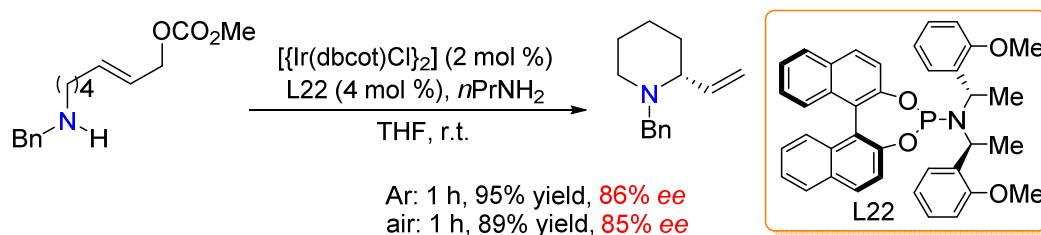
Scheme 2.11. Intramolecular allylic amination mediated by Ir(phosphoramidite) catalysts.

In 2016, You and co-workers applied the diPh-THQphos ligand (**L23**) in the Ir-catalyzed enantioselective amination of *ortho*-substituted cinnamyl carbonates.[17] Good to excellent yields and high enantioselectivity were obtained, whereas poor to moderate yields and enantioselectivity were found when the Feringa ligand **L1** was used (Scheme 2.12).

(16) S. Spiess, C. Welter, G. Franck, J.-P. Taquet, G. Helmchen, *Angew. Chem. Int. Ed*. **2008**, *47*, 7652.
(17) X. Zhang, W.-B. Liu, Q. Cheng, S.-L. You, *Organometallics* **2016**, *35*, 2467.
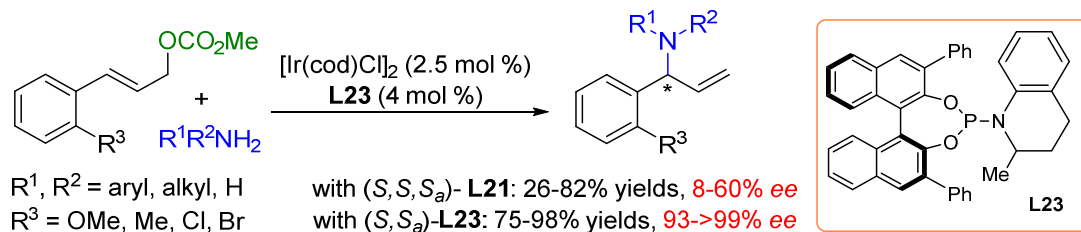
Scheme 2.12. Ir-catalyzed asymmetric amination of *ortho*-substituted cinnamyl carbonates.

Recently, Krische and co-workers developed a new catalytic system for Ir-catalyzed allylic amination reactions.[18] Highly amenable and commercially available π-allyl-Ir *C,O*-benzoate ligated complexes (stable to air, water and chromatographic purification conditions) and well-known to catalyze nucleophilic carbonyl allylation,[19] proved to be also excellent catalysts for the chemo-, regio- and enantioselective electrophilic amination of branched allylic acetates bearing linear alkyl groups. This latter example of an AAA methodology broadened the access to chiral N-containing building blocks and established unique amphiphilic properties of the π-allyl-Ir(benzoate) complex. A series of branched alkyl allyl amines was obtained in good to excellent yield and regio- and enantioselectivities, complementing the allylic amination scope of previously reported alkyl allylic substrates (Scheme 2.13).
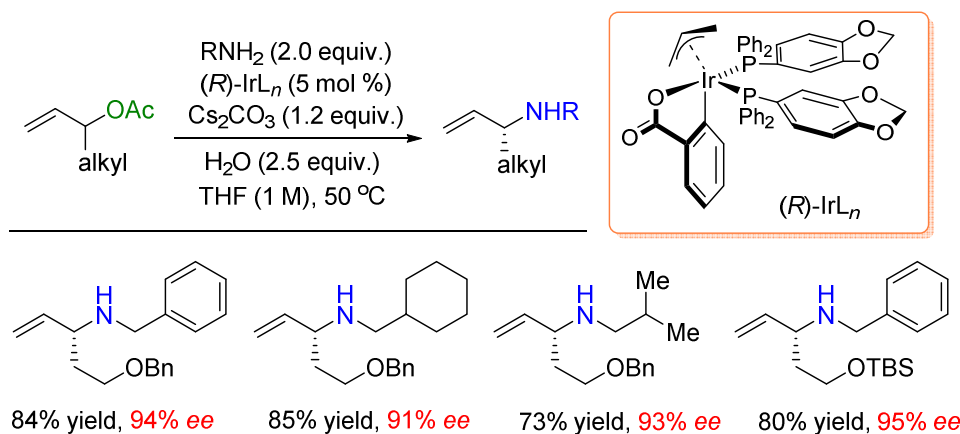
Scheme 2.13. Asymmetric allylic amination reactions catalyzed by a π-ally-Ir *C,O*-benzoate ligated complex.

(18) A. T. Meza, T. Wurm, L. Smith, S. W. Kim, J. R. Zbieg, C. E. Stivala, M. J. Krische, *J. Am. Chem. Soc.* **2018**, *140*, 1275.
(19) S. W. Kim, W. Zhang, M. J. Krische, *Acc. Chem. Res.* **2017**, *50*, 2371.

Ir-catalyzed enantioselective allylic substitution of linear allylic electrophiles has become a powerful tool to prepare optically active allylic amines and ethers. However, Ir-catalyzed reactions of branched allylic electrophiles occur with low enantioselectivities.[20] In 2006, an alternative approach was reported by Hartwig and co-workers, using a Pd-catalyzed isomerization to first transform the racemic branched allylic substrates into their linear isomers, and then subject these to Ir-catalyzed asymmetric allylic substitution reactions (Scheme 2.14). Anilines, alkyl amines, lithium phenoxide, and sodium malonate were used as nucleophiles under these conditions providing the branched products in good yield and with excellent selectivities.
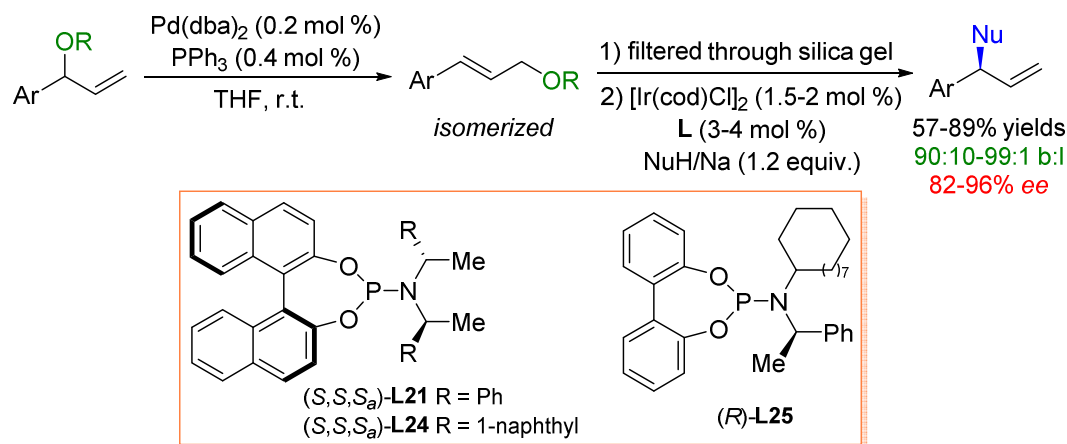
Scheme 2.14. Sequential Pd-catalyzed allylic isomerization of branched allylic substrates, and Ir-catalyzed asymmetric allylic substitution reactions.

Enantioselective substitution of allylic esters by carbon- and heteroatom based nucleophiles has become a classical catalytic asymmetric transformation,[2c,21] However, enantioselective substitution of allylic alcohols is more challenging. Since allylic esters are typically prepared from allylic alcohols, the use of allylic alcohols in asymmetric allylic substitution would streamline synthetic sequences and would provide more atom-economical procedures. The poor leaving group ability of an OH group requires that these conversions are carried out at high temperatures, neat conditions,[22] and/or in the presence

(20) a) B. Bartels, C. Garcia-Yebra, F. Rominger, G. Helmchen, *Eur. J. Inorg. Chem.* **2002**, 2569; b) D. Polet, A. Alexakis, K. Tissot-Croset, C. Corminboeuf, K. Ditrich, *Chem. Eur. J.* **2006**, *12*, 3596.

(21) a) B. M. Trost, M. L. Crawley, *Chem. Rev.* **2003**, *103*, 2921; b) E.-I. Negishi, *Handbook of Organopalladium Chemistry for Organic Synthesis*; WileyInterscience: New York, **2002**.

(22) a) D. E. Bergbreiter, D. A. Weatherford, *J. Chem. Soc., Chem. Commun.* **1989**, 883; b) H. Saburi, S. Tanaka, M. Kitamura, *Angew. Chem. Int. Ed.* **2005**, *44*, 1730; c) G. Onodera, H. Imajima, M. Yamanashi, Y. Nishibayashi, M. Hidai, S. Uemura, *Organometallics* **2004**, *23*, 5841; d) Y. Kayaki, T. Koda, T. Ikariya, *J. Org. Chem.* **2004**, *69*, 2595.

of an activator.[23] Thus far, direct asymmetric substitutions of allylic alcohols is rather rare and embodies a largely unexplored landscape in allylic chemistry. In 2007, Hartwig and co-workers accomplished an Ir-catalyzed enantioselective allylic amination reaction in the presence of ligand (R)-**L25** and using allylic alcohols as substrates.[24] Two procedures have been developed for Ir-catalyzed allylic amination of allylic alcohols to form branched allylic amine products with high levels of regio- and enantioselectivity. Nb-$(OEt)_5$ was found to serve as an *in situ* activator of the allylic alcohol, and catalytic amounts of BPh_3 were also found to serve as activating agent (Scheme 2.15).
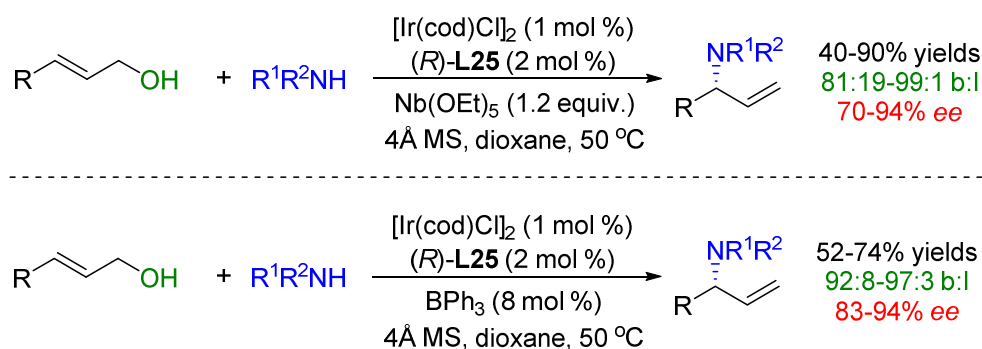
Scheme 2.15. Ir-catalyzed asymmetric allylic amination of linear allylic alcohols.

2.1.4 TM-catalyzed Synthesis of α,α-Disubstituted Allylic Amines

Despite significant progress in this area, the catalytic formation of chiral **di**substituted allylic amines incorporating tetrasubstituted tertiary carbons through allylic amination processes has proven to be very challenging and remains a largely unexplored field of science. In this respect, in 2007, Yudin and co-workers reported that Pd-catalyzed regioselective synthesis of racemic branched α,α-disubstituted allylic amines,[25] and they showed that the presence of DBU was essential for branched allylic amine formation. Various examples of such allylic amines were reported with excellent yields and high b/l ratios using inexpensive ligands (Scheme 2.16).

(23) a) C. Chuit, H. Felkin, C; Frajerma, G. Roussi, G. Swiercze, *Chem. Commun.* **1968**, 1604; b) I. Stary, I. G. Stara, P. Kocovsky, *Tetrahedron Lett.* **1993**, *34*, 179; c) Y. Tamaru, *Eur. J. Org. Chem.* **2005**, 2647; d) S. C. Yang, C. W. Hung, *J. Org. Chem.* **1999**, *64*, 5000; e) N. T. Patil, Y. Yamamoto, *Tetrahedron Lett.* **2004**, *45*, 3101.
(24) Y. Yamashita, A. Gopalarathnam, J. F. Hartwig, *J. Am. Chem. Soc.* **2007**, *129*, 7508.
(25) I. Dubovyk, I. D. G. Watson, A. K. Yudin, *J. Am. Chem. Soc.* **2007**, *129*, 14172.
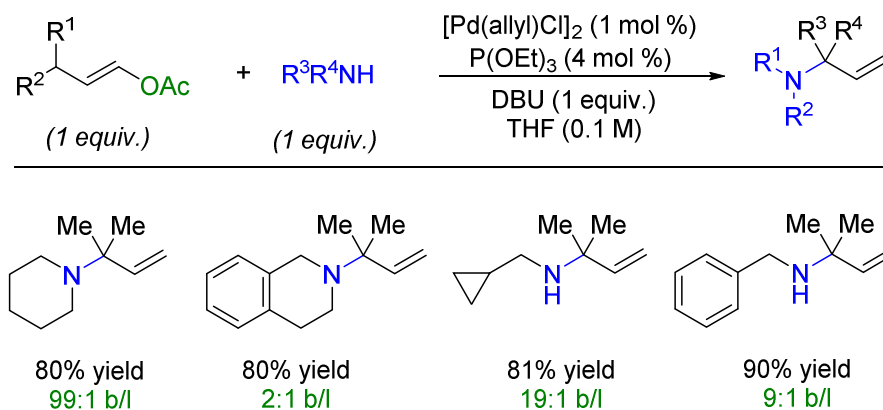
Scheme 2.16. Pd-catalyzed synthesis of α,α-disubstituted allylic amines.

In 2008, Widenhoefer and co-workers described a gold(I)-catalyzed protocol for the intermolecular hydroamination of allenes.[26] The method was efficient for a number of *N*-unsubstituted carbamates and was effective for monosubstituted, 1,1- and 1,3-disubstituted, trisubstituted, and tetrasubstituted allenes. Furthermore, a series of α,α-disubstituted allylic amine could be obtained in moderate to good yields (Scheme 2.17).
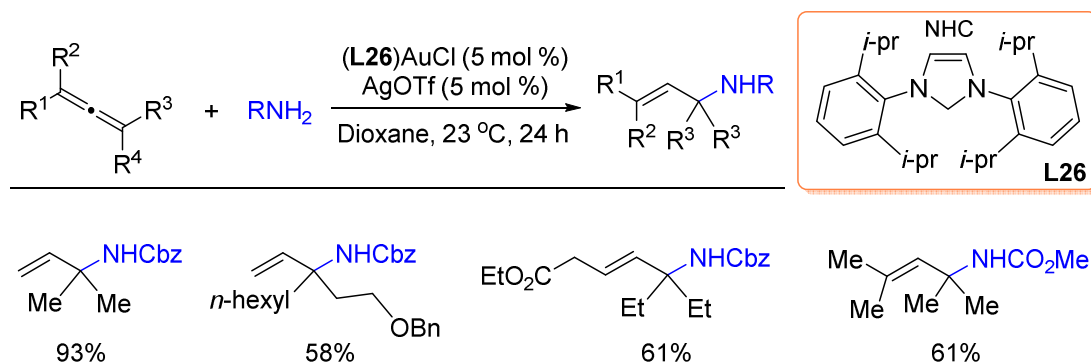
Scheme 2.17. Hydroamination of allenes catalyzed by a Au(I) N-heterocyclic carbene complex.

Recently, an iron-catalyzed allylic amination reaction of 1,1-dimethyl-2-propenyl carbonate was reported to work with *para*- and *meta*-substituted anilines, providing the α,α-disubstituted allylic aryl amines in good yield and with excellent levels of regioselectivity.[27] Substituents at the *ortho* position of the aniline reagent, however, did not result in desired allylic amine products. As a complementary strategy, in 2011 Nguyen and co-workers presented a Rh-catalyzed regioselective allylic amination of tertiary

---

(26) R. E. Kinder, Z. Zhang, R. A. Widenhoefer, *Org. Lett.* **2008**, *10*, 3157.
(27) B. Plietker, *Angew. Chem. Int. Ed.* **2006**, *45*, 6053.

allylic trichloroacetimidates with aromatic amines providing a rare methodology for the preparation of α,α-disubstituted allylic aryl amines in good yield and with excellent regioselectivity (Scheme 2.18).[28]
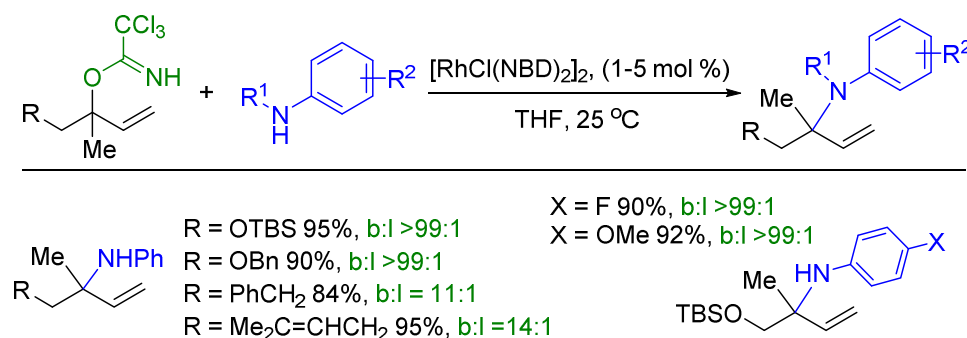
Scheme 2.18. Synthesis of α,α-disubstituted aryl amines by Rh-catalyzed amination of tertiary allylic trichloroacetimidates.

In 2013, the Stanley group developed three strategies based on Pd-catalyzed allylic alkylation reactions to generate *N-tert*-prenylindoles. In the presence of a suitable Pd precursor, good yields and high regioselectivity were observed for α,α-disubstituted amine derivatives.[29] Later on, Kawatsura and co-workers examined the ruthenium-catalyzed regioselective allylic amination of tertiary allylic acetates with several types of amines.[30] The Ru catalyst effectively catalyzed the formation of branched allylic amines while using several types of aliphatic amines and primary aromatic amines, and the desired α,α-disubstituted allylic amines were attained in moderate to good yields (Scheme 2.19).
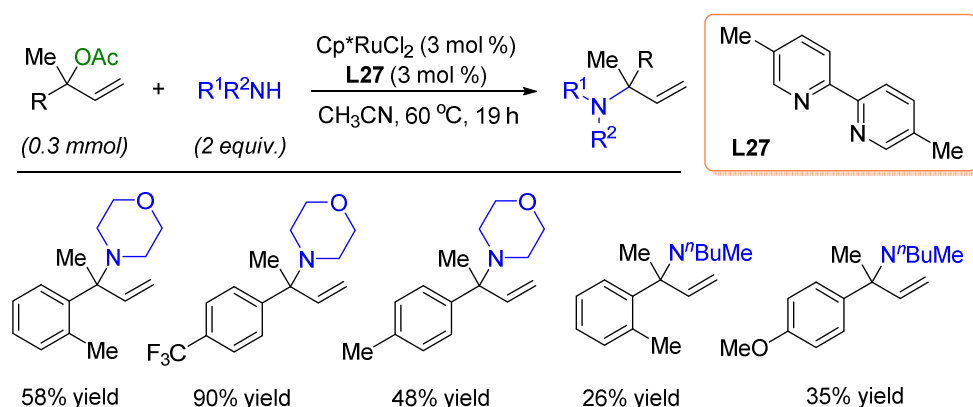
Scheme 2.19. Ru-catalyzed construction of α,α-disubstituted allylic amines.

(28) J. S. Arnold, G. T. Cizio, H. M. Nguyen, *Org. Lett.* **2011**, *13*, 5576.
(29) K. F. Johnson, R.V. Zeeland, L. M. Stanley, *Org. Lett.* **2013**, *15*, 11.
(30) S. Mizuno, S. Terasaki, T. Shinozawa, M. Kawatsura, *Org. Lett.* **2017**, *19*, 504.

In this context, there is only one example known for the regio- and *enantioselective* synthesis of chiral α,α-disubstituted allylic amines based on Pd-catalyzed allylic substitution reactions. In 2000, Trost and co-workers utilized dynamic kinetic asymmetric transformation (DYKAT) in the Pd-catalyzed asymmetric allylic alkylation (AAA) based on butadiene monoepoxides as the allylic precursors. This process required a new ligand design with a higher degree of conformational restrains.[31] The reaction of phthalimide and isoprene monoepoxide demonstrated the remarkable ability of the chiral ligand to control both regio- and enantioselectivity and showed the effectiveness of this protocol in creating a new quaternary stereocenter (Scheme 2.20); albeit, the reported chemistry was limited to only one example.
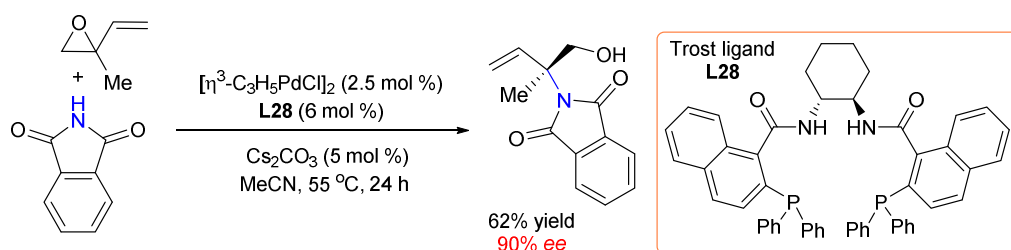
Scheme 2.20. Pd-catalyzed enantioselective synthesis of an α,α-disubstituted allylic amine.

In 2012, Nguyen and co-workers described the first DYKAT of racemic tertiary allylic electrophiles with anilines utilizing a chiral diene-ligated rhodium catalyst. With this catalyst, regio- and enantioselective amination of racemic tertiary allylic trichloroacetimidates was achieved using a variety of aromatic amine nucleophiles and this protocol thus offers a direct and efficient route to chiral α,α-disubstituted allylic *N*-aryl amines. The method allows for the preparation of desired branched products in moderate to good yields with good to excellent levels of regio- and enantioselectivity. However, this chemistry was found to be limited the use of tertiary allylic precursors having an oxygen atom at the β-position, which provides additional chelation control to increase the regio- and enantioselectivity of these reactions. Furthermore, the current method seems to be limited to ethyl- and aryl-substituted imidates (Scheme 2.21). Trichloroacetimidate substrates having a aryl group at the α-position rapidly underwent [3,3]-sigmatropic rearrangement. Allylic imidates bearing an ethyl group at the α-position could not be prepared presumably because the requisite tertiary alcohol precursors were too sterically

---

(31) B. M. Trost, R. C. Bunt, R. C. Lemoine, T. L. Calkins, *J. Am. Chem. Soc.* **2000**, *122*, 5968.

hindered to react with tricloroacetonitrile and thus did not afford the targeted allylic substrates.[32]
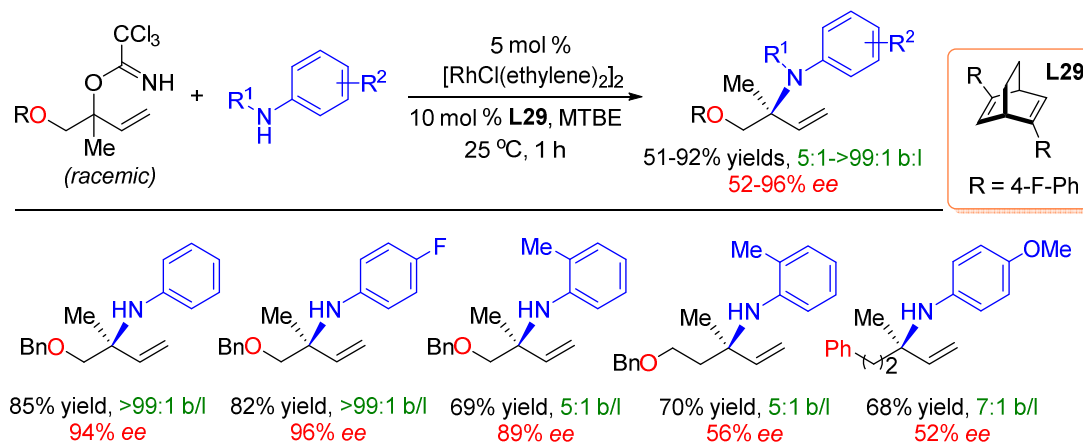
Scheme 2.21. Rh-catalyzed enantioselective synthesis of α,α-disubstituted allylic amines.

2.1.5 Cycloaddition of Vinyl Cyclic Carbonates with Electrophiles

Previous success in Pd-catalyzed transformations of vinyl cyclic carbonates with various electrophiles showed wide potential toward the construction of enantioenriched compounds. A key to this success was the *in situ* formation of a postulated zwitterionic π-allyl-Pd-intermediate that results from a Pd-catalyzed decarboxylation of vinyl cyclic carbonates (Scheme 2.22). In 2014, the Zhang group reported an efficient method for the enantioselective construction of tertiary vinyl glycols and related heterocycles through a Pd-catalyzed asymmetric decarboxylative cycloaddition of vinylethylene carbonates to formaldehyde or Michael acceptors (Schemes 2.22 and 2.23). [33] While using formaldehyde as reaction partner, the reactions proceeded smoothly in the presence of a suitable Pd precursor and the phosphoramidite (S,S,S_a)-**L21** under mild reaction conditions, thus providing the 4,4′-disubstituted 1,3-dioxolanes in high yields (up to 98%) with good to excellent enantioselectivities (82–99% *ee*).

(32) J. S. Arnold, H. M. Nguyen, *J. Am. Chem. Soc*. **2012**, *134*, 8380.
(33) A. Khan, R. Zheng, Y. kan, J. Xiang, Y. J. Zhang, *Angew. Chem. Int. Ed*. **2014**, *53*, 6439.
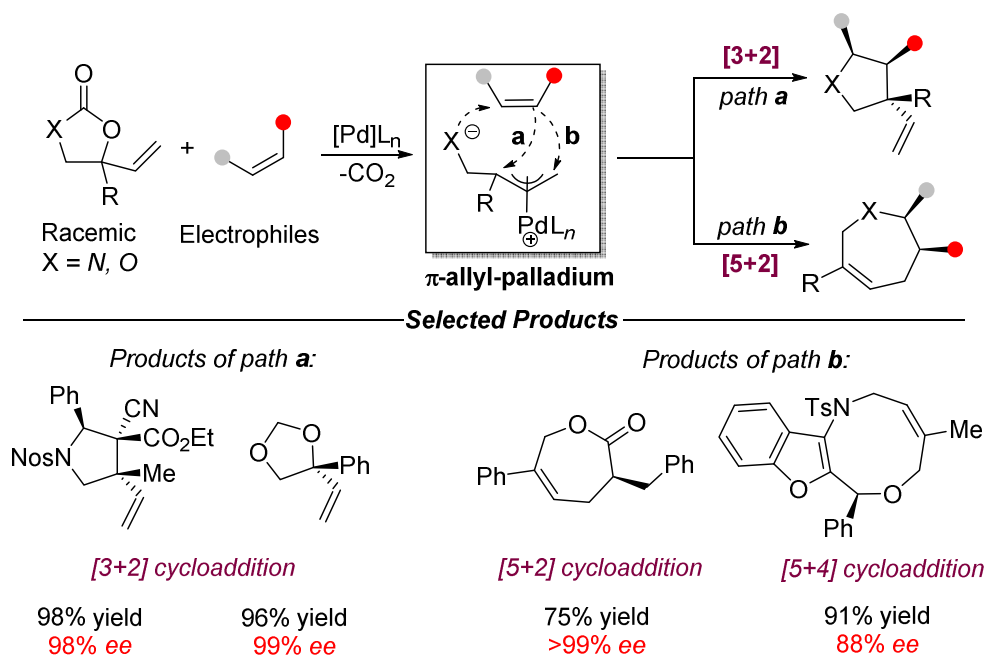
Scheme 2.22. Pd-catalyzed cycloaddition of vinyl cyclic carbonates with electrophiles.
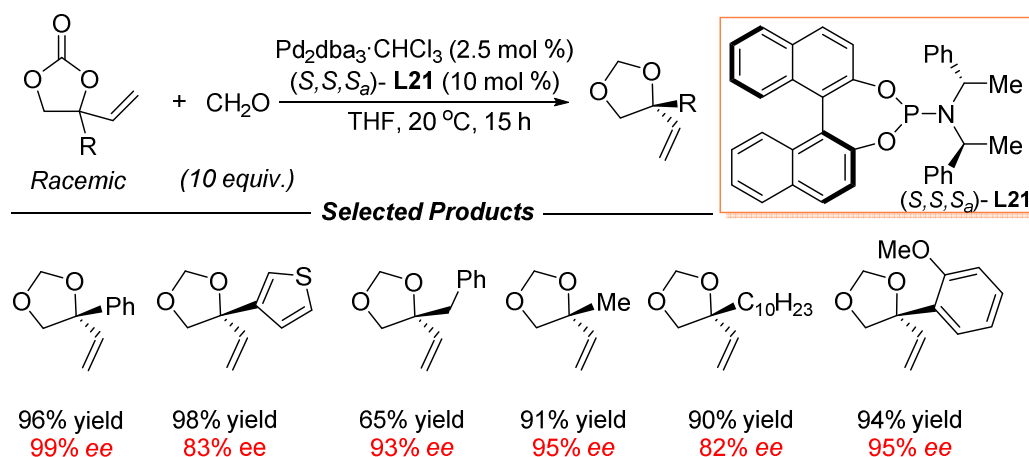
Scheme 2.23. Pd-catalyzed cycloaddition of vinylethylene carbonates for the construction of tertiary vinyl glycols.

In 2017, the first enantioselective formal [5+4] cycloaddition was realized by Zhao and co-workers under Pd catalysis to deliver benzofuran-fused nine-membered ring products in good yields and with excellent enantioselectivity.[34] These medium-sized heterocycles and derivatives undergo unique rearrangements induced by transannular bond formation, resulting in the production of two classes of densely substituted

(34) a) L.-C. Yang, Z.-Q. Rong, Y.-N. Wang, Z. Y. Tan, M. Wang, Y. Zhao, *Angew. Chem. Int. Ed.* **2017**, *56*, 2927; b) Z.-Q. Rong, L.-C. Yang, S. Liu, Z. Yu, Y.-N. Wang, Z. Y. Tan, R.-Z. Huang, Y. Lan, Y. Zhao, *J. Am. Chem. Soc.* **2017**, *139*, 15304.

polycyclic heterocycles with excellent efficiency and high stereoselectivity (Scheme 2.24).
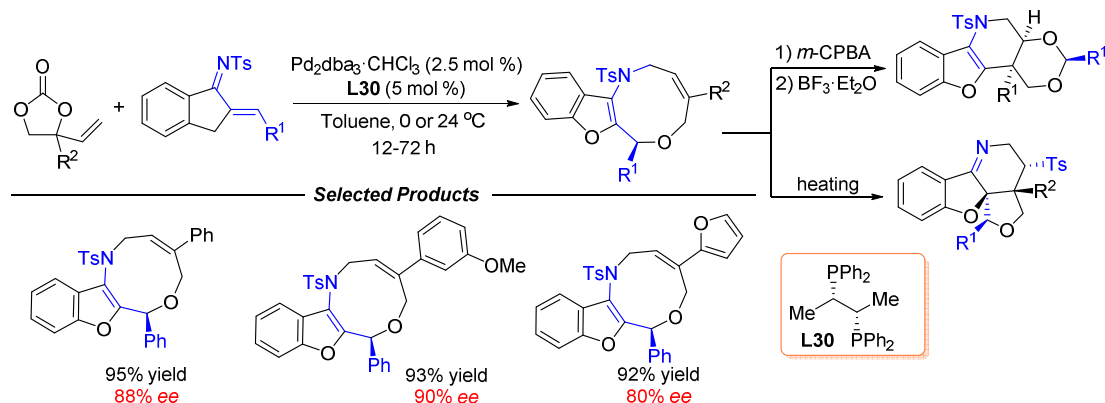
Scheme 2.24. Enantioselective formal [5+4] cycloaddition under Pd catalysis to deliver benzofuran-fused nine-membered rings.

Recently, Glorius *et al.* reported highly enantioselective [5+2] annulation of enals with vinyl cyclic carbonates through a cooperative *N*-heterocyclic carbene/Pd dual catalytic system.[35] Mechanistic studies revealed that the use of a bidentate phosphine ligand was crucial to prevent coordination of the NHC organocatalyst to the active Pd intermediate. The complementary and matched combination of the chiral NHC catalyst and chiral phosphine ligand promotes high levels of reactivity and enantioselectivity (Scheme 2.25).
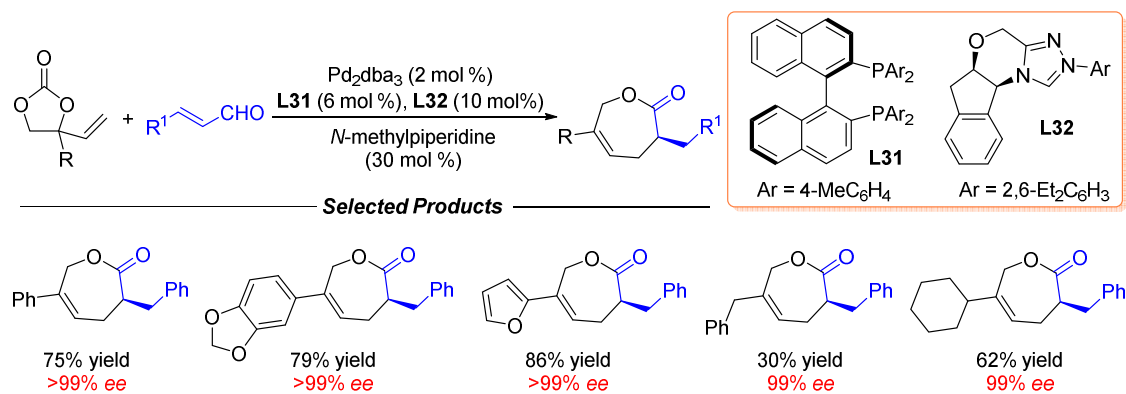
Scheme 2.25. Highly enantioselective [5 + 2] annulations through cooperative *N*-heterocyclic carbene (NHC) organocatalysis and Pd catalysis.

---

(35) S.Singha, T. Patra, C. G. Daniliuc, F. Glorius, *J. Am. Chem. Soc*. **2018**, *140*, 3551.

2.1.6 Aim of the Work presented in this Chapter

Despite the massive attention that has been paid to the synthesis of chiral allylic amines in the past decades, a general Pd-catalyzed asymmetric synthesis of α,α-disubstituted allylic amines featuring a quaternary stereocenter continues to be an unsolved yet inspiring synthetic problem.
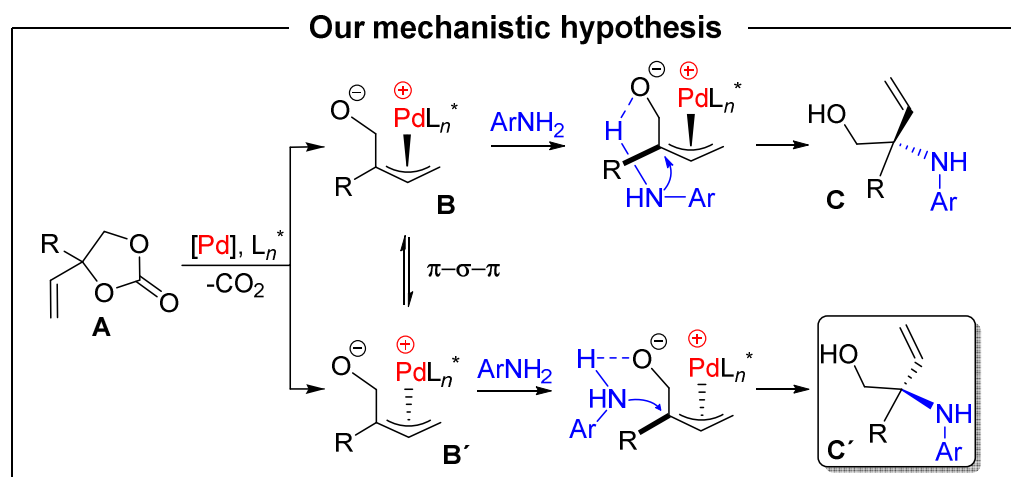
Scheme 2.26. Envisioned approach toward chiral allylic amines from vinyl carbonates and amine nucleophiles under Pd catalysis.

We hypothesized that in the presence of a suitable chiral ligand and amine nucleophile,[36] a dynamic kinetic asymmetric transformation (DYKAT) would be feasible if the isomerization of intermediates **B** and **B′** through $\pi-\sigma-\pi$ interconversion occurs faster than subsequent nucleophilic attack.[37] The asymmetric environment around the Pd center would then kinetically favor the formation of one of the possible allylic amine enantiomers **C** or **C′** upon nucleophilic attack by amines (Scheme 2.26). In this chapter, we disclose the first regio- and enantioselective synthesis of α,α-disubstituted branched allylic aryl amines based on a Pd-catalyzed allylic amination protocol using substituted vinyl cyclic carbonates **A** and unactivated aryl amine nucleophiles as reaction partners.

---

(36) a) T. Hayashi, M. Kawatsura, Y. Uozumi, *Chem. Commun.* **1997**, 561; b) R. J. van Haaren, P. H. Keeven, L. A. van der Veen, K. Goubitz, G. P. F. van Strijdonck, H. Oevering, J. N. H. Reek, P. C. J. Kamer, P. W. N. M. van Leeuwen, *Inorg. Chim. Acta* **2002**, *327*, 108. For a review, see: c) B. M. Trost, M. R. Machacek, A. Aponick, *Acc. Chem. Res.* **2006**, *39*, 747. Hydrogen-bond promoted attack of the amine nucleophilic onto the Pd−allyl species has previously been discussed by Trost and co-workers. We recently reported a related hydrogen-bond mediated formation of linear allylic amines. See: d) W. Guo, L. Martínez-Rodríguez, R. Kuniyil, E. Martin, E. C. Escudero-Adán, F. Maseras, A. W. Kleij, *J. Am. Chem. Soc.* **2016**, *138*, 11970.

(37) B. M. Trost, D. R. Fandrick, *Aldrichimica Acta* **2007**, *40*, 59.

2.2 Results and Discussion

2.2.1 Optimization of the Reaction Conditions

To challenge our mechanistic hypothesis, the reaction of a phenyl-substituted vinyl cyclic carbonate and aniline was selected as a model system (Table 2.1). No reaction was observed in the presence of White catalyst [*i.e*, 1,2-bis(phenylsulfinyl)ethane palladium(II) acetate] and phosphoramidite ligand **L1** (Table 2.1, entries 1-3). To our delight, we could obtain the desired α,α-disubstituted allylic amine product **1** in 19% yield when using $Pd_2(dba)_3 \cdot CHCl_3$ as precursor and **L1** as catalytic system. The use of DCM as solvent increased the yield of the allylic amine product to 67% and with 64% enantiomeric excess (Table 2.1, entry 10). These preliminary investigations suggested that a reaction temperature of 0 ºC and combination of $Pd_2(dba)_3 \cdot CHCl_3$ and **L1** are key to obtain an appreciable yield of branched allylic amine product **1**. Notably, at this temperature the formation of a 1,4-but-2-ene diol byproduct is significantly suppressed.[38] A further decrease in the reaction temperature led to very low conversion. Typically, in the reactions described in Table 2.1, we found a branched-to-linear (b:l) product ratio of up to 80:20.

Product **1** (after isolation) could be analyzed by X-ray crystallography (see the Experimental Section for details), and the configuration of the product was determined to be (*S*).

---

(38) Water can react as a pro-nucleophile with the decarboxylated vinyl cyclic carbonate in the presence of a suitable palladium catalyst to afford a 1,4-but-2-ene diol product. See: W. Guo, L. Martínez-Rodríguez, E. Martin, E. C. Escudero-Adán, A. W. Kleij, *Angew. Chem. Int. Ed*. **2016**, *55*, 11037.

Table 2.1: Preliminary screening of ligands and catalysts towards the branched allylic amine product **1**.[a]
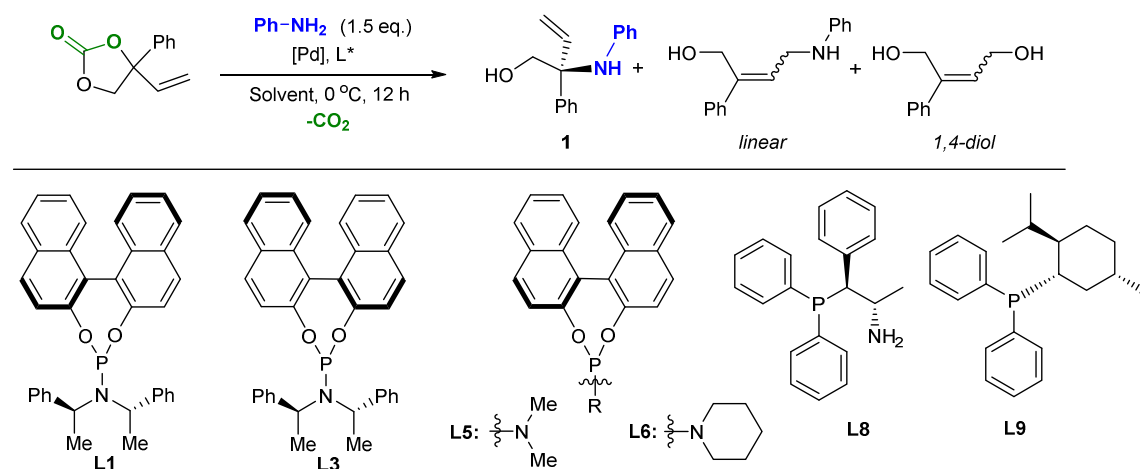
Entry	Ligand (mol %)	Catalyst (mol %)	Solvent (200 μL)	T [°C]	Yield of 1 [%][b]	ee [%]
1	**L1** (5)	White catalyst (2)	-	25	0	-
2	**L3** (5)	White catalyst (2)	-	25	trace	-
3	**L5** (5)	White catalyst (2)	-	25	trace	-
4	**L1** (5)	Pd$_2$(dba)$_3$·CHCl$_3$ (1.25)	-	25	19	-
5	**L1** (5)	Pd$_2$(dba)$_3$·CHCl$_3$ (1.25)	MeOH	25	0	-
6	**L5** (5)	Pd$_2$(dba)$_3$·CHCl$_3$ (1.25)	-	25	0	-
7	**L3** (5)	Pd$_2$(dba)$_3$·CHCl$_3$ (1.25)	-	25	<2	-
8	**L1** (5)	Pd$_2$(dba)$_3$·CHCl$_3$ (1.25)	DCM	25	25	-
9	**L1** (5)	Pd$_2$(dba)$_3$·CHCl$_3$ (1.25)	THF	25	20	-
10	**L1** (5)	Pd$_2$(dba)$_3$·CHCl$_3$ (1.25)	DCM	0	67[c]	64[d]
11	**L1** (5)	Pd$_2$(dba)$_3$·CHCl$_3$ (1.25)	MeOH	0	0	-
12	**L1** (5)	Pd$_2$(dba)$_3$·CHCl$_3$ (1.25)	dioxane	0	57	-
13	**L1** (5)	Pd$_2$(dba)$_3$·CHCl$_3$ (1.25)	DMF	25	18	-
14	**L6** (5)	Pd$_2$(dba)$_3$·CHCl$_3$ (1.25)	DCM	0	50	-
15	**L1** (5)	Pd(OAc)$_2$ (2)	DCM	0	0	-
16	**L1** (5)	Pd(CH$_3$CN)$_4$(BF$_4$)$_2$ (2)	DCM	0	0	-
17	**L1** (5)	Pd(dppf)Cl$_2$ (2)	DCM	0	0	-
18	**L1** (5)	(Ph$_3$P)$_4$Pd (2)	DCM	0	<2	-
19	**L1** (5)	White catalyst (2)	DCM	0	0	-
20[e]	**L1** (5)	Pd$_2$(dba)$_3$·CHCl$_3$ (1.25)	DCM	-5	45	-
21[e]	**L1** (5)	Pd$_2$(dba)$_3$·CHCl$_3$ (1.25)	DCM	-5	trace	-
22[e]	**L3** (5)	Pd$_2$(dba)$_3$·CHCl$_3$ (1.25)	DCM	-5	trace	-
23	**L8** (5)	Pd$_2$(dba)$_3$·CHCl$_3$ (1.25)	DCM	0	0	-
24	**L9** (5)	Pd$_2$(dba)$_3$·CHCl$_3$ (1.25)	DCM	0	0	-

[a]Reaction conditions: carbonate (0.2 mmol), aniline (1.5 equiv.), open to air, 12 h. [b]NMR yield with toluene as internal standard. [c]Isolated yield. [d]Determined by UPC2. [e]36 h.

Table 2.2: Effect of ligands on the asymmetric Pd-catalyzed allylic amination.[a]

Entry	L	Solvent	Yield [%][b]	ee [%][c]
1	**L1**	THF	76	95 (S)
2	**L2**	THF	39	68 (S)
3	**L3**	THF	60	73 (S)
4	**L4**	THF	<2	-
5	**L5**	THF	<2	-
6	**L6**	THF	<2	-
7	**L7**	THF	<2	-

[a] Reaction conditions unless stated otherwise: 0.2 mmol (1 equiv.) of carbonate, aniline (1.5 equiv.), Pd₂(dba)₃·CHCl₃ (1.25 mol %), **L** (5.0 mol %), 0.20 mL of solvent, 0 ºC, open to air, 12 h. [b] Isolated yield. [c] Determined by UPC2; the absolute configuration was assigned on the basis of comparison with the UPC2 trace of crystalline **1**.

Encouraged by our preliminary investigations, then the nature of the chiral phosphoramidite ligand was varied to examine the effect on the regio- and enantioselectivity, and these experiments were carried out at 0 ºC (Table 2.2). We were pleased to find that the yield of the branched allylic amine **1** further increased to 76% with excellent enantiocontrol (96% *ee*) when THF was used as the solvent (Table 2.2, entry 1). The use of **L2** and **L3** gave lower yield and lower levels of enantioselectivity (Table 2.2, entries 2 and 3). These results indicate that the steric hindrance around the nitrogen center in the ligand and its absolute configuration exert a key influence on the

regio- and enantioselectivity in this Pd-catalyzed allylic amination reaction. Therefore, we next investigated a series of chiral phosphoramidite ligands (Table 2.2; **L4-L7**, entries 4-7), however, inferior results were noted when compared to the use of **L1** under similar conditions.

Table 2.3: Effect of the solvent on the asymmetric Pd-catalyzed allylic amination towards **1**.[a]
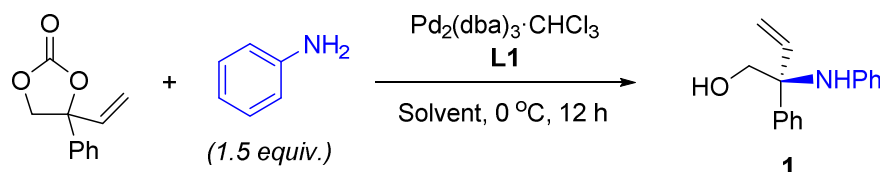
Entry	L	Solvent	Yield [%][b]	ee [%][c]
1	**L1**	CH$_2$Cl$_2$	67	64 (*S*)
2	**L1**	Toluene	52	59 (*S*)
3	**L1**	CH$_3$CN	52	76 (*S*)
4	**L1**	Et$_2$O	67	75 (*S*)
5	**L1**	THF	76	95 (*S*)
6	**L1**	DMF	37	84 (*S*)

[a] Reaction conditions unless stated otherwise: 0.2 mmol (1 equiv.) of carbonate, aniline (1.5 equiv.), Pd$_2$(dba)$_3$·CHCl$_3$ (1.25 mol %), **L1** (5.0 mol %), 0.20 mL of solvent, 0 °C, open to air, 12 h. [b] Isolated yield. [c] Determined by UPC2. See Table 2.2 for the assignment of the absolute configurations.

In light of these results, we next set out to explore the effect of the solvent in this reaction, and these results are summarized in Table 2.3. The solvent had a marked influence on both yield and selectivity. It was found that **1** could be obtained in 52% yield and with 59% enantiomeric excess in toluene. Other solvents such as CH$_3$CN, Et$_2$O, or DMF also gave lower yields and enantioinduction. In addition, we found that trace amount of H$_2$O had positive effects on the rate of the reaction, as the use of anhydrous THF did not allow full conversion of the carbonate substrate after 16 h.

Table 2.4: Effect of other reaction parameters on the asymmetric Pd-catalyzed allylic amination towards **1**.[a]
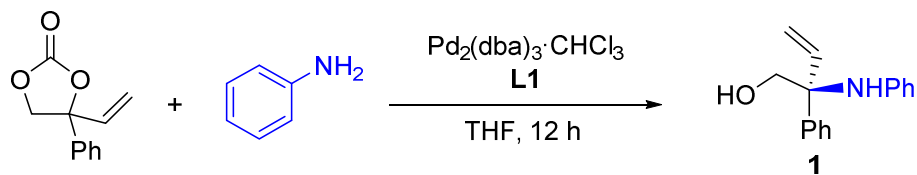
Entry	L	Solvent	Yield [%][b]	ee [%][c]
1[d]	L1	THF	73	95 (S)
2[e]	L1	THF	38	91 (S)
3[f]	L1	THF	59	71 (S)
4[g]	L1	THF	<15	-
5[h]	L1	THF	63	71 (S)

[a] Reaction conditions unless stated otherwise: 0.2 mmol (1.0 equiv.) of carbonate, aniline (1.5 equiv.), $Pd_2(dba)_3 \cdot CHCl_3$ (1.25 mol %), **L1** (5.0 mol %), 0.20 mL of solvent, 0 ºC, open to air, 12 h. [b] Isolated yield. [c] Determined by UPC2, absolute configurations assigned as for Table 2.2. [d] Using $Pd(dba)_2$ (2.5 mol %) as catalyst. [e] Reaction was done at room temperature. [f] 0.10 mL of THF. [g] 0.30 mL of THF. [h] 5.0 equiv. of aniline used.

Taking into consideration the above data, we next set up to explore the influence of the others reaction parameters. The use of $Pd(dba)_2$ was also productive (Table 2.4, entry 1) but showed poor reproducibility. The room-temperature conversion gave lower *ee* value (91%; Table 2.4, entry 2) and a significantly lower isolated yield (38%). Similar erosion of the asymmetric induction was noted when the reaction was performed at higher concentration (71% *ee*; Table 2.4, entry 3). Lowering the concentration of the reactants resulted in rather low conversion (Table 2.4, entry 4). The use of a large excess of aniline also led to a decrease in the enantioselectivity (Table 2.4, entry 5). The experimental observations reported in entries 3, 4, and 5 align well with the mechanistic hypothesis that the asymmetric induction is less efficient when the nucleophilic attack by the amine is favored.[39] Notably, base additives are not required in this catalytic process, which is crucial to control the chemoselectivity of this transformation as their presence may cause side-product formation.[40]

---

(39) Increasing the reaction temperature, concentration, or amount of aniline would give faster nucleophilic addition. This combined with a relatively slow equilibration between reactive species **B** and **B′** (Scheme 2.26) would consequently lead to lower enantio-discrimination.

(40) Addition of external base may lead to 1,2-diol or carbamate formation, see: a) W. Guo, J. Gónzalez-Fabra, N. A. G. Bandeira, C. Bo, A. W. Kleij, *Angew. Chem. Int. Ed*. **2015**, *54*, 11686; b) V. Laserna, G. Fiorani, C. J. Whiteoak, E. Martin, E. C. Escudero-Adán, A. W. Kleij, *Angew. Chem. Int. Ed*. **2014**, *53*, 10416.

2.2.2 Scope of Aryl Amines

Table 2.5: Scope of aryl amines.
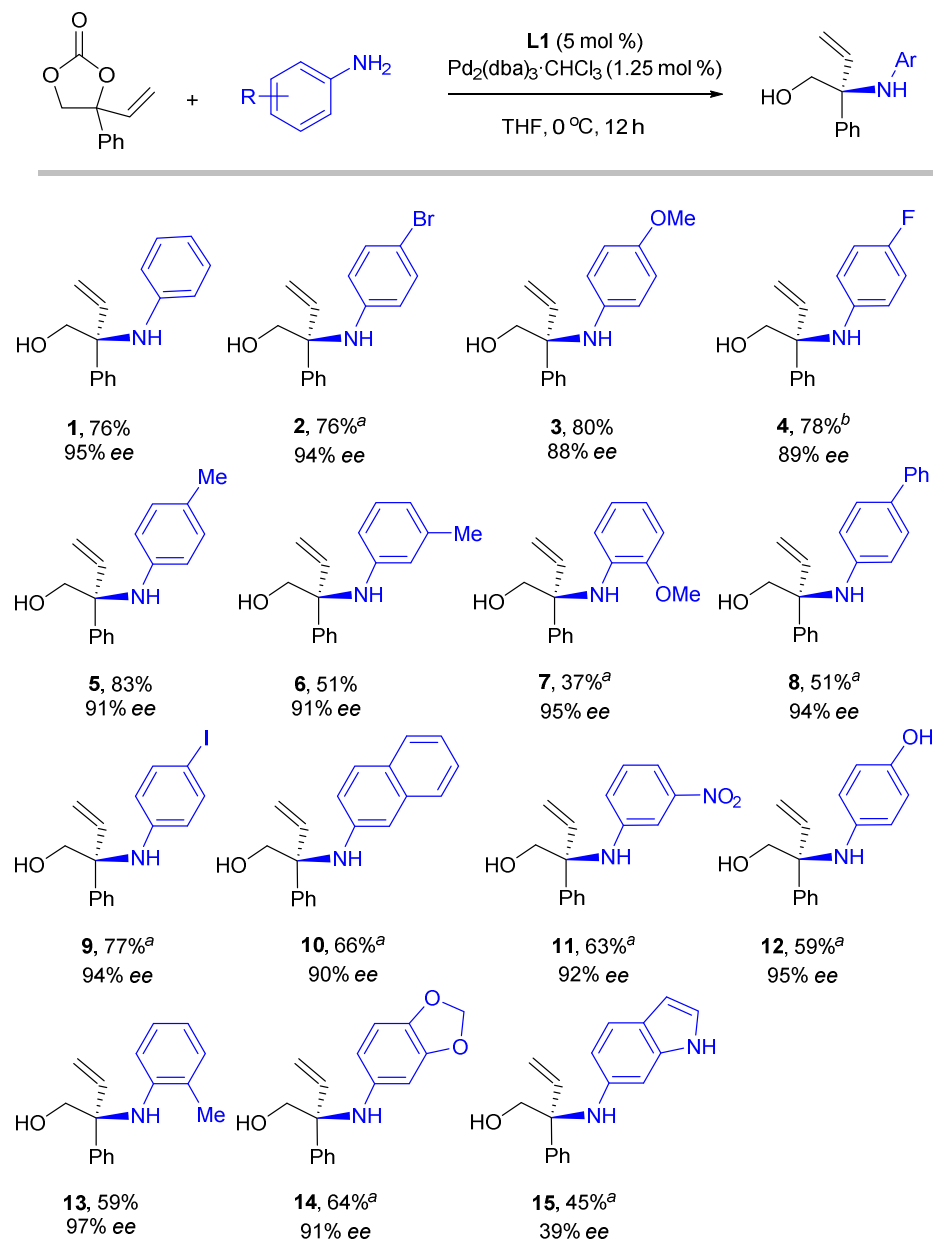
Reaction conditions: 0.2 mmol carbonate, 0.3 mmol of aniline, $Pd_2(dba)_3 \cdot CHCl_3$ (1.25 mol %), **L1** (5.0 mol %), 0.20 mL THF, 0 °C, open to air, 12 h. All reported yields are isolated ones after column purification. [a] $Pd_2(dba)_3 \cdot CHCl_3$ (2.5 mol %), **L1** (10 mol %). [b] 24 h.

With the optimized conditions in hand, we then investigated the scope in aryl amines towards the formation of the branched allylic amines **1–15** (Table 2.5).[41] In general, the formation of these products proceeds with excellent enantioselectivity of up to 97% (except for allylic amine **15**). The protocol is quite efficient for various aryl amine reaction partners, including those having aryl groups with *para-* (**2-5**, **8**, **9** and **12**), *meta-* (**6** and **11**) and *ortho-* (**7** and **13**) substitutions. Both electron-donating (**3**, **5-7** and **12**) and -withdrawing groups (**2**, **4** and **9**) are tolerated. The *meta*-nitro substituted aniline was also tolerated affording allylic amine **11** in 63% yield and 93% *ee*. The installation of indole (**15**) and 1,3-benzodioxole (**14**) fragments, which are frequently observed in relevant pharmaceutical compounds,[42] is also possible. The reaction with the *ortho*-methoxy-aniline gave a lower yield (**7**: 37%) indicating some steric limitations of present methodology. The use of sterically more demanding N-methyl aniline resulted in quantitative linear product formation, while no reaction was observed under the optimal conditions utilizing indole or pyrrole nucleophiles. Further attempts to improve the enantioselectivity of product **15** using chloride additives failed.[43] Also, a linear carbonate substrate was tested but gave as major product the linear allylic amine product under the optimized conditions in 51% yield, suggesting that vinyl cyclic carbonate substrates are requisite towards the formation of the branched allylic amines.

2.2.3 Scope of Vinyl Cyclic Carbonates

We then focused on the investigation of the scope in vinyl carbonates (Table 2.6). We gratifyingly noted that a wide range of aryl-substituted vinyl cyclic carbonates were tolerated under the reaction conditions giving access to the corresponding enantioenriched allylic amines **16–27** in appreciable yields and good to excellent levels

---

(41) Alkyl amines can react with cyclic carbonates at room temperature giving carbamate compounds. Such aminolysis behavior has been well-documented, see for instance: a) M. Blain, L. Jean-Gérard, R. Auvergne, D. Benazet, S. Caillol, B. Andrioletti, *Green Chem*. **2014**, *16*, 4286; b) W. Guo, V. Laserna, E. Martin, E. C. Escudero-Adán, A. W. Kleij, *Chem. Eur. J*. **2016**, *22*, 1722; c) S. Sopeña, V. Laserna, W. Guo, E. Martin, E. C. Escudero-Adán, A. W. Kleij, *Adv. Synth. Catal*. **2016**, *358*, 2172. No branched allylic amine product was observed using deactivated alkyl amines of *p*-F and *p*-NO$_2$ substituted benzyl amines.

(42) a) J. D. Bloom, M. D. Dutia, B. D. Johnson, A. Wissner, M. G. Burns, E. E. Largis, J. A. Dolan, T. H. Claus, *J. Med. Chem*. **1992**, *35*, 3081; b) A. Ali, J. Wang, R. S. Nathans, H. Cao, N. Sharova, M. Stevenson, T. M. Rana, *ChemMedChem* **2012**, *7*, 1217; c) N. K. Kaushik, N. Kaushik, P. Attri, N. Kumar, C. H. Kim, A. K. Verma, E. H. Choi, *Molecules* **2013**, *18*, 6620.

(43) The presence of chloride can increase the rate of the π−σ−π process (Scheme 2.26) and potentially improve the enantioselectivity, see: B. M. Trost, M. R. Machacek, H. C. Tsui, *J. Am. Chem. Soc*. **2005**, *127*, 7014. However, no conversion of the substrates towards **15** and **25** was observed in the presence of Bu$_4$NCl or N(Hex)$_4$Cl (30 mol %).

of enantioselectivity. It is worth noting that compounds **1**–**27** also represent chiral vicinal amino alcohols which are of high synthetic interest and have important applications in biology.[44] The presence of substituents with different steric and electronic effects in the vinyl carbonate proved to be useful variations in these reaction partners. Generally, vinyl carbonates equipped with electron-donating aryl groups gave more productive catalysis with high levels of enantioselectivity (**16**–**17**, **20**–**24**; ≥ 88% *ee*). The carbonate substrate having an *ortho*-Br substituent did not show any reactivity under the optimized conditions, while the *meta*-substituted isomer gave the allylic amine product in 88% *ee* though in low yield. Installation of a thiophene moiety in the allylic amine is feasible (**25**; 80% yield, 76% *ee*) albeit with a lower degree of enantiocontrol. This may be explained by the presence of an additional hetero-atom that could interact with the Pd catalyst during the enantio-determining stage of the reaction.

Similar effects were noted when other reaction partners (aryl amines or carbonates) incorporating heteroatoms were utilized (*cf.*, preparation of **15** and **27**). Under the optimized conditions using ligand **L1**, the use of a furyl-substituted carbonate afforded allylic amine **27** with only 12% *ee*. The enantioselectivity could be improved to 41% when bulkier ligand **L7** was utilized at higher catalyst/ligand loading. It is worth noting that in some cases a substantial amount of the linear product was observed and this resulted in a lower isolated yield of the branched product (*cf.*, syntheses of **7**, **15**, **22** and **26**).

(44) For recent relevant literature: a) S.-L. Shi, Z. L. Wong, S. L. Buchwald, *Nature* **2016**, *532*, 353; b) U. Orcel, J. Waser, *Angew. Chem. Int. Ed*. **2015**, *54*, 5250.

Table 2.6: Scope of aryl-substituted vinyl cyclic carbonates.
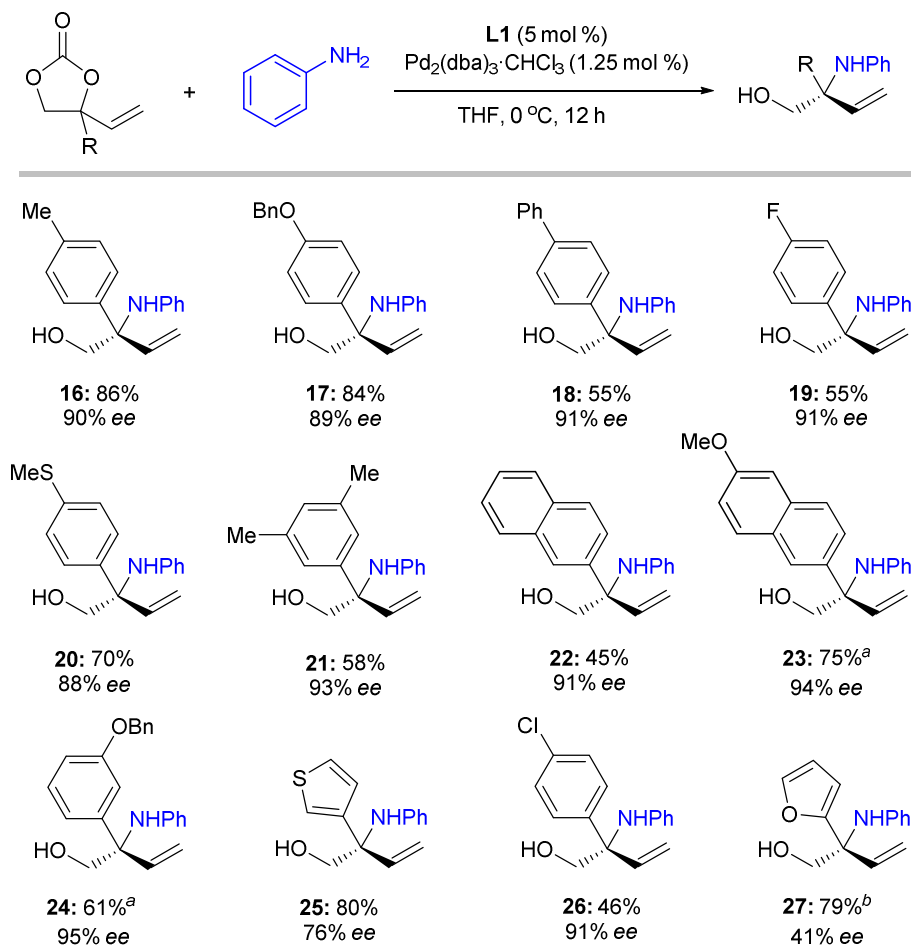
Reaction conditions: 0.2 mmol carbonate, 0.3 mmol of aniline, Pd$_2$(dba)$_3$·CHCl$_3$ (1.25 mol %), **L1** (5.0 mol %), 0.20 mL THF, 0 °C, open to air, 12 h. All reported yields are isolated ones after column purification. [a]Pd$_2$(dba)$_3$·CHCl$_3$ (2.5 mol %), **L1** (10 mol %). [b]Pd$_2$(dba)$_3$·CHCl$_3$ (5 mol%), **L7** (20 mol %).

To further challenge the catalytic protocol, the enantioselective synthesis of methyl- and non-substituted (R = H) allylic amines **28** and **29** was probed (Scheme 2.27). These products were isolated in good yields (71%−77%) though with moderate enantioselectivity (46%−60% *ee*); the use of ligand **L7** did not improve the enantioselectivity. With a bulkier cyclohexyl group (**30**, R = Cy), no product was obtained.

56
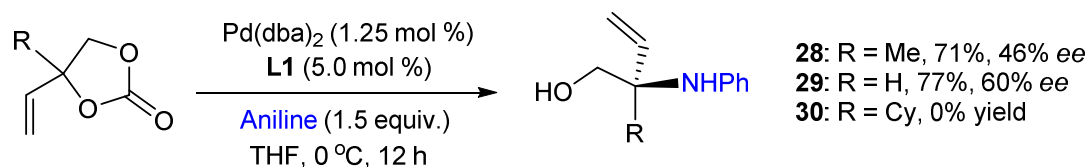
Scheme 2.27. Preparation of methyl- and non-substituted chiral allylic amines **28** and **29**, and attempted synthesis of **30**.

2.2.4 Synthetic Transformations of Allylic Amine (1)

In addition to the potential synthetic value of (chiral) allylic amines reported previously, the synthetic potential of these branched allylic amines was further exemplified by the preparation of chiral ether **31**, oxazolidinone **32**, diamine **33** and carbamate **34** from allylic amine **1** while retaining the original chirality (Table 2.7).

Table 2.7: Synthetic transformations of allylic amine **1**.
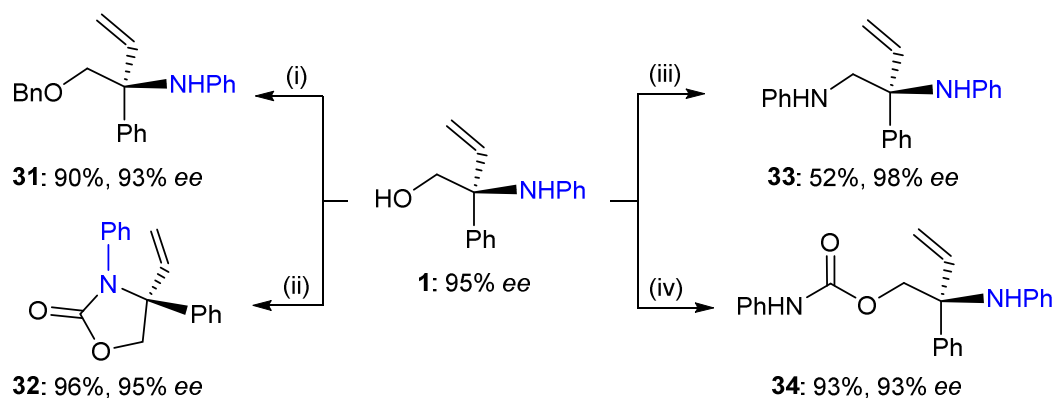
Reaction conditions: (i) BnBr (1.1 equiv.), NaH (2.0 equiv.), THF (1 mL), 0–r.t., 15 h; (ii) pyridine (4.0 equiv.), triphosgene (0.5 equiv.), CH_2Cl_2, 0–r.t., 3 h; (iii) 1) KOH (1.3 equiv.), TsCl (1.3 equiv.), Et_2O, 0 °C, 12 h; 2) aniline (8.0 equiv.), K_2CO_3 (8.0 equiv.), DMF, 0–r.t., 4 h; (iv) phenyl isocyanate (1.3 equiv.), Et_3N (10.0 equiv.), CH_2Cl_2, r.t., 10 min.

2.3   Conclusions

In summary, this chapter presents the first regio- and enantioselective synthesis of α,α-disubstituted allylic *N*-aryl amines based on a Pd-catalyzed allylic amination protocol. This procedure utilizes readily available and modular substituted cyclic vinyl carbonates and unactivated aryl amines as reactants, and can be operated without any special precautions and does not require any additives. Therefore, this user-friendly and efficient methodology marks a significant step forward in the challenging synthesis of these chiral allylic amine scaffolds.

2.4   Experimental Section

2.4.1   General Considerations

Commercially available reagents and solvents were purchased from Aldrich or TCI, and used without further purification. The substituted carbonates were synthesized following a previously reported method.[45] The Pd precursors were purchased from Aldrich or TCI. Phosphoramidites **L1**, **L3-L6** were purchased from Aldrich; **L2**[46] and **L7**[47] were prepared according to previously reported procedures. In the preliminary screening phase (Table 1.1), the internal standard mesitylene was added after the reaction mixture had been stirred at room temperature for 12 h. After that, an aliquot of the resulting mixture was taken and the yield was determined by means of ^1H NMR spectroscopy using $CDCl_3$ as the solvent. ^1H NMR, ^{13}C NMR, ^{19}F NMR spectra were recorded at room temperature on a Bruker AV-400 or an AV-500 spectrometer. All reported NMR values are given in parts per million (ppm) and referenced to the residual deuterated solvent signals. FT-IR measurements were carried out on a Bruker Optics FTIR Alpha spectrometer. Mass spectrometric analyses, ultra-performance convergence chromatography (UPC2) analyses, and X-ray diffraction studies were performed by the Research Support Group at ICIQ.

2.4.2   Procedure for the Preparation of Organocatalyst
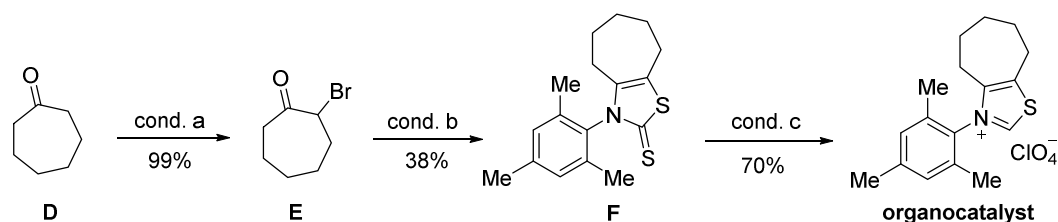
Procedure for obtaining E : To a solution of cycloheptanone **D** (5.0 g, 44.6 mmol, 1.0 equiv.) in CH_2Cl_2 (50 mL) was added *p*-toluenesulfonic acid monohydrate (84 mg, 0.446 mmol, 0.1 equiv.). The reaction was cooled down with an ice bath and *N*-bromosuccinimide (8.7 g, 49.1 mmol, 1.1 equiv.) was added. The reaction was stirred for

(45) a) A. Khan, R. Zheng, Y. Kan, , J. J. YeXing, Y. J. Zhang, *Angew. Chem. Int. Ed*. **2014**, *53*, 6439; b) A. Khan, L. Yang, J. Xu, L. Y. Jin, Y. J. Zhang, *Angew. Chem. Int. Ed*. **2014**, *53*, 11257; c) A. Khan, J. Xing, J. Zhao, Y. Kan, W. Zhang, Y. J. Zhang, *Chem. Eur. J*. **2015**, *21*, 120; d) L. Yang, A. Khan, R. Zheng, L. Y. Jin, Y. J. Zhang, *Org. Lett*. **2015**, *17*, 6230; e) W. Guo, L. Martínez-Rodríguez, E. Martin, E. C. Escudero-Adán, A. W. Kleij, *Angew. Chem. Int. Ed*. **2016**, *55*, 11037.
(46) C. R. Smith, D. J. Mans, T. V. RajanBabu, *Org. Synth*. **2008**, *85*, 238.
(47) D. Polet, A. Alexakis, K. Tissot-Croset, C. Corminboeuf, K. Ditrich, *Chem. Eur. J*. **2006**, *12*, 3596.

16 h and then 20 mL of aqueous saturated solution of thiosulfate was added. The organic phase was extracted with DCM and washed with aqueous saturated solution of bicarbonate (2 × 50 mL) and thereafter with brine (50 mL). The volatiles were removed under reduced pressure. The pure product **E** was obtained as yellow oil (99% yield) and further purification was not necessary. ^{1}H NMR (500 MHz, CDCl$_3$): δ 4.37 (dd, J = 5.1, 9.5 Hz, 1H), 2.92-2.79 (m, 1H), 2.55-2.43 (m, 1H), 2.42-2.29 (m, 1H), 2.09-1.86 (m, 3H), 1.84-1.65 (m, 1H), 1.64-1.48 (m, 2H), 1.46-1.29 (m, 1H).[48]

_Procedure for obtaining F__:_ To a solution of 2,4,6-trimethylaniline (5.82 mL, 41.57 mmol, 1.0 equiv.) in CS$_2$ (2.5 mL, 41.57 mmol, 1.0 equiv.), and DMSO (20 mL) was added 2.1 mL (1.0 equiv.) of aq. NaOH solution (20 M) was added. The reaction was cooled down with an ice bath and the compound **E** was added drop wise stirred for 16 h at room temperature. After that, water (40 mL) was added and the mixture was further stirred for 10 min at 0 °C. The resulting slurry was decanted to remove the water and the suspension was dissolved in EtOH (40 mL), 2 mL of concd. HCl was added and the mixture was refluxed for 1 h. After that, the reaction was cooled down to room temperature, and the organic phase was extracted with ethyl acetate (3 × 30 mL). The volatiles were removed under reduced pressure. The product was purified by chromatography (10−20% ethyl acetate/hexane). The corresponding product **F** was obtained as an oil (38% yield). ^{1}H NMR (500 MHz, CDCl$_3$) δ 7.00 (s, 2H), 2.66-2.60 (m, 2H), 2.33 (s, 3H), 2.23-2.17 (m, 2H), 2.01 (s, 6H), 1.85-1.70 (m, 4H), 1.85-1.70 (m, 4H), 1.63-1.52 (m, 2H).[48]

_Procedure for obtaining organocatalyst__:_ The compound **F** (1200 mg, 4 mmol, 1.0 equiv.) was dissolved in glacial acetic acid (20 mL) and cooled with an ice bath, and then H$_2$O$_2$ (1.14 mL, 13.2 mmol, 3.3 equiv.) was added dropwise and stirred for 30 min. The volatiles were removed under reduced pressure. The residue was dissolved in MeOH (3 mL). Sodium perchlorate monohydrate (2.0 mg, 16.4 mmol, 4.1 equiv.; **CAREFUL perchlorates are potentially explosive**) was added at 0 ºC in a mixture (2:1) of MeOH/H$_2$O (10 mL). The mixture was stirred for 30 min and extracted with DCM (3×20 mL). The volatiles were removed under reduced pressure and a brown oil was obtained. After addition of 20 mL diethyl ether and applying 30 min of sonication, **organocatalyst** was obtained in a 70% yield as a white powder. ^{1}H NMR (500 MHz, CDCl$_3$) δ 9.55 (s,

(48) N. Kuhl, F. Glorius, *Chem. Commun*. **2011**, *47*, 573.

1H), 7.07 (s, 2H), 3.19-3.12 (m, 2H), 2.61-2.54 (m, 2H), 2.37 (s, 3H), 1.99-1.93 (m, 2H), 1.97 (s, 6H), 1.91-1.84 (m, 2H), 1.70-1.62 (m, 2H).[48]

2.4.3 General Procedure for the Synthesis of Vinyl Cyclic Carbonates

A previous reported procedure was followed with minor modifications.[45a]
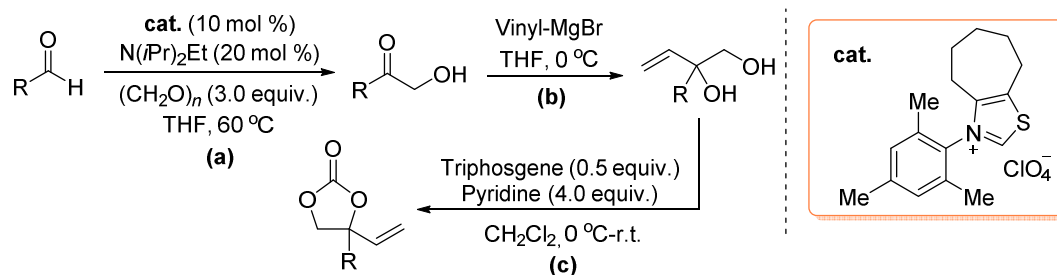
Step (a): In an oven-dried Schlenk-flask sealed with a rubber septum and equipped with a magnetic stirring bar, thiazolium salt **A** (0.1 mmol, 0.1 equiv.), paraformaldehyde (3.0 mmol, 3.0 equiv.) and the aldehyde (1.0 mmol, 1.0 equiv.) were suspended in dry THF (4 mL). N(i-Pr)$_2$Et (0.2 mmol, 0.2 equiv.) was added and the resulting mixture was heated to 60 °C. In the case of aliphatic aldehydes, the aldehyde was added after stirring the other reactants for 5 min at room temperature. After a maximum reaction time of 24 h, the solvent was evaporated and the crude product was purified by flash Chromatography.

Step (b): To a solution of the respective hydroxy methyl ketone (5 mmol, 1 equiv.) in THF (20 mL) was added vinyl magnesium bromide (1.0 M in THF, 2.5 equiv.) at 0 °C. The reaction was stirred under an N$_2$ atmosphere at room temperature for 2 h. The reaction mixture was then quenched with saturated aqueous NH$_4$Cl, and extracted with EtOAc. The combined organic layers were dried over anhydrous Na$_2$SO$_4$, filtered and concentrated affording the crude product which was directly used in next step.

Step (c): To a solution of diol (1 equiv.) and pyridine (4 equiv.) in CH$_2$Cl$_2$ (20 mL) was added triphosgene (0.5 equiv., 1.0 M in CH$_2$Cl$_2$) at 0 °C. The reaction was stirred under an N$_2$ atmosphere at room temperature for 2 h. The reaction mixture was then quenched with saturated aqueous NH$_4$Cl, and extracted with CH$_2$Cl$_2$. The combined organic layers were dried over anhydrous Na$_2$SO$_4$, filtered and concentrated. The residue was purified by flash chromatography on silica to afford the corresponding carbonate.

2.4.4 General Procedure for the Tertiary Allylic Carbonate
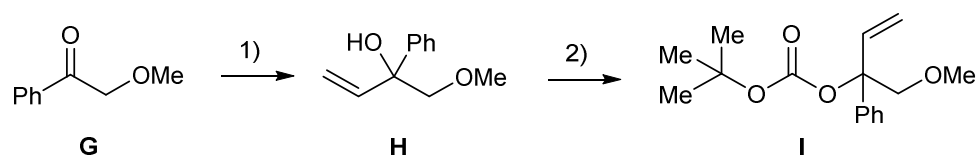
Procedure for obtaining H: To a flame-dried round-bottom flask equipped with a stir bar was added 2-methoxyacetophenone **G** (0.550 g, 3.7 mmol, 1.0 equiv.) in dry THF (5 mL). Then, vinylmagnesium bromide (5.6 mL, 1.5 equiv., 1.0 M THF solution) was added dropwise at 0 °C (ice bath). The reaction was allowed to stir at 0 °C for 4 h and quenched with sat. NH_4Cl (aq.) and extracted with ethyl acetate (3 × 10 mL). The combined organics were washed with brine, dried over Na_2SO_4, filtered, and then concentrated. The tertiary alcohol **H** was obtained (0.528 g, 80% yield) upon purification by flash chromatography (hexane/EtOAc = 10 : 1) as a light yellow oil. (hexane/EtOAc = 3:1, R_f = 0.25).

Procedure for obtaining I: To a flame-dried round-bottom flask equipped with stir bar was added the terciary alcohol **H** (0.500 g, 2.8 mmol, 1.0 equiv.) dissolved in dry THF (5 mL). The solution was cooled to 0 °C (ice bath) followed by dropwise addition of *n*-butyl lithium (1.25 mL, 1.1 equiv, 2.5 M in hexane). The reaction was allowed to stir for 30 minutes at 0 °C, after which Boc_2O (2.5 mmol, 0.57 mL, 0.9 equiv.) was added dropwise. The resultant reaction mixture was allowed to warm to room temperature and stirred for 3 hours. After that, the reaction was then quenched with sat. NH_4Cl (aq.) and extracted with diethyl ether (3 × 10 mL). The combined organic layers were washed with brine, dried over Na_2SO_4, filtered, and then concentrated under vacuum. The linear carbonate **I** was obtained upon purification by flash chromatography (pentane/TEA = 20 : 1, R_f = 0.80) as a yellow oil (0.720 g, 93% yield).

2.4.5 General Procedure for the Synthesis of Allylic Aryl Amines
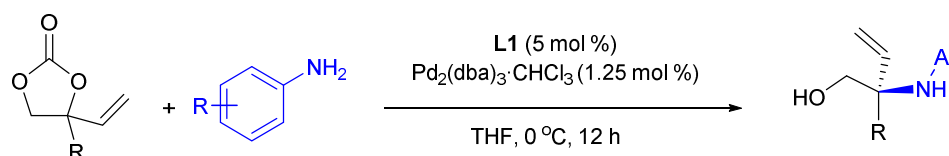
Representative case: To a screw-capped vial equipped with a magnetic stirring bar, vinyl allylic carbonate (0.20 mmol, 1.0 equiv.), $Pd_2(dba)_3 \cdot CHCl_3$ (3.0 mg, 1.25 mol %), **L1** (5.2 mg, 5.0 mol %), aryl amine (0.30 mmol, 1.5 equiv.) and THF (0.2 mL) were added. The

resulting mixture was stirred at 0 ºC for 12 h, and then the reaction mixture was warmed to room temperature, after which the product was purified by flash column chromatography on silica gel (hexane/EA = 10:1) to afford the pure allylic amines. The enantiomeric excess of the product was determined by UPC2 equipped with a chiral column.

2.4.6 Transformations of Allylic Amine (1) into 31-34
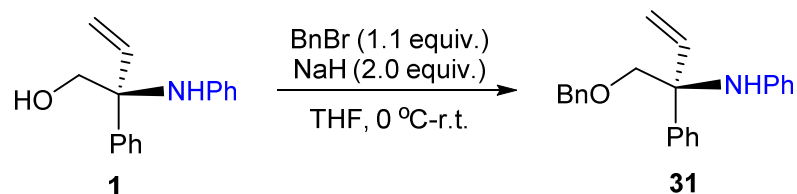
To a screw-capped vial equipped with a magnetic stirring bar, allylic amine **1** (0.20 mmol, 48 mg, 1.0 equiv.), BnBr (31 mg, 1.1 equiv.), NaH (9.6 mg, 2.0 equiv.), and THF (1.0 mL) were added at 0 ºC. The resulting mixture was stirred at room temperature for 15 h, after which the product was purified by flash column chromatography on silica gel to afford the pure chiral ether **31** (51 mg, 77%, hexane : EA = 30 : 1, R_f = 0.45). 93% *ee* (The enantiomeric excess of the product was determined by UPC2 equipped with a chiral column).
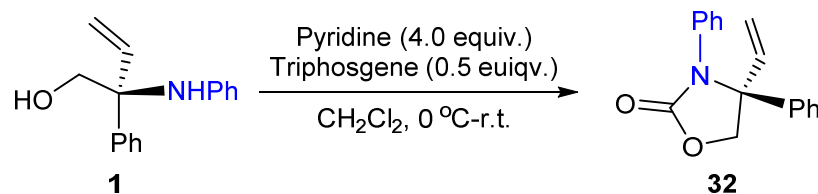
To a solution of allylic amine **1** (48 mg, 1 equiv.) and pyridine (63 mg, 4 equiv.) in CH_2Cl_2 (2 mL) was added triphosgene (30 mg, 0.5 equiv., 1.0 M in CH_2Cl_2) at 0 °C. The reaction was stirred under an N_2 atmosphere at room temperature for 3 h. The reaction mixture was then quenched with saturated aqueous NH_4Cl, and extracted with CH_2Cl_2. The combined organic layers were dried over anhydrous Na_2SO_4, filtered and concentrated. The residue was purified by flash chromatography on silica to afford the corresponding oxazolidinone **32** (51 mg, 96%, hexane : EA = 10 : 1, R_f = 0.12). 95% *ee* (The enantiomeric excess of the product was determined by UPC2 equipped with a chiral column).
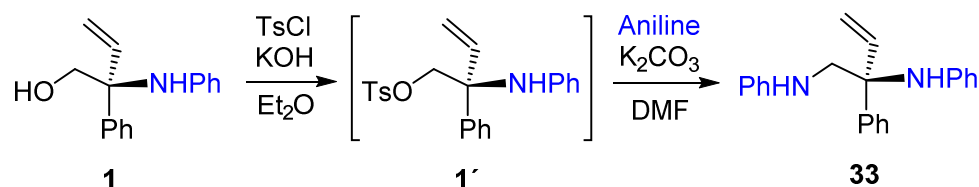
*Note: compounds **1′** and **33** are not highly stable at room temperature for prolonged periods of time*

Experimental procedure: To a mixture of compound **1** (0.048 g, 0.2 mmol, 1 equiv.), KOH (0.015 g, 1.3 equiv.) in Et_2O (0.6 mL) added TsCl (0.050 g, 1.3 equiv.) at 0 °C. The reaction mixture was stirred at 0 °C for 12 h and NMR analysis showed the product **1′** was obtained with quantitative yield. The ether was evaporated under reduced pressure at 0 °C and then aniline (0.149 g, 8 equiv.), K_2CO_3 (0.221 g, 8 equiv.) and DMF (0.8 mL) were added successively. The resultant mixture was stirred at 0 °C for 10 min and allowed to warm at room temperature and stirred for another 4 h. The organics was extracted with ethyl acetate and washed with water. The organic layer was dried over an hour. Na_2SO_4 and concentrated under reduced pressure. The pure product **33** was isolated (0.032 g, 51%) by flash chromatography (hexane : EA = 10 : 1, R_f = 0.53). 95% *ee.*
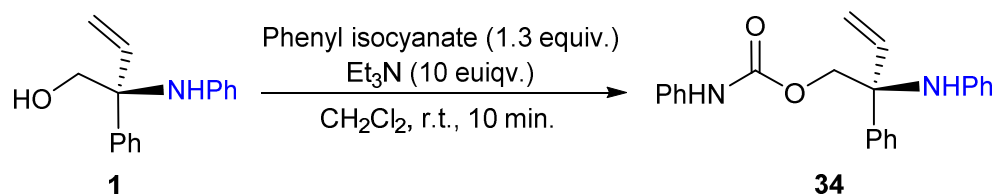
To a vial equipped with a magnetic stirring bar, allylic amine **1** (48 mg, 0.2 mmol), phenyl isocyanate (31 mg, 1.3 equiv.), and Et_3N (202 mg, 10 equiv.) were added in CH_2Cl_2 (1 mL) at room temperature. The resulting reaction mixture was kept while stirring 10 min. The reaction mixture was then diluted with diethyl CH_2Cl_2 and water. The organic layer was separated and the aqueous layer was extracted into diethyl ether (3 × 5 mL). Then, the combined organic layers were dried over Na_2SO_4, filtered, and then concentrated under vaccum. The crude reaction mixture was purified by flash chromatography (hexane/EA=10:1) to afford the pure carbamate **34** (67 mg, 93%, 93 *ee*).

2.4.7 Analytical Data for All Compounds
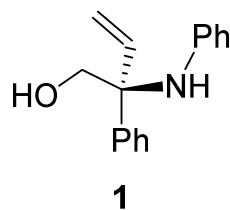
Scale: 0.2 mmol; isolated 36.3 mg (76% yield), Hexane : EA = 5 : 1, R_f = 0.30; 95% *ee*. **^{1}H NMR** (400 MHz, CDCl$_3$): δ 7.55–7.48 (m, 2H), 7.38–7.35 (m, 2H), 7.31–7.27 (m, 1H), 7.04–7.00 (m, 2H), 6.63 (t, *J* = 7.3 Hz, 1H), 6.45 (dd, *J* = 17.3, 10.7 Hz, 1H), 6.41–6.35 (m, 2H), 5.47 (dd, *J* = 10.7, 1.0 Hz, 1H), 5.38 (dd, *J* = 17.3, 1.0 Hz, 1H), 4.89 (s, 1H), 3.68 (s, 2H), 1.76 (s, 1H) ppm. **^{13}C NMR** (101 MHz, CDCl$_3$): δ 145.26, 140.94, 136.46, 128.89, 128.65, 127.50, 127.03, 118.54, 117.31, 115.84, 70.90, 64.85 ppm. **IR** (neat): ν = 3566, 3419, 3021, 1598, 1504, 1322, 1037, 691 cm^{-1}. **HRMS** (ESI+, MeOH): *m/z* calcd. 240.1383 (M + H)$^+$, found: 240.1377. **UPC2** conditions: Chiralpak IA column (100 × 4.6 mm, 3 μm), isocratic CO$_2$/MeOH = 90 : 10; 95% *ee*, 97.5 : 2.5 *er*; $[\alpha]_D^{25}$ = −99.7 (*c* = 0.10, CHCl$_3$).
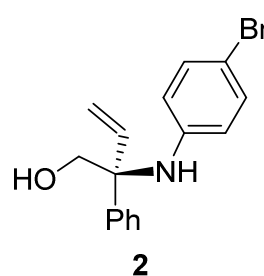
Scale: 0.2 mmol; isolated 48.2 mg (76% yield), Hexane : EA = 5 : 1, R_f = 0.23; 94% *ee*. **^{1}H NMR** (400 MHz, CDCl$_3$): δ 7.49–7.45 (m, 2H), 7.38–7.34 (m, 2H), 7.31–7.26 (m, 1H), 7.11–7.04 (m, 2H), 6.41 (dd, *J* = 17.3, 10.7 Hz, 1H), 6.27–6.21 (m, 2H), 5.47 (dd, *J* = 10.7, 0.8 Hz, 1H), 5.35 (dd, *J* = 17.3, 0.9 Hz, 1H), 4.96 (s, 1H), 3.64 (s, 2H), 1.71 (s, 1H) ppm. **^{13}C NMR** (101 MHz, CDCl$_3$): δ 144.30, 140.31, 135.69, 131.38, 129.02, 127.71, 126.94, 118.95, 117.33, 109.08, 71.10, 64.91 ppm. **IR** (neat): ν = 3398, 3023, 1590, 1490, 1294, 1064, 813, 701 cm^{-1}. **HRMS** (ESI+, MeOH): *m/z* calcd. 340.0307 (M + Na)$^+$, found: 340.0300. **UPC2** conditions: IA column, Isocratic CO$_2$/MeOH = 85 : 15, 3 ml/min, 1500 psi; 94% *ee*, 96.8 : 3.2 *er*; $[\alpha]_D^{25}$ = -93.2 (*c* = 0.11, CHCl$_3$).
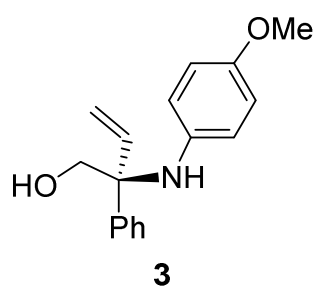
Scale: 0.2 mmol; isolated 43.0 mg (80% yield), Hexane : EA = 5 : 1, R_f = 0.23; 88% *ee*. **^{1}H NMR** (400 MHz, CDCl$_3$): δ 7.54–7.50 (m, 2H), 7.38–7.34 (m, 2H), 7.31–7.26 (m, 1H), 6.83 (d, *J* = 8.1 Hz, 2H), 6.43 (dd, *J* = 17.4, 10.7 Hz, 1H), 6.32–6.27 (m, 2H), 5.46 (dd, *J* = 10.7, 1.1 Hz, 1H), 5.36 (dd, *J* = 17.4, 1.1 Hz, 1H), 3.68 (m, 2H), 2.17 (s, 3H) ppm. **^{13}C NMR** (101 MHz, CDCl$_3$): δ 152.02, 141.28, 139.16, 137.10, 128.83, 127.46, 127.13, 118.25, 117.20, 114.34, 70.48, 65.00, 55.72 ppm. **IR** (neat): ν = 3389, 2930, 2831, 1508, 1445,

1233, 1036, 819, 701 cm^{-1}. **HRMS** (ESI+, MeOH): *m/z* calcd. 292.1308 (M + Na)$^+$, found: 292.1306. **UPC2** conditions: IA column, Isocratic CO_2/MeOH = 90 : 10, 3 ml/min, 1500 psi; 88% *ee*, 93.8 : 6.2 *er*; $[\alpha]_D^{25}$ = -87.9 (*c* = 0.11, CHCl$_3$).
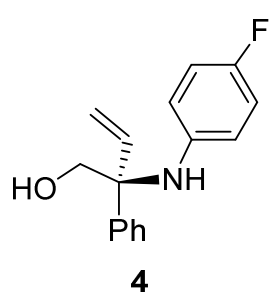
Scale: 0.2 mmol; isolated 40.1 mg (78% yield), Hexane : EA = 5 : 1, R_f = 0.23; 89% *ee*. **^{1}H NMR** (400 MHz, CDCl$_3$): δ 7.53–7.47 (m, 2H), 7.39–7.34 (m, 2H), 7.31–7.27 (m, 1H), 6.75–6.67 (m, 2H), 6.41 (dd, *J* = 17.3, 10.7 Hz, 1H), 6.33–6.27 (m, 2H), 5.47 (dd, *J* = 10.7, 1.1 Hz, 1H), 5.35 (dd, *J* = 17.3, 1.1 Hz, 1H), 4.81 (s, 1H), 3.66 (s, 2H), 1.78 (s, 1H) ppm. **^{19}F NMR** (376 MHz, CDCl$_3$): δ -128.42. **^{13}C NMR** (101 MHz, CDCl$_3$) δ 155.72 (d, *J* = 236 Hz), 141.48 (d, *J* = 1 Hz), 140.76, 136.33, 128.93, 127.60, 127.05, 118.65, 116.59 (d, *J* = 8 Hz), 115.12 (d, *J* = 22 Hz), 70.86, 65.00 ppm. **IR** (neat): ν = 3590, 3414, 2934, 1506, 1402, 1208, 1039, 787, 694 cm^{-1}. **HRMS** (ESI+, MeOH): *m/z* calcd. 280.1108 (M + Na)$^+$, found: 280.1100. **UPC2** conditions: IA column, Isocratic CO_2/MeOH = 90 : 10, 3 ml/min, 1500 psi; 89% *ee*, 94.3 : 5.7 *er*; $[\alpha]_D^{25}$ = -94.0 (*c* = 0.12, CHCl$_3$).
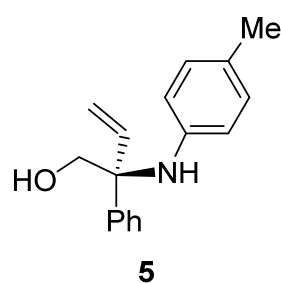
Scale: 0.2 mmol; isolated 42.0 mg (83% yield), Hexane : EA = 5 : 1, R_f = 0.29; 91% *ee*. **^{1}H NMR** (400 MHz, CDCl$_3$): δ 7.56–7.52 (m, 2H), 7.40–7.36 (m, 2H), 7.32–7.28 (m, 1H), 6.85 (d, *J* = 8.1 Hz, 2H), 6.45 (dd, *J* = 17.4, 10.7 Hz, 1H), 6.33–6.31 (m, 2H), 5.48 (dd, *J* = 10.7, 1.1 Hz, 1H), 5.39 (dd, *J* = 17.4, 1.1 Hz, 1H), 3.73–3.67 (m, 2H), 2.20 (s, 3H) ppm. **^{13}C NMR** (126 MHz, CDCl$_3$): δ 142.82, 141.14, 136.73, 129.21, 128.84, 127.43, 127.05, 126.43, 118.37, 115.94, 70.75, 64.82, 20.45 ppm. **IR** (neat): ν = 3398, 2919, 1615, 1515, 1446, 1258, 1039, 807, 700 cm^{-1}. **HRMS** (ESI+, MeOH): *m/z* calcd. 276.1359 (M + Na)$^+$, found: 276.1356. **UPC2** conditions: IA column, Isocratic CO_2/MeOH = 85 : 15, 3 ml/min, 1500 psi; 91% *ee*, 95.7 : 4.3 *er*; $[\alpha]_D^{25}$ = -95.8 (*c* = 0.10, CHCl$_3$).
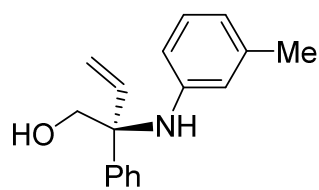
Scale: 0.2 mmol; isolated 25.8 mg (51% yield), Hexane : EA = 5 : 1, R_f = 0.29; 91% *ee*. **^{1}H NMR** (400 MHz, CDCl$_3$): δ 7.52 (d, J = 8.1 Hz, 2H), 7.36 (t, J = 7.6 Hz, 2H), 7.30–7.26 (m, 1H), 6.88 (t, J = 7.8 Hz, 1H), 6.47–6.40 (m, 2H), 6.30 (s, 1H), 6.10 (d, J = 8.1 Hz, 1H), 5.49–5.32 (m, 2H), 4.82 (s, 1H), 3.68 (s, 2H), 2.17 (s, 3H), 1.75 (s, 1H) ppm. **^{13}C NMR** (101 MHz, CDCl$_3$): δ 145.25, 141.07, 138.41, 136.65, 128.84, 128.44, 127.45, 127.03, 118.41, 118.32, 116.64, 113.00, 70.80, 64.82, 21.69 ppm. **IR** (neat): ν = 3399, 2920, 1605, 1589, 1446, 1324, 1040, 699 cm^{-1}. **HRMS** (ESI+, MeOH): *m/z* calcd. 276.1359 (M + Na)$^+$, found: 276.1353. **UPC2** conditions: IA column, Isocratic CO$_2$/MeOH = 90 : 10, 3 ml/min, 1500 psi; 91% *ee*, 95.3 : 4.7 *er*; $[\alpha]_D^{25}$ = -103.2 (*c* = 0.11, CHCl$_3$).
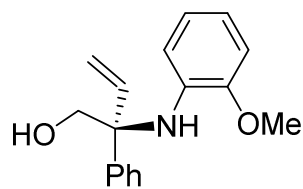
Scale: 0.2 mmol; isolated 20.0 mg (37% yield), Hexane : EA = 5 : 1, R_f = 0.26; 95% *ee*. **^{1}H NMR** (400 MHz, CDCl$_3$): δ 7.54–7.48 (m, 2H), 7.37–7.33 (m, 2H), 7.29–7.26 (m, 1H), 6.80–6.78 (m, 1H), 6.59 (td, J = 7.7, 1.6 Hz, 1H), 6.52 (td, J = 7.7, 1.5 Hz, 1H), 6.43 (dd, J = 17.3, 10.7 Hz, 1H), 6.00–5.98 (m, 1H), 5.44 (dd, J = 10.7, 1.1 Hz, 1H), 5.32 (dd, J = 17.3, 1.1 Hz, 1H), 3.92 (s, 3H), 3.74 (s, 2H), 1.76 (s, 1H) ppm. **^{13}C NMR** (101 MHz, CDCl$_3$): δ 147.40, 141.11, 136.68, 134.80, 128.85, 127.43, 127.04, 120.30, 118.18, 116.58, 115.06, 109.49, 70.69, 64.67, 55.66 ppm. **IR** (neat): ν = 3406, 2935, 1599, 1508, 1454, 1226, 1027, 700 cm^{-1}. **HRMS** (ESI+, MeOH): *m/z* calcd. 292.1308 (M + Na)$^+$, found: 292.1300. **UPC2** conditions: IC column, Isocratic CO$_2$/EtOH = 95 : 5, 3 ml/min, 1500 psi; 95% *ee*, 97.3 : 2.7 *er*; $[\alpha]_D^{25}$ = -100.9 (*c* = 0.11, CHCl$_3$).
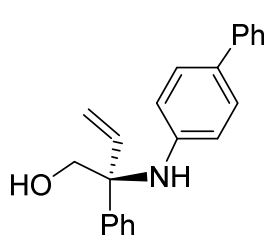
Scale: 0.2 mmol; isolated 32.1 mg (51% yield), Hexane : EA = 5 : 1, R_f = 0.20; 94% *ee*. **^{1}H NMR** (500 MHz, CDCl$_3$): δ 7.57–7.53 (m, 2H), 7.51–7.46 (m, 2H), 7.40–7.34 (m, 7.7 Hz, 4H), 7.32–7.28 (m, 3H), 7.24–7.21 (m, 1H), 6.52–6.41 (m, 3H), 5.50 (dd, J = 10.7, 1.0 Hz, 1H), 5.42 (dd, J = 17.3, 1.0 Hz, 1H), 5.00 (s, 1H), 3.71 (s, 2H), 1.76 (s, 1H) ppm. **^{13}C NMR** (101 MHz, CDCl$_3$): δ 144.73, 141.24, 140.80, 136.29, 130.09, 128.97, 128.68, 127.60, 127.30, 127.04, 126.31, 126.10, 118.74, 116.07, 70.96, 64.94 ppm. **IR** (neat): ν = 3555, 3411, 2930, 1611, 1490, 1321,

1104, 1065, 825, 692 cm^{-1}. **HRMS** (ESI+, MeOH): *m/z* calcd. 338.1515 (M + Na)$^+$, found: 338.1520.**UPC2** conditions: IA column, Isocratic CO_2/MeOH = 70 : 30, 3 ml/min, 1500 psi; 94% *ee*, 97.1 : 2.9 *er*; $[\alpha]_D^{25}$ = -9.5 (*c* = 0.13, CHCl$_3$).
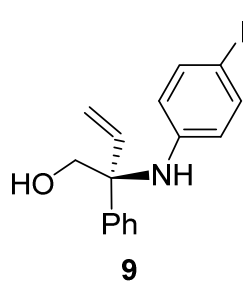
Scale: 0.2 mmol; isolated 56.2 mg (77% yield), Hexane : EA = 5 : 1, R_f = 0.20; 94% *ee*. **^{1}H NMR** (500 MHz, CDCl$_3$): δ 7.49–7.44 (m, 2H), 7.36 (t, *J* = 7.6 Hz, 2H), 7.29 (t, *J* = 7.3 Hz, 1H), 7.27–7.23 (m, 2H), 6.41 (dd, *J* = 17.3, 10.7 Hz, 1H), 6.14 (d, *J* = 8.8 Hz, 2H), 5.47 (d, *J* = 10.7 Hz, 1H), 5.35 (d, *J* = 17.3 Hz, 1H), 4.97 (s, 1H), 3.63 (s, 2H), 1.71 (s, 1H) ppm. **^{13}C NMR** (101 MHz, CDCl$_3$): δ 144.92, 140.26, 137.24, 135.62, 129.02, 127.71, 126.92, 118.96, 117.99, 78.26, 71.11, 64.86 ppm. **IR** (neat): ν = 3394, 3026, 1587, 1488, 1293, 1062, 810, 700 cm^{-1}. **HRMS** (ESI+, MeOH): *m/z* calcd. 366.0349 (M + H)$^+$, found: 366.0353. **UPC2** conditions: IA column, Isocratic CO_2/MeOH = 80 : 20, 3 ml/min, 1500 psi; 94% *ee*, 97.1 : 2.9 *er*; $[\alpha]_D^{25}$ = -66.9 (*c* = 0.14, CHCl$_3$).
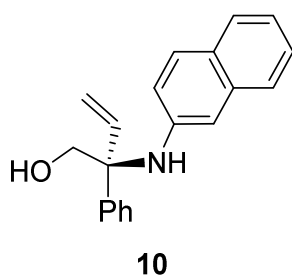
Scale: 0.2 mmol; isolated 38.2 mg (66% yield), Hexane : EA = 5 : 1, R_f = 0.27; 90% *ee*. **^{1}H NMR** (500 MHz, CDCl$_3$): δ 7.62 (d, *J* = 8.1 Hz, 1H), 7.59–7.54 (m, 3H), 7.39–7.33 (m, 3H), 7.31–7.28 (m, 1H), 7.27–7.23 (m, 1H), 7.17–7.12 (m, 1H), 6.87 (dd, *J* = 8.8, 2.4 Hz, 1H), 6.51 (dd, *J* = 17.3, 10.7 Hz, 1H), 6.41 (d, *J* = 2.2 Hz, 1H), 5.48 (dd, *J* = 10.7, 0.9 Hz, 1H), 5.41 (dd, *J* = 17.3, 0.9 Hz, 1H), 5.09 (s, 1H), 3.73 (s, 2H), 1.80 (s, 1H) ppm. **^{13}C NMR** (75 MHz, CDCl$_3$): δ 142.72, 140.53, 135.93, 134.53, 128.95, 128.50, 127.60, 127.57, 127.26, 127.05, 126.15, 126.08, 122.11, 119.29, 118.79, 109.42, 71.06, 65.05 ppm. **IR** (neat): ν = 3389, 3053, 2925, 1627, 1578, 1225, 809, 700 cm^{-1}. **HRMS** (ESI+, MeOH): *m/z* calcd. 312.1359 (M + Na)$^+$, found: 312.1357. **UPC2** conditions: IA column, Isocratic CO_2/EtOH = 80 : 20, 1500 psi, 3 ml/min; 90% *ee*, 95.2 : 4.8 *er*; $[\alpha]_D^{25}$ = -55.0 (*c* = 0.09, CHCl$_3$).
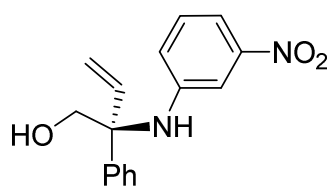
Scale: 0.2 mmol; isolated 36.0 mg (63% yield), Hexane : EA = 5 : 1, R_f = 0.12; 92% *ee*. **¹H NMR** (500 MHz, CDCl₃): δ 7.48 (d, *J* = 7.3 Hz, 2H), 7.44–7.40 (m, 1H), 7.37 (t, *J* = 7.6 Hz, 2H), 7.31 (d, *J* = 7.3 Hz, 1H), 7.21 (t, *J* = 2.2 Hz, 1H), 7.09 (t, *J* = 8.2 Hz, 1H), 6.61–6.59 (m, 1H), 6.46 (dd, *J* = 17.3, 10.7 Hz, 1H), 5.53–5.48 (m, 1H), 5.39–5.34 (m, 1H), 5.31 (s, 1H), 3.67 (s, 2H), 1.80 (s, 1H) ppm. **¹³C NMR** (126 MHz, CDCl₃): δ 148.90, 146.25, 139.53, 135.00, 129.20, 129.12, 128.00, 126.86, 121.21, 119.35, 111.93, 109.80, 71.21, 65.13 ppm. **IR** (neat): ν = 3397, 2927, 1618, 1522, 1346, 1064, 734, 701 cm⁻¹. **HRMS** (ESI+, MeOH): *m/z* calcd. 307.1053 (M + Na)⁺, found: 307.1047. **UPC2** conditions: IA Column, Isocratic CO₂/MeOH = 85 : 15, 3 ml/min, 1500 psi; 92% *ee*, 96.2 : 3.8 *er*; $[\alpha]_D^{25}$ = -102.2 (*c* = 0.13, CHCl₃).
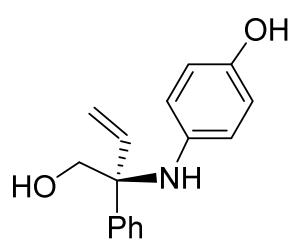
Scale: 0.2 mmol; isolated 30.0 mg (59% yield), Hexane : EA = 5 : 1, R_f = 0.19; 95% *ee*. **¹H NMR** (400 MHz, CD₃OD): δ 7.53– 7.47 (m, 2H), 7.32–7.28 (m, 2H), 7.23–7.20 (m, 1H), 6.46– 6.33 (m, 3H), 6.30–6.23 (m, 2H), 5.35–5.24 (m, 2H), 3.69 (d, *J* = 10.9 Hz, 1H), 3.62 (d, *J* = 10.9 Hz, 1H) ppm. **¹³C NMR** (101 MHz, CD₃OD): δ 149.83, 143.50, 140.18, 139.07, 129.23, 128.54, 127.85, 118.89, 117.40, 116.03, 71.12, 65.98 ppm. **IR** (neat): ν = 3508, 3342, 2932, 1514, 1485, 1206, 756, 693 cm⁻¹. **HRMS** (ESI+, MeOH): *m/z* calcd. 254.1187 (M-H)⁻, found: 254.1184. **UPC2** conditions: IA column, Isocratic CO₂/MeOH = 85 : 15, 3 ml/min, 1500 psi; 95% *ee*, 97.4 : 2.6 *er*; $[\alpha]_D^{25}$ = -20.0 (*c* = 0.10, CHCl₃).
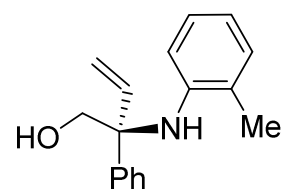
Scale: 0.2 mmol; isolated 30.0 mg (59% yield), Hexane : EA = 5 : 1, R_f = 0.31; 97% *ee*. **¹H NMR** (400 MHz, CDCl₃): δ 7.54– 7.47 (m, 2H), 7.36–7.34 (m, 2H), 7.32–7.26 (m, 1H), 7.07 (d, *J* = 7.3 Hz, 1H), 6.81–6.72 (m, 1H), 6.59–6.56 (m, 1H), 6.48 (dd, *J* = 17.3, 10.7 Hz, 1H), 5.99 (d, *J* = 8.1 Hz, 1H), 5.46 (dd, *J* = 10.7, 1.0 Hz, 1H), 5.30 (dd, *J* = 17.3, 1.0 Hz, 1H), 4.82 (s, 1H), 3.72 (d, *J* = 6.8 Hz, 2H), 2.32 (s, 3H), 1.76 (t, *J* = 7.0 Hz, 1H) ppm. **¹³C NMR** (101 MHz, CDCl₃): δ 142.93, 141.01, 136.41, 130.13, 128.89, 127.47, 126.91, 125.98, 122.72, 118.40, 116.90, 115.22, 71.23, 64.86, 18.02 ppm. **IR** (neat): ν = 3415, 3020, 2924, 1604, 1585, 1506, 1446, 1048, 746, 700 cm⁻¹. **HRMS** (ESI+, MeOH): *m/z* calcd. 276.1359 (M + Na)⁺, found: 276.1356.

UPC2 conditions: IC column, Isocratic CO_2/IPA = 95:5, 3 ml/min, 1500 psi; 97% *ee*, 98.5 : 1.5 *er*; $[\alpha]_D^{25}$ = -124.5 (*c* = 0.11, $CHCl_3$).
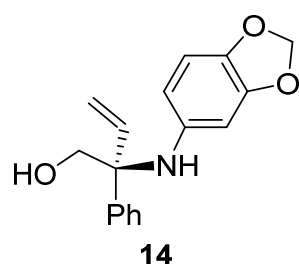
Scale: 0.2 mmol; isolated 36.0 mg (64% yield), Hexane : EA = 5 : 1, R_f = 0.14; 91% *ee*. **^{1}H NMR** (400 MHz, $CDCl_3$): δ 7.54–7.48 (m, 2H), 7.38–7.34 (m, 2H), 7.32–7.27 (m, 1H), 6.50 (d, *J* = 8.4 Hz, 1H), 6.40 (dd, *J* = 17.4, 10.8 Hz, 1H), 5.98 (d, *J* = 2.3 Hz, 1H), 5.86–5.84 (m, 1H), 5.80–5.74 (m, 2H), 5.47 (dd, *J* = 10.8, 1.1 Hz, 1H), 5.37 (dd, *J* = 17.4, 1.1 Hz, 1H), 3.66 (s, 2H), 1.89–1.65 (s, 1H) ppm. **^{13}C NMR** (126 MHz, $CDCl_3$): δ 147.68, 141.03, 140.72, 139.44, 136.73, 128.88, 127.53, 127.06, 118.46, 108.26, 107.90, 100.53, 98.74, 70.62, 65.11 ppm. **IR** (neat): ν = 3389, 2872, 1501, 1485, 1199, 1036, 928, 759, 700 cm^{-1}. **HRMS** (ESI+, MeOH): *m/z* calcd. 306.1101 (M + Na)$^+$, found: 306.1107. **UPC2** conditions: IA column, Isocratic CO_2/MeOH = 85 : 15, 3 ml/min, 1500 psi; 91% *ee*, 95.3 : 4.8 *er*; $[\alpha]_D^{25}$ = -53.7 (*c* = 0.14, $CHCl_3$).
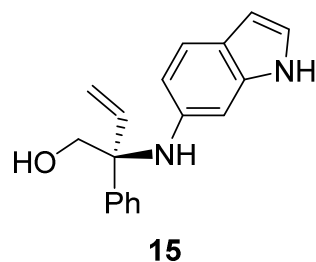
Scale: 0.2 mmol; isolated 25.0 mg (45% yield), Hexane : EA = 5 : 1, R_f = 0.06; 39% *ee*. **^{1}H NMR** (400 MHz, $CDCl_3$): δ 7.63–7.55 (m, 3H), 7.38–7.28 (m, 4H), 6.89–6.87 (m, 1H), 6.53–6.42 (m, 2H), 6.35 (s, 1H), 6.10 (s, 1H), 5.46–5.36 (m, 2H), 3.72 (s, 2H) ppm. **^{13}C NMR** (101 MHz, $CDCl_3$): δ 141.30, 141.11, 136.82, 136.68, 128.85, 127.40, 127.21, 121.71, 120.89, 120.13, 118.39, 112.04, 102.33, 97.55, 70.64, 65.12 ppm. **IR** (neat): ν = 3416, 2925, 1628, 1513, 1445, 1210, 1063, 802, 693 cm^{-1}. **HRMS** (ESI+, MeOH): *m/z* calcd. 279.1492 (M + H)$^+$, found: 279.1490. **UPC2** conditions: IA column, Isocratic CO_2/MeOH = 85 : 15, 1500 psi, 3 ml/min; 40% *ee*, 69.5 : 30.5 *er*; $[\alpha]_D^{25}$ = -19.9 (*c* = 0.11, $CHCl_3$).
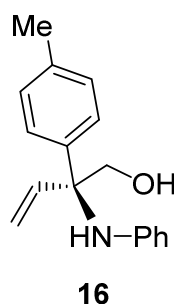
Scale: 0.2 mmol; isolated 44.0 mg (86% yield), Hexane : EA = 5 : 1, R_f = 0.29; 90% *ee*. **^{1}H NMR** (400 MHz, $CDCl_3$): δ *J* = 8.0 Hz 7.40 (d, *J* = 8.2 Hz, 2H), 7.17 (d, *J* = 8.0 Hz, 2H), 7.04–7.00 (m, 2H), 6.62 (t, *J* = 7.3 Hz, 1H), 6.48–6.34 (m, 3H), 5.45 (dd, *J* = 10.7, 1.1 Hz, 1H), 5.36 (dd, *J* = 17.3, 1.0 Hz, 1H), 4.88 (s, 1H), 3.66 (d, *J* = 5.4 Hz, 2H), 2.35 (s, 3H), 1.77 (s, 1H) ppm. **^{13}C NMR** (126 MHz, $CDCl_3$): δ 145.35, 137.85, 137.13, 136.55, 129.60, 128.62, 126.92, 118.37, 117.20, 115.81, 70.94, 64.62, 21.10 ppm. **IR**

(neat): ν = 3399, 2923, 1600, 1499, 1314, 1033, 813, 748, 693 cm^{-1}. **HRMS** (ESI+, MeOH): *m/z* calcd. 276.1359 (M + Na)$^+$, found: 276.1357. **UPC2** conditions: IA column, Isocratic CO_2/MeOH = 90 : 10, 1500 psi, 3 ml/min; 90% *ee*, 94.9 : 5.1 *er*; $[\alpha]_D^{25}$ = -87.0 (*c* = 0.10, CHCl$_3$).
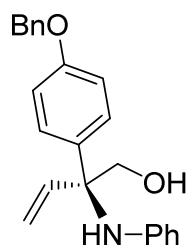
Scale: 0.2 mmol; isolated 58.0 mg (84% yield), Hexane : EA = 5 : 1, R_f = 0.17; 89% *ee*. **^{1}H NMR** (400 MHz, CDCl$_3$) δ 7.46–7.32 (m, 7H), 7.05–7.01 (m, 2H), 7.00–6.95 (m, 2H), 6.67–6.61 (m, 1H), 6.46–6.37 (m, 3H), 5.45 (dd, *J* = 10.7, 1.1 Hz, 1H), 5.36 (dd, *J* = 17.3, 1.1 Hz, 1H), 5.06 (s, 2H), 4.87 (s, 1H), 3.66 (d, *J* = 3.8 Hz, 2H), 1.77 (s, 1H) ppm. **^{13}C NMR** (101 MHz, CDCl$_3$): δ 158.18, 145.33, 137.04, 136.52, 133.05, 128.71, 128.64, 128.22, 128.12, 127.66, 118.33, 117.24, 115.82, 115.12, 70.89, 70.16, 64.37 ppm. **IR** (neat): ν = 3543, 3426, 2927, 1600, 1504, 1236, 1022, 815, 742, 688 cm^{-1}. **HRMS** (ESI+, MeOH): *m/z* calcd. 368.1621 (M + Na)$^+$, found: 368.1619. **UPC2** conditions: IA column, Isocratic CO_2/MeOH = 90 : 10, 1500 psi, 3 ml/min; 90% *ee*, 94.9 : 5.1 *er*; $[\alpha]_D^{25}$ = -58.5 (*c* = 0.10, CHCl$_3$).
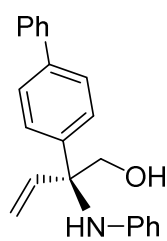
Scale: 0.2 mmol; isolated 40.0 mg (64% yield), Hexane : EA = 5 : 1, R_f = 0.17; 86% *ee*. **^{1}H NMR** (400 MHz, CDCl$_3$): δ 7.62–7.59 (m, 6H), 7.46–7.43 (m, 2H), 7.37–7.33 (m, 1H), 7.06–7.02 (m, 2H), 6.65 (t, *J* = 10.3 Hz, 1H), 6.54–6.39 (m, 3H), 5.49 (dd, *J* = 10.7, 1.0 Hz, 1H), 5.41 (dd, *J* = 17.3, 1.0 Hz, 1H), 3.73 (s, 2H), 1.80 (s, 1H) ppm. **^{13}C NMR** (126 MHz, CDCl$_3$): δ 145.22, 140.61, 140.26, 139.98, 136.36, 128.91, 128.70, 127.54, 127.49, 127.14, 118.63, 117.38, 115.89, 70.87, 64.73 ppm. **IR** (neat): ν = 3568, 3419, 2932, 1596, 1504, 1486, 1319, 1058, 751, 691 cm^{-1}. **HRMS** (ESI+, MeOH): *m/z* calcd. 338.1515 (M + Na)$^+$, found: 338.1506. **UPC2** conditions: IA column, Isocratic CO_2/MeOH = 70 : 30, 1500 psi, 3 ml/min; 86% *ee*, 93.0 : 7.0 *er*; $[\alpha]_D^{25}$ = -105.0 (*c* = 0.10, CHCl$_3$).
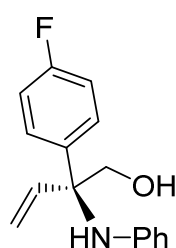
Scale: 0.2 mmol; isolated 28.3 mg (55% yield), Hexane : EA = 5 : 1, R_f = 0.26; 91% *ee* . **^{1}H NMR** (400 MHz, CDCl$_3$): δ 7.52–7.46 (m, 2H), 7.06–7.00 (m, 7.1 Hz, 4H), 6.64 (t, *J* = 7.3 Hz, 1H), 6.44 – 6.34 (m, 3H), 5.50–5.45 (m, 1H), 5.39–5.33 (m, 1H), 4.85 (s, 1H), 3.70–3.60 (m, 2H), 1.80 (s, 1H) ppm. **^{19}F NMR** (376 MHz, CDCl$_3$): δ -115.56 ppm. **^{13}C NMR** (101 MHz, CDCl$_3$): δ 162.18 (d, *J* = 247 Hz), 145.02, 136.64 (d, *J* = 3

Hz), 136.13, 128.80, 128.71, 118.76, 117.50, 115.83, 115.61, 70.78, 64.44 ppm. **IR** (neat): ν = 3560, 3422, 1596, 1503, 1225, 1031, 746, 676 cm^{-1}. **HRMS** (ESI+, MeOH): *m/z* calcd. 258.1289 (M + H)$^+$, found: 258.1287. **UPC2** conditions: IA column, Isocratic CO$_2$/MeOH = 90 : 10, 1500 psi, 3 ml/min; 91% *ee*, 95.5 : 4.5 *er*; $[\alpha]_D^{25}$ = -96.3 (*c* = 0.11, CHCl$_3$).
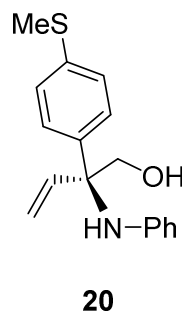
Scale: 0.2 mmol; isolated 40.0 mg (70% yield), Hexane : EA = 5 : 1, R_f = 0.20; 88% *ee*. **¹H NMR** (400 MHz, CDCl$_3$): δ 7.44–7.41 (m, 2H), 7.26–7.20 (m, 2H), 7.04–7.00 (m, 2H), 6.65–6.61 (m, 1H), 6.44–6.35 (m, 3H), 5.46 (dd, *J* = 10.7, 1.0 Hz, 1H), 5.36 (dd, *J* = 17.3, 1.0 Hz, 1H), 4.88 (s, 1H), 3.68–3.62 (m, 2H), 2.47 (s, 3H), 1.80 (s, 1H) ppm. **¹³C NMR** (101 MHz, CDCl$_3$): δ 145.13, 137.69, 137.66, 136.18, 128.66, 127.54, 126.76, 118.59, 117.34, 115.81, 70.79, 64.50, 15.69 ppm. **IR** (neat): ν = 3394, 3019, 2920, 1599, 1495, 1315, 1062, 748, 694 cm^{-1}. **HRMS** (ESI+, MeOH): *m/z* calcd. 308.1080 (M + Na)$^+$, found: 308.1077. **UPC2** conditions: IA column, Isocratic CO$_2$/MeOH = 70 : 30, 1500 psi, 3 ml/min; 88% *ee*, 93.8 : 6.2 *er*; $[\alpha]_D^{25}$ = -65.2 (*c* = 0.10, CHCl$_3$).
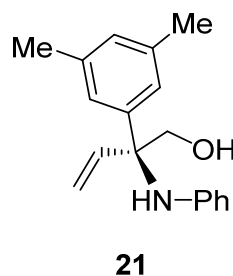
Scale: 0.2 mmol; isolated 31.0 mg (58% yield), Hexane : EA = 5 : 1, R_f = 0.31; 93% *ee*. **¹H NMR** (400 MHz, CDCl$_3$): δ 7.13 (s, 2H), 7.04–7.00 (m, 2H), 6.93 (s, 1H), 6.67–6.56 (m, 1H), 6.50–6.34 (m, 3H), 5.44 (dd, *J* = 10.8, 1.1 Hz, 1H), 5.34 (dd, *J* = 17.4, 1.1 Hz, 1H), 4.84 (s, 1H), 3.67 (s, 2H), 2.31 (s, 6H), 1.75 (s, 1H) ppm. **¹³C NMR** (101 MHz, CDCl$_3$): δ 145.49, 141.01, 138.31, 136.71, 129.19, 128.62, 124.70, 118.23, 117.21, 115.86, 70.76, 64.73, 21.70 ppm. **IR** (neat): ν = 3397, 3016, 2917, 1599, 1499, 1313, 1054, 748, 693 cm^{-1}. **HRMS** (ESI+, MeOH): *m/z* calcd. 268.1696 (M + H)$^+$, found: 268.1698. **HPLC** conditions: Chiralpak IA (250 × 4.6 mm, 5μm), Hex/IPA = 90:10, 1500 psi, 3 ml/min; 93% *ee*, 96.4 : 3.6 *er*; $[\alpha]_D^{25}$ = -78.8 (*c* = 0.10, CHCl$_3$).
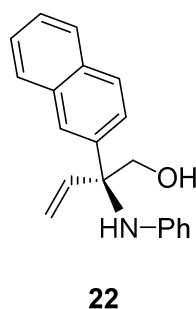
Scale: 0.2 mmol; isolated 26.0 mg (45% yield), Hexane : EA = 5 : 1, R_f = 0.23; 91% *ee*. **¹H NMR** (400 MHz, CDCl$_3$): δ 7.97 (d, *J* = 1.7 Hz, 1H), 7.86–7.80 (m, 3H), 7.69–7.66 (m, 1H), 7.52–7.46 (m, 2H), 7.02–6.94 (m, 2H), 6.64–6.52 (m, 2H), 6.45–6.41 (m, 2H), 5.53 (dd, *J* = 10.7, 0.9 Hz, 1H), 5.43 (dd, *J* = 17.4, 0.9 Hz, 1H), 4.98 (s, 1H), 3.77 (s, 2H), 1.80 (s, 1H) ppm. **¹³C NMR** (126 MHz, CDCl$_3$): δ 145.33, 138.74, 136.44,

133.52, 132.81, 128.75, 128.73, 128.32, 127.66, 126.29, 126.25, 126.09, 125.02, 118.68, 117.43, 115.85, 70.65, 64.99 ppm. **IR** (neat): ν = 3557, 3400, 2931, 1598, 1502, 1177, 1060, 745, 692 cm^{-1}. **HRMS** (ESI+, MeOH): m/z calcd. 312.1359 (M + Na)$^+$, found: 312.1361. **UPC2** conditions: IA column, Isocratic CO_2/MeOH = 85 : 15, 1500 psi, 3 ml/min; 91% ee, 95.3 : 4.7 er; $[\alpha]_D^{25}$ = -123.5 (c = 0.10, CHCl$_3$).
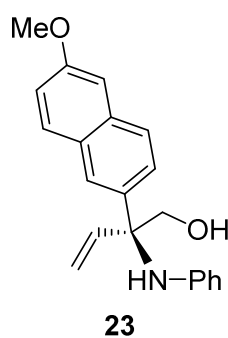
Scale: 0.2 mmol; isolated 48.0 mg (75% yield), Hexane : EA = 5 : 1, R_f = 0.17; 94% ee. ^{1}**H NMR** (400 MHz, CDCl$_3$): δ 7.91–7.87 (m, 1H), 7.72 (d, J = 8.7 Hz, 2H), 7.64–7.62 (m, 1H), 7.18–7.12 (m, 2H), 7.02–6.94 (m, 2H), 6.61 (t, J = 7.3 Hz, 1H), 6.54 (dd, J = 17.4, 10.8 Hz, 1H), 6.43 (d, J = 7.8 Hz, 2H), 5.55–5.47 (m, 1H), 5.46–5.37 (m, 1H), 3.92 (s, 3H), 3.75 (s, 2H) ppm. ^{13}**C NMR** (101 MHz, CDCl$_3$): δ 158.04, 145.41, 136.55, 136.32, 133.93, 129.78, 129.00, 128.70, 127.57, 125.88, 125.55, 119.11, 118.49, 117.35, 115.84, 105.61, 70.69, 64.85, 55.47 ppm. **IR** (neat): ν = 3390, 3015, 2934, 1599, 1498, 1262, 1028, 748, 694 cm^{-1}. **HRMS** (ESI+, MeOH): m/z calcd. 320.1645 (M + H)$^+$, found: 320.1640. **UPC2** conditions: IA column, Isocratic CO_2/MeOH = 85 : 15, 1500 psi, 3 ml/min; 94% ee, 97.1 : 2.9 er; $[\alpha]_D^{25}$ = -98.6 (c = 0.13, CHCl$_3$).
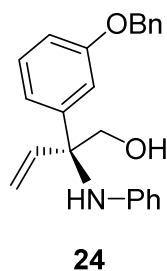
Scale: 0.2 mmol; isolated 42.1 mg (61% yield), Hexane : EA = 5 : 1, R_f = 0.21; 95% ee. ^{1}**H NMR** (400 MHz, CDCl$_3$): δ 7.44–7.39 (m, 4H), 7.37–7.32 (m, 1H), 7.30 (d, J = 8.2 Hz, 1H), 7.21–7.19 (m, 1H), 7.15 (d, J = 7.8 Hz, 1H), 7.07–7.02 (m, 2H), 6.94–6.92 (m, 1H), 6.66 (t, J = 7.3 Hz, 1H), 6.48–6.38 (m, 3H), 5.47 (dd, J = 10.7, 0.9 Hz, 1H), 5.38 (dd, J = 17.3, 0.9 Hz, 1H), 5.04 (s, 2H), 4.90 (s, 1H), 3.70 (d, J = 5.3 Hz, 2H), 1.79 (s, 1H) ppm. ^{13}**C NMR** (101 MHz, CDCl$_3$): δ 159.31, 145.23, 142.86, 136.98, 136.37, 129.89, 128.68, 128.65, 128.12, 127.75, 119.60, 118.51, 117.37, 115.84, 114.23, 113.56, 70.79, 70.22, 64.82 ppm. **IR** (neat): ν = 3566, 3395, 2929, 1598, 1498, 1247, 1026, 744, 696 cm^{-1}. **HRMS** (ESI+, MeOH): m/z calcd. 346.1802 (M + H)$^+$, found: 346.1801. **UPC2** conditions: ID column, Isocratic CO_2/MeOH = 95 : 5, 1500 psi, 3 ml/min; 95% ee, 97.4 : 2.6 er; $[\alpha]_D^{25}$ = -60.7 (c = 0.12, CHCl$_3$).
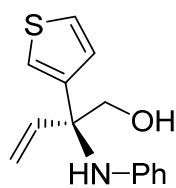
Scale: 0.2 mmol; isolated 39.2 mg (80% yield), Hexane : EA = 5 : 1, R_f = 0.23; 76% *ee*. **^{1}H NMR** (400 MHz, CDCl$_3$): δ 7.31–7.29 (m, 1H), 7.22–7.21 (m, 1H), 7.12–7.10 (m, 1H), 7.06–7.00 (m, 2H), 6.64 (t, *J* = 7.3 Hz, 1H), 6.45–6.43 (m, 2H), 6.33 (dd, *J* = 17.3, 10.6 Hz, 1H), 5.42 (dd, *J* = 10.6, 1.0 Hz, 1H), 5.35 (dd, *J* = 17.3, 0.9 Hz, 1H), 4.86 (s, 1H), 3.74–3.62 (m, 2H), 1.77 (s, 1H) ppm. **^{13}C NMR** (126 MHz, CDCl$_3$): δ 145.40, 143.08, 136.84, 128.66, 126.87, 126.39, 122.33, 118.24, 117.46, 115.73, 70.45, 63.30 ppm. **IR** (neat): ν = 3566, 3409, 2938, 1598, 1500, 1321, 1035, 748, 693 cm^{-1}. **HRMS** (ESI+, MeOH): *m/z* calcd. 268.0767 (M + Na)$^+$, found: 268.0756. **UPC2** conditions: IA column, Isocratic CO$_2$/MeOH = 90 : 10, 1500 psi, 3 ml/min; 76% *ee*, 88.1 : 11.9 *er*; $[\alpha]_D^{25}$ = -57.8 (*c* = 0.11, CHCl$_3$).
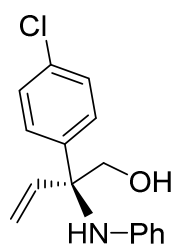
Scale: 0.2 mmol; isolated 25.0 mg (46% yield), Hexane : EA = 5 : 1, R_f = 0.26; 91% *ee*. **^{1}H NMR** (400 MHz, CDCl$_3$): δ 7.48–7.43 (m, 2H), 7.37–7.29 (m, 2H), 7.04–7.00 (m, 2H), 6.66–6.22 (m, 1H), 6.44–6.31 (m, 3H), 5.47 (dd, *J* = 10.7, 0.9 Hz, 1H), 5.36 (dd, *J* = 17.3, 0.9 Hz, 1H), 4.88 (s, 1H), 3.69–3.61 (m, 2H), 1.80 (s, 1H) ppm. **^{13}C NMR** (101 MHz, CDCl$_3$): δ 144.91, 135.90, 135.50, 133.43, 129.03, 128.74, 128.52, 118.92, 117.59, 115.83, 70.68, 64.52 ppm. **IR** (neat): ν = 3401, 3019, 2926, 1600, 1496, 1315, 1062, 748, 699 cm^{-1}. **HRMS** (ESI+, MeOH): *m/z* calcd. 274.0993 (M + H)$^+$, found: 274.0986. **UPC2** conditions: IA column, Isocratic CO$_2$/MeOH = 85 : 15, 1500 psi, 3 ml/min; 91% *ee*, 95.3 : 4.7 *er*; $[\alpha]_D^{25}$ = -51.8 (*c* = 0.10, CHCl$_3$).
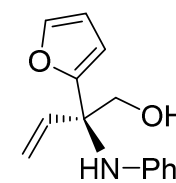
Scale: 0.2 mmol; isolated 36.2 mg (79% yield), Hexane : EA = 5 : 1, R_f = 0.34; 41% *ee*. **^{1}H NMR** (500 MHz, CDCl$_3$): δ 7.39 (dd, *J* = 1.8, 0.9 Hz, 1H), 7.09–7.03 (m, 2H), 6.69–6.66 (m, 1H), 6.56–6.51 (m, 2H), 6.36–6.23 (m, 3H), 5.45 (s, 1H), 5.42 (dd, *J* = 6.5, 1.2 Hz, 1H), 3.86 (d, *J* = 11.1 Hz, 1H), 3.64 (d, *J* = 11.0 Hz, 1H) ppm. **^{13}C NMR** (126 MHz, CDCl$_3$): δ 1534.08, 145.30, 142.35, 135.16, 128.62, 118.59, 117.89, 115.83, 110.54, 108.64, 69.18, 62.29 ppm. **IR** (neat): ν = 3380, 2926, 1599, 1497, 1314, 1012, 740, 693 cm^{-1}. **HRMS** (ESI+, MeOH): *m/z* calcd. 252.0995 (M + Na)$^+$, found: 252.0993. **UPC2** conditions: IA column, Isocratic CO$_2$/MeOH = 90 : 10, 1500 psi, 3 ml/min; 41% *ee*, 70.5 : 29.5 *er*; $[\alpha]_D^{25}$ = 11.8 (*c* = 0.14, CHCl$_3$).
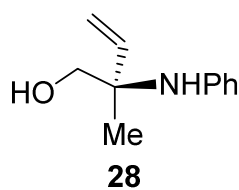
Scale: 0.2 mmol; isolated 25.0 mg (71% yield), Hexane : EA = 5 : 1, R_f = 0.29; 46% *ee*. **^{1}H NMR** (400 MHz, CDCl$_3$): δ 7.16–7.12 (m, 2H), 6.80–6.68 (m, 3H), 5.94 (dd, *J* = 17.5, 10.8 Hz, 1H), 5.31–5.21 (m, 2H), 3.65 (d, *J* = 10.8 Hz, 1H), 3.50 (d, *J* = 10.8 Hz, 1H), 1.39 (s, 3H) ppm. **^{13}C NMR** (101 MHz, CDCl$_3$): δ 146.10, 141.75, 128.97, 118.29, 116.56, 116.14, 69.06, 58.76, 21.91 ppm. **IR** (neat): ν = 3385, 2932, 1600, 1497, 1315, 1030, 748, 694 cm^{-1}. **HRMS** (ESI+, MeOH): *m/z* calcd. 178.1226 (M + H)$^+$, found: 178.1227. **UPC2** conditions: IA column, Isocratic CO$_2$/EtOH = 95 : 5, 1500 psi, 3 ml/min; 46% *ee*, 73.2 : 26.8 *er*; $[\alpha]_D^{25}$ = -4.5 (*c* = 0.12, CHCl$_3$).
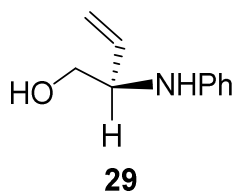
Scale: 0.2 mmol; isolated 25.0 mg (77% yield), Hexane : EA = 5 : 1, R_f = 0.19; 60% *ee*. **^{1}H NMR** (400 MHz, CDCl$_3$): δ 7.21–7.17 (m, 2H), 6.76–6.73 (m, 1H), 6.69–6.66 (m, 2H), 5.81 (ddd, *J* = 17.3, 10.4, 5.5 Hz, 1H), 5.33 (dt, *J* = 17.3, 1.4 Hz, 1H), 5.26 (dt, *J* = 10.4, 1.3 Hz, 1H), 4.06–4.02 (m, 1H), 3.79 (dd, *J* = 11.0, 4.4 Hz, 1H), 3.64 (dd, *J* = 11.0, 6.3 Hz, 1H) ppm. **^{13}C NMR** (101 MHz, CDCl$_3$): δ 147.40, 136.47, 129.33, 118.16, 117.50, 114.03, 65.03, 57.76 ppm. **IR** (neat): ν = 3382, 2929, 1600, 1500, 1315, 1029, 748, 692 cm^{-1}. **HRMS** (ESI+, MeOH): *m/z* calcd. 290.1070 (M + H)$^+$, found: 164.1063. **UPC2** conditions: ID Column, Isocratic CO$_2$/MeOH = 90 : 10, 3 ml/min,1500 psi; 60% *ee*, 80.0 : 20.0 *er*; $[\alpha]_D^{25}$ = 20.9 (*c* = 0.13, CHCl$_3$).
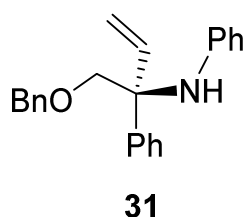
Scale: 0.2 mmol; isolated 51.0 mg, 77% yield, Hexane : EA = 30 : 1, R_f = 0.45; 93% *ee*. **^{1}H NMR** (500 MHz, CDCl$_3$): δ 7.55 (d, *J* = 7.6 Hz, 2H), 7.40–7.25 (m, 8H), 7.03 (t, *J* = 7.8 Hz, 2H), 6.66 (t, *J* = 7.3 Hz, 1H), 6.49–6.35 (m, 3H), 5.48–5.25 (m, 2H), 4.99 (s, 1H), 4.56 (s, 2H), 3.71 (d, *J* = 9.3 Hz, 1H), 3.61 (d, *J* = 9.3 Hz, 1H) ppm. **^{13}C NMR** (126 MHz, CDCl$_3$): δ 145.69, 141.47, 137.95, 137.17, 128.57, 128.55, 127.92, 127.90, 127.78, 127.37, 127.27, 117.36, 116.20, 77.78, 73.59, 63.93 ppm. **IR** (neat): ν = 3400, 3026, 2857, 1498, 1313, 1078, 747, 695 cm^{-1}. **HRMS** (ESI+, MeOH): *m/z* calcd. 352.1672 (M + Na)$^+$, found: 352.1677. **UPC2** conditions: IA Column, CO$_2$:IPA = 100:0, 3 ml/min,1500 psi; 93% *ee*, 96.7 : 3.3 *er*; $[\alpha]_D^{25}$ = -107.7 (*c* = 0.07, CHCl$_3$).
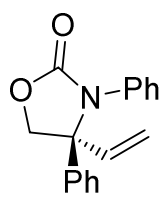
32

Scale: 0.2 mmol; isolated 51.0 mg, 96% yield, Hexane : EA = 10 : 1, R_f = 0.12; 95% *ee.* **^{1}H NMR** (500 MHz, CDCl$_3$): δ 7.44–7.42 (m, 2H), 7.39–7.36 (m, 2H), 7.35–7.31 (m, 1H), 7.22–7.17 (m, 4H), 7.10–7.06 (m, 1H), 6.38 (dd, *J* = 17.4, 10.9 Hz, 1H), 5.59 (d, *J* = 10.9 Hz, 1H), 5.49 (d, *J* = 17.4 Hz, 1H), 4.54 (d, *J* = 8.5 Hz, 1H), 4.40 (d, *J* = 8.5 Hz, 1H) ppm. **^{13}C NMR** (126 MHz, CDCl$_3$): δ 156.31, 139.60, 136.20, 135.56, 129.16, 128.67, 128.65, 126.95, 125.45, 124.15, 119.32, 76.11, 69.57 ppm. **IR** (neat): ν = 3064, 2982, 2912, 1743, 1493, 1381, 1211, 1062, 1022, 771, 699 cm^{-1}. **HRMS** (ESI+, MeOH): *m/z* calcd. 266.1176 (M + H)$^+$, found: 266.1177. **UPC2** conditions: Chiralpak IA column (100 × 4.6 mm, 3 μm), isocratic CO$_2$/MeOH = 90 : 10; 3 ml/min, 1500 psi; 95% *ee*, 97.5 : 2.5 *er*; $[\alpha]_D^{25}$ = -13.1 (*c* = 0.08, CHCl$_3$).
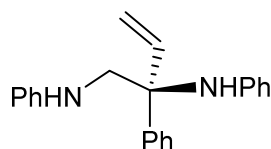
33

Scale: 0.2 mmol, isolated 32 mg, 51% yield, (Hexane : EA = 10 : 1, R_f = 0.53). 95% *ee.* **^{1}H NMR** (400 MHz, CDCl$_3$): δ 7.57–7.55 (m, 2H), 7.37 (t, *J* = 7.5 Hz, 2H), 7.29 (t, *J* = 7.3 Hz, 1H), 7.21–7.17 (m, 2H), 7.01–6.97 (m, 2H), 6.77 (t, *J* = 7.3 Hz, 1H), 6.67 (d, *J* = 7.5 Hz, 2H), 6.60 (t, *J* = 7.3 Hz, 1H), 6.48 (dd, *J* = 17.3, 10.8 Hz, 1H), 6.35–6.32 (m, 2H), 5.47 (dd, *J* = 10.7, 1.1 Hz, 1H), 5.39 (dd, *J* = 17.3, 1.2 Hz, 1H), 3.48 (d, *J* = 12.0 Hz, 1H), 3.34 (d, *J* = 12.0 Hz, 1H) ppm. **^{13}C NMR** (101 MHz, CDCl$_3$): δ 148.05, 145.23, 142.17, 137.32, 129.51, 128.94, 128.63, 127.48, 126.94, 118.63, 118.01, 117.24, 115.82, 113.90, 63.59, 55.50 ppm. **IR** (neat): ν = 3390, 3048, 1597, 1498, 1424, 1263, 1029, 744, 688 cm^{-1}. **HRMS** (ESI+, MeOH): *m/z* calcd. 315.1856 (M + H)$^+$, found: 315.1858. **UPC2** conditions: Chiralpak IA column (100 × 4.6 mm, 3 μm), isocratic CO$_2$/MeOH = 90 : 10; 3 ml/min, 1500 psi; 95% *ee*, 97.5 : 2.5 *er*; $[\alpha]_D^{25}$ = 72.2 (*c* = 0.08, CHCl$_3$).
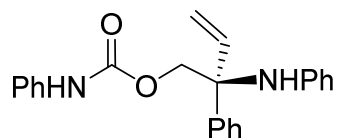
34

Scale: 0.2 mmol; isolated 67.0 mg, 93% yield, Hexane : EA = 10 : 1, R_f = 0.23; 93% *ee.* **^{1}H NMR** (500 MHz, CDCl$_3$): δ 7.56–7.54 (m, 2H), 7.38–7.29 (m, 7H), 7.10 (t, *J* = 7.1 Hz, 1H), 7.03–7.00 (m, 2H), 6.68–6.63 (m, 2H), 6.43–6.38 (m, 3H), 5.42–5.37 (m, 2H), 4.55 (d, *J* = 11.1 Hz, 1H), 4.32 (d, *J* = 11.3 Hz, 1H) ppm. **^{13}C NMR** (126 MHz, CDCl$_3$): δ 153.44, 145.07, 140.32, 137.55, 136.46, 129.22, 128.80, 128.63, 127.66, 127.29, 123.95, 118.95, 117.98, 117.62, 116.10, 71.16, 63.82 ppm. **IR** (neat): ν = 3891, 3052, 1591, 1498, 1444, 1208, 1057, 1028, 746, 689 cm^{-1}. **HRMS** (ESI+,

MeOH): m/z calcd. 359.1754 (M + H)$^+$, found: 359.1747. **UPC2** conditions: Chiralpak IA column (100 × 4.6 mm, 3 μm), isocratic CO$_2$/MeOH = 85 : 15; 3 ml/min, 1500 psi; 93% *ee*, 96.6 : 3.4 *er*; $[\alpha]_D^{25}$ = -34.2 (*c* = 0.15, CHCl$_3$).

Analytical data for other New Compounds:
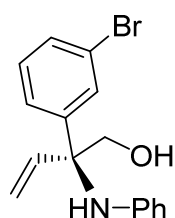
Scale: 0.2 mmol; isolated 18.0 mg (28% yield), Hexane : EA = 5 : 1, R_f = 0.23; 88% *ee.* **^{1}H NMR** (400 MHz, CDCl$_3$): δ 7.66 (t, *J* = 1.8 Hz, 1H), 7.48–7.39 (m, 2H), 7.22 (t, *J* = 7.9 Hz, 1H), 7.05–7.01 (m, 2H), 6.66–6.63 (m, 1H), 6.43–6.30 (m, 3H), 5.48 (dd, *J* = 10.8, 0.9 Hz, 1H), 5.36 (dd, *J* = 17.3, 0.9 Hz, 1H), 4.83 (s, 1H), 3.71–3.60 (m, 2H), 1.77 (s, 1H) ppm. **^{13}C NMR** (101 MHz, CDCl$_3$): δ 144.83, 143.72, 135.71, 130.72, 130.48, 130.05, 128.77, 125.85, 123.11, 119.11, 117.68, 115.88, 70.62, 64.63 ppm. **IR** (neat): ν = 3398, 3018, 1599, 1498, 1474, 1314, 1062, 748, 693 cm^{-1}. **HRMS** (ESI+, MeOH): *m/z* calcd. 318.0488 (M + H)$^+$, found: 318.0479. **UPC2** conditions: IA Column, Isocratic CO$_2$/MeOH = 95 : 5, 3 ml/min,1500 psi; 88% *ee*, 94.0 : 6.0 *er*; $[\alpha]_D^{25}$ = -71.9 (*c* = 0.08, CHCl$_3$).
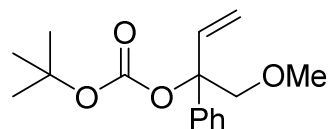
Scale: 2.8 mmol; isolated 720.0 mg (93% yield), Pentane : TEA = 20 : 1, R_f = 0.80. **^{1}H NMR** (400 MHz, CDCl$_3$): δ 7.41–7.33 (m, 4H), 7.29–7.27 (m, 1H), 6.37 (dd, *J* = 17.6, 11.1 Hz, 1H), 5.40 (dd, *J* = 11.1, 0.9 Hz, 1H), 5.35 (dd, *J* = 17.6, 0.9 Hz, 1H), 4.00–3.94 (m, 2H), 3.34 (s, 3H), 1.41 (s, 9H) ppm. **^{13}C NMR** (101 MHz, CDCl$_3$): δ 151.50, 140.62, 137.64, 128.31, 127.73, 125.83, 117.13, 84.63, 82.15, 76.91, 59.71, 27.87 ppm. **IR** (neat): ν = 2980, 2930, 1743, 1252, 1153, 1114, 766, 698 cm^{-1}. **HRMS** (ESI+, MeOH): *m/z* calcd. 301.1410 (M + Na)$^+$, found: 301.1407.
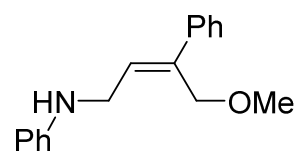
Scale: 0.2 mmol; isolated 26.0 mg (51% yield), Hexane : EA = 30 : 1, R_f = 0.20. **^{1}H NMR** (400 MHz, CDCl$_3$): δ 7.45–7.42 (m, 2H), 7.36–7.32 (m, 2H), 7.29–7.26 (m, 1H), 7.23–7.19 (m, 2H), 6.76–6.73 (m, 1H), 6.69–6.67 (m, 2H), 6.13 (t, *J* = 6.6 Hz, 1H), 4.40 (s, 2H), 4.02 (d, *J* = 6.7 Hz, 2H), 3.40 (s, 3H) ppm. **^{13}C NMR** (101 MHz, CDCl$_3$): δ 148.15, 140.99, 139.13, 130.53, 129.45, 128.52, 127.57, 126.36, 117.88, 113.20, 69.76,

58.39, 42.24 ppm. **IR** (neat): ν = 3367, 2924, 1752, 1601, 1498, 1255, 1090, 745, 692 cm^{-1}. **HRMS** (ESI+, MeOH): *m/z* calcd. 254.1539 (M + H)$^{+}$, found: 254.1536.

2.4.8 X-ray Crystallographic Data for Allylic Amine 1

Table 2.8. Crystal data and structure refinement for allylic amine **1** (CCDC-1496759).

Empirical formula	$C_{16}H_{17}NO$
Formula weight	239.30
Temperature	100(2) K
Wavelength	0.71073 Å
Crystal system	Orthorhombic
Space group	$P2(1)2(1)2(1)$
Unit cell dimensions	$a = 5.78299(6)$Å $\quad\quad \alpha = 90°$
	$b = 12.54070(14)$Å $\quad \beta = 90°$
	$c = 17.36504(15)$Å $\quad \gamma = 90°$
Volume	1259.36(2) Å^3
Z	4
Density (calculated)	1.262 mg/m^3
Absorption coefficient	0.078 mm^{-1}
F(000)	512
Theta range for data collection	2.003 to 63.013°
Index ranges	-14<=h<=13,-27<=k<=27,-42<=l<=43
Reflections collected	113700
Independent reflections	18084 [R(int) = 0.0249]
Completeness to theta =63.013°	92.1%
Absorption correction	Multi-scan
Max. and min. transmission	0.991 and 0.762
Refinement method	Full-matrix least-squares on F^2
Data / restraints / parameters	18084/ 310/ 393
Goodness-of-fit on F^2	1.109
Final R indices [I>2sigma(I)]	$R_1 = 0.0260, wR_2 = 0.0787$
R indices (all data)	$R_1 = 0.0278, wR_2 = 0.0796$
Flack parameter	$x = 0.05(8)$
Largest diff. peak and hole	0.508 and -0.187 e·Å^{-3}
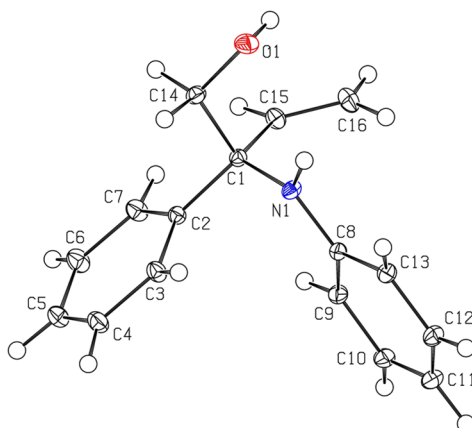
The measured crystal of **1** was stable under atmospheric conditions; nevertheless, it was treated under inert conditions immersed in perfluoro-polyether as protecting oil for manipulation. Data Collection: measurements were made on a Bruker-Nonius diffractometer equipped with an APPEX II 4K CCD area detector, a FR591 rotating anode with Mo Kα radiation, Montel mirrors and a Kryoflex low temperature device (T = −173 °C). Full-sphere data collection was used with ω and φ scans. Programs used: Data collection Apex2 V2011.3 (Bruker-Nonius 2008), data reduction Saint+Version 7.60A (Bruker AXS 2008) and absorption correction SADABS V. 2008−1 (2008). Structure Solution: SHELXTL Version 6.10 (Sheldrick, 2000) was used.[49] Structure Refinement: SHELXTL-97-UNIX VERSION.

---

(49) G. M. Sheldrick, *SHELXTL Crystallographic System*, version 6.10; Bruker AXS, Inc.: Madison, WI, **2000**.

Chapter 3.

Asymmetric Synthesis of α,α-Disubstituted Allylic Amines through Palladium-Catalyzed Allylic Substitution

3.1 Introduction

3.1.1 General Background

Pd-catalyzed regio- and enantioselective allylic substitution towards branched allylic amines has traditionally been extremely challenging. Nucleophilic attack by the amine on the less crowded terminal carbon atom of the π-allyl-Pd intermediate is much more favored than attack on the sterically hindered internal carbon atom, thus giving the linear derivative as the major product.[1] In this context, there are rather few examples of successful preparation of sterically demanding (*rac*)-α,α-disubstituted allylic amines through Pd-catalyzed allylic substitution, and these show limitations in the α,α-disubstitution pattern (often two methyl groups) and functional group diversity.[2]

Chiral α,α-disubstituted allylic amines represent a class of amines featuring a quaternary stereocenter which have found important applications in biology and pharmaceutical industry,[3] and their synthesis is thus of high significance.[4] Despite notable success in the preparation of allylic amines via transition metal catalyzed allylic substitution in the last decade,[5] the asymmetric synthesis of α,α-disubstituted allylic

---

(1) a) I. Dubovyk, I. D. G. Watson, A. K. Yudin, *J. Am. Chem. Soc.* **2007**, *129*, 14172; b) A. M. Johns, Z. Liu, J. F. Hartwig, *Angew. Chem. Int. Ed.* **2007**, *46*, 7259; c) I. Dubovyk, I. D. G. Watson, A. K. Yudin, *J. Org. Chem.* **2013**, *78*, 1559; d) K. F. Johnson, R. V. Zeeland, L. M. Stanley, *Org. Lett.* **2013**, *15*, 2798; e) I. D. G. Watson, A. K. Yudin, *J. Am. Chem. Soc.* **2005**, *127*, 17516.
(2) The regioselective allylic substitution toward branched *α-mono*-substituted allylic amines based on palladium catalysis is already challenging with few exceptions, see: a) O. G. Mancheno, J. Priego, S. Cabrera, R. G. Arrayas, T. Llamas, J. C. Carretero, *J. Org. Chem.* **2003**, *68*, 3679; b) J. W. Faller, J. C. Wilt, *Org. Lett.* **2005**, *7*, 633; c) S. You, X. Zhu, Y. Luo, X. Hou, L. Dai, *J. Am. Chem. Soc.* **2001**, *123*, 7471.
(3) *Chiral Amine Synthesis*; T. C. Nugent, Ed.; Wiley-VCH: New York, 2008.
(4) For reviews on the application and synthesis of allylic amines: a) L. Huang, M. Arndt, K. Gooßen, H. Heydt, L. J. Gooßen, *Chem. Rev.* **2015**, *115*, 2596; b) B. M. Trost, M. L. Crawley, *Chem. Rev.* **2003**, *103*, 2921; c) B. M. Trost, T. Zhang, J. D. Sieber, *Chem. Sci.* **2010**, *1*, 427; d) M. Johannsen, K. A. Jørgensen, *Chem. Rev.* **1998**, *98*, 1689; e) B. M. Trost, D. L. Van Vranken, *Chem. Rev.* **1996**, *96*, 395; f) T. E. Müller, K. C. Hultzsch, M. Yus, F. Foubelo, M. Tada, *Chem. Rev.* **2008**, *108*, 3795; g) S. Hong, T. J. Marks, *Acc. Chem. Res.* **2004**, *37*, 673; h) T. E. Müller, M. Beller, *Chem. Rev.* **1998**, *98*, 675; i) J. F. Hartwig, L. M. Stanley, *Acc. Chem. Res.* **2010**, *43*, 1461; j) B. M. Trost, D. R. Fandrick, *Aldrichimica Acta* **2007**, *40*, 59.
(5) For representative examples using Ir catalysis: a) M. J. Pouy, A. Leitner, D. J. Weix, S. Ueno, J. F. Hartwig, *Org. Lett.* **2007**, *9*, 3949; b) M. Roggen, E. M. Carreira, *J. Am. Chem. Soc.* **2010**, *132*, 11917; c) L. M. Stanley, J. F. Hartwig, *Angew. Chem. Int. Ed.* **2009**, *48*, 7841; d) A. Leitner, S. Shekhar, M. J. Pouy, J. F. Hartwig, *J. Am. Chem. Soc.* **2005**, *127*, 15506; e) O. V. Singh, H. Han, *J. Am. Chem. Soc.* **2007**, *129*, 774; f) S. Shekhar, B. Trantow, A. Leitner, J. F. Hartwig, *J. Am. Chem. Soc.* **2006**, *128*, 11770; g) A. Leitner, C. Shu, J. F. Hartwig, *Org. Lett.* **2005**, *7*, 1093; h) R. Takeuchi, N. Ue, K. Tanabe, K. Yamashita, N. Shiga, *J. Am. Chem. Soc.* **2001**, *123*, 9525; i) Y. Yamashita, A. Gopalarathnam, J. F. Hartwig, *J. Am. Chem. Soc.* **2007**, *129*, 7508; j) T. Ohmura, J. F. Hartwig, *J. Am. Chem. Soc.* **2002**, *124*, 15164; k) R. Weihofen, O. Tverskoy, G. Helmchen, *Angew. Chem. Int. Ed.* **2006**, *45*, 5546; l) A. Leitner, C. T. Shu, J. F. Hartwig, *Proc. Natl. Acad. Sci. U.S.A.* **2004**, *101*, 5830; m) L. M. Stanley, J. F. Hartwig,

amines based on allylic substitution using economically more attractive Pd catalysis has remained extremely challenging and to date underdeveloped.[5, 6]

In previous seminal contributions, Trost and co-workers reported the Pd-catalyzed ring-opening of isoprene monoxide with amines/phthalimides towards enantioenriched α,α-disubstituted allylic N-alkyl amines though with limited substrate scope.[7] In 2007, the Peters group reported the asymmetric formation of α,α-disubstituted allylic trifluoroacetimidates through Pd-catalyzed aza-claissen rearrangements (Scheme 3.1).[8] They found that the enantioselectivity-determining step involves enantioface-selective olefin coordination to the Pd(II) center, allowing high enantioselectivities even when using 3,3-disubstituted substrates in which the two substituents at the 3-position have an identical size.
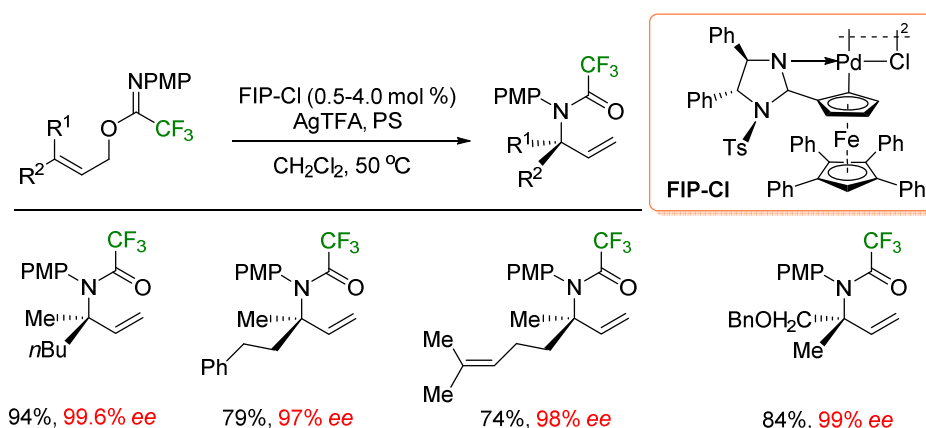
Scheme 3.1. The asymmetric formation of α,α-disubstituted allylic trifluoro-acetimidates through Pd-catalyzed aza-claissen rearrangement.

We recently developed a Pd-catalyzed decarboxylative allylic amination process toward the construction of enantioenriched α,α-disubstituted allylic N-aryl amines (chapter 2 of this thesis) from substituted vinyl cyclic carbonates and anilines.[9] The protocol uses highly modular vinyl cyclic carbonates and unactivated amine nucleophiles

---

J. Am. Chem. Soc. **2009**, *131*, 8971; n) C. Shu, A. Leitner, J. F. Hartwig, *Angew. Chem. Int. Ed.* **2004**, *43*, 4797.

(6) For Rh-catalyzed allylic amine formation: a) J. S. Arnold, E. T. Mwenda, H. M. Nguyen, *Angew. Chem. Int. Ed.* **2014**, *53*, 3688; b) P. A. Evans, J. E. Robinson, J. D. Nelson, *J. Am. Chem. Soc.* **1999**, *121,* 6761; c) J. S. Arnold, G. T. Cizio, H. M. Nguyen, *Org. Lett.* **2011**, *13*, 5576; For utilization of Ru catalysis: d) M. Kawatsura, K. Uchida, S. Terasaki, H. Tsuji, M. Minakawa, T. Itoh, *Org. Lett.* **2014**, *16*, 1470; e) S. Mizuno, S. Terasaki, T. Shinozawa, M. Kawatsura, *Org. Lett.* **2017**, *19*, 504.

(7) a) B. M. Trost, C. Jiang, K. Hammer, *Synthesis* **2005**, 3335; b) B. M. Trost, R. C. Bunt, R. C. Lemoine, T. L. Calkins*, J. Am. Chem. Soc.* **2000**, *122*, 5968.

(8) D. F. Fischer, Z. Xin, R. Peters, *Angew. Chem. Int. Ed.* **2007**, *46*, 7704.

(9) A. Cai, W. Guo, L. Martínez-Rodríguez, A. W. Kleij, *J. Am. Chem. Soc*. **2016**, *138*, 14194.

as substrates, and this method features minimal waste production (only CO_2), ample scope in reaction partners.[10] The use of a Me-protected linear carbonate analogue of the vinyl cyclic carbonate substrate in this decarboxylative process resulted mainly in linear allylic amine formation, which points toward a privileged selectivity for branched product when using vinyl cyclic carbonate and aromatic amines. As a consequence, this decarboxylative approach is limited to the use of aryl amines only since the more nucleophilic aliphatic amines quickly attack the carbonate carbon of the vinyl cyclic carbonates, leading to an undesired carbamate formation through ring-opening aminolysis (Scheme 3.2).[11]
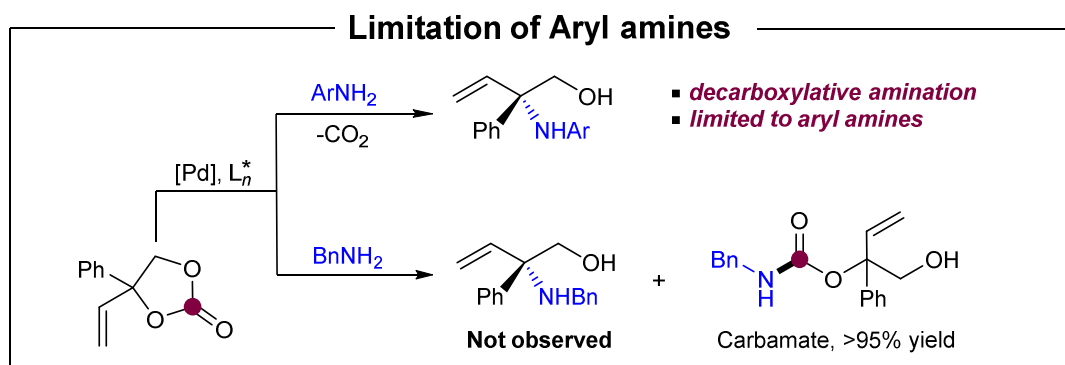
Scheme 3.2. Pd-catalyzed decarboxylative amination for the construction of enantioenriched α,α-disubstituted allylic *N*-aryl amines.

3.1.2 Aim of the Work presented in this Chapter

Although massive attention has been paid to the synthesis of allylic amines in the past decades,[5, 6] to the best of our knowledge, there is still no general approach available for the asymmetric synthesis of α,α-disubstituted allylic *N*-alkyl amines based on transition-metal-catalyzed allylic substitution, which is a long-lasting challenge in organic synthesis.

Based on our previous success with a Pd-catalyzed decarboxylative amination method (Scheme 3.2),[9] we reasoned that in the presence of a suitable Pd complex and a chiral phosphoramidite ligand, the conversion of alkyl amines and racemic tertiary allylic precursors with an appropriate and efficient leaving group (LG) would allow to access

---

(10) For more details, see ref. 9.

(11) The reaction of cyclic carbonate (Scheme 2.1) with $BnNH_2$ or $BuNH_2$ (4 equiv.) at r.t. for 10 min gave rise to quantitative yield of the carbamate product. Relevant contributions describing this aminolysis reactivity: a) M. Blain, L. Jean-Gérard, R. Auvergne, D. Benazet, S. Caillol, B. Andrioletti, *Green Chem*. **2014**, *16*, 4286; b) W. Guo, V. Laserna, E. Martin, E. C. Escudero-Adán, A. W. Kleij, *Chem. Eur. J.* **2016**, *22*, 1722; c) S. Sopeña, V. Laserna, W. Guo, E. Martin, E. C. Escudero-Adán, A. W. Kleij, *Adv. Synth. Catal*. **2016**, *358*, 2172; No reaction is observed between the cyclic carbonate precursor and aniline at 100 ºC for 20 h: d) W. Guo, J. Gónzalez-Fabra, N. A. G. Bandeira, C. Bo, A. W. Kleij, *Angew. Chem. Int. Ed.* **2015**, *54*, 11686.

α,α-disubstituted allylic *N*-alkyl amines (Scheme 3.3). Such a simple and concise approach would offer a general and tunable route towards enantioenriched α,α-disubstituted allylic amine products.
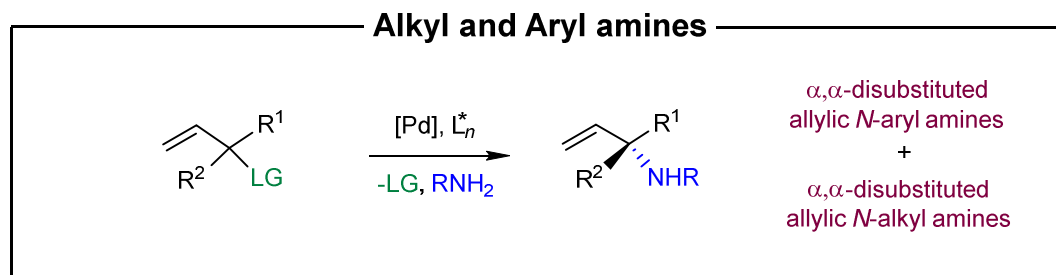
Scheme 3.3. Enantioselective synthesis of α,α-disubstituted allylic *N*-alkyl/aryl amines.

3.2   Results and Discussion

3.2.1 Optimization of the Reaction Conditions

Table 3.1: Preliminary screening of allylic precursors **A−F** towards the synthesis of **(1)**.
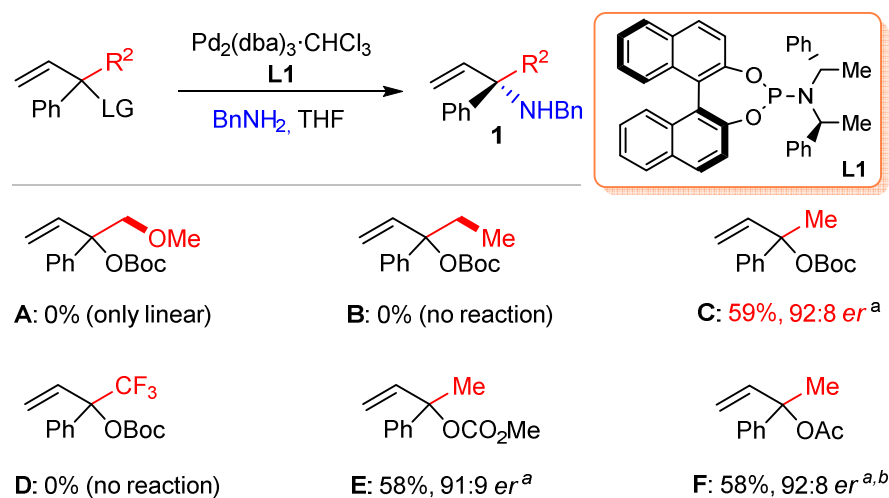
Reaction conditions: allylic precursors: **A−F** (0.15 mmol), BnNH$_2$ (0.23 mmol, 1.5 equiv.), THF (150 μL), Pd$_2$(dba)$_3$·CHCl$_3$ (3.5 mol %), **L1** (14 mol %), open to air, r.t., 12 h. [a] Isolated yield, *er* determined by UPC2 analysis. [b] 36 h.

We started our investigation using the model reaction between benzyl amine and a series of highly substituted allylic precursors **A**–**F** (Table 3.1). In the presence of Pd$_2$(dba)$_3$·CHCl$_3$ (3.5 mol %) and phosphoramidite ligand **L1** (14 mol %),[12] allylic precursor **A** (a Me-protected linear analogue of vinyl cyclic carbonate) was converted quantitatively into a *linear* allylic amine,[9] thus confirming the challenging nature of α,α-disubstituted allylic amine formation.

We reasoned that the steric impediment in the allylic precursor would probably be crucial to bias the regioselectivity towards the formation of branched product **1**. A less bulky, ethyl-substituted tertiary allylic precursor **B** was then tested but no conversion was noted, and we totally recovered the starting materials. To our delight, by decreasing the bulkiness of the alkyl group to a methyl group, conversion of the allylic precursor **C** resulted in a substantial amount of the desired branched allylic amine product **1** in 59% yield and with a high enantiomeric ratio (92.5:7.5 *er*). No reaction was observed when the methyl group was replaced by a CF$_3$ group; this may be explained by the presence of a rather electron-withdrawing group (CF$_3$) that may destabilize the π-allyl-Pd intermediate. Changing the leaving group from OBoc to OCO$_2$Me did not significantly improve the reaction outcome (**C** versus **E**), while the presence of an OAc leaving group (**F**) slowed down the rate of the reaction. These combined results indicated that the leaving group is crucial for the reactivity and selectivity of the reaction.

Encouraged by this first screening phase, we next set up to explore the effect of the solvent using allyl precursor **C** and benzyl amine as reaction partners (Table 3.2). The use of CH$_2$Cl$_2$, acetonitrile (ACN), and DMF increased the yield of the branched allylic amine **1** but with low enantioselectivity (Table 3.2; entries 1, 3 and 5). Both yield and enantiocontrol of the product were decreased when the toluene was used as medium (entry 2). By using 1,4-dioxane and Et$_2$O in this reaction, the desired α,α-disubstituted allylic *N*-alkyl amine **1** was obtained only in 20% and 28% yield, respectively (entries 4 and 6). Whereas the reaction in THF provides high enantioselectivity but low yield of product, and ACN gave the allylic amine in good yield and lower enantiomeric excess, a higher (80%) isolated yield was achieved when the reaction was performed in a mixed solvent system consisting of THF/ACN = 1:1 (*er* 86:14, entry 7). Upon increasing the amount of

---

(12) The use of chiral phosphoramidites is based on our previous success toward branched *N*-aryl amines, see ref. 9. The use of other type of (bidentate) ligands leads to the linear product, see: W. Guo, L. Martínez-Rodríguez, R. Kuniyil, E. Martin, E. C. Escudero-Adán, F. Maseras, A. W. Kleij, *J. Am. Chem. Soc.* **2016**, *138*, 11970.

THF in the mixed solvent medium (THF/CAN = 3:1) the enantioselectivity could be improved without affecting the overall reactivity (entries 7-9).

Table 3.2: Effect of the solvent on the asymmetric synthesis of **(1)**.[a]
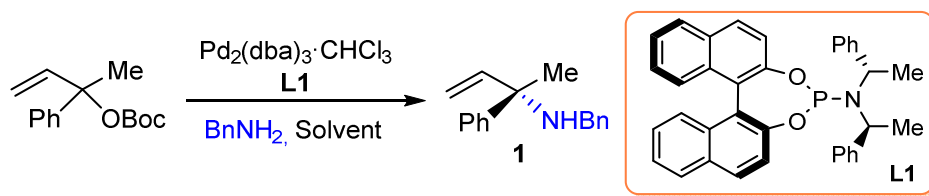
Entry	L	Solvent	T [°C]	Yield [%][b]	er [%][c]
1	L1	CH₂Cl₂	25	63	86:14
2	L1	Toluene	25	34	88:12
3	L1	ACN	25	79	86:14
4	L1	Dioxane	25	20	–
5	L1	DMF	25	83	85:15
6	L1	Et₂O	25	28	87:13
7	L1	THF/ACN (1:1)	25	80	86:14
8	L1	THF/ACN (2:1)	25	79	89:11
9	L1	THF/ACN (3:1)	25	80	91:9

[a] Allyl precursor **C** (0.15 mmol), BnNH₂ (0.23 mmol, 1.5 equiv.), solvent (150 µL), Pd₂(dba)₃·CHCl₃ (3.5 mol %), **L** (14 mol %). [b] Isolated yield. [c]Determined by UPC2.

Subsequently, other phosphoramidite ligands (**L2**–**L7**) were investigated in this benchmark reaction, but their use proved to be less efficient under these conditions (Table 3.3; entry 9 *vs* entries 1–6). The increase of the amount of solvent and decreasing the amount of amine reagent (Table 3.3; entry 7) or catalyst loading (Table 3.3; entry 8) did not significantly change the reaction outcome. The reaction was further optimized using more diluted conditions and lowering the reaction temperature to 0 °C giving the allylic amine target in 78% yield and with an *er* of 95.5:4.5 (Table 3.3; entries 9-10). When the temperature was decreased to -10 °C, a deceleration of the reaction process was observed (Table 3.3; entry 11).

Table 3.3: Effect of other phosphoramidite ligands and reaction parameters on the asymmetric Pd-catalyzed allylic amination towards (**1**).[a]

Entry	L	Solvent	T [ºC]	Yield [%][b]	er [%][c]
1	**L2**	THF/ACN (3:1)	25	57	88:12
2	**L3**	THF/ACN (3:1)	25	74	68:32
3	**L4**	THF/ACN (3:1)	25	40	26:74
4	**L5**	THF/ACN (3:1)	25	18	–
5	**L6**	THF/ACN (3:1)	25	20	–
6	**L7**	THF/ACN (3:1)	25	50	65:35
7[d,e]	**L1**	THF/ACN (3:1)	25	74	92:8
8[d-f]	**L1**	THF/ACN (3:1)	25	74	93:7
9[d-f]	**L1**	THF/ACN (3:1)	0	75	95:5
10[e-g]	**L1**	THF/ACN (3:1)	0	78	95.5:4.5
11[e-g]	**L1**	THF/ACN (3:1)	−10	trace	–

[a] Allyl precursor **C** (0.15 mmol), BnNH$_2$ (0.23 mmol, 1.5 equiv.), solvent (150 μL), Pd$_2$(dba)$_3$·CHCl$_3$ (3.5 mol %), **L** (14 mol %). [b] Isolated yield. [c] Determined by UPC2. [d] Solvent (300 μL). [e] BnNH$_2$ (1.1 equiv.). [f] Pd$_2$(dba)$_3$·CHCl$_3$ (2 mol %), **L1** (10 mol %). [g] Solvent (350 μL).

Table 3.4: Reaction condition screening for *N*-**aryl** allyl amine formation.
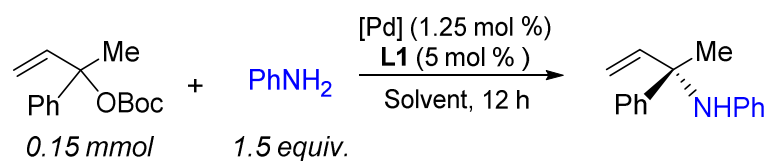
Entry	Aniline (equiv.)	Solvent	T (°C)	Yield (%)[a]	er (%)[b]
1	1.5	THF:CH$_3$CN (3:1, 200 µL)	0	85	85:15
2	**1.5**	**THF (200 µL)**	**0**	**87**	**88:12**
3[c]	1.5	THF (200 µL)	0	85	80.5:19.5
4	1.1	THF (300 µL)	0	82	86.5:13.5
5	1.1	THF (100 µL)	0	83	82:18
6	1.5	THF (200 µL)	−10	89	82.5:17.5
7	1.5	THF (200 µL)	−20	96	77.5:22.5
8	1.5	THF (200 µL)	−30	95	74.5:25.5
9	1.5	THF (200 µL)	25	85	81:19
10	1.5	EtOAc (200 µL)	0	86	82:18
11	1.5	DCE (200 µL)	0	87	79:21
12	1.5	DCM (200 µL)	0	trace	-
13	1.5	Toluene (200 µL)	0	90	74.5:25.5
14	1.5	Et$_2$O (200 µL)	0	80	60.5:39.5

[a] Isolated yield. [b] Determined by HPLC. [c] [Pd]: 2.5 mol %, **L1**: 10 mol %.

Stimulated by the optimization of asymmetric synthesis of *N*-alkyl allyl amine **1**, the preparation of α,α-disubstituted *N*-**aryl** allylic amines was then probed (Table 3.4). Initially the reaction of racemic tertiary allylic carbonate **C** and aniline was selected as a model system. In the presence Pd precursor and phosphoramidite ligand **L1**, in a mixed solvent system consisting of THF/ACN = 3:1 providing the corresponding allylic *N*-aryl amine product in 85% yield and with a moderate *er* value of 80:20 (Table 3.4, entry 1). By further optimization, the *er* value could be improved to 88:12 when the reaction was performed in THF and with a lower catalyst loading (Table 3.4; entry 2: 1.25 mol % [Pd] precursor and 5 mol % of **L1**). Subsequently, the exploration of the volume of solvent, temperature, and various solvents did not further improve the yield or enantioselectivity of the product (Table 3.4, entries 4-14).

3.2.2 Scope of Tertiary Allylic Carbonates

The scope of tertiary allylic Boc-protected precursors was then examined under the optimized conditions (Table 3.5, products **1**-**13**). The absolute configuration for **1** (*S*) was unambiguously confirmed by X-ray analysis of its HCl salt (see Experimental Section). Both electron-donating (**6**, **8**, **9**, **12** and **13**) and withdrawing (**2**, **3**, **5** and **11**) groups in the aryl substituents were tolerated while providing high levels of enantio-induction with *er* values up to 98.5:1.5. The presence of *meta*-, *para*- or *ortho*-substitutions in the aryl group proved to be feasible (**2-6**, **9**, **11-13**). The presence of larger aromatic fragments did not affect the efficiency of the catalysis (**7** and **8**), while the preparation of enantioenriched allylic amines with two α-alkyl substituents was also endorsed as exemplified by the synthesis of compound **10** though with a moderate *er* value.

Table 3.5: Scope of tertiary allylic carbonates.
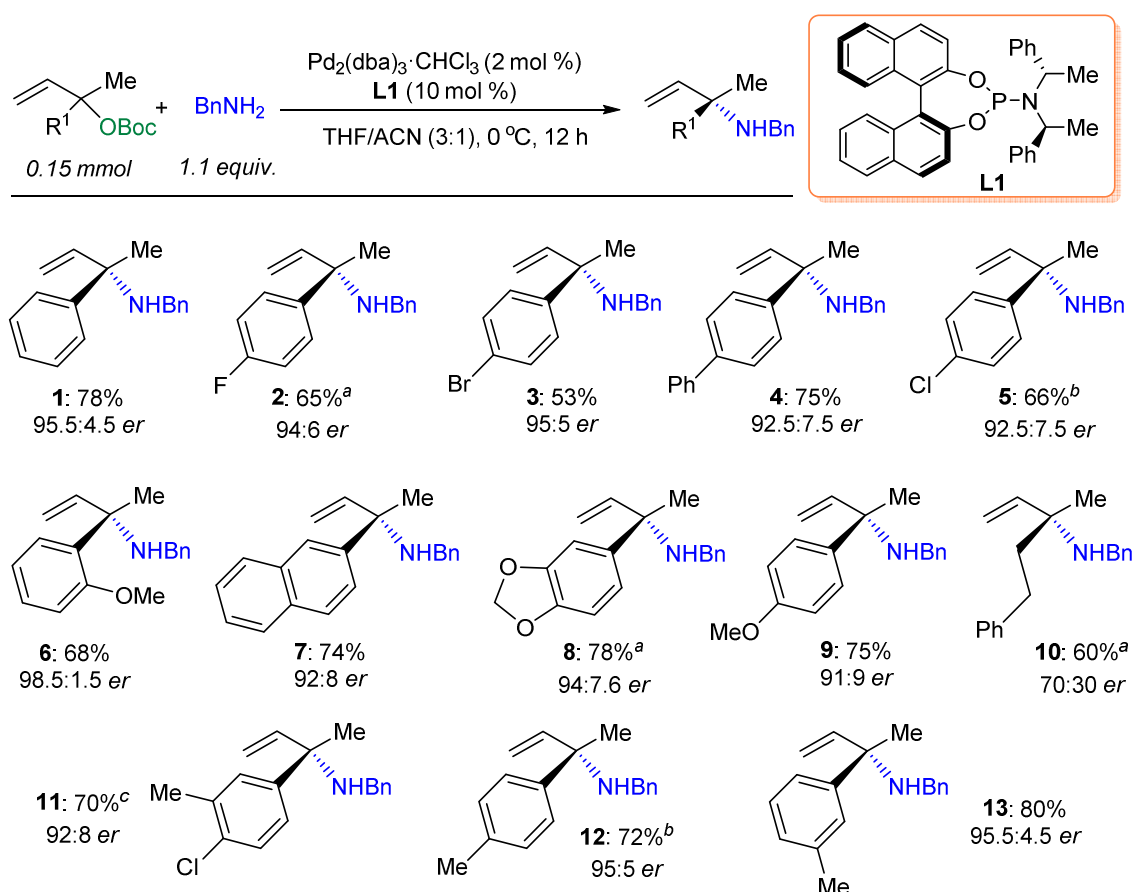
Reaction conditions: allylic precursor (0.15 mmol), BnNH$_2$ (0.17 mmol, 1.1 equiv.), Pd$_2$(dba)$_3$·CHCl$_3$ (2 mol %), **L1** (10 mol %), THF/ACN (3:1; 0.35 mL), 0 °C, open to air, 12 h. Isolated yields are reported, and the *er* values were determined by UPC2. [a] The *er* values were determined by using a chiral shift reagent. [b] 24 h. [c] 36 h.

3.2.3 Scope of Alkyl and Aryl Amines

Table 3.6: Scope of alkyl amines.

14: 53%, 96:4 *er*[a]
64%, 93:7 *er*[a,b]

15: 63%[c]
93:7 *er*

16: 82%
94:6 *er*

17: 45%, 95:5 *er*
74%, 93:7 *er*[b]

18: 86%
94:6 *er*

19: 62%[d]
96:4 *er*

20: 43%
96:4 *er*

21: 66%[e]
94:6 *er*

22: X = O, 86%, 86:14 *er*
23: X = C, 78%, 89:11 *er*

24: 66%[d]
94:6 *er*

25: 32%[d]
92.5:7.5 *er*

26: 72%[e]
96:4 *er*

27: 72%
80.5:19.5 *er*

28: 81%
94:6 *er*

29: 48%, 95:5 *er*[d]
64%, 91:9 *er*[b]
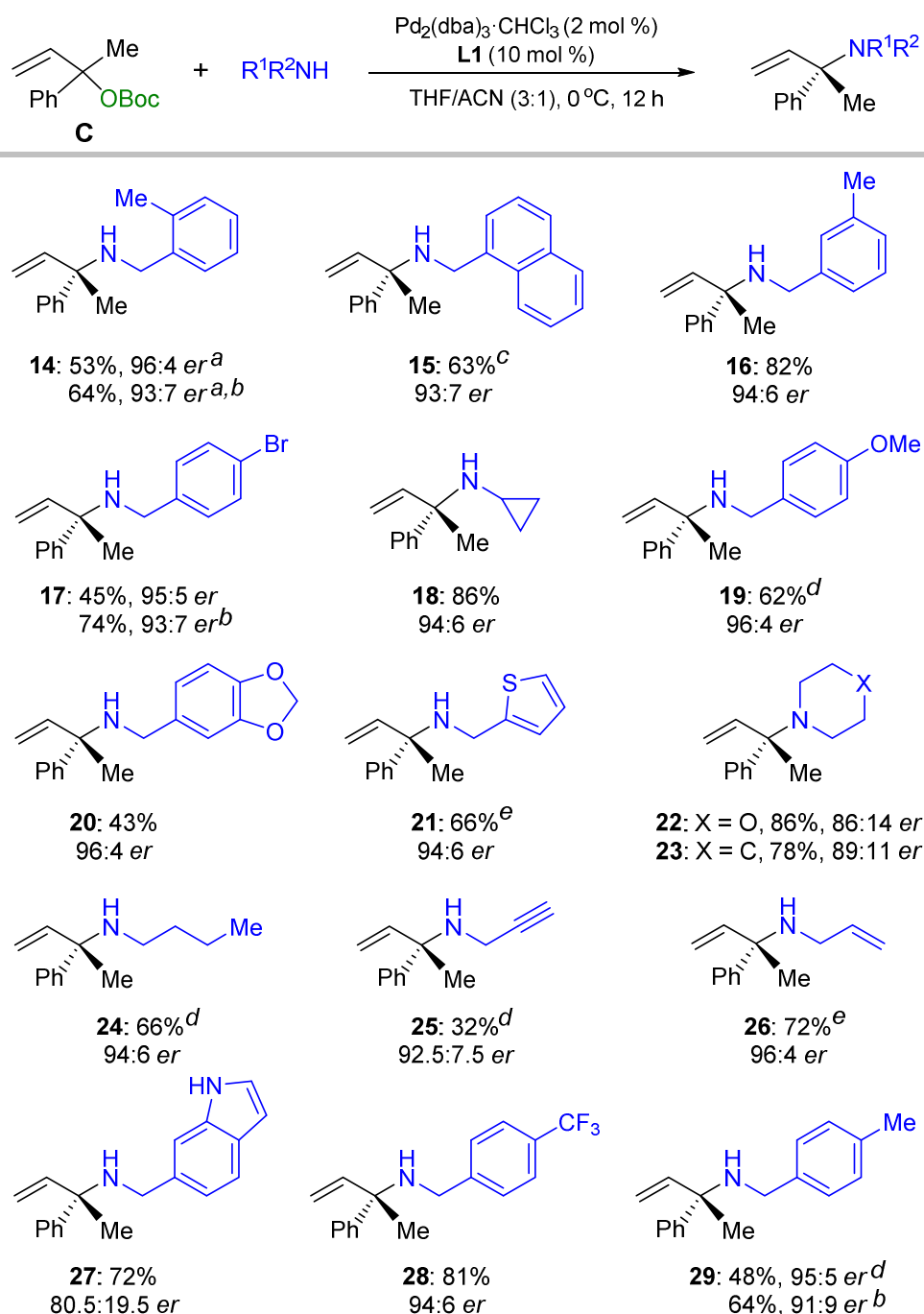
Reaction conditions: allylic precursor **C** (0.15 mmol), amine (0.17 mmol, 1.1 equiv.), Pd$_2$(dba)$_3$·CHCl$_3$ (2 mol %), **L1** (10 mol %), THF/ACN (3:1; 0.35 mL), 0 °C, open to air, 12 h; isolated yields are reported and the *er* values were determined by UPC2. [a] 24 h. [b] CsF (3 equiv.) was added, THF/ACN/H$_2$O (3:1:0.4). [c] Amine (1.5 equiv.). [d] 36 h. [e] The *er* values were determined by using a chiral shift reagent.

Various (functionalized) alkyl amines were found to be suitable reaction partners (Table 3.6, **14-29**). Importantly, more functional amines showed appreciable reactivity and provided good to high *er* values (**18**, **22-26**) unlike in previous reports.[7,8] The presence of a thiophene group did not hamper the successful preparation of **21** despite the potential for catalyst poisoning in the presence of sulfur-containing compounds.[13] Although the use of a propargylic amine reagent resulted in a sluggish reaction, upon reaction for 36 h, only 63% conversion was noted. Longer reaction times did not lead to higher conversion. Allylic amine **25** could be obtained with a 92.5:7.5 *er* value, and may be useful for *in vivo* bio-orthogonal applications through the use of click chemistry.[14]

The amine products comprising of an indole (**27**) or 1,3-benzodioxole fragment (**8** and **20**) are of interest for pharmaceutical development.[15] It is interesting to note that in most cases only trace amounts of the corresponding *linear* allylic amine product were observed (cf., Tables 3.5 and Table 3.6). However, in some cases (Table 3.6; for **14**, **17** and **29**) substantial amount of a 1,3-diene elimination product[16] was detected under the optimized reaction conditions thus resulting in a poorer yield of the desired allylic amine. This side-reaction could be suppressed by addition of CsF which significantly improved the yield of the branched product, although with somewhat lower enantioinduction.

Encouraged by the asymmetric synthesis of various *N*-alkyl allyl amines, the preparation of α,α-disubstituted *N*-**aryl** allylic amines was then further investigated (Table 3.7). The reaction of racemic tertiary allylic precursors and various anilines gave the desired allylic *N*-aryl amines products **30-35** in good yields with appreciable enantioselectivities. Both the aniline and allylic precursor with either electron-donating (**31**, **34** and **35**) or electron-withdrawing (**32** and **33**) aryl substituents were successfully employed in our approach. The use of *N*-methyl aniline (a secondary amine), however, resulted in quantitative formation of the linear product.

(13) J. E. Gómez, W. Guo, A. W. Kleij, *Org. Lett.* **2016**, *18*, 6042.

(14) a) M. Yang, J. Li, P. R. Chen, *Chem. Soc. Rev.* **2014**, *43*, 6511; b) R. K. V. Lim, Q. Lin, *Chem. Commun.* **2010**, *46*, 1589.

(15) 1,3-Benzodioxole and indole motifs are frequently encountered fragments in pharmaceuticals: a) A. Ali, J. Wang, R. S. Nathans, H. Cao, N. Sharova, M. Stevenson, T. M. Rana, *ChemMedChem* **2012**, *7*, 1217; b) J. D. Bloom, M. D. Dutia, B. D. Johnson, A. Wissner, M. G. Burns, E. E. Largis, J. A. Dolan, T. H. Claus, *J. Med. Chem.* **1992**, *35*, 3081.

(16) P. Zhang, H. Le, R. E. Kyne, J. P. Morken, *J. Am. Chem. Soc.* **2011**, *133*, 9716. Base was found to increase the isomerization rate from branched allylic amine to linear product. In our case, all the compounds are stable under the applied reaction conditions.

Table 3.7: Scope of aryl amines.
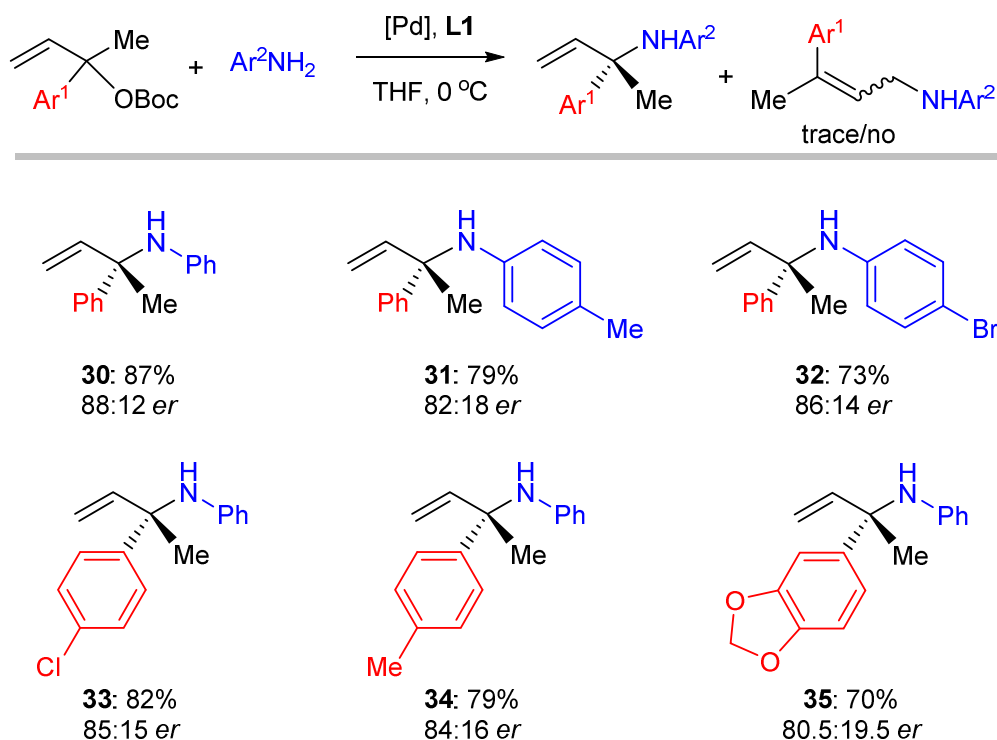
Reaction conditions: allylic precursor (0.15 mmol), aniline reagent (0.23 mmol, 1.5 equiv.), Pd$_2$(dba)$_3$·CHCl$_3$ (1.25 mol %), **L1** (5 mol %), THF (0.2 mL), 0 °C, open to air, 12 h. Isolated yields are reported and the *er* values were determined by UPC2.

3.2.4 Synthetic Transformations of Allylic Alkyl Amine (1)

The catalytic reaction could be easily performed on a 7 mmol scale, which was exemplified by the successful isolation of 1.24 g (75% yield) of allylic amine **1** with high enantioselectivity (*er* 95:5). The synthetic potential of these allylic amines was demonstrated by further transformation of **1** into the enantioenriched amide **36** by treatment with benzoyl chloride, and oxidation of **1** with 3-chloroperbenzoic acid (*m*-CPBA) to afford allylic nitrone **37** in 76% yield while retaining the enantiopurity (Table 3.8). Reaction of allylic amine **1** with phenyl isocyanate gave access to asymmetric urea **38** in 93% yield and 95:5 enantiomeric excess. Finally, by judiciously variation and optimization of the amount of *m*-CPBA, allylic amine **1** could be transformed into chiral epoxide **39**. Additionally, α,α-disubstituted allylic amines can also be transformed into highly functionalized aziridines as reported previously.[17]

---

(17) S. Hayashi, H. Yorimitsu, K. Oshima, *Angew. Chem. Int. Ed*. **2009**, *48*, 7224.

Table 3.8: Synthetic transformations of α,α-disubstituted allylic amine (**1**).

36: 70%, 95:5 *er*

37: 76%, 96:4 *er*

1: 1.24 g, 75% 95:5 *er*

38: 93%, 95:5 *er*

39: 57%, 26:74 *dr* 94.5:5.5 *er*
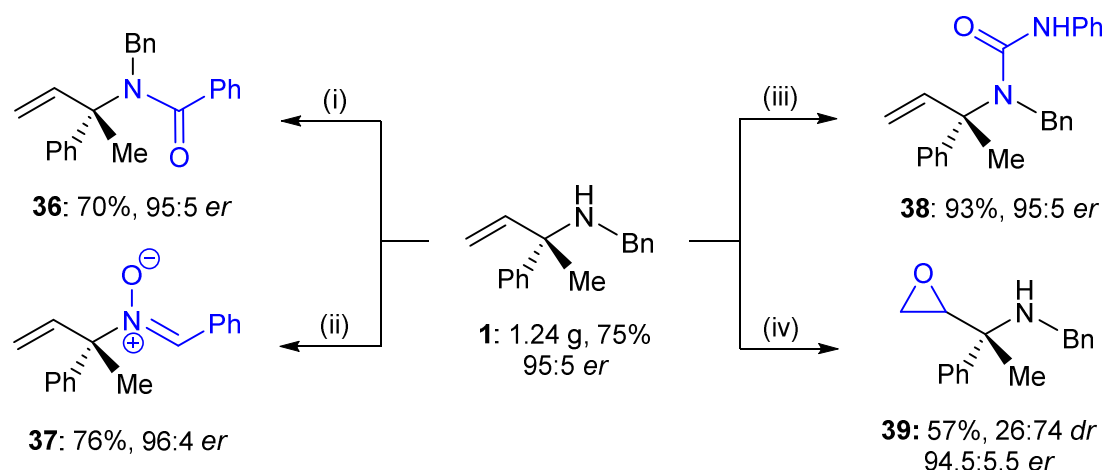
Reaction conditions: (i) Benzoyl chloride (1.3 equiv.), NEt$_3$ (5.0 equiv.), CH$_2$Cl$_2$, r.t., 50 min. (ii) *m*-CPBA (2.3 equiv.), CH$_2$Cl$_2$, 0–r.t., 2 h. (iii) Phenyl isocyanate (1.3 equiv.), NEt$_3$ (10.0 equiv.), CH$_2$Cl$_2$, r.t., 10 min. (iv) TsOH (1.02 equiv.), *m*-CPBA (1.2 equiv.), CH$_2$Cl$_2$, 0–r.t., 3 h.

3.3   Conclusions

In summary, chiral α,α-disubstituted allylic *N*-**alkyl** amines are important building blocks in organic synthesis and medicinal chemistry, but to data no general TM-catalyzed approach has been developed regarding their synthesis. The regio- and enantioselectivity of Pd-catalyzed allylic substitution toward α,α-disubstituted allylic *N*-alkyl amines has been a long-standing challenge. Our contribution represents a first, huge step forward in this area. Despite the fact that some substrate combinations deliver moderately high asymmetric induction levels and some limitations are pertinent to the allylic precursors, this new catalytic approach represents the only general method reported to date. Our work also highlights the key role of the steric modulation in the allylic substrate to prepare challenging chiral allylic amines via economically attractive Pd catalysis compared to Ir- and Rh-based approaches.

3.4 Experimental Section

3.4.1 General Considerations

Commercially available reagents were purchased from Aldrich or TCI, and used without further purification. The Pd precursors were purchased from Aldrich. Phosphoramidites **L1** and **L3**-**L6** were purchased from Aldrich; **L2**[18] and **L7**[19] were prepared according to a previously reported protocol. ^{1}H, ^{13}C$\{^1$H$\}$ and ^{19}F$\{^1$H$\}$ NMR spectra were recorded at room temperature on a Bruker AV-400 or AV-500 spectrometer and referenced to the residual deuterated solvent signals. All reported NMR values are given in parts per million (ppm). FT-IR spectra were collected using a Bruker Optics FTIR Alpha spectrometer. Mass spectrometric analyses, ultra-performance convergence chromatography (UPC2) analyses, and X-ray diffraction studies were performed by the Research Support Group at ICIQ.

3.4.2 Procedure for the Formation of Tertiary Allylic Carbonates
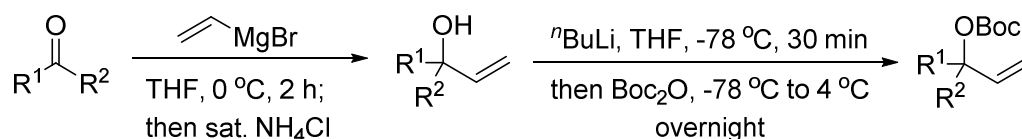
Representative Procedure: The allylic carbonates were prepared according to a reported procedure:[20] to a flame-dried round-bottom flask equipped with a stirring bar was added vinyl magnesium bromide in THF (1.0 M, 15.0 mL, 15.0 mmol) and THF (10 mL). The solution was cooled to 0 ºC and the respective ketone (10.0 mmol) in THF (10 mL) was added dropwise *via* a cannula. The reaction was allowed to stir at 0 ºC for 4 h. The reaction mixture was then quenched with saturated NH$_4$Cl (aq.), and the product extracted with diethyl ether (3 × 20 mL). The combined organic layers were washed with brine, dried over Na$_2$SO$_4$, filtered, and then concentrated under reduced pressure. The crude allylic alcohol product was directly used in the next step.

To a separate flame-dried round-bottom flask equipped with a stirring bar was added the respective allylic alcohol (8 mmol) and THF (16 mL). The solution was cooled to −78 °C (dry ice/acetone) followed by dropwise addition of *n*-butyl lithium (3.55 mL, 8.51 mmol) in hexane (2.40 M). The reaction was allowed to stir for 30 min at -78 °C, after

(18) C. R. Smith, D. J. Mans, T. V. RajanBabu, *Org. Synth.* **2008**, *85*, 238.
(19) D. Polet, A. Alexakis, K. Tissot-Croset, C. Corminboeuf, K. Ditrich, *Chem. Eur. J.* **2006**, *12*, 3596.
(20) P. Zhang, H. Le, R. E. Kyne, J. P. Morken, *J. Am. Chem. Soc.* **2011**, *133*, 9716.

which Boc$_2$O (2.29 g, 10.5 mmol) in THF (5.0 mL) was added dropwise *via a* cannula. The reaction was allowed to warm to 4 $^\circ$C and stirred overnight. The reaction was then diluted with diethyl ether and water. The organic layer was separated and the aqueous layer was extracted into diethyl ether (3 × 20 mL). The combined organic layers were washed with brine, dried over Na$_2$SO$_4$, filtered, and then concentrated *in vacuo*. The crude mixture was purified on silica gel (neutralized with 5% TEA, eluted with 100:1 hexane/EA) to afford the corresponding allylic carbonate.

Preparation of 2-(4-bromophenyl)but-3-en-2-yl-tert-butyl carbonate.

From commercially available 4'-bromoacetophenone, the general procedure was followed for the synthesis of the allylic alcohol intermediate, which was then converted to the carbonate as shown below.
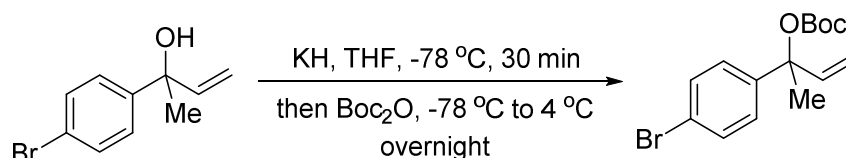
A flame-dried round-bottom flask was charged with KH (562.0 mg, 30 wt % in mineral oil, 4.2 mmol) and purged with N$_2$ three times. Dry hexane (5 mL) was added and the flask was gently swirled. Once the KH settled on the bottom of the flask, hexane was removed *via* cannula. This process was repeated twice, then THF (4.0 mL) was added to create a suspension. The suspension was transferred *via* cannula to another flame-dried round-bottom flask containing a solution of allylic alcohol (852.0 mg, 4.0 mmol) in THF (3.0 mL) at -78 $^\circ$C. The reaction was allowed to stir for 30 minutes at this temperature, followed by addition of Boc$_2$O (1.13 g, 5.2 mmol) in THF (1.0 mL) *via* cannula. The reaction was allowed to warm to 4 $^\circ$C in a cold room and stir overnight. The reaction was diluted with diethyl ether and water. The organic layer was separated and the aqueous layer was extracted into diethyl ether three times. The combined organics were washed with brine, dried over Na$_2$SO$_4$, filtered, and concentrated *in vacuo*. The unpurified reaction mixture was purified on silica gel (neutralized with 5% TEA, eluted with 100:1 hexanes/EA) to afford 1.10 g (84% yield) of a light yellow oil. R_f = 0.50 (8:1 hexanes/EA).[20]

3.4.3 General Procedure for the Synthesis of Chiral Allylic Amines
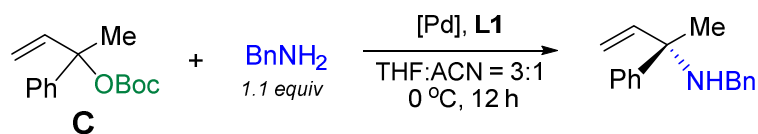
Preparation of allylic N-alkyl amines: The Boc-protected allylic precursor **C** (0.15 mmol, 37 mg, 1 equiv.) was combined with $Pd_2(dba)_3 \cdot CHCl_3$ (3.1 mg, 2 mol %), **L1** (8.1 mg, 10 mol %) and benzyl amine (18 mg, 1.1 equiv.; 0.17 mmol), and then a mixture of THF/CH_3CN (3:1, 0.35 mL) was added at 0 °C open to air. The reaction mixture was stirred at 0 °C for 12 h. Analysis of the unpurified reaction mixture using ^1H NMR was used to determine the conversion of the reaction, then the reaction mixture was purified by flash chromatography (hexane:EA = 10:1, R_f = 0.30) to give the desired product (28 mg, 78%). The *er* value was determined by UPC2 equipped with a chiral column. EA stands for ethyl acetate.
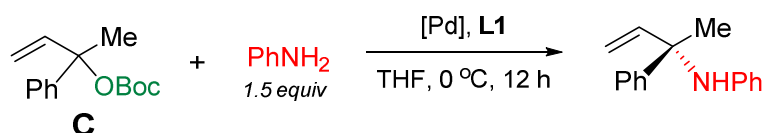
Preparation of allylic N-aryl amines: The tertiary allylic precursor **C** (0.15 mmol, 37 mg, 1 equiv.) was combined with the $Pd_2(dba)_3 \cdot CHCl_3$ (1.95 mg, 1.25 mol %), **L1** (4.05 mg, 10 mol %), aniline (21 mg, 1.5 equiv.; 0.23 mmol), and then a mixture of THF (0.20 mL) was added at 0 °C open to air. The reaction mixture was stirred at 0 °C for 12 h. Analysis of the unpurified reaction mixture using ^1H NMR was used to determine the conversion of the reaction, and then the reaction mixture was purified by flash chromatography (hexane:EA = 25:1, R_f = 0.36) to give the desired product (29 mg, 87%). The *er* value was determined by UPC2 equipped with a chiral column.

3.4.4 Determination of *er* Value with a Chiral Shift Reagent
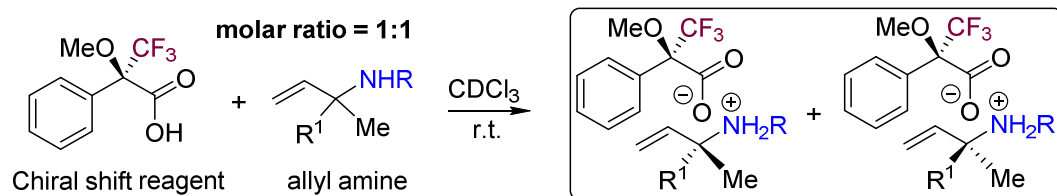
When the separation of the two enantiomers of the allyl amines could not be achieved via UPC2 equipped with different chiral columns, a chiral shift reagent (see scheme above) was used to determine the *er* value on the basis of a previously reported procedure.[21]

Procedure: The chiral shift reagent (0.01 mmol) and allyl amine (0.01 mmol) were mixed in CDCl$_3$ (0.6 mL). The ^{1}H NMR spectrum of the resultant mixture (containing two diastereoisomers) was then measured at room temperature. The *er* value was calculated based on the integral ratio of the proton of the vinyl or methyl group of both diastereoisomers.

3.4.5 Procedures for Transformation of Chiral Allylic Alkyl Amine (1)
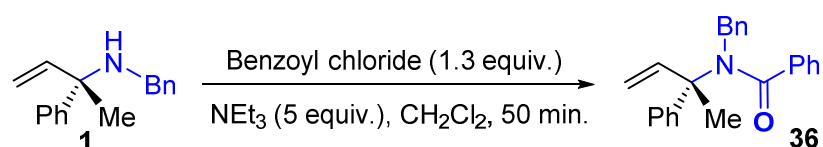
(**i**) To a solution of allylic amine **1** (36 mg, 0.15 mmol, 1 equiv.) and NEt$_3$ (105 μL, 5 equiv.) in CH$_2$Cl$_2$ (300 μL) was added benzoyl chloride (27 mg, 23 μL, 1.3 equiv.) and the resultant reaction mixture was stirred at room temperature for 50 min. The pure product **36** was isolated by chromatography (36 mg, 70% yield) as a light yellow solid (hexane:EA = 50 : 1, R_f = 0.11).
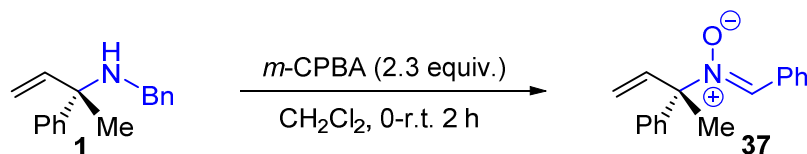
(**ii**) To a cold solution (0 °C) of allylic amine **1** (36 mg, 0.15 mmol, 1 equiv.) in CH$_2$Cl$_2$ (300 μL) was added *m*-CPBA (85 mg, 2.3 equiv.; considering 70% of pure *m*-CPBA from the commercial source) and the resultant solution was allowed to warm up to room temperature and stirred for 2 h. When the reaction was finished (checked by ^{1}H NMR), saturated NaHCO$_3$ aqueous solution (3 mL) was added to the reaction mixture and the mixture further stirred at room temperature for 20 min. The organic components were extracted with CH$_2$Cl$_2$, dried with anhydrous Na$_2$SO$_4$, and concentrated under reduced pressure. The pure product **37** was obtained as a white solid after chromatography

---

[21] A. Nemes, T. Csóka, S. Béni, V. Farkas, J. Rábai, D. Szabó, *J. Org. Chem.* **2015**, *80*, 6267.

purification (29 mg, 76% yield; hexane:EA = 10 : 1, R_f = 0.11). Note: the amount of the

m-CPBA is crucial to achieve the reported yield of the product.[22]
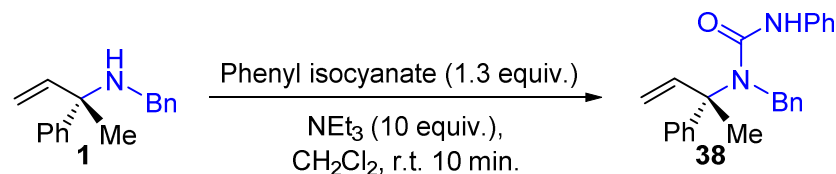
(**iii**) To a solution of allylic amine **1** (36 mg, 0.15 mmol, 1 equiv.) and NEt$_3$ (210 μL, 10

equiv.) in CH$_2$Cl$_2$ (500 μL) was added phenyl isocyanate (23 mg, 21 μL, 1.3 equiv.) and

the resultant reaction mixture was stirred at room temperature for 10 min. The pure

product **38** was isolated by chromatographic purification (50 mg, 93% yield; hexane:EA

= 10 : 1, R_f = 0.38) as a light yellow oil.
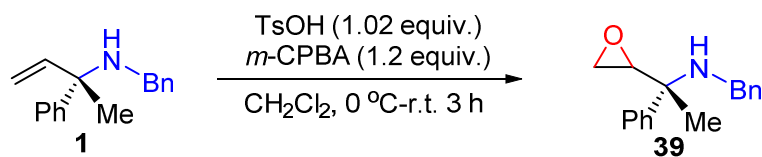
(**iv**) Compound **39** was prepared following a previously reported procedure[23] but with

small modifications: to a stirred cold (0 °C) solution of allylic amine **1** (0.15 mmol, 35

mg) in diethyl ether (300 μL), was added dropwise a solution of benzene sulfonic acid

(24 mg, 0.15 mmol) in diethyl ether (300 μL). The formed precipitate was filtered off,

washed with cold diethyl ether and dried under vacuum. After that, to a stirred cold (0 °C)

solution of the above-mentioned dry precipitate in dichloromethane (2 mL) was added a

solution of *m*-CPBA (44 mg, 1.2 equiv., considering 30% of water content in reagent) in

dichloromethane (2 mL). The resulting reaction mixture was kept under stirring at 0 °C

until the proton signal of the double bond in the ^{1}H NMR spectrum disappeared (about 4

h, followed by NMR). Then dimethyl sulfide (6 μL) was added and the mixture stirred at

0 °C for 30 min, followed by the addition of NaOH solution (2 mL, 5M) and further

stirring at 0 °C for 1 h. The organic components were extracted with dichloromethane.

Upon removal of the solvent, the reaction crude was purified by flash chromatography

(hexane:EA = 50 : 1, R_f = 0.18) to afford the pure epoxide **39** (22 mg, 57%) as a colorless

oil. $[\alpha]_D^{25}$ = −17.0 (*c* = 0.10, CHCl$_3$).

(22) For related research please refer to: a) D. Christensen, K. A. Jørgemen, *J. Org. Chem.* **1989**, *54*, 126; b) D. Mostowicz, C. Bełżecki, *J. Org. Chem.* **1977**, *42*, 3917.
(23) G. Asensio, R. Mello, C. Boix-Bernardini, M. E. González-Núñez, G. Castellano, *J. Org. Chem.* **1995**, *60*, 3692.

3.4.6 Analytical Data for all Compounds

The characterization data of non-reported starting materials:
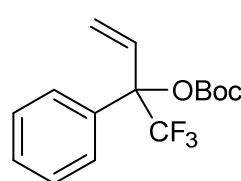
allylic precursor **D**

¹H NMR (400 MHz, CDCl₃): δ 7.54–7.47 (m, 2H), 7.45–7.39 (m, 3H), 6.56 (dd, *J* = 17.7, 11.4 Hz, 1H), 5.78–5.68 (m, 2H), 1.44 (s, 9H) ppm. **¹⁹F NMR** (376 MHz, CDCl₃): δ -76.73 ppm. **¹³C NMR** (101 MHz, CDCl₃): δ 149.90, 134.49, 130.75, 129.19, 128.44, 127.02, 123.33 (q, *J* = 285.8 Hz), 121.82, 83.64, 82.7 (q, *J* = 29.3 Hz), 27.75 ppm. **IR** (neat): *v* = 2989, 1759, 1370, 1273, 1255, 1177, 1154, 946, 762, 699 cm⁻¹. **HRMS** (ESI+, MeOH): *m/z* calcd. 325.1019 (M + Na)⁺, found: 325.1023.
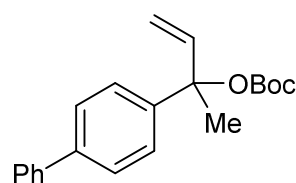
¹H NMR (500 MHz, CDCl₃): δ 7.61–7.58 (m, 4H), 7.48–7.42 (m, 4H), 7.37–7.33 (m, 1H), 6.44–6.35 (m, 1H), 5.37–5.30 (m, 2H), 1.93 (s, 3H), 1.45 (s, 9H) ppm. **¹³C NMR** (126 MHz, CDCl₃): δ 151.69, 142.91, 141.13, 140.86, 140.22, 128.85, 127.39, 127.22, 127.13, 125.67, 115.24, 83.79, 81.98, 27.94, 25.90 ppm. **IR** (neat): *v* = 2976, 1745, 1486, 1278, 1154, 1073, 1007, 770, 702 cm⁻¹. **HRMS** (ESI+, MeOH): *m/z* calcd. 347.1618 (M + Na)⁺, found: 347.1610.
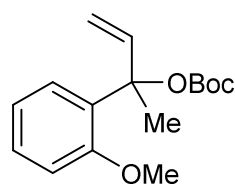
¹H NMR (500 MHz, CDCl₃): δ 7.35 (dd, *J* = 7.8, 1.7 Hz, 1H), 7.27–7.23 (m, 1H), 6.94 (m, 1H), 6.89 (d, *J* = 8.2 Hz, 1H), 6.49 (dd, *J* = 17.5, 10.8 Hz, 1H), 5.23–5.16 (m, 2H), 3.81 (s, 3H), 1.90 (s, 3H), 1.42 (s, 9H) ppm. **¹³C NMR** (126 MHz, CDCl₃): δ 156.52, 151.72, 141.30, 131.59, 128.78, 126.75, 120.50, 113.97, 111.80, 83.41, 81.41, 55.47, 27.97, 24.92 ppm. **IR** (neat): *v* = 2981, 1740, 1459, 1278, 1243, 1115, 1063, 1029, 845, 752 cm⁻¹. **HRMS** (ESI+, MeOH): *m/z* calcd. 301.1410 (M + Na)⁺, found: 301.1405.
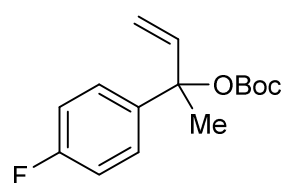
¹H NMR (500 MHz, CDCl₃): δ 7.38–7.34 (m, 2H), 7.04–6.99 (m, 2H), 6.31 (dd, *J* = 17.2, 11.1 Hz, 1H), 5.28–5.24 (m, 2H), 1.86 (s, 3H), 1.41 (s, 9H) ppm. **¹⁹F NMR** (376 MHz, CDCl₃): δ -115.70 ppm. **¹³C NMR** (126 MHz, CDCl₃): δ 162.05 (d, *J* = 247 Hz), 151.55, 141.04, 139.63 (d, *J* = 2.5 Hz), 127.12 (d, *J* = 7.6 Hz), 115.29, 115.14 (d, *J* = 8.8 Hz), 83.42, 81.98, 27.88, 25.88 ppm. **IR** (neat): *v* = 2982, 1509, 1369, 1276, 1255, 1229,

1154, 1090, 1070, 833, 792 cm^{-1}. **HRMS** (ESI+, MeOH): *m/z* calcd. 289.1210 (M + Na)$^{+}$, found: 289.1200.
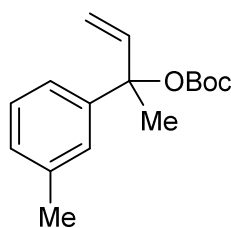
^{1}H NMR (500 MHz, CDCl$_3$): δ 7.25–7.19 (m, 3H), 7.11–7.07 (m, 1H), 6.36 (dd, *J* = 17.4, 10.8 Hz, 1H), 5.33–5.26 (m, 2H), 2.37 (s, 3H), 1.88 (s, 3H), 1.45 (s, 9H) ppm. **^{13}C NMR** (126 MHz, CDCl$_3$): δ 151.61, 143.82, 141.20, 137.81, 128.22, 128.05, 125.75, 122.17, 114.97, 83.85, 81.72, 27.86, 25.91, 21.67 ppm. **IR** (neat): *ν* = 2980, 1368, 1257, 1154, 1105, 862, 787, 706 cm^{-1}. **HRMS** (ESI+, MeOH): *m/z* calcd. 285.1461 (M + Na)$^{+}$, found: 285.1463.
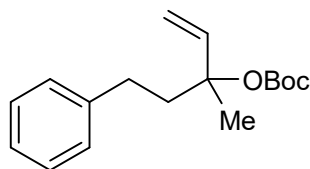
^{1}H NMR (400 MHz, CDCl$_3$): δ 7.31–7.26 (m, 2H), 7.21–7.17 (d, *J* = 6.5 Hz, 3H), 6.10 (dd, *J* = 17.6, 11.0 Hz, 1H), 5.28–5.19 (m, 2H), 2.70–2.63 (m, 2H), 2.19–2.13 (m, 2H), 1.63 (s, 3H), 1.51 (s, 9H) ppm. **^{13}C NMR** (101 MHz, CDCl$_3$): δ 152.01, 142.01, 141.61, 128.49, 128.45, 125.93, 113.88, 83.38, 81.54, 41.70, 30.15, 27.97, 23.72 ppm. **IR** (neat): *ν* = 2980, 1736, 1368, 1280, 1254, 1150, 1097, 747, 698 cm^{-1}. **HRMS** (ESI+, MeOH): *m/z* calcd. 299.1618 (M + Na)$^{+}$, found: 299.1610.
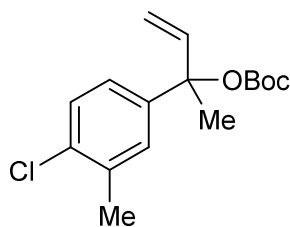
^{1}H NMR (400 MHz, CDCl$_3$): δ 7.29 (d, *J* = 8.4 Hz, 1H), 7.23 (d, *J* = 2.2 Hz, 1H), 7.14 (dd, *J* = 8.4, 2.2 Hz, 1H), 6.30 (dd, *J* = 17.5, 10.7 Hz, 1H), 5.31–5.25 (m, 2H), 2.37 (s, 3H), 1.84 (s, 3H), 1.43 (s, 9H) ppm. **^{13}C NMR** (101 MHz, CDCl$_3$): δ 151.56, 142.49, 140.81, 135.88, 133.35, 128.99, 127.80, 124.05, 115.42, 83.35, 82.04, 27.89, 25.86, 20.35 ppm. **IR** (neat): *ν* = 2980, 1743, 1481, 1368, 1276, 1253, 1154, 1096, 1047, 824, 791 cm^{-1}. **HRMS** (ESI+, MeOH): *m/z* calcd. 319.1071 (M + Na)$^{+}$, found: 319.1062.

The characterization data of the allylic amine products:
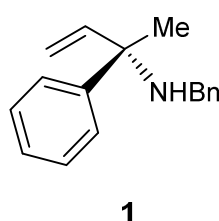
Scale: 0.15 mmol; isolated 27 mg (72% yield), light yellow oil, Hexane : EA = 10 : 1, R_f = 0.17; 95.5:4.5 *er*; the racemic compound has been reported.[24] **¹H NMR** (400 MHz, CDCl₃): δ 7.57–7.54 (m, 2H), 7.39–7.30 (m, 6H), 7.27–7.21 (m, 2H), 6.11 (dd, *J* = 17.5, 10.7 Hz, 1H), 5.26 (dd, *J* = 12.0, 1.2 Hz, 1H), 5.23 (dd, *J* = 5.2, 1.2 Hz, 1H), 3.62 (d, *J* = 2.7 Hz, 2H), 1.59 (s, 3H) ppm. **¹³C NMR** (101 MHz, CDCl₃): δ 146.40, 145.05, 141.42, 128.48, 128.34, 128.27, 126.92, 126.74, 126.69, 113.13, 60.88, 47.45, 26.26 ppm. **UPC2** conditions: OJ-3 Column, Isocratic CO₂/IPA/DEA = 90 : 10 : 0.1, 2000 psi, 2 ml/min; 95.5 : 4.5 *er*; $[\alpha]_D^{25}$ = -28.9 (*c* = 0.13, CHCl₃).
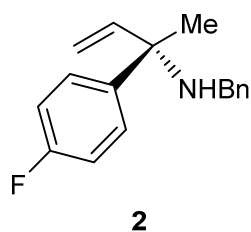
Scale: 0.15 mmol; isolated 25 mg (65% yield), light yellow oil, Hexane : EA = 10 : 1, R_f = 0.33. **¹H NMR** (400 MHz, CDCl₃): δ 7.56–7.50 (m, 2H), 7.38–7.33 (m, 4H), 7.27–7.22 (m, 1H), 7.05–6.99 (m, 2H), 6.08 (dd, *J* = 17.7, 10.5 Hz, 1H), 5.28–5.22 (m, 2H), 3.61 (d, *J* = 1.7 Hz, 2H), 1.57 (s, 3H) ppm. **¹⁹F NMR** (376 MHz, CDCl₃): δ -116.94 ppm. **¹³C NMR** (101 MHz, CDCl₃): δ 161.76 (d, *J* = 245 Hz), 144.89, 142.21 (d, *J* = 3 Hz), 141.32, 128.50, 128.36 (d, *J* = 7 Hz), 128.22, 126.97, 114.98 (d, *J* = 21 Hz), 113.32, 60.49, 47.39, 26.41 ppm. **IR** (neat): *ν* = 2976, 1600, 1505, 1453, 1222, 1157, 835, 729, 698 cm⁻¹. **HRMS** (ESI+, MeOH): *m/z* calcd. 256.1496 (M + H)⁺, found: 256.1505.
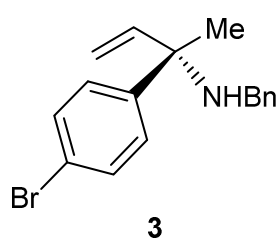
Scale: 0.15 mmol; isolated 25 mg (53% yield), light yellow oil, Hexane : EA = 10 : 1, R_f = 0.22. **¹H NMR** (400 MHz, CDCl₃): δ 7.48–7.42 (m, 4H), 7.37–7.30 (m, 4H), 7.27–7.22 (m, 1H), 6.06 (dd, *J* = 17.7, 10.5 Hz, 1H), 5.2 –5.21 (m, 2H), 3.60 (s, 2H), 1.56 (s, 3H) ppm. **¹³C NMR** (101 MHz, CDCl₃): δ 145.62, 144.46, 141.18, 131.37, 128.65, 128.52, 128.21, 127.01, 120.68, 113.62, 60.63, 47.39, 26.28 ppm. **IR** (neat): *ν* = 2974, 2925, 1724, 1604, 1486, 1452, 1368, 1008, 823, 697 cm⁻¹. **HRMS** (ESI+, MeOH): *m/z* calcd. 316.0695 (M + H)⁺, found: 316.0706. **UPC2** conditions: OJ-3 Column, Isocratic CO₂/IPA/DEA = 60 : 40 : 0.1, 2000 psi, 2 ml/min; 95 : 5 *er*; $[\alpha]_D^{25}$ = − 9.7 (*c* = 0.12, CHCl₃).

(24) D. T. H. Phan, V. M. Dong, *Tetrahedron* **2013**, *69*, 5726.
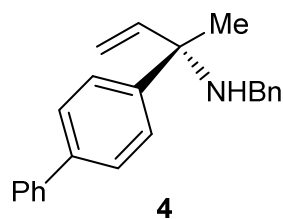
Scale: 0.15 mmol; isolated 35 mg (75% yield), light yellow oil, Hexane : EA = 10 : 1, R_f = 0.19. **^{1}H NMR** (400 MHz, CDCl$_3$): δ 7.66–7.59 (m, 6H), 7.47–7.39 (m, 4H), 7.38–7.33 (m, 3H), 7.29–7.25 (m, 1H), 6.17 (dd, J = 17.5, 10.7 Hz, 1H), 5.35–5.26 (m, 2H), 3.68 (d, J = 2.0 Hz, 2H), 1.65 (s, 3H) ppm. **^{13}C NMR** (101 MHz, CDCl$_3$): δ 145.53, 144.99, 141.41, 141.03, 139.59, 128.86, 128.49, 128.27, 127.28, 127.19, 127.15, 127.06, 126.93, 113.23, 60.74, 47.48, 26.26 ppm. **IR** (neat): v = 3027, 2925, 1734, 1601, 1485, 1074, 838, 765, 733, 695 cm^{-1}. **HRMS** (ESI+, MeOH): m/z calcd. 314.1903 (M + H)$^+$, found: 314.1892. **UPC2** conditions: OJ-3 Column, Isocratic CO$_2$/IPA/DEA = 60 : 40 : 0.1, 2000 psi, 2 ml/min; 92.5 : 7.5 er; $[\alpha]_D^{25}$ = –22.8 (c = 0.12, CHCl$_3$).
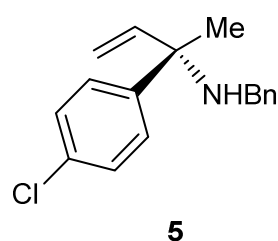
Scale: 0.15 mmol; isolated 27 mg (66% yield), light yellow oil, Hexane : EA = 10 : 1, R_f = 0.23. **^{1}H NMR** (400 MHz, CDCl$_3$): δ 7.53–7.48 (m, 2H), 7.38–7.30 (m, 6H), 7.28–7.24 (m, 1H), 6.08 (dd, J = 17.6, 10.5 Hz, 1H), 5.30–5.22 (m, 2H), 3.61 (s, 2H), 1.57 (s, 3H) ppm. **^{13}C NMR** (101 MHz, CDCl$_3$): δ 145.07, 144.55, 141.20, 132.49, 128.51, 128.40, 128.23, 128.21, 126.99, 113.55, 60.56, 47.38, 26.30 ppm. **IR** (neat): v = 2927, 1735, 1490, 1367, 1253, 1094, 1012, 827, 698 cm^{-1}. **HRMS** (ESI+, MeOH): m/z calcd. 272.1201 (M + H)$^+$, found: 272.1197. **UPC2** conditions: IG Column, Isocratic CO$_2$/IPA/DEA = 90 : 10 : 0.1, 2000 psi, 2 ml/min; 93 : 7 er; $[\alpha]_D^{25}$ = -14.3 (c = 0.09, CHCl$_3$).
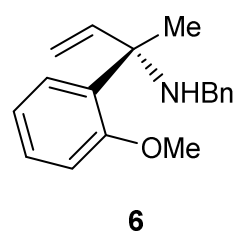
Scale: 0.15 mmol; isolated 27 mg (68% yield), light yellow oil, Hexane : EA = 5 : 1, R_f = 0.15. **^{1}H NMR** (400 MHz, CDCl$_3$): δ 7.37 (dd, J = 7.7, 1.7 Hz, 1H), 7.31–7.25 (m, 5H), 7.24–7.20 (m, 1H), 6.97 (td, J = 7.5, 1.2 Hz, 1H), 6.93 (d, J = 8.2 Hz, 1H), 6.25 (dd, J = 17.4, 10.7 Hz, 1H), 5.13–5.04 (m, 2H), 3.80 (s, 3H), 3.50 (d, J = 12.1 Hz, 1H), 3.39 (d, J = 12.1 Hz, 1H), 1.65 (s, 3H) ppm. **^{13}C NMR** (101 MHz, CDCl$_3$): δ 157.88, 145.21, 141.58, 133.40, 128.70, 128.44, 128.41, 128.35, 126.72, 120.67, 111.92, 111.62, 61.28, 55.27, 48.17, 25.10 ppm. **IR** (neat): v = 2929, 2835, 1713, 1581, 1488, 1452, 1435, 1236, 1026, 750, 698 cm^{-1}. **HRMS** (ESI+, MeOH): m/z calcd. 290.1515 (M + Na)$^+$, found: 290.1515. **UPC2** conditions: CELL-2 Column, Isocratic CO$_2$/IPA/DEA = 90 : 10 : 0.1, 2000 psi, 2 ml/min; 98.5 : 1.5 er; $[\alpha]_D^{25}$ = -64.3 (c = 0.11, CHCl$_3$).
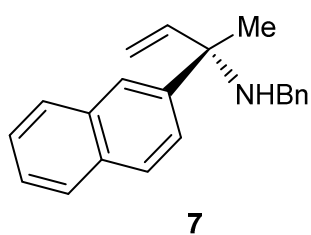
Scale: 0.15 mmol; isolated 32 mg (74% yield), light yellow oil, Hexane : EA = 10 : 1, R_f = 0.15; the racemic compound has been reported.[25] **^{1}H NMR** (500 MHz, CDCl$_3$): δ 7.96 (s, 1H), 7.87–7.83 (m, 3H), 7.74–7.72 (m, 1H), 7.50–7.47 (m, 2H), 7.40 (d, J = 7.3 Hz, 2H), 7.34 (t, J = 7.5 Hz, 2H), 7.28–7.24 (m, 1H), 6.22 (dd, J = 17.5, 10.7 Hz, 1H), 5.37–5.26 (m, 2H), 3.65 (q, J = 12.6 Hz, 2H), 1.71 (s, 3H) ppm. **^{13}C NMR** (126 MHz, CDCl$_3$): δ 145.02, 143.77, 141.42, 133.39, 132.51, 128.50, 128.30, 128.23, 128.01, 127.58, 126.94, 126.04, 125.82, 125.52, 125.10, 113.35, 61.00, 47.55, 26.21 ppm. **UPC2** conditions: OJ-3 Column, Isocratic CO$_2$/MeOH/DEA = 90 : 10 : 0.1, 2000 psi, 2 ml/min; 92 : 8 *er*; $[\alpha]_D^{25}$ = −3.7 (*c* = 0.09, CHCl$_3$).
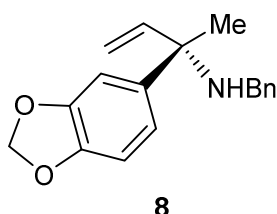
Scale: 0.15 mmol; isolated 33 mg (78% yield), light yellow oil, Hexane : EA = 10 : 1, R_f = 0.14. **^{1}H NMR** (400 MHz, CDCl$_3$): δ 7.39–7.35 (m, 2H), 7.32 (m, 2H), 7.26–7.21 (m, 1H), 7.11 (d, J = 1.8 Hz, 1H), 6.99 (dd, J = 8.1, 1.8 Hz, 1H), 6.78 (d, J = 8.1 Hz, 1H), 6.07 (dd, J = 17.5, 10.7 Hz, 1H), 5.95 (s, 2H), 5.27–5.19 (m, 2H), 3.61 (d, J = 2.0 Hz, 2H), 1.55 (s, 3H) ppm. **^{13}C NMR** (101 MHz, CDCl$_3$): δ 147.79, 146.25, 145.15, 141.44, 140.74, 128.47, 128.23, 126.90, 119.71, 112.96, 107.81, 107.61, 101.04, 60.67, 47.37, 26.38 ppm. **IR** (neat): ν = 2973, 2919, 1501, 1483, 1452, 1431, 1237, 1038, 918, 809, 698 cm^{-1}. **HRMS** (ESI+, MeOH): *m/z* calcd. 304.1308 (M + Na)$^+$, found: 304.1309. The *ee* of allylic amine **8** was determined using a chiral shift reagent, and was based on the integration of the methyl group.
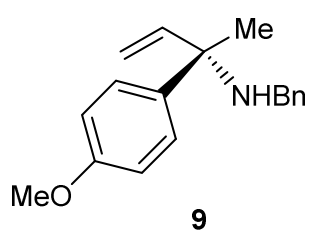
Scale: 0.15 mmol; isolated 30 mg (75% yield), light yellow oil, Hexane : EA = 5 : 1, R_f = 0.14; ; the racemic compound has been reported.[25] **^{1}H NMR** (500 MHz, CDCl$_3$): δ 7.49–7.45 (m, 2H), 7.37 (d, J = 7.2 Hz, 2H), 7.32 (t, J = 7.5 Hz, 2H), 7.24 (t, J = 7.2 Hz, 1H), 6.92–6.87 (m, 2H), 6.10 (dd, J = 17.5, 10.7 Hz, 1H), 5.26–5.19 (m, 2H), 3.82 (s, 3H), 3.64–3.58 (m, 2H), 1.58 (s, 3H) ppm. **^{13}C NMR** (126 MHz, CDCl$_3$): δ 158.38, 145.32, 141.44, 138.42, 128.46, 128.28, 127.84, 126.89, 113.62, 112.85, 60.42, 55.38, 47.42, 26.28 ppm. **UPC2** conditions: OJ-3 Column,

(25) S. Mizuno, S. Terasaki, T. Shinozawa, M. Kawatsura, *Org. Lett.* **2017**, *19*, 504.

Isocratic CO_2/IPA/DEA = 95 : 5 : 0.1, 2000 psi, 2 ml/min; 91 : 9 *er*; $[\alpha]_D^{25}$ = –50.2 (*c* = 0.10, $CHCl_3$).
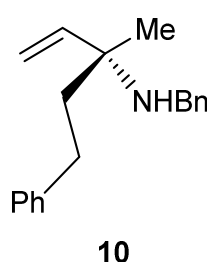
Scale: 0.15 mmol; isolated 24 mg (60% yield), light yellow oil, Hexane : EA = 10 : 1, R_f = 0.14; the racemic compound has been reported.[25] **^{1}H NMR** (400 MHz, $CDCl_3$): δ 7.39–7.27 (m, 6H), 7.26–7.22 (m, 1H), 7.19 (d, *J* = 7.5 Hz, 3H), 5.85 (dd, *J* = 17.5, 10.9 Hz, 1H), 5.22–5.13 (m, 2H), 3.68 (s, 2H), 2.65 (ddd, *J* = 11.3, 6.4, 3.0 Hz, 2H), 1.87–1.78 (m, 2H), 1.29 (s, 3H) ppm. **^{13}C NMR** (101 MHz, $CDCl_3$): δ 145.31, 142.98, 141.47, 128.53, 128.50, 128.47, 128.36, 126.94, 125.81, 113.48, 57.33, 47.15, 42.33, 30.48, 23.89 ppm. The *ee* of allylic amine **10** was determined using a chiral shift reagent, and was based on the integration of the methyl group.
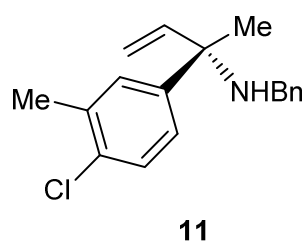
Scale: 0.15 mmol; isolated 30 mg (70% yield), light yellow oil, Hexane : EA = 10 : 1, R_f = 0.25. **^{1}H NMR** (400 MHz, $CDCl_3$): δ 7.45–7.42 (m, 1H), 7.41–7.33 (m, 6H), 7.31–7.28 (m, 1H), 6.14–6.05 (m, 1H), 5.31–5.25 (m, 2H), 3.63 (d, *J* = 1.4 Hz, 2H), 2.42 (s, 3H), 1.59 (s, 3H) ppm. **^{13}C NMR** (101 MHz, $CDCl_3$): δ 145.11, 144.70, 141.30, 135.68, 132.64, 129.37, 128.87, 128.51, 128.24, 126.97, 125.59, 113.38, 60.51, 47.43, 26.26, 20.41 ppm. **IR** (neat): *v* = 2975, 2924, 1478, 1452, 1390, 1046, 919, 697 cm^{-1}. **HRMS** (ESI+, MeOH): *m/z* calcd. 286.1357 (M + H)$^+$, found: 286.1354. **UPC2** conditions: OJ-3 Column, Isocratic CO_2/IPA/DEA = 98 : 2 : 0.1, 2000 psi, 2 ml/min; 92 : 8 *er*; $[\alpha]_D^{25}$ = –38.3 (*c* = 0.11, $CHCl_3$).
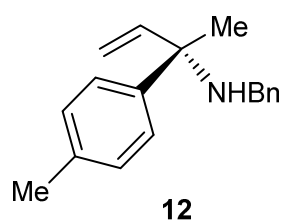
Scale: 0.15 mmol; isolated 27 mg (72% yield), light yellow oil, Hexane : EA = 10 : 1, R_f = 0.17; ; the racemic compound has been reported.[25] **^{1}H NMR** (500 MHz, $CDCl_3$): δ 7.44 (d, *J* = 8.2 Hz, 2H), 7.38 (d, *J* = 7.4 Hz, 2H), 7.32 (t, *J* = 7.5 Hz, 2H), 7.25 (d, *J* = 7.4 Hz, 1H), 7.17 (d, *J* = 8.0 Hz, 2H), 6.11 (dd, *J* = 17.5, 10.7 Hz, 1H), 5.28–5.19 (m, 2H), 3.65–3.58 (m, 2H), 2.36 (s, 3H), 1.59 (s, 3H) ppm. **^{13}C NMR** (126 MHz, $CDCl_3$): δ 145.28, 143.42, 141.52, 136.26, 129.04, 128.45, 128.27, 126.87, 126.61, 112.88, 60.62, 47.44, 26.28, 21.11 ppm. **UPC2** conditions: IG Column, Isocratic CO_2/MeOH/DEA = 95 : 5 : 0.1, 2000 psi, 2 ml/min; 95 : 5 *er*; $[\alpha]_D^{25}$ = –19.3 (*c* = 0.09, $CHCl_3$).
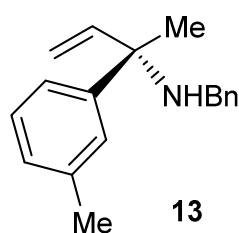
Scale: 0.15 mmol; isolated 30 mg (80% yield), light yellow oil, Hexane : EA = 10 : 1, R_f = 0.27. **^{1}H NMR** (400 MHz, CDCl$_3$): δ 7.31–7.40 (m, 6H), 7.28–7.23 (m, 2H), 7.08 (d, J = 7.4 Hz, 1H), 6.12 (dd, J = 17.5, 10.7 Hz, 1H), 5.30–5.22 (m, 2H), 3.63 (d, J = 2.3 Hz, 2H), 2.39 (s, 3H), 1.59 (s, 3H) ppm. **^{13}C NMR** (101 MHz, CDCl$_3$): δ 146.42, 145.15, 141.52, 137.82, 128.46, 128.28, 128.22, 127.46, 127.37, 126.88, 123.72, 112.96, 60.79, 47.48, 26.23, 21.81 ppm. **IR** (neat): v = 2975, 2856, 1739, 1604, 1494, 1452, 1367, 1253, 1028, 785, 698. **HRMS** (ESI+, MeOH): m/z calcd. 252.1747 (M + H)$^+$, found: 252.1744 cm^{-1}. **UPC2** conditions: OJ-3 Column, Isocratic CO$_2$/ACN/DEA = 99 : 1 : 0.1, 2000 psi, 2 ml/min; 95.5 : 4.5 *er*; $[\alpha]_D^{25}$ = –6.6 (c = 0.09, CHCl$_3$).
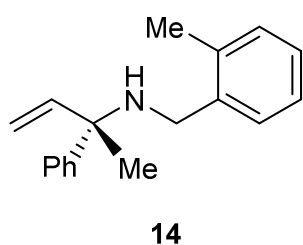
Scale: 0.15 mmol; isolated 24 mg (64% yield), light yellow oil, Hexane : EA = 10 : 1, R_f = 0.34; the racemic compound has been reported.[24] **^{1}H NMR** (400 MHz, CDCl$_3$): δ 7.59–7.57 (m, 2H), 7.41–7.35 (m, 3H), 7.29–7.25 (m, 1H), 7.22–7.18 (m, 3H), 6.14 (dd, J = 17.5, 10.7 Hz, 1H), 5.33–5.25 (m, 2H), 3.61 (d, J = 3.3 Hz, 2H), 2.35 (s, 3H), 1.64 (s, 3H) ppm. **^{13}C NMR** (101 MHz, CDCl$_3$): δ 146.64, 145.09, 139.26, 136.70, 130.29, 128.75, 128.28, 126.97, 126.73, 126.65, 126.06, 113.14, 60.80, 45.06, 25.91, 19.13 ppm. **UPC2** conditions: OJ-3 column, Isocratic CO$_2$/IPA/DEA = 85 : 15 : 0.1, 2 ml/min, 2000 psi; 96.0 : 4.0 *er*; $[\alpha]_D^{25}$ = –37.8 (c = 0.10, CHCl$_3$).
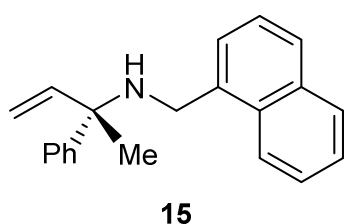
Scale: 0.15 mmol; isolated 27 mg (63% yield), light yellow oil, Hexane : EA = 10 : 1, R_f = 0.30. **^{1}H NMR** (400 MHz, CDCl$_3$): δ 8.13–8.06 (m, 1H), 7.8–97.86 (m, 1H), 7.79 (d, J = 8.2 Hz, 1H), 7.64–7.60 (m, 2H), 7.58 (d, J = 6.5 Hz, 1H), 7.55–7.49 (m, 2H), 7.49–7.44 (m, 1H), 7.41–7.37 (m, 2H), 7.31–7.27 (m, 1H), 6.21 (dd, J = 17.5, 10.7 Hz, 1H), 5.37–5.29 (m, 2H), 4.09 (s, 2H), 1.71 (s, 3H) ppm. **^{13}C NMR** (101 MHz, CDCl$_3$): δ 146.56, 145.00, 137.01, 133.94, 132.09, 128.70, 128.34, 127.68, 126.82, 126.74, 126.13, 126.00, 125.85, 125.68, 124.16, 113.35, 61.08, 45.00, 26.00 ppm. **IR** (neat): v = 3056, 2974, 2926, 1736, 1597, 1490, 1445, 1366, 766, 699 cm^{-1}. **HRMS** (ESI+, MeOH): m/z calcd. 288.1747 (M + H)$^+$, found: 288.1742. **UPC2** conditions: OJ-3 column, Isocratic CO$_2$/IPA/DEA = 80 : 20 : 0.1, 2 ml/min, 2000 psi; 93 : 7 *er*; $[\alpha]_D^{25}$ = –70.0 (c = 0.09, CHCl$_3$).

16
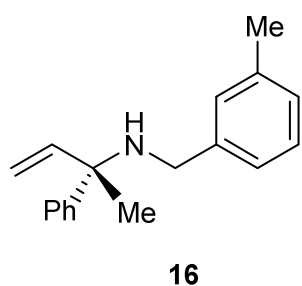
Scale: 0.15 mmol; isolated 31 mg (82% yield), light yellow oil, Hexane : EA = 10 : 1, R_f = 0.32. **^{1}H NMR** (400 MHz, CDCl$_3$): δ 7.58–7.55 (m, 2H), 7.39–7.34 (m, 2H), 7.29–7.21 (m, 2H), 7.21–7.17 (m, 2H), 7.09–7.05 (m, 1H), 6.13 (dd, J = 17.5, 10.7 Hz, 1H), 5.30–5.23 (m, 2H), 3.59 (d, J = 2.3 Hz, 2H), 2.37 (s, 3H), 1.60 (s, 3H) ppm. **^{13}C NMR** (101 MHz, CDCl$_3$): δ 146.31, 144.96, 141.21, 137.95, 128.92, 128.27, 128.20, 127.53, 126.58, 125.19, 112.99, 60.74, 47.31, 26.18, 21.44 ppm. **IR** (neat): v = 2974, 1737, 1607, 1489, 1445, 1072, 917, 764, 699 cm^{-1}. **HRMS** (ESI+, MeOH): m/z calcd. 252.1747 (M + H)$^+$, found: 252.1748. **UPC2** conditions: IG column, Isocratic CO$_2$/ACN/DEA = 95 : 5 : 0.1, 2 ml/min, 2000 psi; 94 : 6 er; $[\alpha]_D^{25}$ = –26.6 (c = 0.11, CHCl$_3$).

17
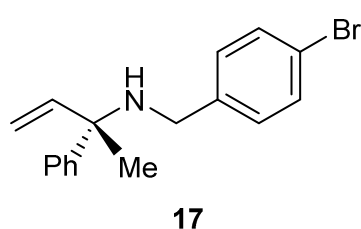
Scale: 0.15 mmol; isolated 35 mg (74% yield), light yellow oil, Hexane : EA = 10 : 1, R_f = 0.30. **^{1}H NMR** (400 MHz, CDCl$_3$): δ 7.55–7.51 (m, 2H), 7.45–7.41 (m, 2H), 7.37–7.33 (m, 2H), 7.27–7.23 (m, 3H), 6.09 (dd, J = 17.4, 10.7 Hz, 1H), 5.28–5.20 (m, 2H), 3.56 (d, J = 2.0 Hz, 2H), 1.57 (s, 3H) ppm. **^{13}C NMR** (101 MHz, CDCl$_3$): δ 146.24, 144.90, 140.53, 131.49, 129.93, 128.38, 126.83, 126.63, 120.60, 113.22, 60.88, 46.80, 26.25 ppm. **IR** (neat): v = 2935, 2926, 1739, 1486, 1254, 1070, 1011, 918, 764, 699 cm^{-1}. **HRMS** (ESI+, MeOH): m/z calcd. 316.0695 (M + H)$^+$, found: 316.0691. **UPC2** conditions: OJ-3 column, Isocratic CO$_2$/IPA/DEA = 70 : 30 : 0.1, 2 ml/min, 2000 psi; 95 : 5 er; $[\alpha]_D^{25}$ = –39.7 (c = 0.11, CHCl$_3$).

18
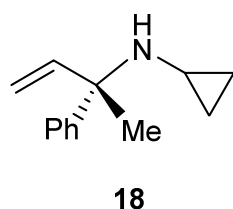
Scale: 0.15 mmol; isolated 23 mg (86% yield), light yellow oil, Hexane : EA = 10 : 1, R_f = 0.30. **^{1}H NMR** (400 MHz, CDCl$_3$): δ 7.48–7.45 (m, 2H), 7.35–7.30 (m, 2H), 7.25–7.19 (m, 1H), 6.05 (dd, J = 17.4, 10.7 Hz, 1H), 5.27–5.05 (m, 2H), 1.95 (ddd, J = 10.3, 6.3, 4.0 Hz, 1H), 1.57 (s, 3H), 0.42–0.32 (m, 4H) ppm. **^{13}C NMR** (101 MHz, CDCl$_3$): δ 147.20, 145.68, 128.19, 126.62, 126.50, 112.62, 61.62, 25.54, 25.23, 7.59, 6.75 ppm. **IR** (neat): v = 3084, 2980, 1746, 1446, 1365, 916, 762, 698. **HRMS** (ESI+, MeOH): m/z calcd. 131.0855 (M - cyclopropylamine)$^+$, found: 131.0855. **UPC2** conditions: OJ-3 column,

Isocratic CO_2/MeOH/DEA = 95 : 5 : 0.1, 2 ml/min, 2000 psi; 94 : 6 *er*; $[\alpha]_D^{25}$ = −13.5 (*c* = 0.11, $CHCl_3$).
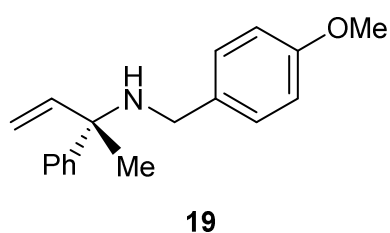
Scale: 0.15 mmol; isolated 25 mg (62% yield), light yellow oil, Hexane : EA = 10 : 1, R_f = 0.12. **¹H NMR** (400 MHz, $CDCl_3$): δ 7.56–7.53 (m, 2H), 7.38–7.33 (m, 2H), 7.29–7.22 (m, 3H), 6.88–6.84 (m, 2H), 6.10 (dd, *J* = 17.5, 10.7 Hz, 1H), 5.28–5.20 (m, 2H), 3.80 (s, 3H), 3.54 (d, *J* = 2.9 Hz, 2H), 1.58 (s, 3H) ppm. **¹³C NMR** (101 MHz, $CDCl_3$): δ 158.66, 146.48, 145.13, 133.59, 129.38, 128.31, 126.69, 113.90, 113.03, 60.83, 55.43, 46.82, 26.27 ppm. **IR** (neat): *v* = 2931, 2834, 1611, 1570, 1443, 1244, 1172, 1034, 917, 761, 700 cm⁻¹. **HRMS** (ESI+, MeOH): *m/z* calcd. 268.1696 (M + H)⁺, found: 268.1693. **UPC2** conditions: OJ-3 column, Isocratic CO_2/IPA/DEA = 70 : 30 : 0.1, 2 ml/min, 2000 psi; 96 : 4 *er*; $[\alpha]_D^{25}$ = −15.5 (*c* = 0.12, $CHCl_3$).
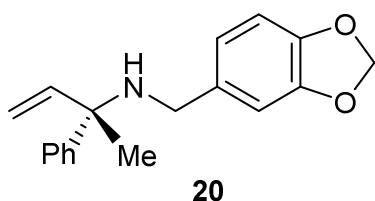
Scale: 0.15 mmol; isolated 18 mg (43% yield), light yellow oil, Hexane : EA = 10 : 1, R_f = 0.14; the racemic compound has been reported.[24] **¹H NMR** (500 MHz, $CDCl_3$): δ 7.57–7.52 (m, 2H), 7.36 (t, *J* = 7.7 Hz, 2H), 7.27–7.23 (m, 1H), 6.91 (d, *J* = 1.2 Hz, 1H), 6.81–6.73 (m, 2H), 6.10 (dd, *J* = 17.5, 10.7 Hz, 1H), 5.93 (s, 2H), 5.27–5.21 (m, 2H), 3.52 (d, *J* = 3.3 Hz, 2H), 1.58 (s, 3H) ppm. **¹³C NMR** (126 MHz, $CDCl_3$): δ 147.71, 146.46, 146.39, 145.05, 135.46, 128.32, 126.73, 126.65, 121.12, 113.07, 108.93, 108.15, 100.95, 60.79, 47.24, 26.26 ppm. **UPC2** conditions: OJ-3 column, Isocratic CO_2/MeOH/DEA = 95 : 5 : 0.1, 2 ml/min, 2000 psi; 96 : 4 *er*; $[\alpha]_D^{25}$ = −24.3 (*c* = 0.08, $CHCl_3$).
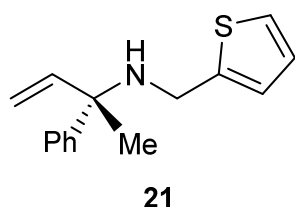
Scale: 0.15 mmol; isolated 24 mg (66% yield), light yellow oil, Hexane : EA = 10 : 1, R_f = 0.16. **¹H NMR** (400 MHz, $CDCl_3$): δ 7.57–7.54 (m, 2H), 7.37–7.34 (m, 2H), 7.27–7.23 (m, 1H), 7.20 (dd, *J* = 5.0, 1.3 Hz, 1H), 6.98–6.88 (m, 2H), 6.09 (dd, *J* = 17.5, 10.7 Hz, 1H), 5.30–5.22 (m, 2H), 3.82 (s, 2H), 1.58 (s, 3H) ppm. **¹³C NMR** (101 MHz, $CDCl_3$): δ 146.10, 145.59, 144.69, 128.39, 126.81, 126.67, 126.62, 124.16, 124.03, 113.28, 60.89, 42.53, 26.36 ppm. **IR** (neat): *v* = 3057, 2974, 1741, 1444, 1092, 1072, 918,

764, 696 cm^{-1}. **HRMS** (ESI+, MeOH): *m/z* calcd. 244.1154 (M + H)$^+$, found: 244.1149. The *ee* of allylic amine **21** was determined using a chiral shift reagent, and was based on the integration of the vinyl group.
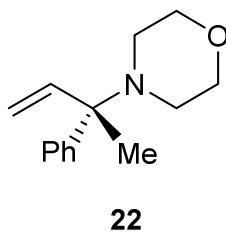
Scale: 0.15 mmol; isolated 28 mg (86% yield), light yellow oil, Hexane : EA = 10 : 1, R_f = 0.30; the racemic compound has been reported.[25] **^{1}H NMR** (400 MHz, CDCl$_3$): δ 7.54–7.51 (m, 2H), 7.36–7.27 (m, 2H), 7.25–7.17 (m, 1H), 6.04 (dd, *J* = 17.6, 10.9 Hz, 1H), 5.23–5.12 (m, 2H), 3.69 (t, *J* = 4.6 Hz, 4H), 2.48 (dtd, *J* = 16.7, 11.6, 5.9 Hz, 4H), 1.46 (s, 3H) ppm. **^{13}C NMR** (101 MHz, CDCl$_3$): δ 146.45, 143.04, 128.34, 126.91, 126.65, 114.25, 68.01, 64.60, 47.22, 18.05 ppm. **UPC2** conditions: OJ-3 column, Isocratic CO$_2$/MeOH/DEA = 95 : 5 : 0.1, 2 ml/min, 2000 psi; 86 : 14 *er*; $[\alpha]_D^{25}$ = 26.6 (*c* = 0.11, CHCl$_3$).
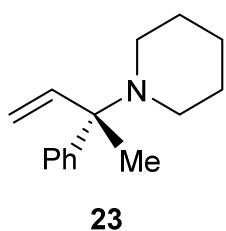
Scale: 0.15 mmol; isolated 25 mg (78% yield), light yellow oil, Hexane : EA = 10 : 1, R_f = 0.35; the racemic compound has been reported.[25] **^{1}H NMR** (400 MHz, CDCl$_3$): δ 7.53–7.51 (m, 2H), 7.32–7.27 (m, 2H), 7.22–7.15 (m, 1H), 6.02 (dd, *J* = 17.6, 10.9 Hz, 1H), 5.14–5.05 (m, 2H), 2.49–2.33 (m, 4H), 1.61–1.46 (m, 6H), 1.43 (s, 3H) ppm. **^{13}C NMR** (101 MHz, CDCl$_3$): δ 147.72, 144.55, 128.17, 126.76, 126.28, 112.96, 65.12, 47.97, 27.15, 25.38, 17.73 ppm. **UPC2** conditions: OJ-3 column, Isocratic CO$_2$/IPA/DEA = 95 : 5 : 0.1, 2 ml/min, 2000 psi; 89 : 11 *er*; $[\alpha]_D^{25}$ = 38.8 (*c* = 0.15, CHCl$_3$).
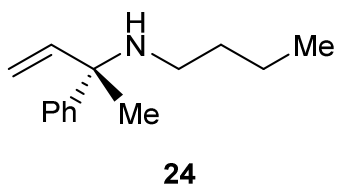
Scale: 0.15 mmol; isolated 20 mg (66% yield), light yellow oil, Hexane : EA = 5 : 1, R_f = 0.11; the racemic compound has been reported.[25] **^{1}H NMR** (400 MHz, CDCl$_3$): δ 7.46–7.44 (m, 2H), 7.34–7.29 (m, 2H), 7.24–7.19 (m, 1H), 6.02 (dd, *J* = 17.1, 11.0 Hz, 1H), 5.21–5.11 (m, 2H), 2.47–2.36 (m, 2H), 1.50 (s, 3H), 1.46–1.43 (m, 2H), 1.36–1.30 (m, 2H), 0.88 (t, *J* = 7.3 Hz, 3H) ppm. **^{13}C NMR** (101 MHz, CDCl$_3$): δ 146.67, 145.36, 128.23, 126.60, 126.56, 112.73, 60.55, 42.71, 33.28, 26.14, 20.71, 14.20 ppm. **UPC2** conditions: IG column, Isocratic CO$_2$/MeOH/DEA = 95 : 5 : 0.1, 2 ml/min, 2000 psi; 94 : 6 *er*; $[\alpha]_D^{25}$ = −9.0 (*c* = 0.13, CHCl$_3$).
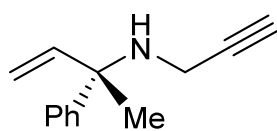
Scale: 0.15 mmol; isolated 9 mg (32% yield), light yellow oil, Hexane : EA = 10 : 1, R_f = 0.16. **^{1}H NMR** (500 MHz, CDCl$_3$): δ 7.47–7.45 (m, 2H), 7.35–7.32 (m, 2H), 7.25–7.22 (m, 1H), 6.02 (dd, J = 17.4, 10.8 Hz, 1H), 5.25–5.19 (m, 2H), 3.23 (d, J = 2.5 Hz, 2H), 2.19 (t, J = 2.5 Hz, 1H), 1.53 (s, 3H) ppm. **^{13}C NMR** (126 MHz, CDCl$_3$): δ 145.36, 144.06, 128.44, 126.97, 126.61, 113.75, 83.22, 70.96, 60.98, 32.71, 26.10 ppm. **IR** (neat): v = 3301, 2924, 2803, 1732, 1445, 1028, 920, 759, 697 cm^{-1}. **HRMS** (ESI+, MeOH): m/z calcd. 186.1277 (M + H)$^+$, found: 186.1281. **UPC2** conditions: OJ-3 column, Isocratic CO$_2$/MeOH/DEA = 98 : 2 : 0.1, 2 ml/min, 2000 psi; 93 : 7 er; $[\alpha]_D^{25}$ = −13.6 (c = 0.14, CHCl$_3$).

25
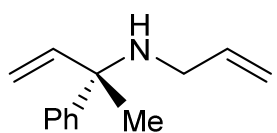
Scale: 0.15 mmol; isolated 20 mg (72% yield), light yellow oil, Hexane : EA = 10 : 1, R_f = 0.10. **^{1}H NMR** (500 MHz, CDCl$_3$): δ 7.48–7.46 (m, 2H), 7.34–7.31 (m, 2H), 7.25–7.20 (m, 1H), 6.04 (dd, J = 17.8, 10.4 Hz, 1H), 5.99–5.89 (m, 1H), 5.22–5.16 (m, 3H), 5.05 (dq, J = 10.2, 1.4 Hz, 1H), 3.11–3.03 (m, 2H), 1.53 (s, 3H) ppm. **^{13}C NMR** (126 MHz, CDCl$_3$): δ 146.31, 144.99, 137.70, 128.30, 126.69, 126.60, 115.26, 113.01, 60.63, 46.04, 26.22 ppm. **IR** (neat): v = 2977, 2926, 2853, 1738, 1620, 1600, 1446, 1337, 1073, 992, 764, 698 cm^{-1}. **HRMS** (ESI+, MeOH): m/z calcd. 188.1434 (M + H)$^+$, found: 188.1426. The ee of allylic amine **26** was determined using a chiral shift reagent, and was based on the integration of the vinyl group.

26
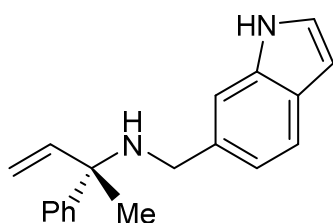
Scale: 0.15 mmol; isolated 30 mg (72% yield), white powder, Hexane : EA = 10 : 1, R_f = 0.30. **^{1}H NMR** (300 MHz, CDCl$_3$): δ 8.21 (s, 1H), 7.59 (d, J = 8.4 Hz, 3H), 7.42–7.35 (m, 3H), 7.30–7.24 (m, 1H), 7.18–7.14 (m, 1H), 7.10 (d, J = 8.1 Hz, 1H), 6.53 (s, 1H), 6.16 (dd, J = 17.5, 10.7 Hz, 1H), 5.33–5.21 (m, 2H), 3.73 (d, J = 2.0 Hz, 2H), 1.64 (s, 3H) ppm. **^{13}C NMR** (101 MHz, CDCl$_3$): δ 146.48, 145.15, 136.17, 135.27, 128.32, 126.96, 126.72, 126.70, 124.23, 120.69, 120.61, 113.08, 110.62, 102.52, 60.95, 47.87, 26.28 ppm. **IR** (neat): v = 3080, 2920, 1422, 1336, 1260, 1052, 922, 814, 770, 698 cm^{-1}. **HRMS** (ESI+, MeOH): m/z calcd. 277.1699 (M + H)$^+$, found: 277.1686. **UPC2** conditions: OJ3 column,

27

Isocratic CO_2/CAN/DEA = 85 : 15 : 0.1, 2 ml/min, 2000 psi; 81:19 *er*; $[\alpha]_D^{25}$ = −39.7 (*c* = 0.11, $CHCl_3$).
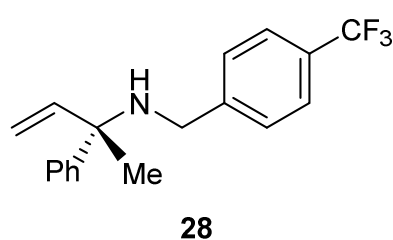
Scale: 0.15 mmol; isolated 37 mg (81% yield), light yellow oil, Hexane : EA = 10 : 1, R_f = 0.30. **^{1}H NMR** (400 MHz, $CDCl_3$): δ 7.60–7.54 (m, 4H), 7.51 (d, *J* = 8.0 Hz, 2H), 7.39–7.34 (m, 2H), 7.29–7.24 (m, 1H), 6.12 (dd, *J* = 17.5, 10.7 Hz, 1H), 5.31–5.24 (m, 2H), 3.69 (s, 2H), 1.60 (s, 3H). **^{19}F NMR** (376 MHz, $CDCl_3$) δ -62.45 ppm. **^{13}C NMR** (101 MHz, $CDCl_3$): δ 146.17, 145.71, 144.84, 129.17 (q, *J* = 32.3 Hz), 128.42, 128.38, 126.89, 126.63, 125.5 (q, *J* = 272.7 Hz), 125.34 (q, *J* = 3.0 Hz), 113.30, 60.93, 47.02, 26.26 ppm. **IR** (neat): *v* = 2977, 2927, 1619, 1416, 1332, 1161, 1121, 1066, 1018, 700. **HRMS** (ESI+, MeOH): *m/z* calcd. 306.1464 (M + H)$^+$, found: 306.1476 cm^{-1}. **UPC2** conditions: OJ-3 column, Isocratic CO_2/IPA/DEA = 85 : 15 : 0.1, 2 ml/min, 2000 psi; 94 : 6 *er*; $[\alpha]_D^{25}$ = −23.1 (*c* = 0.12, $CHCl_3$).
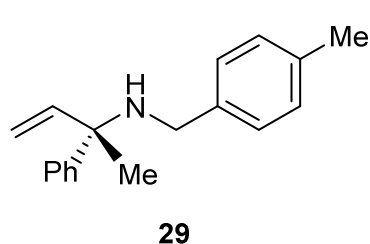
Scale: 0.15 mmol; isolated 24 mg (64% yield), light yellow oil, Hexane : EA = 10 : 1, R_f = 0.33. **^{1}H NMR** (400 MHz, $CDCl_3$): δ 7.61–7.57 (m, 2H), 7.41–7.36 (m, 2H), 7.32–7.27 (m, 3H), 7.17 (d, *J* = 7.8 Hz, 2H), 6.14 (dd, *J* = 17.5, 10.7 Hz, 1H), 5.32–5.24 (m, 2H), 3.61 (d, *J* = 2.9 Hz, 2H), 2.38 (s, 3H), 1.62 (s, 3H) ppm. **^{13}C NMR** (101 MHz, $CDCl_3$): δ 146.48, 145.12, 138.40, 136.45, 129.15, 128.31, 128.21, 126.69, 113.04, 60.84, 47.15, 26.27, 21.23 ppm. **IR** (neat): *v* = 2975, 2922, 1490, 1445, 1140, 916, 803, 762, 699 cm^{-1}. **HRMS** (ESI+, MeOH): *m/z* calcd. 252.1747 (M + H)$^+$, found: 252.1737. **UPC2** conditions: OJ-3 column, Isocratic CO_2/IPA/DEA = 85 : 15 : 0.1, 2 ml/min, 2000 psi; 95 : 5 *er*; $[\alpha]_D^{25}$ = −22.4 (*c* = 0.11, $CHCl_3$).
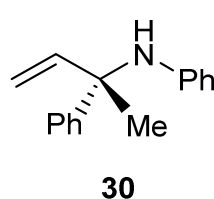
Scale: 0.15 mmol; isolated 29 mg (87% yield), light yellow oil, Hexane : EA = 25 : 1, R_f = 0.36; the racemic compound has been reported.[6] **^{1}H NMR** (500 MHz, $CDCl_3$): δ 7.53 (d, *J* = 7.3 Hz, 2H), 7.35 (t, *J* = 7.7 Hz, 2H), 7.26 (t, *J* = 7.3 Hz, 1H), 7.06–7.00 (m, 2H), 6.65 (t, *J* = 7.3 Hz, 1H), 6.45–6.35 (m, 3H), 5.30–5.21 (m, 2H), 4.16 (s, 1H), 1.71 (s, 3H)

ppm. **^{13}C NMR** (126 MHz, CDCl$_3$): δ 145.83, 145.41, 143.00, 128.73, 128.64, 126.81, 126.39, 117.48, 115.88, 113.96, 60.38, 29.40 ppm. **UPC2** conditions: OJ-3 column, Isocratic CO$_2$/IPA/DEA = 80 : 20 : 0.1, 2 ml/min, 2000 psi; 88 : 12 *er*; $[\alpha]_D^{25}$ = −66.7 (*c* = 0.11, CHCl$_3$).
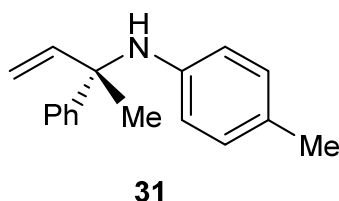
Scale: 0.15 mmol; isolated 28 mg (79% yield), light yellow oil, Hexane : EA = 25 : 1, R_f = 0.35. **^{1}H NMR** (400 MHz, CDCl$_3$): δ 7.56–7.54 (m, 2H), 7.39–7.34 (m, 2H), 7.30–7.25 (m, 1H), 6.87 (d, *J* = 8.1 Hz, 2H), 6.43–6.34 (m, 3H), 5.31–5.20 (m, 2H), 4.05 (s, 1H), 2.21 (s, 3H), 1.71 (s, 3H) ppm. **^{13}C NMR** (101 MHz, CDCl$_3$): δ 145.61, 143.43, 143.22, 129.28, 128.61, 126.75, 126.71, 126.43, 116.09, 113.83, 60.39, 29.30, 20.47 ppm. **IR** (neat): *v* = 3411, 2979, 2919, 1615, 1572, 1445, 1253, 1027, 808, 700 cm^{-1}. **HRMS** (ESI+, MeOH): *m/z* calcd. 238.1590 (M + H)$^+$, found: 238.1586. **UPC2** conditions: OJ-3 column, Isocratic CO$_2$/IPA/DEA = 85 : 15 : 0.1, 2 ml/min, 2000 psi; 82 : 18 *er*; $[\alpha]_D^{25}$ = -45.2 (*c* = 0.12, CHCl$_3$).
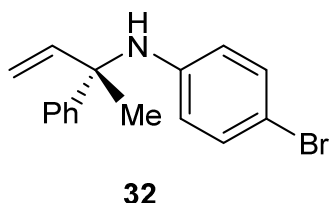
Scale: 0.15 mmol; isolated 33 mg (73% yield), light yellow oil, Hexane : EA = 25 : 1, R_f = 0.33. **^{1}H NMR** (500 MHz, CDCl$_3$): δ 7.50–7.43 (m, 2H), 7.33 (t, *J* = 7.6 Hz, 2H), 7.27–7.23 (m, 1H), 7.12–7.04 (m, 2H), 6.34 (dd, *J* = 17.3, 10.7 Hz, 1H), 6.27 (d, *J* = 8.8 Hz, 2H), 5.28–5.19 (m, 2H), 4.19 (s, 1H), 1.68 (s, 3H) ppm. **^{13}C NMR** (101 MHz, CDCl$_3$): δ 144.79, 142.26, 131.46, 128.76, 127.01, 126.31, 117.33, 114.33, 109.27, 60.46, 29.79 ppm. **IR** (neat): *v* = 3413, 2968, 2924, 1591, 1490, 1445, 1293, 1254, 1074, 923, 813, 700 cm^{-1}. **HRMS** (ESI+, MeOH): *m/z* calcd. 131.0855 (M − *p*-Br-C$_6$H$_4$NH)$^+$, found: 131.0855. **UPC2** conditions: IG column, Isocratic CO$_2$/MeOH/DEA = 80 : 20 : 0.1, 2 ml/min, 2000 psi; 86 : 14 *er*; $[\alpha]_D^{25}$ = −48.8 (*c* = 0.11, CHCl$_3$).
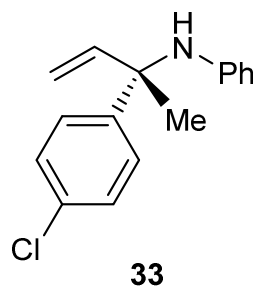
Scale: 0.15 mmol; isolated 32 mg (82% yield), light yellow oil, Hexane : EA = 25 : 1, R_f = 0.34. **^{1}H NMR** (400 MHz, CDCl$_3$): δ 7.48–7.41 (m, 2H), 7.32–7.28 (m, 2H), 7.05–7.01 (m, 2H), 6.67–6.64 (m, 1H), 6.43–6.26 (m, 3H), 5.29–5.19 (m, 2H), 4.12 (s, 1H), 1.67 (s, 3H) ppm. **^{13}C NMR** (101 MHz, CDCl$_3$): δ 145.47, 143.95, 142.42, 132.63, 128.82, 128.77, 127.96, 117.75, 115.87, 114.41,

60.07, 29.58 ppm. **IR** (neat): ν = 3411, 3052, 2980, 1600, 1490, 1315, 1256, 1093, 924, 748, 693 cm^{-1}. **HRMS** (ESI+, MeOH): m/z calcd. 258.1044 (M + H)$^+$, found: 258.1055. **UPC2** conditions: IG column, Isocratic CO_2/MeOH/DEA = 80 : 20 : 0.1, 2 ml/min, 2000 psi; 85 : 15 er; $[\alpha]_D^{25}$ = −51.6 (c = 0.11, CHCl$_3$).
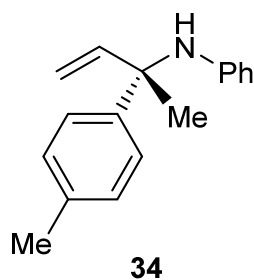
Scale: 0.15 mmol; isolated 28 mg (79% yield), light yellow oil, Hexane : EA = 25 : 1, R_f = 0.35; the racemic compound has been reported.[25] **¹H NMR** (400 MHz, CDCl$_3$): δ 7.39 (d, J = 8.2 Hz, 2H), 7.14 (d, J = 8.0 Hz, 2H), 7.04–7.00 (m, 2H), 6.63 (t, J = 7.3 Hz, 1H), 6.48–6.40 (m, 2H), 6.35 (dd, J = 17.3, 10.6 Hz, 1H), 5.29–5.16 (m, 2H), 4.12 (s, 1H), 2.34 (s, 3H), 1.68 (s, 3H) ppm. **¹³C NMR** (101 MHz, CDCl$_3$): δ 145.95, 143.23, 142.47, 136.37, 129.36, 128.72, 126.30, 117.40, 115.88, 113.74, 60.19, 29.32, 21.13 ppm. **UPC2** conditions: IF column, Isocratic CO_2/MeOH/DEA = 98 : 2 : 0.1, 2 ml/min, 2000 psi; 84 : 16 er; $[\alpha]_D^{25}$ = -42.3 (c = 0.10, CHCl$_3$).
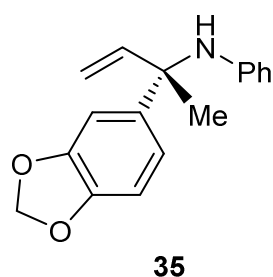
Scale: 0.15 mmol; isolated 28 mg (70% yield), light yellow oil, Hexane : EA = 25 : 1, R_f = 0.26. **¹H NMR** (400 MHz, CDCl$_3$): δ 7.08–7.00 (m, 3H), 6.98 (dd, J = 8.2, 1.9 Hz, 1H), 6.77 (d, J = 8.1 Hz, 1H), 6.67–6.62 (m, 1H), 6.45–6.42 (m, 2H), 6.33 (dd, J = 17.3, 10.6 Hz, 1H), 5.94 (s, 2H), 5.27–5.17 (m, 2H), 4.09 (s, 1H), 1.66 (s, 3H) ppm. **¹³C NMR** (101 MHz, CDCl$_3$): δ 148.09, 146.38, 145.76, 143.04, 139.65, 128.77, 119.37, 117.57, 115.86, 113.78, 108.15, 107.30, 101.12, 60.18, 29.25 ppm. **IR** (neat): ν = 3426, 2965, 2905, 1600, 1435, 1318, 1107, 922, 806, 747, 690 cm^{-1}. **HRMS** (ESI+, MeOH): m/z calcd. 268.1332 (M + H)$^+$, found: 268.1328. **UPC2** conditions: IG column, Isocratic CO_2/MeOH/DEA = 80 : 20 : 0.1, 2 ml/min, 2000 psi; 80.5 : 19.5 er; $[\alpha]_D^{25}$ = −30.4 (c = 0.13, CHCl$_3$).
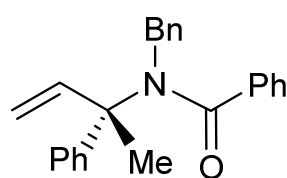
¹H NMR (400 MHz, CDCl3): δ 7.44-7.40 (m, 4H), 7.37-7.20 (m, 11H), 6.52 (dd, J = 17.5, 10.7 Hz, 1H), 5.13 (dd, J = 10.7, 0.8 Hz, 1H), 4.92 (dd, J = 17.5, 0.8 Hz, 1H), 4.78 (d, J = 3.9 Hz, 2H), 1.83 (s, 3H) ppm. **¹³C NMR** (101 MHz, CDCl3): δ 173.10, 146.16, 142.43, 139.56, 138.26, 129.49, 128.54, 128.43, 128.37,

127.17, 126.89, 126.73, 126.49, 125.10, 114.75, 66.50, 52.54, 25.02 ppm. **IR** (neat): $v =$ 3024, 2965, 1623, 1445, 1387, 1131, 920, 721, 694, 647 cm^{-1}. **HRMS** (ESI+, MeOH): *m/z* calcd. 342.1852 (M + H)+, found: 342.1847. **UPC2** conditions: OJ-3 Column, Isocratic CO_2/IPA/DEA = 85 : 15 : 0.1, 1500 psi, 3 ml/min; 95 : 5 *er*; $[\alpha]_D^{25} = -9.8$ (*c* = 0.11, CHCl$_3$).
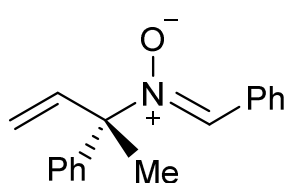
37: 76%, 96:4 *er*

^{1}H NMR (400 MHz, CDCl3): δ 8.27–8.23 (m, 2H), 7.53 (s, 1H), 7.43-7.31 (m, 8H), 6.51 (dd, *J* = 17.3, 10.7 Hz, 1H), 5.45 (d, *J* = 10.7 Hz, 1H), 5.18 (d, *J* = 17.3 Hz, 1H), 2.09 (s, 3H) ppm. **^{13}C NMR** (101 MHz, CDCl3): δ 141.33, 140.40, 133.70, 130.74, 130.48, 129.00, 128.79, 128.59, 128.16, 126.87, 118.03, 80.99, 25.12 ppm. **IR** (neat): *v* = 3057, 2985, 1555, 1444, 1410, 1120, 1072, 1028, 809, 749, 690 cm^{-1}. **HRMS** (ESI+, MeOH): *m/z* calcd. 274.1202 (M + Na)+, found: 274.1203. **UPC2** conditions: IA Column, Isocratic CO_2/MeOH/DEA = 95 : 5 : 0.1, 1500 psi, 3 ml/min; 96 : 4 *er*; $[\alpha]_D^{25} = 12.9$ (*c* = 0.10, CHCl$_3$).
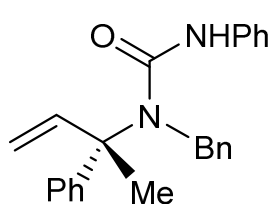
38: 93%, 95:5 *er*

^{1}H NMR (360 MHz, CDCl3): δ 7.51-7.29 (m, 10H), 7.16-7.11 (m, 2H), 6.94-6.90 (m, 3H), 6.36-6.27 (m, 2H), 5.21 (d, *J* = 10.6 Hz, 1H), 5.13 (d, *J* = 17.3 Hz, 1H), 4.93-4.79 (m, 2H), 1.83 (s, 3H) ppm. **^{13}C NMR** (101 MHz, CDCl3): δ 156.55, 145.10, 142.24, 140.74, 138.95, 129.50, 128.82, 128.78, 127.91, 127.27, 127.04, 126.00, 122.89, 119.52, 114.49, 66.19, 49.66, 25.94 ppm. **IR** (neat): *v* = 3403, 3027, 1656, 1526, 1496, 1439, 1311, 1177, 1028, 750, 692 cm^{-1}. **HRMS** (ESI-, MeOH): *m/z* calcd. 355.1816 (M − H)+, found: 355.1815. **SFC** conditions: OJ-3 Column, Isocratic CO_2/IPA/DEA = 90 : 10 : 0.1, 1500 psi, 2 ml/min; 95 : 5 *er*; $[\alpha]_D^{25} = -$4.6 (*c* = 0.05, CHCl$_3$).
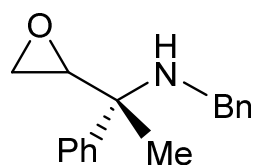
39: 57%, 26:74 *dr*
94.5:5.5 *er*

^{1}H NMR (500 MHz, CDCl3): δ 7.61-7.57 (m, 2H), 7.43-7.37 (m, 2H), 7.35-7.29 (m, 5H), 7.25-7.22 (m, 1H), 3.67-3.41 (m, 2H), 3.28-3.08 (m, 1H), 3.02-2.93 (m, 1H), 2.79-2.66 (m, 1H), 1.75-1.45 (2 s, 3H) ppm. **^{13}C NMR** (126 MHz, CDCl3): δ 144.38, 143.46, 143.09, 141.27, 128.61, 128.50, 128.45, 128.42, 128.17, 128.10, 127.36, 127.23, 127.22, 126.92, 126.62, 60.39, 59.08,

57.91, 57.58, 46.87, 46.40, 44.80, 44.50, 22.39, 21.52 ppm. **IR** (neat): v = 3060, 2979, 2929, 1493, 1450, 1028, 907, 756, 698 cm^{-1}. **HRMS** (ESI+, MeOH): *m/z* calcd. 254.1539 (M + H)+, found: 254.1537. The *ee* of allylic amine **39** was determined using a chiral shift reagent, and was based on the integration of the methyl protons.

3.4.7 X-ray Crystallographic Data for 1·HCl

Table 3.9. Crystal data and structure refinement for allylic amine **1**·HCl (CCDC 1554683).

Empirical formula	$C_{17}H_{20}ClN$
Formula weight	273.79
Temperature	100(2) K
Wavelength	0.71073 Å
Crystal system	Monoclinic
Space group	$P2(1)$
Unit cell dimensions	a = 10.1383(2)Å $\quad$ α= 90°
	b = 12.8743(2)Å $\quad$ β = 104.671(2)°
	c = 11.8748(2)Å $\quad$ γ = 90°
Volume	1499.40(5) Å^3
Z	4
Density (calculated)	1.213 mg/m^3
Absorption coefficient	0.242 mm^{-1}
F(000)	584
Crystal size	0.10 × 0.10 × 0.08 mm^3
Theta range for data collection	2.364 to 28.954°.
Index ranges	-13<=h<=13,-16<=k<=17,-14<=l<=16
Reflections collected	20725
Independent reflections	7045[R(int) = 0.0228]
Completeness to theta = 28.954°	92.0%
Absorption correction	Multi-scan
Max. and min. transmission	0.981 and 0.755
Refinement method	Full-matrix least-squares on F^2
Data / restraints / parameters	7045/ 1/ 339
Goodness-of-fit on F^2	1.057
Final R indices [I>2sigma(I)]	R_1 = 0.0358, wR_2 = 0.0928
R indices (all data)	R_1 = 0.0385, wR_2 = 0.0943
Flack parameter	x =0.025(15)
Largest diff. peak and hole	0.420 and -0.334 e·Å^{-3}
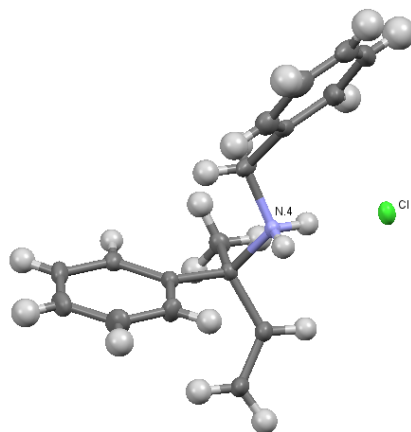
ORTEP view of the molecular structure of **1**·HCl with the adopted numbering scheme.

Note that the structure was measured using the same method as described in chapter 2.

Chapter 4.

A Mechanistic Analysis of the Palladium-Catalyzed Formation of Branched Allylic Amines Reveals the Origin of the Regio- and Enantioselective through a Unique Inner-Sphere Pathway

4.1 Introduction

4.1.1 General Background

Pd-catalyzed allylic substitution reactions provide one of the most powerful and straightforward approaches for the construction of C–C and C–X bonds in organic synthesis.[1] Phenomena that involve efficient discrimination of enantiotopic complex faces followed by ionization to lead to asymmetric induction so far have not been very successful in Pd-catalyzed processes.[2] Scheme 4.1 outlines one of the issues that complicates this target. A key obstacle in Pd-catalyzed allylic substitution reactions is the propensity of nucleophiles to attack at the sterically more accessible terminal position (path b) which leads to a linear product.[3] A second challenge is the facility of migration of the Pd ion from one enantiotopic face to the other (path c) via π–σ–π isomerization. Such a phenomenon, if faster than nucleophilic attack, can lead to asymmetric induction if the difference in activation energies for path a and *ent*-path a is sufficiently large in the presence of a suitable chiral ligand. In such an event, the nucleophilic addition step determines the asymmetric induction.[4] A third obstacle relates to the preferred motions with chiral scalemic ligands during the ionization and alkylation steps which must be opposite. Thus, if the former is a matched event, the latter must become a mismatched one and *vice versa*. Such stereochemical mismatching would tend to favor pathways b and c competing with path a or *ent*-path a. Considering the above mentioned issues, a key challenging in this field is the development of Pd-mediated regiodivergent strategies to

(1) For selected reviews, see: a) B. M. Trost, M. L. Crawley, *Chem. Rev.* **2003**, *103*, 2921; b) B. M. Trost, M. R. Machacek, A. Aponick, *Acc. Chem. Res.* **2006**, *39*, 747; c) Y.-N. Wang, L.-Q. Lu, W.-J. Xiao, *Chem. Asian J.* **2018**, *13*, 2174; d) N. A. Butt, W. Zhang, *Chem. Soc. Rev.* **2015**, *44*, 7929; e) J. D. Weaver, A. Recio III, A. J. Grenning, J. A. Tunge, *Chem. Rev.* **2011**, *111*, 1846; f) B. M. Trost, T. Zhang, J. D. Sieber, *Chem. Sci.* **2010**, *1*, 427; g) Z. Lu, S. Ma, *Angew. Chem. Int. Ed.* **2008**, *47*, 258; h) S. Oliver, P. A. Evans, *Synthesis* **2013**, *45*, 3179; i) G. Helmchen, A. Pfaltz, *Acc. Chem. Res.* **2000**, *33*, 336; j) C.-H. Ding, X.-L. Hou, *Top. Organomet. Chem.* **2011**, *36*, 247; k) C.-X. Zhuo, C. Zheng, S.-L. You, *Acc. Chem. Res.* **2014**, *47*, 2558.
(2) a) T. Hayashi, K. Kishi, H. Yamamoto, Y. Ito, *Tetrahedron Lett.* **1990**, *31*, 1743; b) T. Hayashi, A. Yamamoto, Y. Ito, *Tetrahedron Lett.* **1988**, *29*, 669; c) T. Hayashi, A. Ohno, S. Lu, Y. Matsumoto, Y. Uozumi, M. Miki, K. Yanagi, *J. Am. Chem. Soc.* **1994**, *116*, 775; d) K. Yamamoto, R. Deguchi, Y. Ogimura, J. Tsuji, *Chem. Lett.* **1984**, 1657; e) J. P. Genét, S. Grisone, *Tetrahedron Lett.* **1988**, *29*, 4543.
(3) a) S. A. Godleski, *Comprehensive Organic Synthesis*; B. M. Trost, I. Fleming, M. F. Semmelhack, Eds.; Pergamon Press: Oxford: Vol. 4, Chapter 3.3, pp 585-662; b) B. M. Trost, M.-H. Hung, *J. Am. Chem. Soc.* **1984**, *106*, 6837.
(4) a) B. M. Trost, R. C. Bunt, *Angew. Chem., Int. Ed. Engl.* **1996**, *35*, 99; b) G. J. Dawson, J. M. J. Williams, S. J. Coote, *Tetrahedron Lett.* **1995**, *36*, 461; c) P. R. Auburn, P. B. Mackenzie, B. Bosnich, *J. Am. Chem. Soc.* **1985**, *107*, 2033.

realize highly selective formation of either the linear or the branched product from allylic precursors.
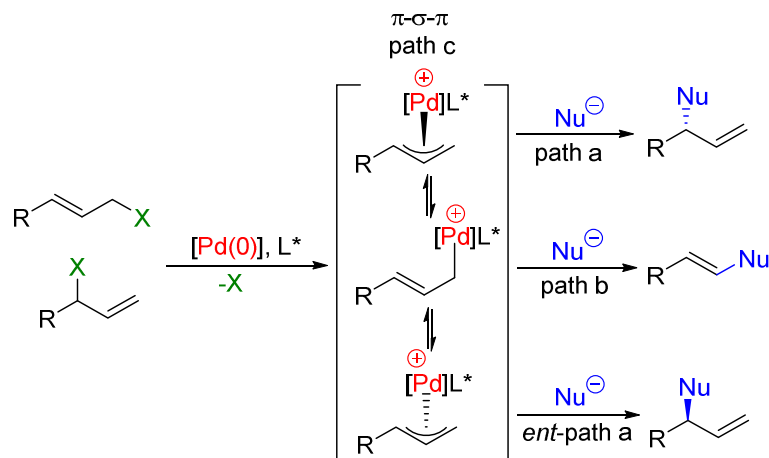
Scheme 4.1. Asymmetric induction via enantiotopic facial discrimination.

From a mechanistic point of view, it is generally accepted that Pd-catalyzed allylic substitutions take place through an outer-sphere pathway (Scheme 4.2). Thus, the formation of the linear products is predominant in most cases since the nucleophilic attacks at the less hindered, terminal carbon and is favored over the attack at the internal carbon center. Previous studies have revealed that the regioselectivity of an outer-sphere pathway can be controlled to a certain extent through a rational design of the allylic substitution process (*i.e.*, using a specific substrate, ligand and/or additive).[5]
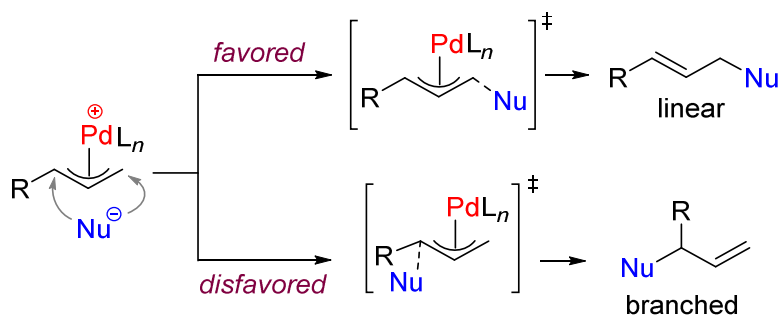
Scheme 4.2. An outer-sphere pathway typically favors the linear product.

(5)   For selected examples, see: a) Y.-N. Wang, B.-C. Wang, M.-M. Zhang, X.-W. Gao, T.-R. Li, L.-Q. Lu, W.-J. Xiao, *Org. Lett.* **2017**, *19*, 4094; b) H. Inami, T. Ito, H. Ura-be, F. A. Sato, *Tetrahedron Lett.* **1993**, *34*, 5919; c) J.-P. Chen, C.-H. Ding, W. Liu, X.-L. Hou, L.-X. Dai, *J. Am. Chem. Soc.* **2010**, *132*, 15493; d) H. Steinhagen, M. Reggelin, G. Helmchen, *Angew. Chem. Int. Ed. Engl.* **1997**, *36*, 2108; e) T. Hayashi, M. Kawatsura, Y. Uozumi, *J. Am. Chem. Soc.* **1998**, *120*, 1681; f) S.-L. You, X.-Z. Zhu, Y.-M. Luo, X.-L. Hou, L.-X. Dai, *J. Am. Chem. Soc.* **2001**, *123*, 7471; g) I. Dubovyk, I. D. G. Watson, A. K. Yudin, *J. Org. Chem.* **2013**, *78*, 1559; h) X. Wang, P. Guo, Z. Han, X. Wang, Z. Wang, K. Ding, *J. Am. Chem. Soc.* **2014**, *136*, 405.

For instance, in 2000, Trost and co-workers developed a Pd-catalyzed branched selective allylic amination of vinyl epoxides, in which a hydrogen-bonding interaction between the nucleophile and the oxo-anion of the π-allyl-Pd intermediate was proposed to be crucial in guiding the regioselectivity towards the formation of the branched product (Scheme 4.3).[6]
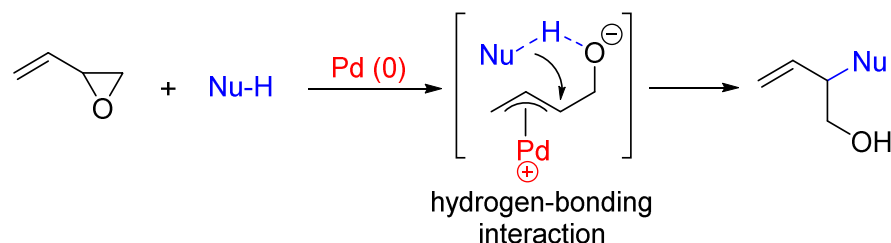
Sheme 4.3. Pd-catalyzed branched selective allylic substitution of vinyl epoxide.

4.1.2 Inner-Sphere Pathway
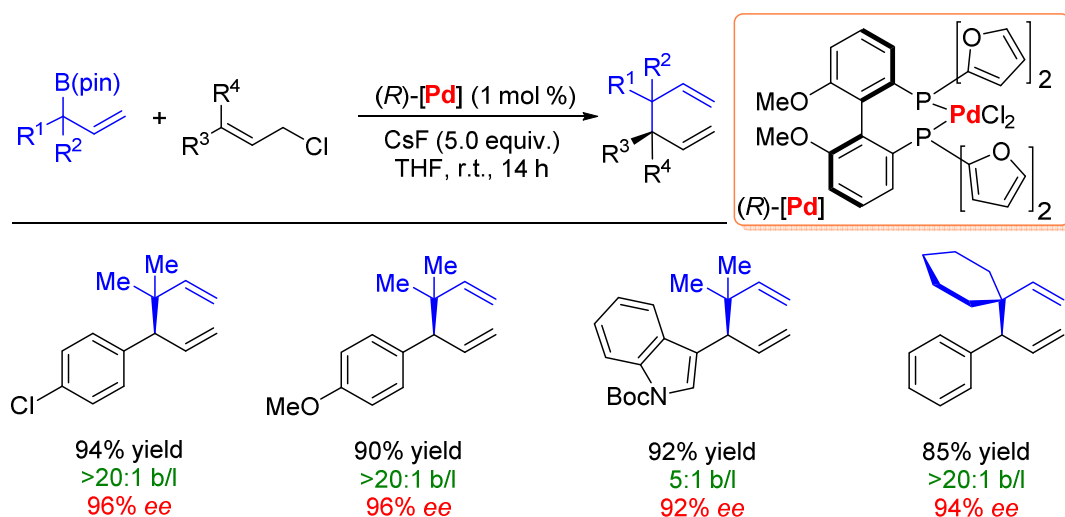
Scheme 4.4. Pd-catalyzed allyl−allyl couplings.

Although limited in scope, some recent cases have shown that the selective formation of branched allylic products can also be achieved by an inner-sphere pathway. In 2014, Morken and co-worker reported the development of an effective catalyst for Pd-catalyzed allyl-allyl couplings (Scheme 4.4).[7] Under the influence of a chiral bidentate diphosphine ligand, the Pd-catalyzed asymmetric cross-coupling of allylboron reagents and allylic precursors establishes 1,5-dienes with adjacent stereocenters in high regio- and

(6) B. M. Trost, R. C. Bunt, R. C. Lemoine, T. L. Calkins, T. *J. Am. Chem. Soc.* **2000**, *122*, 5968.
(7) a) M. J. Ardolino, J. P. Morken, *J. Am. Chem. Soc.* **2014**, *136*, 7092.

enantioselectivity. A mechanistic study through reaction progress kinetic analysis, labeling studies, and DFT calculations suggested that the reaction operates through an inner-sphere 3,3′-reductive elimination pathway, which is both rate-limiting and stereo-controlling. Additionally, these new reaction conditions and insight allowed for the extension of this coupling reaction to forge products containing vicinal quaternary and tertiary centers as well as having unique ring systems.

Recently, Goddard, Stoltz and co-workers communicated a detailed reaction mechanism of the Tsuji allylation involving prochiral nucleophiles and allylic substrates (Scheme 4.5). They further showed that the observed enantioselectivity in the Pd-catalyzed intramolecular decarboxylative allylic alkylation of allyl enol carbonates is best explained through an inner-sphere pathway.[8] In this chemistry, although conclusive identification of the enantioselective step was not possible, they noted that three different types of computational analyses using different levels of theory all revealed that inner-sphere pathways are lower in energy than outer-sphere pathways. These results qualitatively contrast with established allylation reaction mechanisms involving prochiral nucleophiles and prochiral allylic fragments.
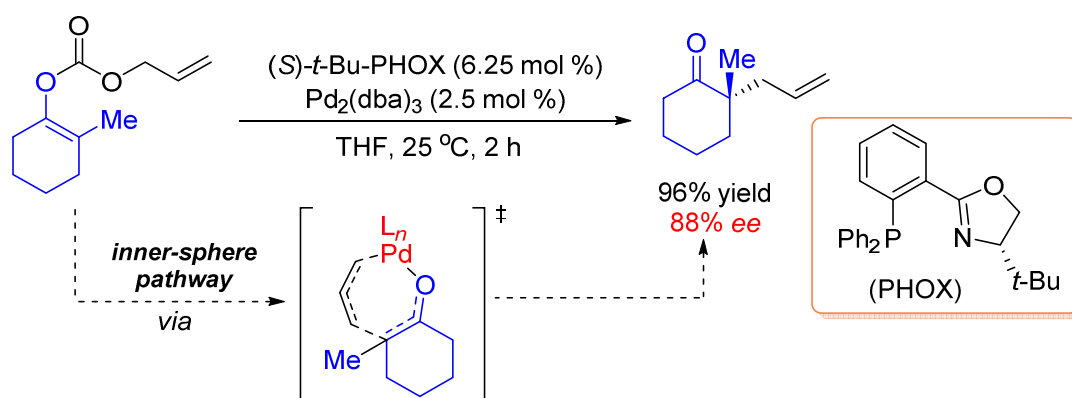
Scheme 4.5. Enantioselective allylation through an inner-sphere pathway.

In 2011, Hou and co-workers reported chemo- and regioselectivity-tunable Pd-catalyzed allylic alkylation of imines. α-Carbanions of cyclic and acyclic imines were successfully applied as nucleophiles in the allylic alkylation reaction. Tuning of the chemo- and regioselectivity was realized by using bases with different counterions.[9]

---

(8) a) J. A. Keith, D. C. Behenna, J. T. Mohr, S. Ma, S. C. Marinescu, J. Oxgaard, B. M. Stoltz, W. A. Goddard III, *J. Am. Chem. Soc.* **2007**, *129*, 11876; b) J. A. Keith, D. C. Behenna, N. Sherden, J. T. Mohr, S. Ma, S. C. Marinescu, R. J. Nielsen, J. Oxgaard, B. M. Stoltz, W. A. Goddard III, *J. Am. Chem. Soc.* **2012**, *134*, 19050.

(9) J.-P. Chen, Q. Peng, X.-L. Hou, Y.-D. Wu, *J. Am. Chem. Soc.* **2011**, *133*, 14180.

When the hard-acid ion Li$^+$ was used, the linear product was produced. In the presence of the soft-acid counterions Na$^+$ or K$^+$, the branched product was obtained. A novel mechanism involving a transmetalation and a Pd-mediated 3,3′-reductive elimination was proposed to account for the formation of the branched product using Na$^+$ or K$^+$ as the counterion. DFT calculations suggested that the unique branched selectivity of the reaction occurs through an inner-sphere pathway. Subsequently, they reported an efficient Pd-catalyzed protocol for reactions of β-substituted ketones as nucleophiles with mono-substituted allylic precursors using an N-heterocyclic carbene as ligand, leading to branched products with up to three contiguous stereocenters with excellent regio- and diastereoselectivities.[10] Mechanistic studies by both DFT calculations and experiments revealed that the reaction proceeds via an inner-sphere mechanism, i.e. nucleophilic attack of an enolate oxygen on Pd followed by C–C bond-forming [3,3′]-reductive elimination (Scheme 4.6).
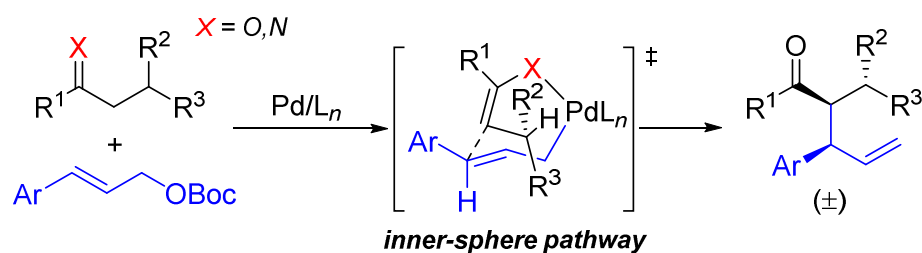
Scheme 4.6. Pd-catalyzed allylic alkylation with *N*- and *O*- based nucleophiles affording branched products.

4.1.3 Pd-catalyzed Decarboxylation of VCCs with Nucleophiles

Previous success in Pd-catalyzed decarboxylative transformations of vinylethylene carbonates (VCCs) with various electrophiles and (pro)nucleophiles has been reported.[11] In this context, Kleij, Maseras and co-workers developed a Pd-catalyzed allylic substitution of VCCs **1** with aryl- and alkyl-amines (Scheme 4.7).[12] Notably, with the diphosphine ligand **L1**, complete linear regioselectivity and high (*Z*)-stereoselectivity was observed, thus providing a general method for the stereoselective construction of tri- and tetrasubstituted allylic amines (*Z*)-**2**. A detailed reaction mechanism was also provided

(10) D.-C. Bai, F.-L. Yu, W.-Y. Wang, D. Chen, H. Li, Q.-R. Liu, C.-H. Ding, B. Chen, X.-L. Hou, *Nat. Commun.* **2016**, *7*, 11806.
(11) For a recent review, see: W. Guo, J. E. Gómez, À. Cristòfol, J. Xie, A. W. Kleij, *Angew. Chem. Int. Ed.* **2018**, *57*, 13735.
(12) W. Guo, L. Martínez-Rodríguez, R. Kuniyil, E. Martin, E. C. Escudero-Adán, F. Maseras, A. W. Kleij, *J. Am. Chem. Soc.* **2016**, *138*, 11970.

by DFT calculations, and the computational results showed that the reaction follows a generally accepted outer-sphere pathway in line with the experimental results.
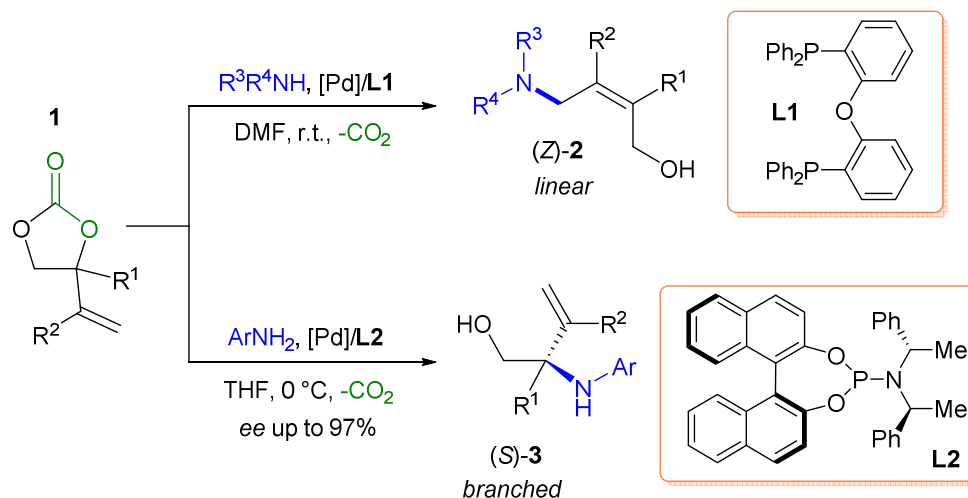
Scheme 4.7. Ligand-controlled linear or branched allylic amination of VCC **1**.

At a later stage, Kleij and co-workers found that the regioselectivity of this reaction can be switched towards the branched product through ligand control.[13] The use of phosphoramidite **L2** afforded the elusive α,α-disubstituted allylic *N*-aryl amines such as (*S*)-**3** in good yields under excellent regio- and enantiocontrol (Scheme 4.7).
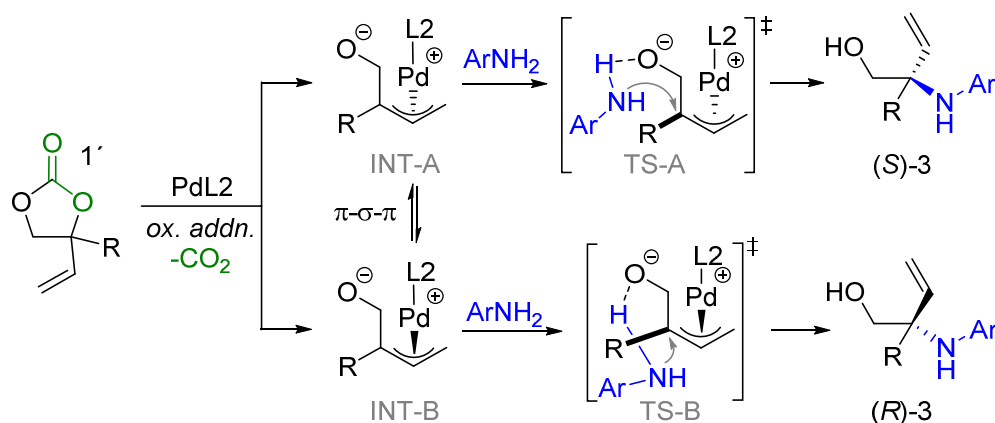
Scheme 4.8. Previous proposed outer-sphere branched allylic amination of VCC **1′**.

The manifold responsible for this rare regio- and enantio-controlled synthesis of these sterically encumbered chiral allylic amines was proposed to go through a dynamic kinetic resolution (DKR) process[14] after initial oxidative addition of the VCC **1′** to Pd(0)

(13) A. Cai, W. Guo, L. Martínez-Rodríguez, A. W. Kleij, *J. Am. Chem. Soc.* **2016**, *138*, 14194.
(14) B. M. Trost, D. R. Fandrick, *Aldrichimica Acta* **2007**, *40*, 59; b) B. M. Trost, F. D. Toste, *J. Am. Chem. Soc.* **2003**, *125*, 3090; c) R. Noyori, M. Tokunaga, M. Kitamura, *Bull. Chem. Soc. Jpn.* **1995**, *68*, 36; d) F. Huerta, A. B. E. Minidis, J-E. Backvall, *Chem. Soc. Rev.* **2001**, *30*, 321.

following CO_2 extrusion (Scheme 4.8). Then, the amine attacks the zwitterionic Pd(allyl) intermediate at the internal carbon center of intermediates **INT-A** or **INT-B** guided by the alkoxy fragment in an outer-sphere mechanism through transition states **TS-A** or **TS-B** to afford branched-products (*S*)-**3** or (*R*)-**3**, respectively. The phosphoramidite ligand **L2** allows to kinetically differentiate between both outer-sphere attacks (Scheme 4.8), and hence high enantiomeric excess in the allylic amine product is observed.[15]

4.1.4 Aim of the Work presented in this Chapter
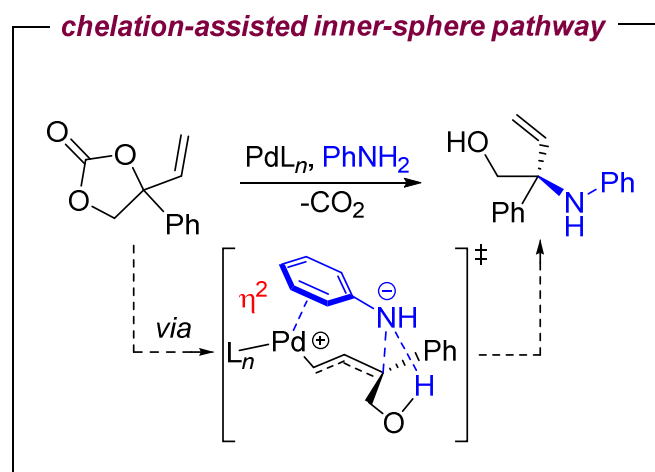
Scheme 4.9. A unique chelation-assisted inner-sphere pathway for the Pd-catalyzed allylic amination of VCCs with aryl amines.

Despite the notable progress in the formation of elusive and sterically encumbered α,α-disubstituted allylic amines,[16] the origin of both the branched regioselectivity and high asymmetric induction exerted by ligand effects is not well-understood. Therefore, it is appealing to investigate both computationally and experimentally the underlying mechanistic features that govern this unusual selectivity behavior in the Pd-mediated allylic amination. Our efforts show (*vide infra*), unlike previously assumed,[16] that the manifold involves a unique inner-sphere activation of the amine nucleophile that pre-organizes the nucleophilic attack to occur onto the internal carbon center of the Pd(allyl)

(15) A Pd-catalyzed asymmetric formation of α,α-disubstituted aliphatic allylic amines has been developed *via* DKR using related linear carbonate substrates, see: W. Guo, A. Cai, J. Xie, A. W. Kleij, *Angew. Chem. Int. Ed.* **2017**, *56*, 11797.

(16) a) J. S. Arnold, H. M. Nguyen, *J. Am. Chem. Soc.* **2012**, *134*, 8380; b) J. S. Arnold, E. T. Mwenda, H. M. Nguyen, *Angew. Chem. Int. Ed.* **2014**, *53*, 3688; c) J. S. Arnold, G. T. Cizio, H. M. Nguyen, *Org. Lett.* **2011**, *13*, 5576; d) M. Kawatsura, K. Uchida, S. Terasaki, H. Tsuji, M. Minakawa, T. Itoh, *Org. Lett.* **2014**, *16*, 1470; e) S. Mizuno, S. Terasaki, T. Shinozawa, M. Kawatsura, *Org. Lett.* **2017**, *19*, 504; f) M. Kawatsura, K. Uchida, S. Terasaki, H. Tsuji, M. Minakawa, T. Itoh, *Org. Lett.* **2014**, *16*, 1470; g) I. Dubovyk, I. D. G. Watson, A. K. Yudin, *J. Am. Chem. Soc.* **2007**, *129*, 14172.

intermediate (Scheme 4.9), with a key role for the experimentally optimized phosphoramidite ligand **L2** to favor the formation of one product enantiomer.

4.2   Results and Discussion

4.2.1 Formation of the Palladacyclic Intermediate INT4

The experimentally used (*rac*) vinyl cyclic carbonate **1a** and aniline ($PhNH_2$) were selected as model substrates for the computational studies (Figure 4.1).[17] Experimentally, the racemic vinylethylene carbonate **1a** is converted to a chiral allylic amine in a formal dynamic kinetic asymmetric transformation.[13] The calculations indeed show that after the C–O oxidative addition step and CO_2 extrusion starting from either (*R*)-**1a** or (*S*)-**1a**, the formation of the key palladacyclic intermediate is relatively easy (Figure 4.1; all energies in kcal/mol). For each intermediate/transition state, the energy of two possible states were computed, with L is thf (black numbers) or with no ligand (red numbers). Further on, we will thus only focus on the energetically most favorable pathway leading to the palladacyclic intermediates based on (*R*)-**1a** and (*S*)-**1a** (Figure 4.1).

The reaction is initiated by C–O oxidative addition of the cyclic carbonate substrate to the Pd(0) precursor (*i.e.*, $Pd_2(dba)_3 \cdot CHCl_3$). The computations show that the coordination of the double bond of (*R*)-**1a** and (*S*)-**1a** to the Pd center gives intermediates **INT1a** and **INT1b**, and these coordination steps were calculated to be exergonic by 20.0 and 18.1 kcal/mol, respectively. **INT1a** and **INT1b** then undergo a C–O oxidative addition via an S_N2 back-side attack passing through transition states **TS1a** and **TS1b**,[18] leading to zwitterionic, π-allyl-Pd complexes **INT2a** and **INT2b**, respectively. It should be noted here that in principle, four possible π-allyl-Pd complexes can be generated after the C–O oxidative addition, and all were considered in our calculation. Upon formation of the zwitterionic, π-allyl-Pd complexes **INT2a** and **INT2b**, the subsequent CO_2 extrusion step

---

(17) For selected examples of DFT studies on Pd-catalyzed allylic substitution reactions: a) J. Kleimark, P.-O. Norrby, *Top. Organomet. Chem.* **2012**, *38*, 65; b) M. Kalek, F. Himo, *J. Am. Chem. Soc.* **2017**, *139*, 10250; c) C. Zheng, C.-X. Zhuo, S.-L. You, *J. Am. Chem. Soc.* **2014**, *136*, 16251; d) C. Johansson, G. C. Lloyd-Jones, P.-O. Norrby, *Tetrahedron: Asymmetry* **2010**, *21*, 1585; e) P. Fristrup, T. Jensen, J. Hoppe, P.-O. Norrby, *Chem. Eur. J.* **2006**, *12*, 5352; f) K. E. McPherson, M. P. Croatt, A. T. Morehead Jr., A. L. Sargent, *Organometallics* **2018**, *37*, 3791; g) O. Piechaczyk, C. Thoumazet, Y. Jean, P. I. Floch, *J. Am. Chem. Soc.* **2006**, *128*, 14306; h) N. Solin, J. Kjellgren, K. J. Szabó, *J. Am. Chem. Soc.* **2004**, *126*, 7026; i) G. Jindal, R. B. Sunoj, *J. Org. Chem.* **2014**, *79*, 7600; j) S. T. Madrahimov, Q. Li, A. Sharma, J. F. Hartwig, *J. Am. Chem. Soc.* **2015**, *137*, 14968.
(18) S.-Q. Zhang, B. L. H. Taylor, C.-L. Ji, Y. Gao, M. R. Harris, L. E. Hanna, E. R. Jarvo, K. N. Houk, *J. Am. Chem. Soc.* **2017**, *139*, 12994.
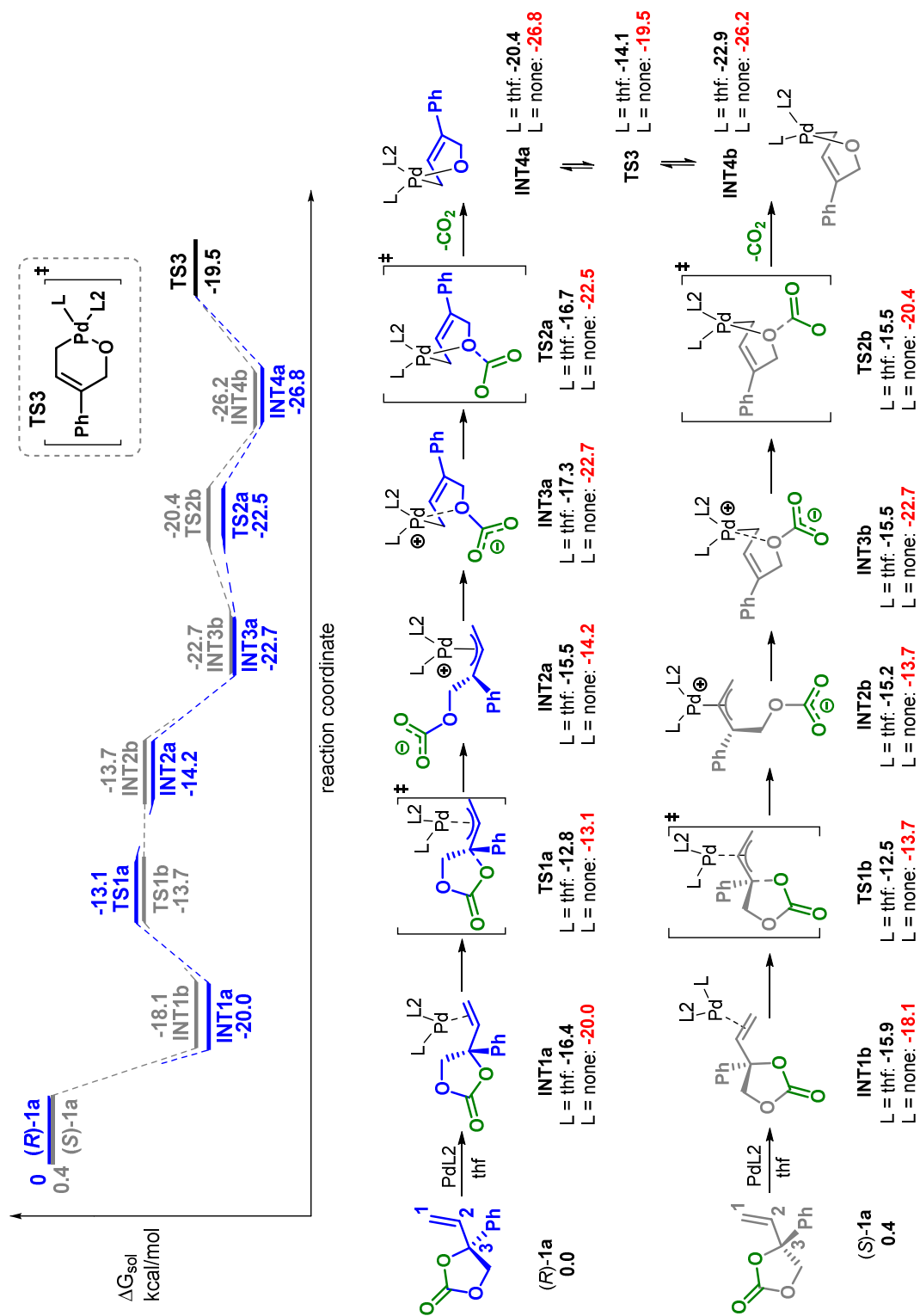
Figure 4.1. C–O oxidative addition and CO_2 extrusion from both enantiomers of the substrate **1a** leading to transition state **TS3**.

leading to the formation of the six-membered palladacyclic intermediate is assisted by a coordinative Pd–O chelating interaction, and affords intermediates **INT3a** and **INT3b**, which were calculated to be more stable than **INT2a** and **INT2b** by 8.5 and 9.0 kcal/mol, respectively. The CO_2 extrusion from **INT3a** and **INT3b** *via* transition states **TS2a** and **TS2b** was found to be virtually barrierless evolving thus into the palladacyclic intermediates **INT4a** and **INT4b**.

We have also evaluated CO_2 extrusion directly from **INT2a** and **INT2b**. However, the energies of the corresponding transition states were found to be much higher than **TS2a** and **TS2b**. The computed results are indeed consistent with the DFT study performed by Maseras and co-workers on a related Pd(**L1**)-catalyzed allylic amination reaction (towards formation of a linear (*Z*)-configured allylic amine) for which a chelation effect enabled by Pd–O coordination was revealed to be a key factor to control the stereoselectivity.[12] The reactions of (*R*)-**1a** and (*S*)-**1a** were found to converge at the stage of the formation of the palladacycle intermediate **INT4**. Since the DFT studies so far discussed revealed that both coordinatively saturated and unsaturated **INT4** intermediates are energetically feasible (Figure 4.1), we next turned our attention on the influence of the Pd/**L2** ratio on the outcome of the catalytic conversion of **1a**, and the spectroscopic and mass spectrometric analysis of relevant reaction mixtures composed of the Pd precursor and phosphoramidite ligand **L2** under various conditions (*vide infra*).

4.2.2 Influence of the Pd/L Ratio in the Allylic Amination Reaction

In order to gain insight into the role of the ratio of Pd to phosphoramidite ligand in the allylic amination reaction, we first carried out a series of control experiments (Table 4.1) showing that the overall kinetics of the allylic amination is significantly affected by the ratio between the Pd precursor and **L2** (entries 1-3; Pd-to-**L2** ratios increasing from 1:1 to 1:2). Interestingly, neither the relative amount of **L2** nor the reaction time affects the regio- and enantioselectivity of the reaction (entries 2-5), and compared well with the previously reported experimental data (entry 6).[13] This apparent requirement of two equivalents of phosphoramidite ligand to activate the $Pd_2(dba)_3 \cdot CHCl_3$ precursor has been well-documented and allows to reach equilibrium concentration of the pre-catalytic species.[19]

---

(19) a) H. Du, B. Zhao, Y. Shi, *J. Am. Chem. Soc*. **2008**, *130*, 8590; b) E. Janusson, H. S. Zijlstra, P. P. T. Nguyen, L. MacGillivray, J. Martelino, J. S. McIndoe, *Chem. Commun*. **2017**, *53*, 854; c) B. M. Trost,

Table 4.1 Influence of the ratio of [Pd]/**L2** on the overall performance in the allylic amination reaction between cyclic carbonate **1a** and aniline to afford (**S**)-**3a**.[a]
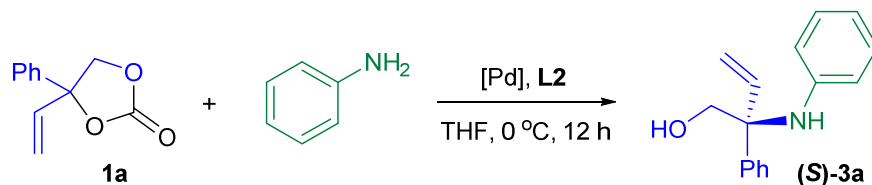
Entry	[**Pd₂**] [mol %]	**L2** [mol %]	B/L[b]	Conv.[b] [%]	Yield[c] [%]	ee[d]
1[e]	1.25	2.5	72:28	15	11[b]	nd
2[e]	1.25	3.75	76:24	50	35	97
3	1.25	5.0	78:22	>99	71	95
4[f]	1.25	5.0	81:19	57	42	98
5	1.25	7.5	76:24	>99	68	95
6[g]	1.25	5.0	79:21	>99	76	95

[a] Reaction conditions unless stated otherwise: 0.20 mmol (1.0 equiv.) of carbonate **1a**, aniline (1.5 equiv.), Pd₂(dba)₃·CHCl₃ [**Pd₂**] and **L2**: amounts are indicated, 0.20 mL of THF, 0 ºC, 12 h, open to air. B/L stands for branched-to-linear product ratio, nd for not determined. [b] Determined by ^{1}H NMR analysis (CDCl₃) of the crude reaction mixture: for entry 1 using toluene as an internal standard. [c] Isolated yield after chromatographic purification. [d] Determined by UPC2. [e] After 48 h. [f] After 6 h. [g] Reference data taken from footnote 15.

To examine whether classical kinetic resolution of the cyclic carbonate **1a** takes place (entry 4), the reaction was stopped after 6 h and the remaining carbonate was isolated and analysed by UPC2. The isolated substrate **1a** (37%) was virtually a racemic mixture, while the allylic amine product **3a** (42%) was isolated with 98% *ee*. Further to this, the interconversion of the palladacycle intermediates **INT4a** and **INT4b** (see Figure 4.1) via transition state **TS3** was calculated to be feasible with an energy barrier 7.3 kcal/mol, being in agreement with the experimental observation that indeed a dynamic kinetic asymmetric transformation can occur.

4.2.3 Analysis of the Coordination Mode of L2 to the Pd Precursor

To further determine the coordination behavior of the phosphoramidite ligand **L2** to the Pd precursor, we first combined stoichiometric amounts of Pd₂(dba)₃·CHCl₃ with ligand

W.-J. Bai, C. Hohn, Y. Bai, J. J. Cregg, *J. Am. Chem. Soc.* **2018**, *140*, 6710; d) B. M. Trost, J. P. Stambuli, S. M. Silverman, U. Schwörer, *J. Am. Chem. Soc.* **2006**, *128*, 13328.

L2 and analyzed the mixture by ^{31}P NMR (Figure 4.2, entries 1 and 2). It is clear from this analysis that two ^{31}P resonances for two Pd complexes are noted, which are assigned to structures involving different positions of the allyl ligands with respect to the chiral phosphoramidite ligand. [20] It is worth to note that we were unable to find the corresponding ^{31}P NMR peak of the free **L2** ligand under these conditions.
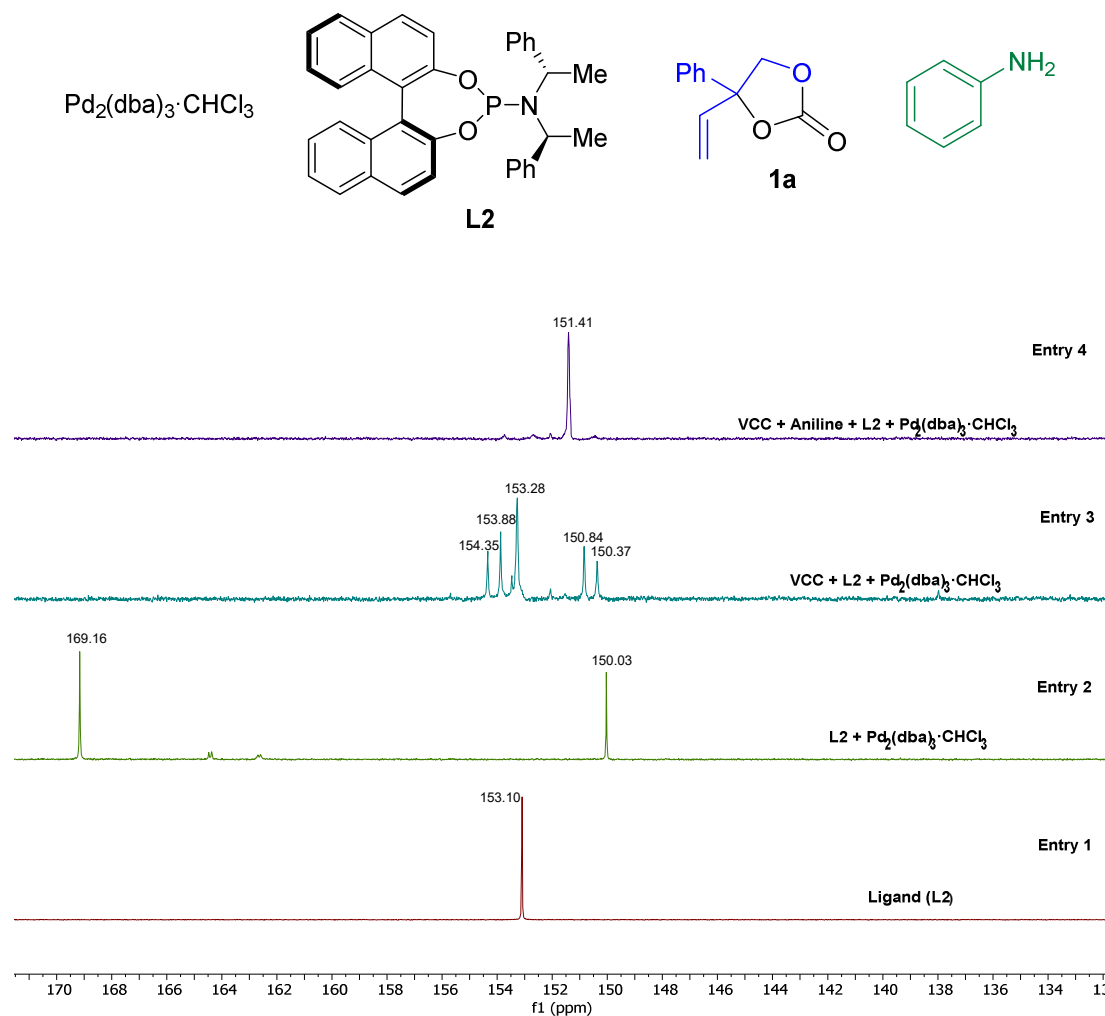
Entry 1: ligand **L2** only
Entry 2: ligand **L2** and $Pd_2(dba)_3 \cdot CHCl_3$ (2:1 molar ratio)
Entry 3: ligand **L2**, $Pd_2(dba)_3 \cdot CHCl_3$ and VCC **1a** (10:5:100 molar ratio)
Entry 4: ligand **L2**, $Pd_2(dba)_3 \cdot CHCl_3$, VCC **1a** and aniline (10:5:100:150 molar ratio)

Figure 4.2. ^{31}P NMR analyses of $Pd_2(dba)_3 \cdot CHCl_3$ and ligand **L2** in d_8-THF at 0 ºC.

The addition of vinyl cyclic carbonate **1a** to a d_8-THF solution of the Pd precursor and ligand **L2** affords the ^{31}P NMR trace reported in entry 3 and reveals the presence of a species having two diastereotopic P-atoms,[20] together with free non-coordinated **L2**.

---

(20) S. Filipuzzi, P. S. Pregosin, *Organometallics,* **2006***, 25,* 5957.

This may suggest that upon coordination of the VCC (through its vinyl group) to the Pd precursor there may be several species in dynamic equilibrium. After addition of aniline to this mixture, the spectrum collapses into the one shown in entry 4, resembling the starting point for the catalytic reaction. It is clear from the spectra reported in Figure 4.2 that multiple species may be involved at the pre-activation stage, including Pd complexes having one or two **L2** ligands coordinated to the metal center, and possibly multinuclear Pd complexes with a Pd/**L2** ratio of 1:1. These NMR data align with the DFT prediction that multiple species may indeed be involved at the initial stage of the reaction.

Experimental evidence for the formation of the key palladacycle **INT4** was obtained by ESI(+)-MS (Figure 4.3). Analyzing a catalytic mixture by ESI(+) revealed that both mono- as well as di-**L2** complexes based on **INT4** are energetically feasible intermediates resulting from the pre-activation of the Pd precursor.[21]
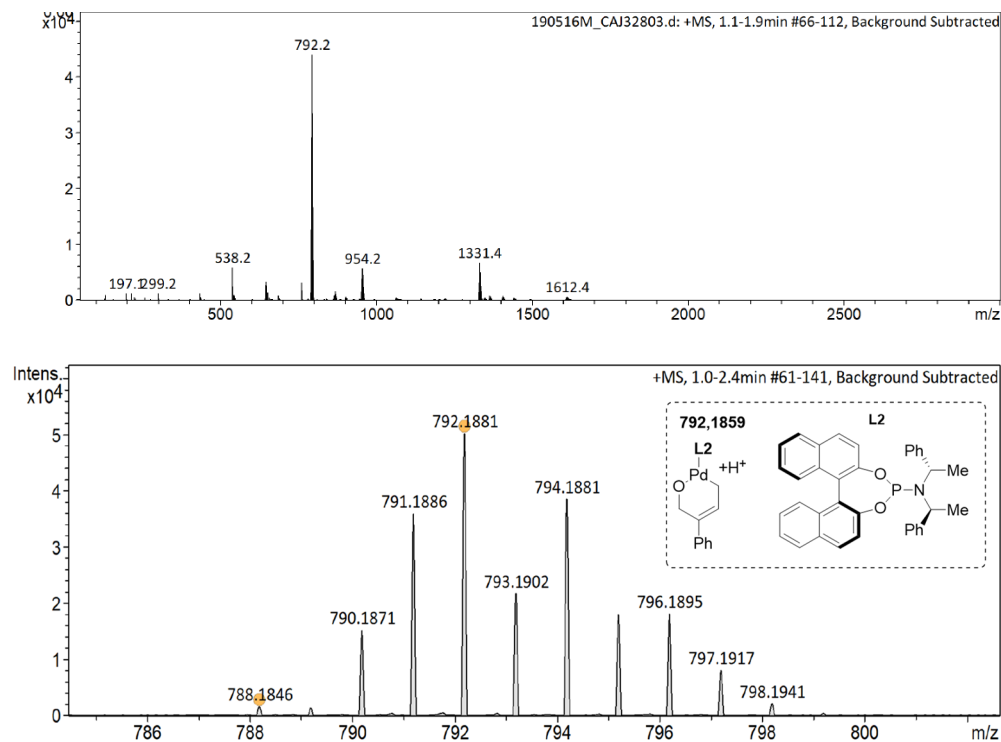
Figure 4.3. ESI-MS analysis of a pre-catalytic mixture. <u>Top</u>: full mass trace, showing at m/z = 792 the mono-**L2** Pd complex, and at m/z = 1331.4 the di-**L2** Pd complex. Note that the peak at m/z = 538 corresponds to "free" ligand **L2**. <u>Below</u>: high-resolution mass analysis of the mono-**L2** Pd complex.

---

(21) Recently, Lu, Xiao and coworkers nicely showed the use of ESI(+) to examine Pd(allyl) intermediates derived from vinyl cyclic carbonates, see: Y. Wei, S. Liu, M.-M. Li, Y. Li, Y. Lan, L.-Q. Lu, W.-J. Xiao, *J. Am. Chem. Soc.* **2019**, *141*, 133.

4.2.4 Outer-Sphere Nucleophilic Attack

Next, the regio- and enantio-control in this allylic amination process was scrutinized focusing first on the previously proposed outer-sphere pathway involving the amine species. The calculated energies of the nucleophilic attack via a previously proposed outer-sphere pathway are shown in Figure 4.4 starting from intermediates **INT4a** and **INT4b** having three distinct starting points, with L being either a THF or dba ligand, or none. Note that for the computed pathways Pd complexes with either thf, dba or without additional ligand were evaluated: the calculations generally show that most of the involved intermediates/transition states having a single sterically demanding phosphoramidite (**L2**) coordinating to the Pd (*i.e.*, with L = none) are equal or lower in energy compared against the (allyl)Pd**L2**(L) complexes (with L = thf or dba).

Two types of nucleophilic attack, namely at C1 (see both **TS6**) and C3 atoms (see both **TS7**), were considered, which eventually leads to the formation of the linear and branched products, respectively. It is worth to note that intramolecular H-transfer within **INT4a** and **INT4b** was also considered in the current calculations but these processes were calculated to be much higher in energy than the nucleophilic attack.

The process begins with the formation of intermediates **INT5a** and **INT5b** through a hydrogen bond interaction between the incoming aniline ($PhNH_2$) and the anionic oxygen atom of the π-allyl-Pd moiety. From **INT5a** and **INT5b**, the pathway that represents a nucleophilic attack on C1 was found to take place via a stepwise fashion. First, the formation of an O-H bond occurs via proton-transfer from the N to the O center followed by a nucleophilic attack of the amide onto the allyl-Pd intermediate (cf., **TS6a** and **TS6b**) enabling C1–N bond formation, and resulting into coordinated product- complexes **INT7a** and **INT7b**.[22] Subsequent ligand exchange in the presence of the racemic substrate [(*rac*)-1a] regenerates **INT1a/INT1b** and releases the linear product (*Z*)-2a.

---

(22) Notably, **TS5b** was calculated to be slightly lower in energy than the connecting intermediate **INT6b**.
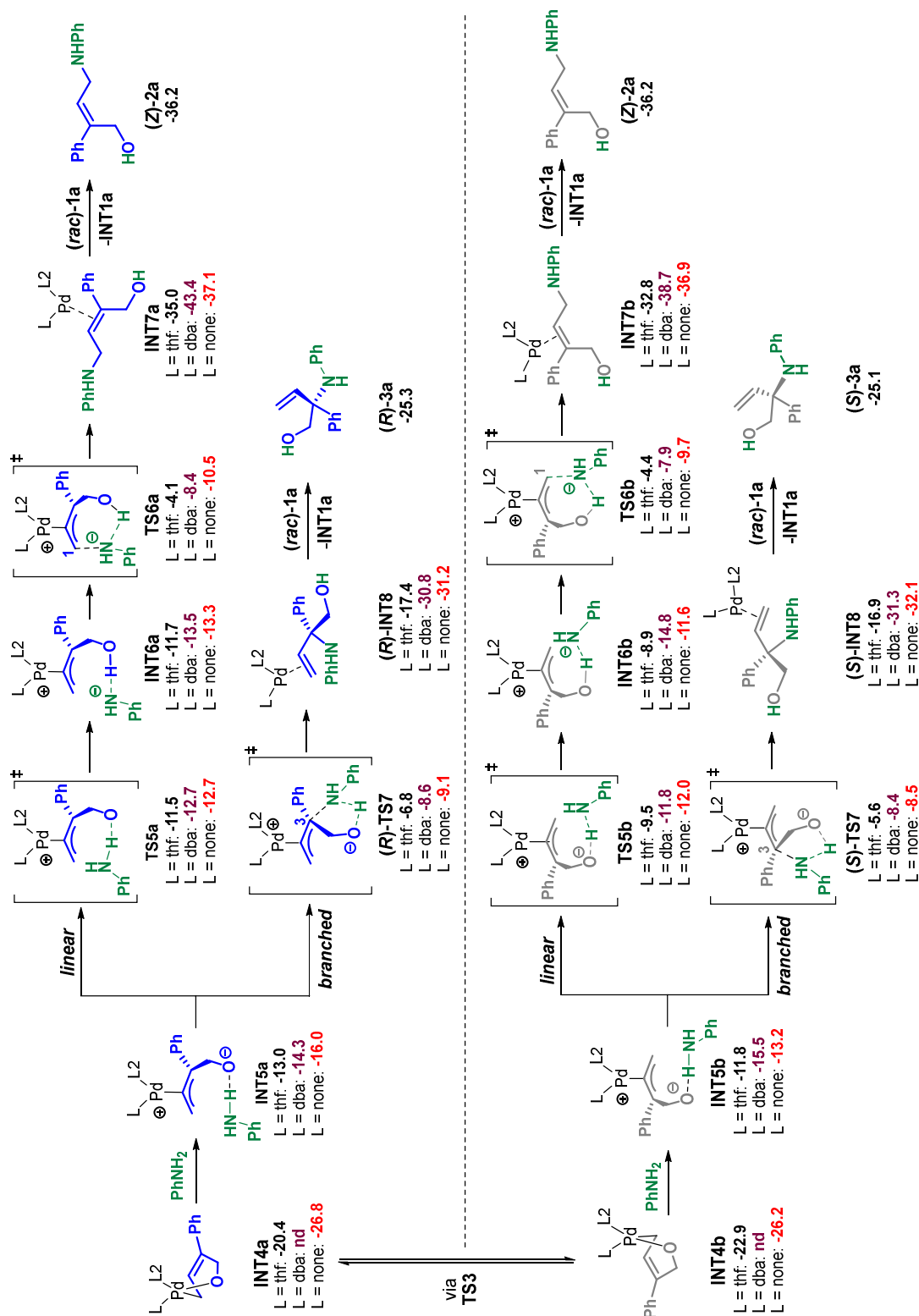
Figure 4.4. Nucleophilic attack via an outer-sphere pathway starting from **INT4a** and **INT4b** leading to linear product **(Z)-2a** or branched products **(R)-3a** or **(S)-3a**.

On the other hand, the nucleophilic attack at C3 was found to take place through a concerted fashion via transition states **(R)-TS7** and **(S)-TS7**, in which the proton-transfer and C3–N bond formation occur simultaneously. The ligand exchange process between the resultant intermediates **(R)-INT8** and **(S)-INT8** and substrate **(rac)-1a** regenerates **INT1a/INT1b** and releases the branched products **(R)-3a** and **(S)-3a**, respectively. The computations show that for both starting points in Figure 4.6 (**INT4a** and **INT4b**), an outer-sphere nucleophilic attack of aniline at the terminal C1 carbon of the allyl-Pd complex is more favorable (see Figure 4.4) than at the internal C3 atom for the pathway that involves intermediates/transition displaying the lowest barrier (L = none, *i.e.* at an apparent low-coordinate Pd species). In the latter case, the barriers determined for the highest transition states **TS6a** and **TS6b** arising from **INT4a** and **INT4b** leading to linear allylic amine product **(Z)-2a** are located at −10.5 and −9.7 kcal/mol, respectively, whereas the attack at C3 going through transition states **TS7a** and **TS7b** need to overcome barriers positioned at −9.1 and −8.5 kcal/mol, respectively.
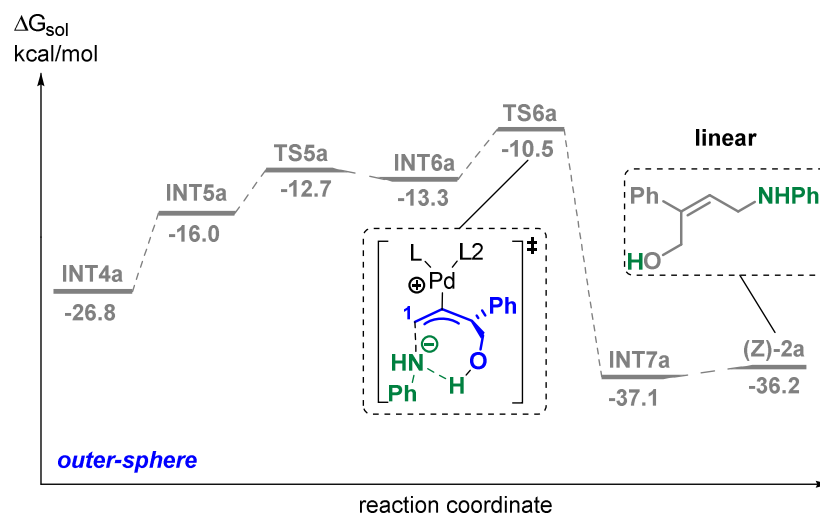
Figure 4.5. The energetically most favored outer-sphere pathway leading to preferred formation of linear allylic amine product **(Z)-2a**.

These calculated results indicate that linear product **(Z)-2a** should be observed as the major product (Figure 4.5; favored by at least 1.2 kcal/mol) in the reaction, which is in contrast with the experimental results that show the opposite trend.[13] Moreover, the experimentally observed enantioselectivity (95% *ee*) of the product **3a** can also not be correctly reproduced by this outer-sphere pathway, with a $\Delta\Delta G^{\ddagger}$ of only 0.6 kcal/mol (−8.5 kcal/mol for **(S)-TS7** *versus* -9.1 kcal/mol for **(R)-TS7**).[13] Importantly, the outer-

sphere pathway also predicts the branched product to have an (*R*) configuration, which is in contrast to the experimental findings as the product **3a** was determined to have an (*S*) configuration by X-ray analysis.[13] Therefore, an alternative pathway has to be examined to account for the experimental observations.

4.2.5 Inner-Sphere Nucleophilic Attack

We found that the formation of the branched products **(*S*)-3a** and **(*R*)-3a** can also take place via an inner-sphere pathway (Figure 4.6). The computations show that this pathway is initiated by the formation of intermediates **(*S*)-INT9** and **(*R*)-INT9** through a hydrogen-bonding interaction between aniline ($PhNH_2$) and the oxygen atom of **INT4a** and **INT4b**. A subsequent proton transfer (as also proposed for the outer-sphere pathway, Figure 4.4) takes place via transition states **(*S*)-TS8** and **(*R*)-TS8**, generating intermediates **(*S*)-INT10** and **(*R*)-INT10**, respectively. Surprisingly, the formation of the latter intermediates further reveals the involvement of the amine nucleophile through a η^2-coordination of the aryl group and thus a ditopic, stabilizing interaction with the Pd(allyl) intermediate. This ditopic interaction is preserved up to the actual formation of the branched allylic amine products **(*S*)-3a** and **(*R*)-3a**. The intermediates **(*S*)-INT10** and **(*R*)-INT10** undergo C3–N bond formation via transition states **(*S*)-TS9** and **(*R*)-TS9** to deliver product-coordinated intermediates **(*S*)-INT8** and **(*R*)-INT8**, from which the branched products **(*S*)-3a** and **(*R*)-3a** are furnished by ligand exchange in the presence of **(*rac*)-1a**.
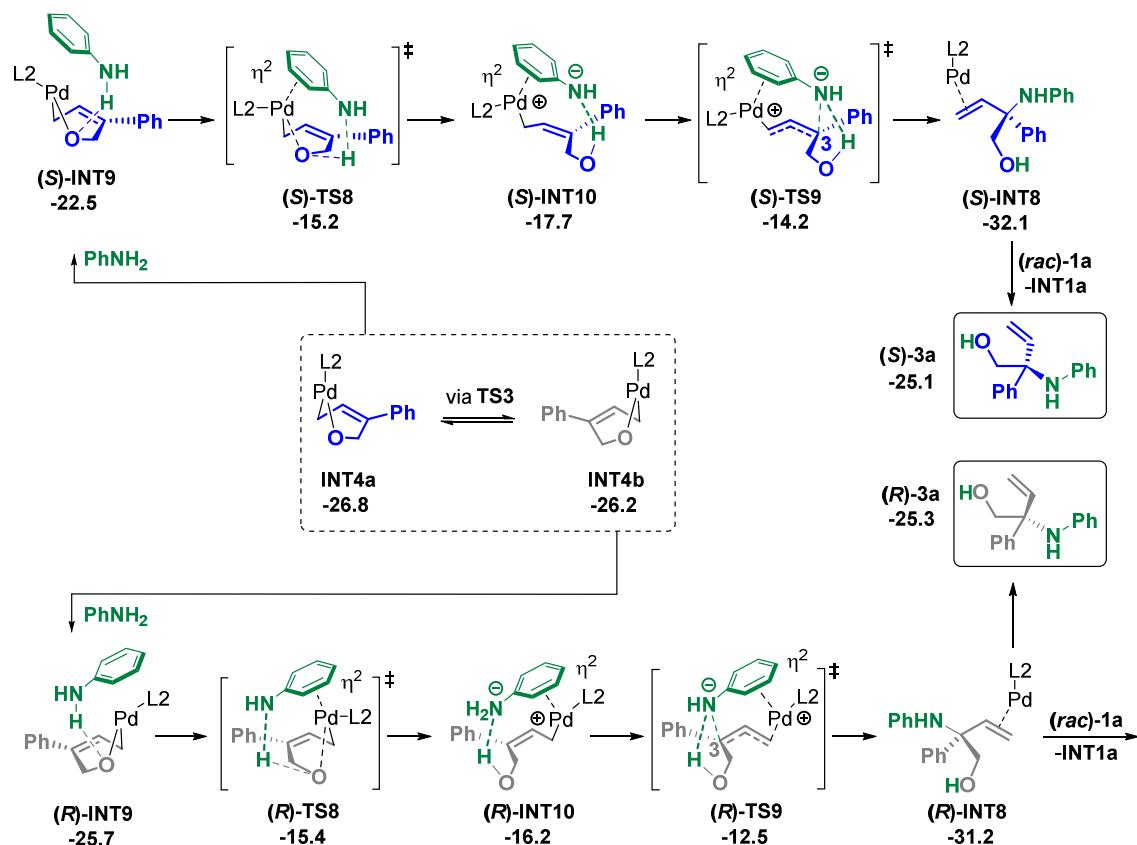
Figure 4.6. Nucleophilic attack via an inner-sphere pathway starting from **INT4a** and **INT4b** leading to branched products **(S)-3a** and **(R)-3a**.

The results show that the formation of branched type products via this alternative, and unexpected inner-sphere pathway is more favorable than the originally proposed outer-sphere pathway by at least 3.4 kcal/mol. The highest transition states **(S)-TS7** and **(R)-TS7** for the outer-sphere pathway are at −8.5 kcal/mol and −9.1 kcal/mol, respectively, whereas the highest barriers located in the inner-sphere manifold (**(S)-TS9** and **(R)-TS9**) reside at −14.2 and −12.5 kcal/mol, respectively. Importantly, with this inner-sphere pathway, the experimentally observed and preferred branched regioselectivity in the presence of the phosphoramidite ligand **L2** is well reproduced, since the highest barrier in the lowest energy pathway giving linear product **(Z)-2a** is at −10.5 kcal/mol, while that of the lowest energy pathway for branched allylic amine formation based on an inner-sphere mechanism is at −14.2 kcal/mol. Thus, the difference of 3.7 kcal/mol between these two pathways is in line with the experimentally observed preferable formation of **(S)-3a**.

Moreover, the calculated energy difference between the enantioselectivity determining transition states **(S)-TS9** and **(R)-TS9** is 1.7 kcal/mol, which corresponds to a calculated

asymmetric induction of 92% *ee* at 273.15 K being in good agreement with the experimentally observed 95% *ee*.[13] With these combined results, we thus conclude that the reaction leading to branched allylic amine product **(S)-3a** should proceed through an inner-sphere pathway. It is particularly noteworthy that the η^2-aryl coordination of the nucleophile to the Pd center was identified as a key interaction with important implications for the enantiocontrol (see below). To the best of our knowledge, this type of unusual inner-sphere pathway in the area of Pd-catalyzed allylic substitution has not yet been considered.
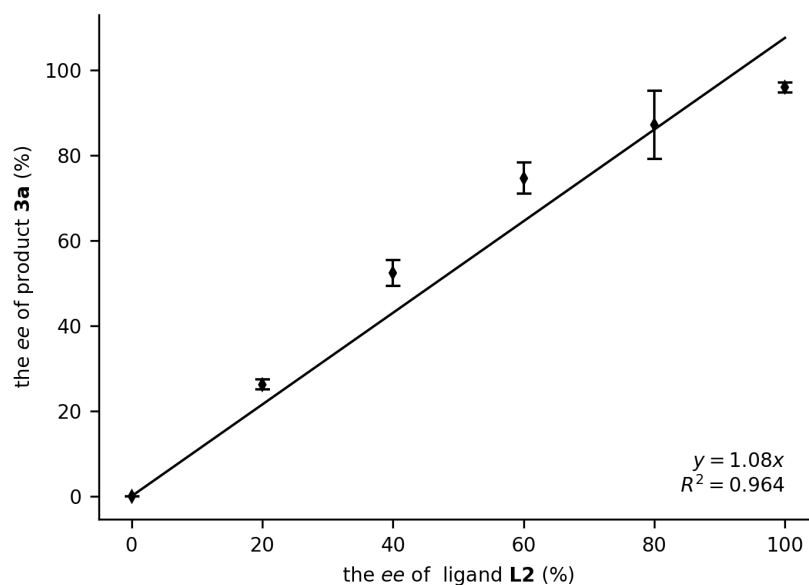
Figure 4.7. Relationship between the *ee* of product **3a** versus *ee* of ligand **L2**.

To gain further insight into the coordination mode of the phosphoramidite ligand **L2** during the enantio- and regio-determining step of the reaction (*cf.*, **TS9** in Figure 4.4), we performed a set of experiments using ligand **L2** with various optical purities under standard catalytic conditions. As shown in Figure 4.7, a small non-linear effect was observed between the *ee* of the ligand and that of the allylic amine product.[23] These results imply that the palladium center coordinated with one phosphoramidite ligand is likely to be an active species during the transfer of the chiral information, which is in agreement with previous findings in allylic alkylation reactions.[24]

---

(23) Figure 4.7 is based on averaging three series of experimental data and displaying the standard deviation as a 99% confidence interval.

(24) Minimal nonlinear effects using phosphoramidite ligands in Pd-catalyzed allylic substitution reactions were also reported by van Leeuwen: M. D. K. Boele, P. C. J. Kamer, M. Lutz, A. L. Spek, J. G. de Vries, P.W. N. M. van Leeuwen, G. P. F. van Strijdonck, *Chem. Eur. J.* **2004**, *10*, 6232.

Table 4.2. Influence of the amine nucleophile on the B/L ratio and overall performance in the allylic amination reaction using cyclic carbonate **1a**.[a]
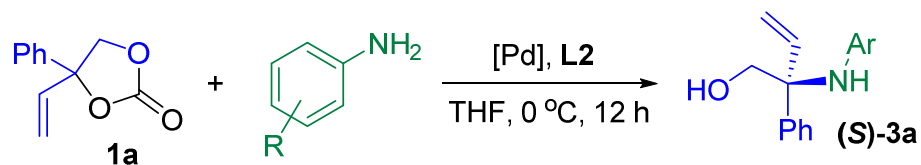
Entry	R	B/L[b]	Conversion [%][b]	Yield [%][b]
1	p-OMe	83:17	>99	77
2	m-NO$_2$	80:20	>99	67
3	H	80:20	>99	78
4	p-Cl	76:24	>99	63
5	m-Br	75:25	>99	57
6	o-OMe	70:30	>99	53
7	p-OH	68:32	>99	62
8	o-Me	65:35	>99	60
9	m-Me	60:40	>99	56
10	o-iPr	57:43	51	22
11	o-Et	53:47	32	14
12	o-tBu	nd	<1	<1

[a] Reaction conditions unless stated otherwise: 0.20 mmol (1.0 equiv.) of carbonate **1a**, aniline (1.5 equiv.), Pd$_2$(dba)$_3$·CHCl$_3$ [**Pd$_2$**] (2.5 mol %) and **L2** (10 mol %), 0.20 mL of THF, 0 ºC, 12 h, open to air. B/L stands for branched-to-linear product ratio, and nd for not determined. [b] Determined by ^{1}H NMR analysis (CDCl$_3$) of the crude reaction mixture: NMR yields of the *branched* products were determined by using toluene as an internal standard.

Additional control experiments were conducted to investigate the role of the substitution on the aromatic ring of the amine nucleophile (see Table 4.2). These latter data illustrate that any increasing steric bulk near the nitrogen center of the nucleophile (cf., entries 8–12) reduces the overall kinetics of the process and/or produces also more linear product with the outer-sphere manifold thus becoming more competitive. However, there seems also some degree of electronic control in these conversions (cf., entries 1 versus 7 and 2 versus 9).
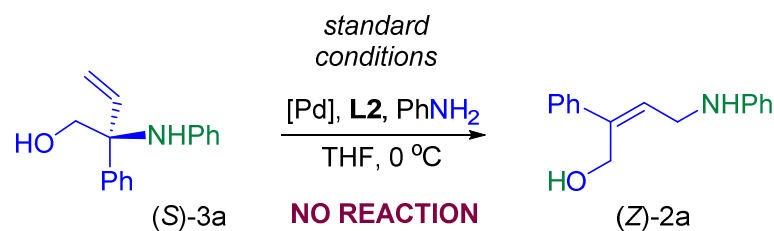
Scheme 4.10. Control experiment to examine potential **(S)-3a**-to-**(Z)-2a** interconversion.

To further testify that both types of allylic amine products do not interconvert and that the observed selectivity patterns are not the result of thermodynamic process control (note that **Z-2a** has a much lower calculated free energy than **(S)-3a**), an isolated sample of **(S)-3a** was subjected to the standard catalytic conditions and afterwards analyzed by ^{1}H NMR spectroscopy (Scheme 4.10). No observable conversion could be noted, and **(S)-3a** was recovered quantitatively.

4.2.6 Origin of the Enantiocontrol

The origin of the experimentally observed enantioselectivity can be ascribed to steric effects. The comparison of the optimized geometries of **(S)-TS9** and **(R)-TS9** shows that the key computed bond distances are similar in both transition states (Figure 4.8). However, the relative orientation of the phenyl ring of the aniline was found to be quite different. In **(S)-TS9**, the phenyl ring is more distant from the steric bulk present on the N-center of the phosphoramidite ligand, whereas in **(R)-TS9** the same phenyl ring is nearer the same moiety. Therefore, an increase in steric repulsion between the phosphoramidite ligand and the incoming nucleophile in **(R)-TS9** is expected. To minimize this steric repulsion, the dihedral angles made up by an O, P, C and N atom (∠CNPO, as indicated in Figure 4.8) markedly changes with this angle for **(S)-TS9** amounting to 111.2° and being significantly larger within **(R)-TS9** (138.5°): this likely causes the energy of **(R)-TS9** to be higher than computed for **(S)-TS9**.[25]

---

(25) The CNPO dihedral angles in **INT4a** and **INT4b** are nearly the same, being 108.4 and 110.0°, respectively.
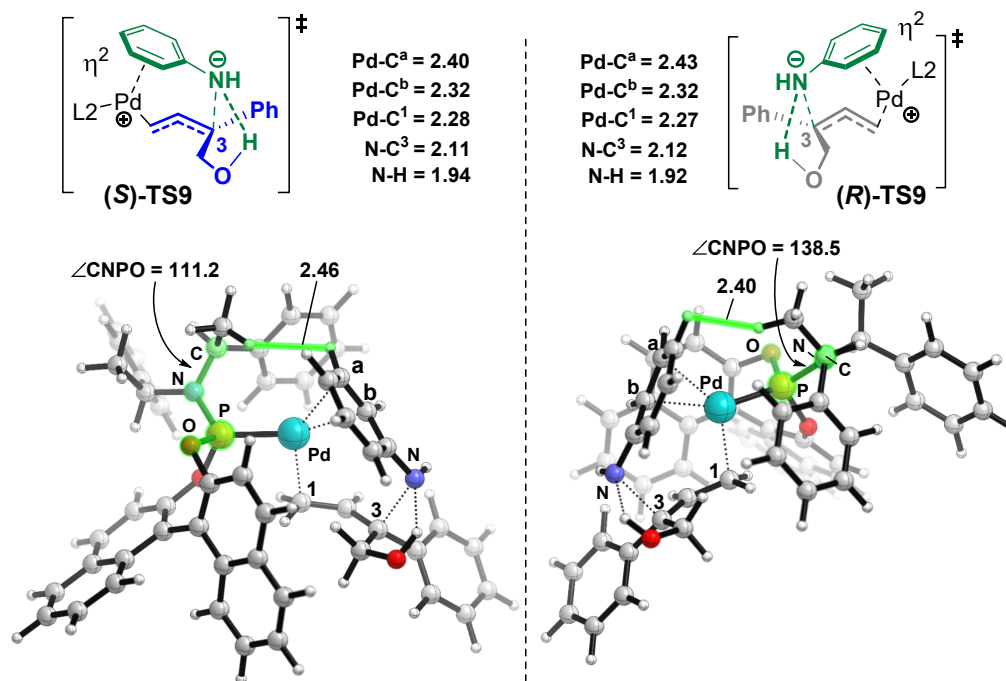
Figure 4.8. Optimized geometries of **(S)-TS9** and **(R)-TS9**. The reported computed bond distances and dihedral angles (highlighted in green) are in Å and degrees, respectively.

Control calculations by the modification of the substituents of the N-center in the phosphoramidite moiety were performed to gain deeper insights into the origins of enantioselectivity (Figure 4.9). First, the substituents were replaced with methyl groups (**L3**), in which smaller steric repulsion between the phosphoramidite ligand and the incoming nucleophile can be envisioned. The comparison of the optimized geometries indeed shows that ∠CNPO for **(R)-TS9'** is 159.4º, which is slightly larger than that for **(S)-TS9'** (153.4º).[26] As a consequence, the energy difference was calculated to be 0.9 kcal/mol (**(S)-TS9'** versus **(R)-TS9'**). Furthermore, changing the substituents to "H" atoms results in an energy difference of only 0.4 kcal/mol (**L4**, **(S)-TS9''** versus **(R)-TS9''**). These additional data provide further support for steric control in the enantio-discriminating transition state of the inner-sphere pathway.[27]

---

(26) With ligand **L3**, the CNPO dihedral angles in **INT4a** and **INT4b** are 157.1 and 156.2º, respectively.

(27) The energies of **(R)-TS9** relative to **INT4a** are 14.3, 11.2, and 9.6 kcal/mol using **L2**, **L3**, and **L4**, respectively. This additional result further demonstrates that the steric repulsion plays an important role in the nucleophilic attack step.
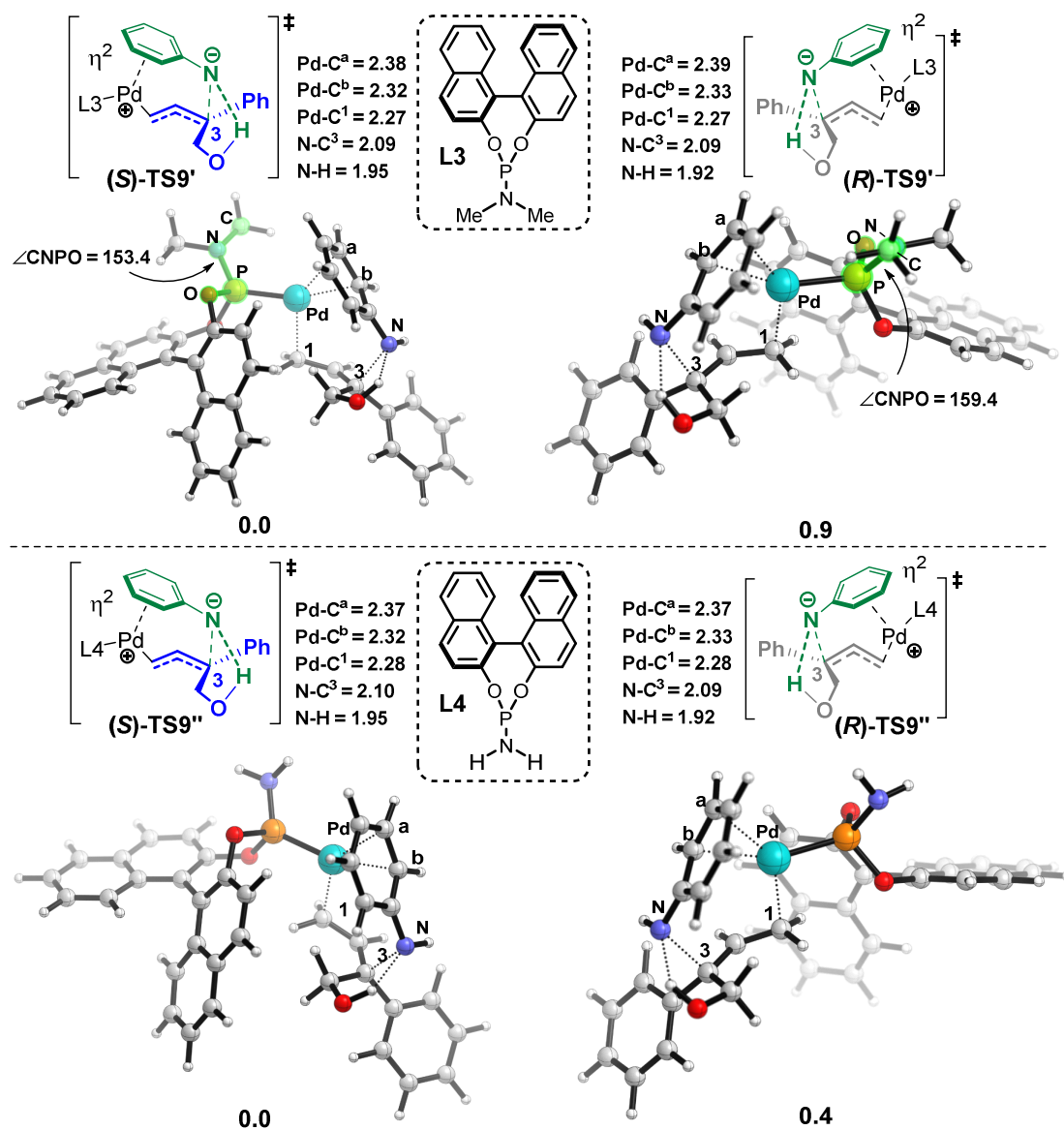
Figure 4.9. Control calculations with **L3** and **L4**. The reported computed energies, bond distances and dihedral angles (highlighted in green) are in kcal/mol, Å and degrees, respectively.

4.2.7 Results Obtained Using Aliphatic Amines

Table 4.3. Product analysis using aliphatic amines and **1a** as substrates.

Conditions **A**: 100% conv., 95% yield
Conditions **B**: 100% conv., 92% yield

Conditions **A**: 91% conv., 85% yield[a]
Conditions **B**: 100% conv., 90% yield

Conditions **A**: 24% conv., 19% yield[a]

Conditions **A**: 87% conv., 80% yield[b]
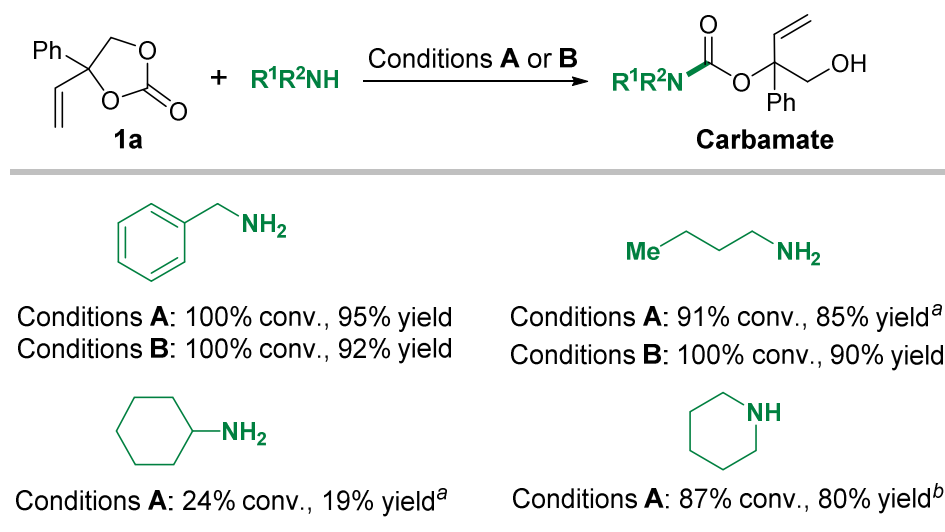
Reaction conditions unless stated otherwise: 0.20 mmol (1.0 equiv.) of cyclic carbonate **1a**, aliphatic amine (1.5 equiv.); conversion and yield determined by ^{1}H NMR analysis of the crude reaction mixture using toluene as internal standard. Conditions **A**: $Pd_2(dba)_3 \cdot CHCl_3$ [**Pd₂**] (1.25 mol %) and **L2** (5 mol %), THF (200 μL), 0 ºC, 12 h; Conditions **B**: without [**Pd₂**] and **L2,** THF (200 μL), r.t., 4 h. [a] Reaction time was 24 h. [b] Reaction time was 24 h, isolated yield reported.

Several aliphatic amines were also scrutinized and in all cases the formation of the allylic amine product could not be detected. The reason for this is that aliphatic amines (*i.e.*, *n*-butyl amine, benzyl amine, cyclohexyl amine, and piperidine) are much more nucleophilic than aromatic ones and preferentially attack the electrophilic carbon center of the carbonate unit (a formal aminolysis takes place) to afford almost exclusively the carbamate products (Table 4.3). This is also in line with previous control experiments[15] showing that the use of benzyl amine yields >95% linear carbamate product and not the allylic amine target.

4.3 Conclusions

In summary, in this chapter we present a mechanistic study on the Pd-catalyzed allylic substitution of vinylethylene carbonates with aryl amines by means of DFT calculations and various control reactions. The computations reveal that after oxidative addition/CO_2 extrusion, the nucleophilic attack leading to branched allylic amine product proceeds through a novel type of inner-sphere pathway comprising of a η^2-aryl coordination of the aromatic group of the amine to the Pd center. While the outer-sphere pathway predicts a preference for the linear product and the formation of an (*R*)-configured product in the "branched" manifold, the new inner-sphere mechanism predicts correctly the preferential formation of the branched product, is energetically significantly more favored than the route leading to linear product and also forecasts the (*S*)-configured branched allyl amine (including the level of asymmetric induction) as experimentally observed. The enantioselectivity was found to be mainly triggered by steric repulsion between the coordinated η^2-aryl and the substituted N-center of the phosphoramidite ligand. Pd-catalyzed allylic substitution reactions that proceed via this new inner-sphere pathway are distinct from those previously observed, and should have important implications for the design of new catalytic systems for the formation of elusive, sterically congested quaternary stereocenters.

4.4 Experimental Section

4.4.1 General Considerations

Commercially available amines and solvents were purchased from Aldrich or TCI, and used without further purification. The substituted carbonates were synthesized following a previously reported method.[28] The Pd precursors were purchased from Aldrich or TCI. Phosphoramidites **L2**[29] was prepared according to previously reported procedures. In the control experiments (Table 4.2), the internal standard toluene was added after the reaction mixture had been stirred at 0 °C for 12 h. After that, an aliquot of the resulting mixture was taken and the yield was determined by means of ^{1}H NMR spectroscopy using CDCl$_3$ as the solvent. ^{1}H NMR, ^{13}C NMR, ^{19}F NMR spectra were recorded at room temperature on a Bruker AV-400 or AV-500 spectrometer and referenced to the residual deuterated solvent signals. Ultra-performance convergence chromatography (UPC2) and the ESI-MS analyses were performed by the Research Support Group at ICIQ.

4.4.2 Computational Details

All of the calculations were performed in THF solvent (ε = 7.4257) using the SMD model[30] at the B97D[31] level of theory with the Gaussian 09 package.[32] Geometry optimizations were carried out with a mixed basis set of SDD[33] for Pd and 6-31G(d) for other atoms. Vibrational frequencies were computed analytically at the same level of theory to confirm whether the structures are minima (no imaginary frequencies) or transition states (only one imaginary frequency). Selected key transition-state structures were confirmed to connect corresponding reactants and products by intrinsic reaction

(28) A. Khan, R. Zheng, Y. Kan, J. J. YeXing, Y. J. Zhang, *Angew. Chem. Int. Ed.* **2014**, *53*, 6439.

(29) C. R. Smith, D. J. Mans, T. V. RajanBabu, *Org. Synth.* **2008**, *85*, 238.

(30) A. V. Marenich, C. J. Cramer, D. G. Truhlar, *J. Phys. Chem. B.* **2009**, *113*, 6378.

(31) a) S. Grimme, *J. Comput. Chem.* **2006**, *27*, 1787; b) A. D. Becke, *J. Chem. Phys.* **1997**, *107*, 8554.

(32) Gaussian 09, Revision E.01, M. J. Frisch, G. W. Trucks, H. B. Schlegel, G. E. Scuseria, M. A. Robb, J. R. Cheeseman, G. Scalmani, V. Barone, B. Mennucci, G. A. Petersson, H. Nakatsuji, M. Caricato, X. Li, H. P. Hratchian, A. F. Izmaylov, J. Bloino, G. Zheng, J. L. Sonnenberg, M. Hada, M. Ehara, K. Toyota, R. Fukuda, J. Hasegawa, M. Ishida, T. Nakajima, Y. Honda, O. Kitao, H. Nakai, T. Vreven, J. A. Montgomery, Jr., J. E. Peralta, F. Ogliaro, M. Bearpark, J. J. Heyd, E. Brothers, K. N. Kudin, V. N. Staroverov, R. Kobayashi, J. Normand, K. Raghavachari, A. Rendell, J. C. Burant, S. S. Iyengar, J. Tomasi, M. Cossi, N. Rega, J. M. Millam, M. Klene, J. E. Knox, J. B. Cross, V. Bakken, C. Adamo, J. Jaramillo, R. Gomperts, R. E. Stratmann, O. Yazyev, A. J. Austin, R. Cammi, C. Pomelli, J. W. Ochterski, R. L. Martin, K. Morokuma, V. G. Zakrzewski, G. A. Voth, P. Salvador, J. J. Dannenberg, S. Dapprich, A. D. Daniels, Ö. Farkas, J. B. Foresman, J. V. Ortiz, J. Cioslowski, S11D. J. Fox, Gaussian, Inc., Wallingford CT, 2013.

(33) a) D. Andrae, U. Haeussermann, M. Dolg, H. Stoll, H. Preuss, *Theor. Chim. Acta.* **1991**, *78*, 247; b) D. Andrae, U. Haeussermann, M. Dolg, H. Stoll, H. Preuss, *Theor. Chim. Acta.* **1990**, *77*, 123.

coordinate (IRC) calculations.[34] To obtain better accuracy, energies for the optimized geometries were recalculated using single-point calculations with a larger basis set, which is SDD for Pd and 6-311++G(d,p) for all other atoms. The final free energies reported in the article (ΔG_{sol}) are the large basis set single-point energies with Gibbs free energy correction (at 298.15 K). The same method has been applied in the DFT studies on the Pd(L1)-catalyzed reactions, which has been proven to provide reliable results. To further validate our computations, the energies of the key nucleophilic attack step were recalculated using PBE0-D3(BJ) functional.[35] The results show that the same conclusions were obtained compared with those from B97D functional. In order to ensure that the lowest energy conformation of intermediates and transition states was presented and discussed in the text, extensive conformational searches were conducted.

4.4.3 Standard Catalytic Experiment

To a vial equipped with a magnetic stirring bar, vinyl cyclic carbonate **1a** (0.20 mmol, 38 mg, 1.0 equiv.), Pd$_2$(dba)$_3$·CHCl$_3$ (2.6 mg, 0.0025 mmol, 2.5 mol % Pd), **L2** (5.4 mg, 0.010 mmol, 5.0 mol %), aniline (28 mg, 0.30 mmol, 1.5 equiv.) and THF (0.20 mL) were added. The resulting mixture was stirred at 0 °C for 12 h, and then the reaction mixture was warmed to room temperature, after which the product was purified by flash column chromatography on silica gel (hexane : ethyl acetate = 5 : 1, R_f = 0.30) to afford the corresponding allylic amine **3a**. The enantiomeric excess of the product was determined by UPC2 equipped with a chiral column.

4.4.4 General Procedure for the ESI-MS Analysis

To a vial equipped with a magnetic stirring bar, vinyl cyclic carbonate **1a** (0.20 mmol, 38 mg), Pd$_2$(dba)$_3$·CHCl$_3$ (2.6 mg, 0.0025 mmol, 2.5 mol % Pd), **L2** (5.4 mg, 0.010 mmol, 5.0 mol %), and THF (0.20 mL) were added. The resulting mixture was stirred at 0 °C for 30 min, then a small aliquot was injected in the mass spectrometer following detection

---

(34) a) K. Fukui, *J. Phys. Chem.* **1970**, *74*, 4161; b) K. Fukui, *Acc. Chem. Res*. **1981**, *14*, 363.

(35) a) C. Adamo, V. Barone, *J. Chem. Phys*. **1999**, *110*, 6158; b) S. Grimme, S. Ehrlich, L. Goerigk, *J. Comput. Chem.* **2011**, *32*, 1456.

and analysis of the present Pd-species. Under these conditions, a mono-**L2** ligated Pd complex was noted as the major species.

[M+H]+ calcd: 792.1853
Found: 792.1881
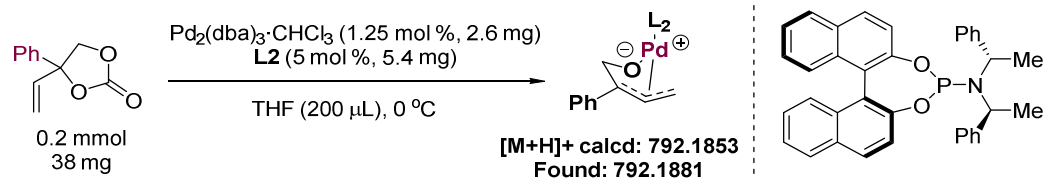
4.4.5 Procedure for the ^{31}P NMR Analyses

To an NMR tube, vinyl cyclic carbonate **1a** (0.40 mmol, 76 mg, 1.0 equiv.), Pd$_2$(dba)$_3$·CHCl$_3$ (5.2 mg, 0.0025 mmol, 2.5 mol % Pd), **L2** (10.8 mg, 0.010 mmol, 5.0 mol %), aniline (56 mg, 0.30 mmol, 1.5 equiv.) and d$_8$-THF (0.40 mL) were added (*cf.*, entry 4, Figure 4.2). The resulting mixture was kept at 0 ºC, then quickly transferred to a Bruker AV-500 spectrometer and the ^{31}P NMR spectrum measured at 0 ºC.

4.4.6 Procedure for the DYKAT Experiment
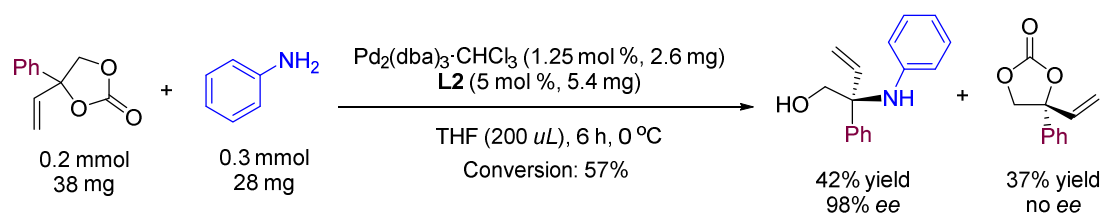
To a vial equipped with a magnetic stirring bar, vinyl cyclic carbonate **1a** (0.20 mmol, 38 mg, 1.0 equiv.), Pd$_2$(dba)$_3$·CHCl$_3$ (2.6 mg, 0.0025 mmol, 2.5 mol % Pd), **L2** (5.4 mg, 0.010 mmol, 5.0 mol %), aniline (28 mg, 0.30 mmol, 1.5 equiv.) and THF (0.20 mL) were added. The resulting mixture was stirred at 0 ºC, and stopped after 6 h; the conversion was determined to be 57%. Then the reaction mixture was warmed to room temperature, recycling the carbonate **1a** in 37% isolated yield by flash column chromatography on silica gel, and the corresponding allylic amine **3a** was obtained in 42% yield. The enantiomeric excess of the vinyl cyclic carbonate **1a** and allylic amine product was determined by UPC2 equipped with a chiral column.

UPC2 trace of the chiral allylic amine product:
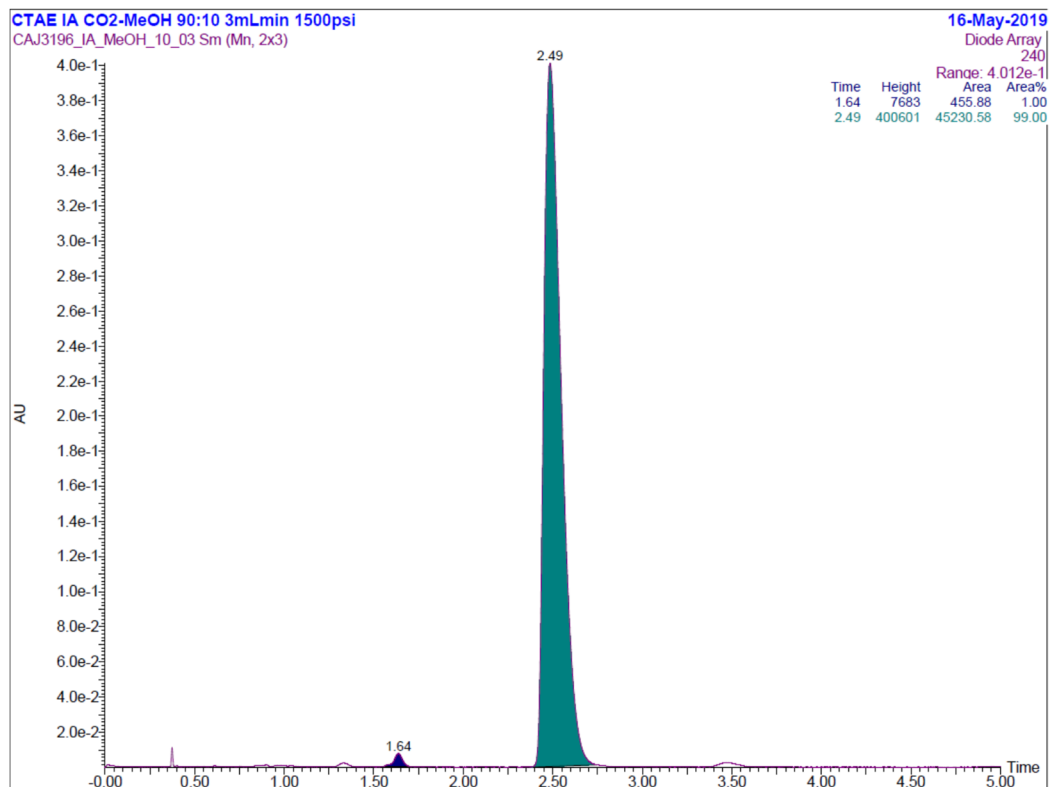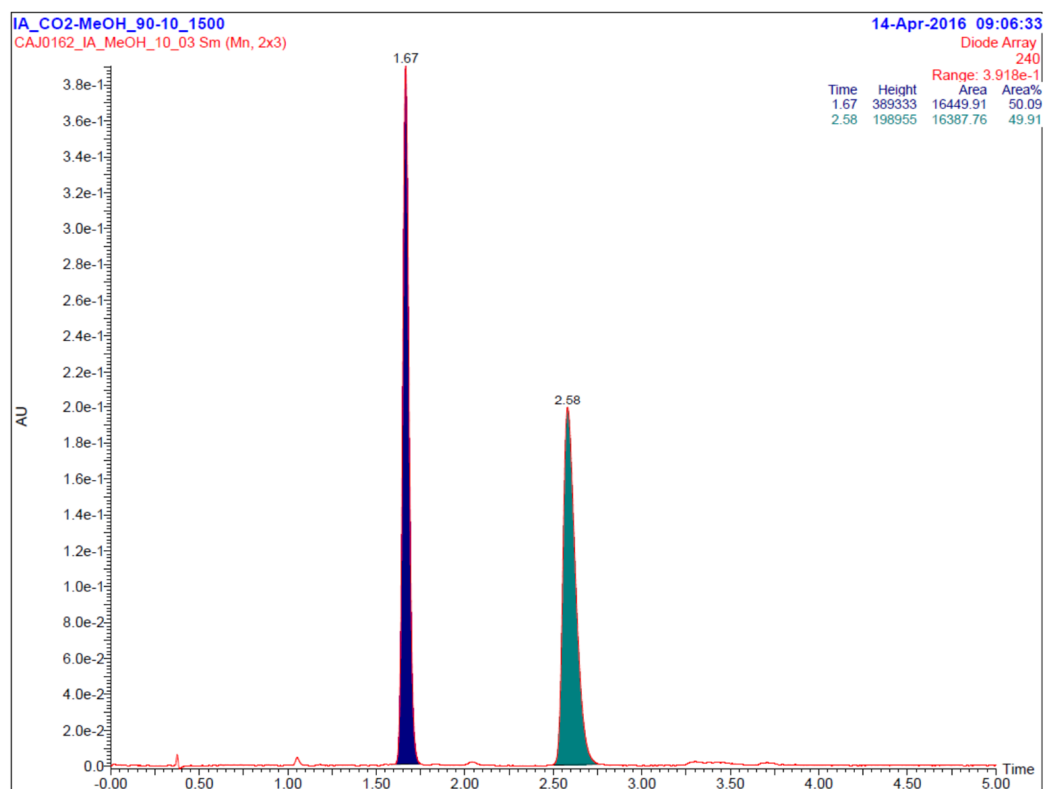
UPC2 trace of the isolated starting material 1a:
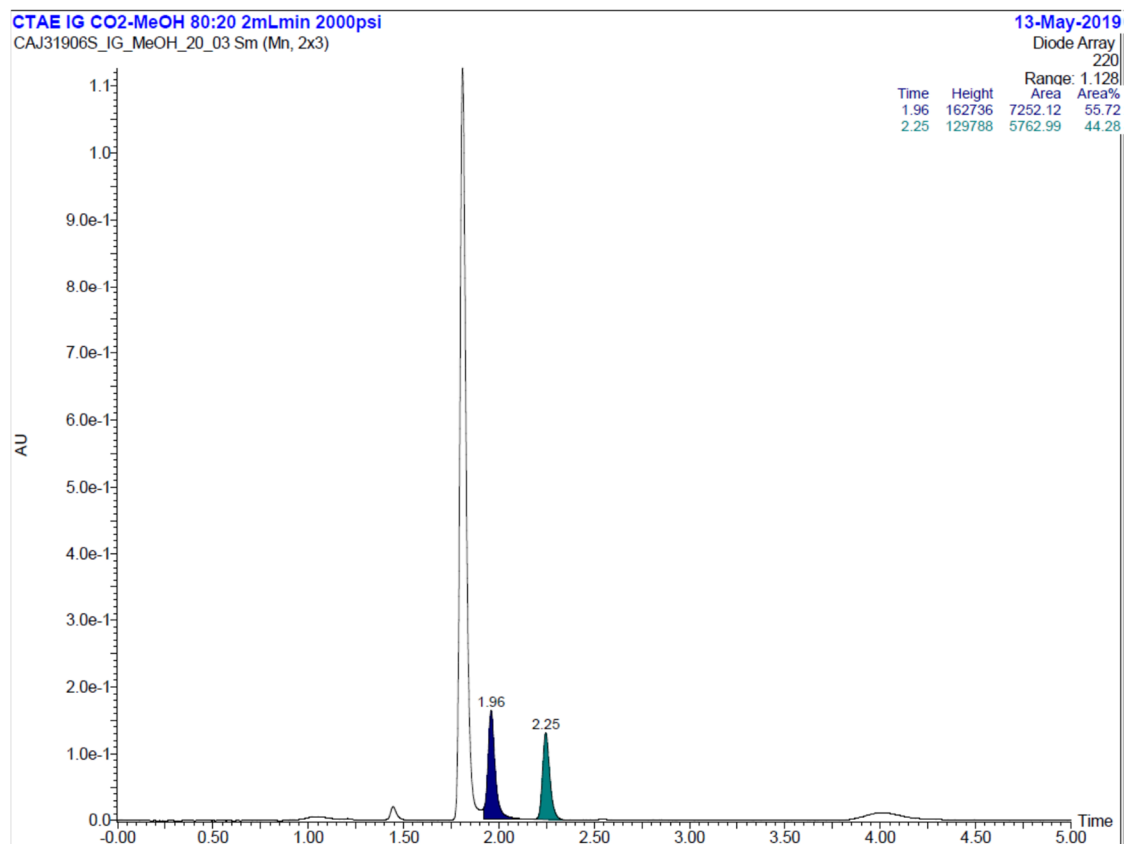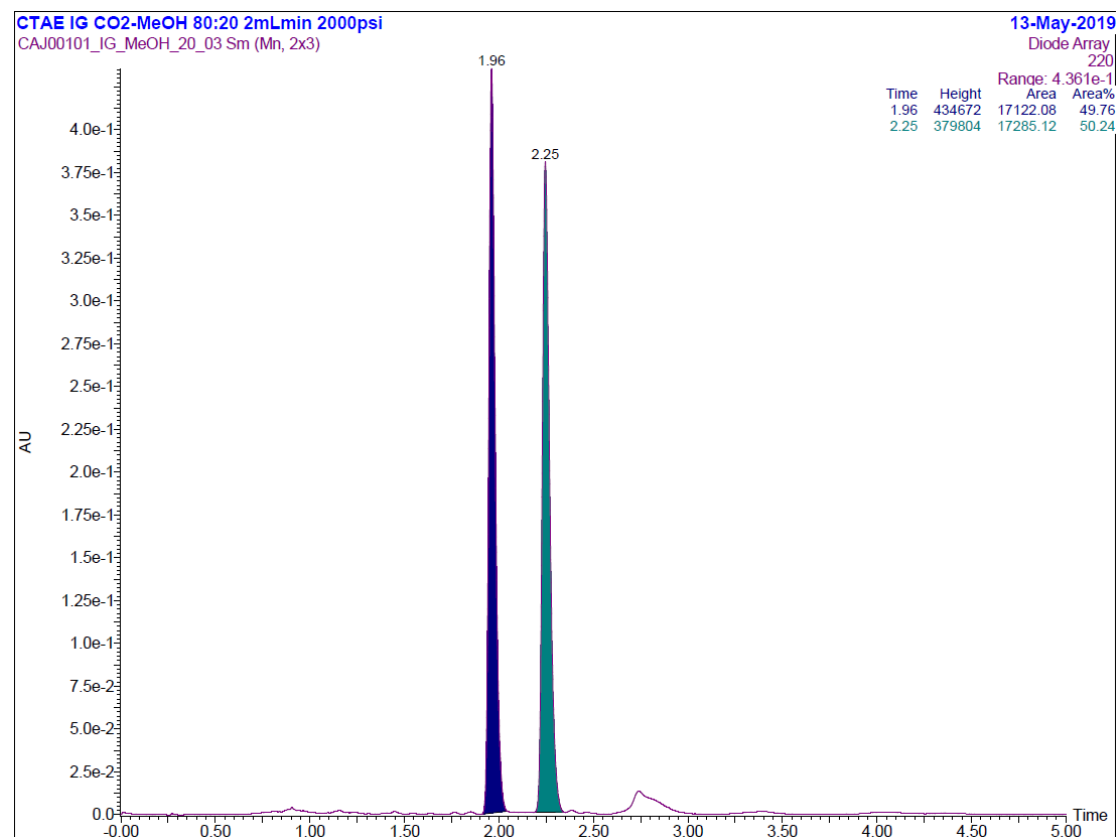
4.4.7 (Non)linear Effects
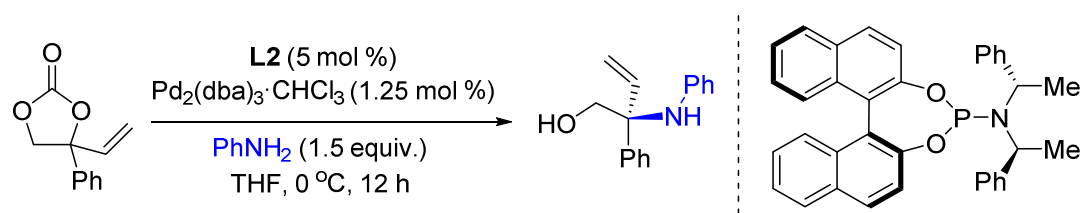
We carried out this study with chiral phosphoramidite ligand **L2** under the optimized reaction conditions. Six different reactions were performed with chiral ligand **L2** with different levels of enantiopurity (racemic, 20%, 40%, 60%, 80%, and >99% *ee*) using the following procedure. To a vial equipped with a magnetic stirring bar, vinyl cyclic carbonate **1a** (0.20 mmol, 38 mg, 1.0 equiv.), Pd$_2$(dba)$_3$·CHCl$_3$ (2.6 mg, 0.0025 mmol, 2.5 mol % Pd), **L2** (5.4 mg, 0.010 mmol, 5.0 mol %), aniline (28 mg, 0.30 mmol, 1.5 equiv.) and THF (0.20 mL) were added. The resulting mixture was stirred at 0 °C for 12 h, and then the reaction mixture was warmed to room temperature, after which the product was purified by flash column chromatography on silica gel (hexane : ethyl acetate = 5 : 1, R_f = 0.30) to afford the corresponding allylic amine **3a**. The enantiomeric excess of each of the products was determined by UPC2 equipped with a chiral column. The enantioselectivity of the obtained product were plotted against the enantiopurity of the chiral ligand (see Figure 4.7).

4.4.8 Validation of the Computational Method

The energies of the key nucleophilic attack step were recalculated using the PBE0-D3(BJ) functional. As shown below, the results show that the same conclusions are obtained compared with those from B97D functional. The originally proposed outer-sphere pathway predicts the enantioselectivity opposite to the experimental results. With B97D, (**R**)-**TS7** is lower in energy than (**S**)-**TS7** by 0.6 kcal/mol. With PBE0-D3(BJ), (**R**)-**TS7** is lower in energy than (**S**)-**TS7** by 1.6 kcal/mol. Both functionals yield the same conclusion that the proposed inner-sphere pathway is more favorable than the outer-sphere pathway. Importantly, the experimentally observed enantioselectivity was reproduced quite well. With B97D, (**S**)-**TS9** is lower in energy than (**R**)-**TS9** by 1.7 kcal/mol. With PBE0-D3(BJ), (**S**)-**TS9** is lower in energy than (**R**)-**TS9** by 2.4 kcal/mol.

Results obtained for the **outer**-sphere manifold based on PBE0-D3(BJ):
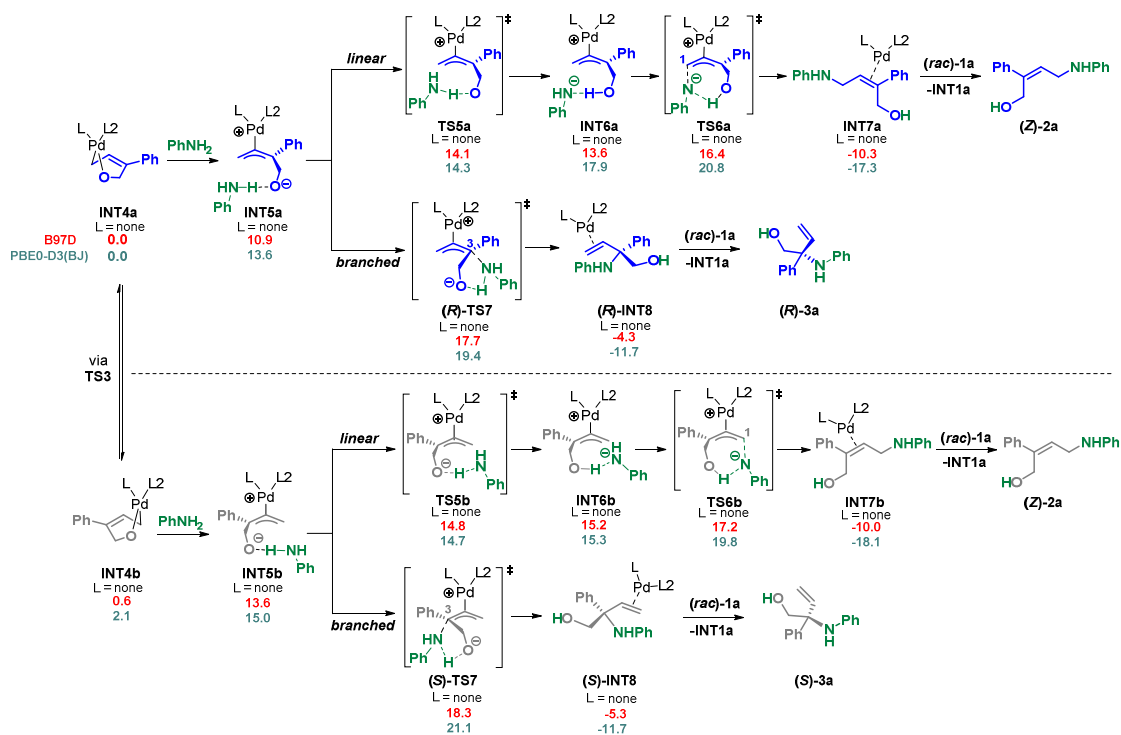
Results obtained for the **inner**-sphere manifold based on PBE0-D3(BJ):

152
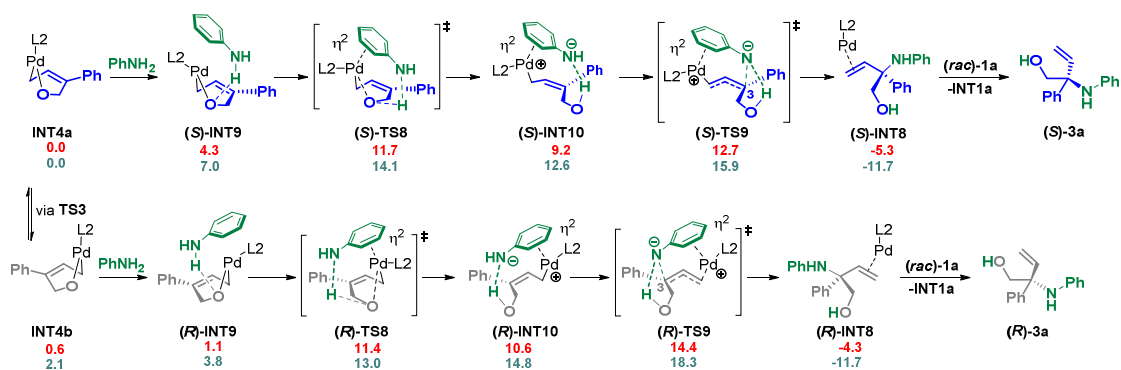
Chapter 5.

Regio- and Enantioselective Preparation of Chiral Allylic Sulfones Featuring Elusive Quaternary Stereocenters

5.1 Introduction

5.1.1 Allylic Sulfones
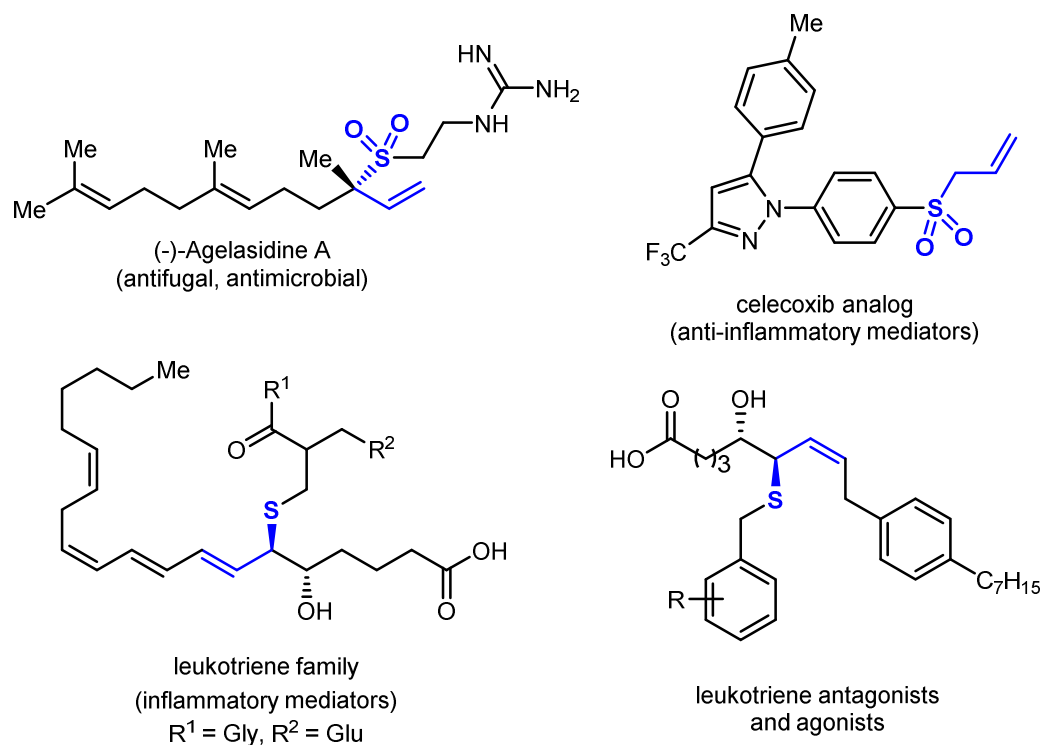
Scheme 5.1. Chiral allylic thioether and sulfone substructures present in drugs and natural products.

Allylic sulfones, owing to their widespread distribution in biological active molecules, have received increasing attention in the past few years. Allylic sulfones particularly serve as versatile building blocks in modern organic synthesis[1] and pharmaceutical chemistry.[2]

---

(1) For the applications of sulfones please refer to: a) N. S. Simpkins, *Sulfones in Organic Synthesis*; Pergamon: Oxford, **1993**; b) S. Patai, Z. Rapoport, C. Stirling, *The Chemistry Functional Groups: Sulfones and Sulfoxides*; Wiley: New York, **1988**; c) *Organosulfur Chemistry in Asymmetric Synthesis*, eds. T. Toru, C. Bolm, Wiley-VCH: Weinheim, **2008**; d) A. El-Awa, M. N. NoShi, Mollat du X. Jourdin, P. L. Fuchs, *Chem. Rev.* **2009**, *109*, 2315; e) M. Nielsen, C. B. Jacobsen, N. Holub, M. W. Paixão, K. A. Jørgensen, *Angew. Chem. Int. Ed.* **2010**, *49*, 2668; f) A. R. Alba, X. Companyó, R. Rios, *Chem. Soc. Rev.* **2010**, *39*, 2018; g) M. Feng, B. Tang, S. H. Liang, X. Jiang, *Curr. Top. Med. Chem.* **2016**, *16*, 1200.

(2) a) A. El-Awa, M. N. Noshi, X. M. du Jourdin, P. L. Fuchs, *Chem. Rev.* **2009**, *109*, 2315; b) X. Chen, S. Hussain, S. Parveen, S. Xhang, Y. Yang, C. Zhu, *Curr. Med. Chem.* **2012**, *19*, 3578; c) T. G. Back, K. N. Clary, D. Gao, *Chem. Rev.* **2010**, *110*, 4498; d) A. S. Morgan, P. E. Sanderson, R. F. Borch, K. D. Tew, Y. Niitsu, T. Takayama, D. D. Von Hoff, E. Izbicka, G. Mangold, C. Paul, U. Broberg, B. Mannervik, W. D. Henner, L. M. Kauvar, *Cancer Res.* **1998**, *58*, 2568; e) F. Reck, F. Zhou, M. Girardot, G. Kern, C. J. Eyermann, N. J. Hales, R. R. Ramsay, M. B. Gravestock, *J. Med. Chem.* **2005**, *48*, 499; f) E. C. Bohl, W. Gao, D. D. Miller, C. E. Bell, J. T. Dalton, *Proc. Natl. Acad. Sci. U.S.A.* **2005**, *102*, 6201; g) N. Neamati, G. W. Kabalka, B. Venkataiah, R. Dayam, W.O. Patent 081966, **2007**; h) C. L. Percicot, C. R. Schnell, C. Debon, C. Hariton, *J. Pharmacol. Toxicol. Methods* **1996**, *36*, 223; i) J. D. Buynak, V. R. Doppalapudi, A. S. Rao, S. D. Nidamarthy, G. Adam, *Bioorg. Med. Chem. Lett.* **2000**, *10*, 847; j) F. G. Pilkiewicz, L. Boni, C. Mackinson, J. B. Portnoff, A. Scotto, An inhalation system for prevention and treatment of intracellular infections. WO 2003075889 A1, Sep 18, **2003**; k) M. C.

Furthermore, chiral allylic sulfones are important motifs in biological research that strives towards the discovery of new anticancer agents,[2g] antibacterial agents[2e] and TSH receptor antagonists.[2j] Approximately 20% of all FDA approved drugs are organosulfur compounds[3] and their preparation is thus of high significance.[1-3] For example, (−)-Agelasidine A (Scheme 5.1), which is an antifungal and antimicrobial agent isolated from marine sponges of the genus *Agelas*,[4] it is the first marine natural product containing both guanidine and sulfone groups and its unique structure is characterized by the presence of a quaternary stereocenter. Therefore, the synthesis of highly substituted allylic sulfones could be seen as an important synthetic tool in modern organic chemistry and drug synthesis.

5.1.2 Enantioselective Synthesis of Allylic Sulfones

Vinyl sulfones are excellent Michael acceptors and participate as versatile reagents in various cross coupling reactions. The steric bulk of the sulfone group offers an opportunity to direct reactions aimed at functionalization of an adjacent carbon center. Furthermore, elimination reactions affording alkenes and reductive cleavage of the sulfone unit allows it to function as a selectivity control group. Allylic sulfones are particular useful and modular building blocks.[5] Despite the massive attention that has been paid to the synthesis of allylic sulfones in the past decade,[6] a general catalytic

Gershengorn, S. Neumann, C. J. Thomas, H. Jaeschke, S. Moore, G. Krause, B. Raaka, R. Paschke, G. Kleinau, U.S. Patent 0,203,716, **2009**.

(3) a) N. A. McGrath, M. Brichacek, J. T. Njardarson, *J. Chem. Educ*. **2010**, *87*, 1348; b) K. A. Scott, J. T. Njardarson, *Top. Curr. Chem.* **2018**, *376*, 5.

(4) H. Nakamura, H. Wu, J. Kobayashi, Y. Ohizumi, Y. Hirata, T. Higashijima, T. Miyazawa, *Tetrahedron Lett.* **1983**, *24*, 4105.

(5) a) B. M. Trost, M. R. Ghadiri, *J. Am. Chem. Soc.* **1984**, *106*, 7260; b) B. M. Trost, M. R. Ghadiri, J. *Am. Chem.* Soc. **1986**, *108*, 1098; c) J. P. Adams, J. Bowler, M. A. Collins, D. N. Jones, S. Swallow, *Tetrahedron Lett.* **1990**, *31*, 4355; d) B. M. Trost, M. R. Ghadiri, *Bull. Soc. Chim. Fr.* **1993**, *130*, 433; e) M. Julia, A. Righini, J. N. Verpeaux, *Tetrahedron Lett.* **1979**, 2393; f) Y. Masaki, K. Sakuma, K. Kaji, *J. Chem. Soc., Chem. Commun.* **1980**, 434; g) M. Julia, A. Righini-Tapie, J. N. Verpeaux, *Tetrahedron* **1983**, *39*, 3283; h) M. Julia, J. N. Verpeaux, *Tetrahedron* **1983**, *39*, 3289; i) Y. Masaki, K. Sakumi, K. Kaji, *J. Chem. Soc., Perkin Trans. I* **1985**, 1171; j) B. M. Trost, C. A. Merlic, J. *Am. Chem.* Soc. **1988**, *110*, 5216; k) J. L. Fabre, M. Julia, J. N. Verpeaux, *Bull. Soc. Chim. Fr.* **1985**, 772; l) T. Cuvigny, M. Julia, *J. Organomet. Chem.* **1983**, 250, C21; **1986**, *317*, 383; m) B. M. Trost, N. R. Schmuff, M. J. Miller, *J. Am. Chem.* Soc. **1980**, *102*, 5979; n) B. M. Trost, C. A. Merlic, *J. Org. Chem.* **1990**, *55,* 1127; o) B. M. Trost, C. A. Merlic, *J. Am. Chem. Soc.* **1990**, *112*, 9590.

(6) Selected examples of construction of allylic sulfones synthesis: a) G. W. Kabalka, B. Venkataiah, G. Dong, *Tetrahedron Lett.* **2003**, *44*, 4673; b) V. Garima, P. Srivastava, L. Dhar, S. Yadav, *Tetrahedron Lett.* **2011**, *52*, 4622; c) X.-Q. Chu, H. Meng, X.-P. Xu and S.-J. Ji, *Chem. Eur. J.* **2015**, *21*, 11359; d) L. Jiang, T.-G. Li, J.-F. Zhou, Y.-M. Chuan, H.-L. Li, M.-L. Yuan, *Molecules*, **2015**, *20*, 8213; e) C.-R. Liu, M.-B. Li, D.-J. Cheng, C.-F. Yang, S.-K. Tian, *Org. Lett.* **2009**, *11*, 2543; f) L. Rajender Reddy, B. Hu, M. Prashad, K. Prasad, *Angew. Chem. Int. Ed.* **2009**, *48*, 172; g) E. Jacobsen, M. K. Chavda, K. M. Zikpi, S. L. Waggoner, D. J. Passini, J. A. Wolfe, R. Larson, C. Beckley, C. G. Hamaker, S. R. Hitchcock, *Tetrahedron Lett.* **2017**, *58*, 3073; h) M. Jegelka, B. Plietker, *Chem. Eur. J.* **2011**, *17*, 10417;

asymmetric synthesis of α,α-disubstituted allylic sulfones featuring a quaternary stereocenter remains extremely challenging and underdeveloped. In this context, only a few examples of enantioselective synthesis of sterically less hindered α-mono-functionalized allylic sulfones by traditional allylic substitution reactions (*i.e.*, Tsuji−Trost reactions) have been reported.[7]

In 1995, Trost and co-workers reported a Pd-catalyzed asymmetric synthesis of allylic sulfones via allylic sulfonylation reactions (Scheme 5.2).[7a] A desymmetrization of *meso-*diesters in the presence of a sulfinate anion gave excellent enantioselectivity. On the other hand, conversion of allylic esters into enantiomerically pure allylic sulfones required sodium benzenesulfinate to participate in the enantio-discriminating step. Substrates with five-, six-, and seven-membered rings all provided excellent enantioselectivities in this Pd-mediated manifold.

Scheme 5.2 reaction conditions:

$[PdCl(allyl)]_2$ (2.5 mol %)
Trost-ligand **L1** (7.5 mol %)
$(C_6H_{13})_4NBr$ (3 equiv.)
CH_2Cl_2, 0 °C

LG = OAc or OCO_2Me + $PhSO_2Na$ (3 euiqv.) → products with SO_2Ph

$n = 1$: 95%, *98% ee*
$n = 2$: 87%, *98% ee*
$n = 3$: 95%, *98% ee*
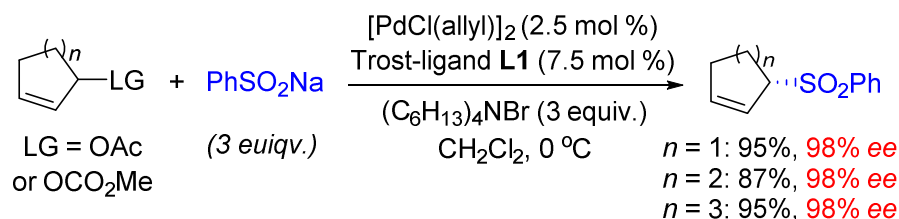
Scheme 5.2. Pd-catalyzed asymmetric synthesis of allylic sulfones (**L1**: see Chapter 1).

i) S. Chandrasekhar, V. Jagadeshwar, B. Saritha, C. Narsihmulu, *J. Org. Chem.* **2005**, *70*, 6506; j) H.-H. Li, D.-J. Dong, Y.-H. Jin, S.-K. Tian, *J. Org. Chem.* **2009**, *74*, 9501; k) M. Jegelka, B. Plietker, *Org. Lett.* **2009**, *11*, 3462; l) M. Billamboz, F. Mangin, N. Drillaud, C. Chevrin-Villette, E. Banaszak-Léonard, C. Len, *J. Org. Chem.* **2014**, *79*, 493; m) X.-T. Ma, R.-H. Dai, J. Zhang, Y. Gu, S.-K. Tian, *Adv. Synth. Catal.* **2014**, *356*, 2984; n) T.-T. Wang, F.-X. Wang, F.-L. Yang, S.-K. Tian, *Chem. Commun.* **2014**, *50*, 3802; o) K. Xu, V. Khakyzadeh, T. Bury, B. Breit, *J. Am. Chem. Soc.* **2014,** *136, 16124;* p) M.-Y. Chang, H.-Y. Chen, H.-S. Wang, *J. Org. Chem.* **2017**, *82*, 10601; q) X. Lei, L. Zheng, C. Zhang, X. Shi, Y. Chen, *J. Org. Chem.* **2018**, *83*, 1772; r) G. Zhang, L. Zhang, H. Yi, Y. Luo, X. Qi, C.-H. Tung, L.-Z. Wu, A. Lei, *Chem. Commun.* **2016**, *52*, 10407; s) R. Mao, Z. Yuan, R. Zhang, Y. Ding, X. Fan, J. Wu, *Org. Chem. Front.* **2016**, *3*, 1498; t) X. Li, X. Xu, C. Zhou, *Chem. Commun.* **2012**, *48*, 12240; u) L. Kadari, R. K. Palakodety, L. P. Yallapragada, *Org. Lett.* **2017**, *19*, 2580; v) V. Khakyzadeh, Y. H. Wang, B. Breit, *Chem. Commun.* **2017**, *53*, 4966.

(7) For representative examples for enantioselective synthesis of α-mono-functionalized chiral allylic sulfones: a) B. M. Trost, M. G. Organ, G. A. Odoherty, *J. Am. Chem. Soc.* **1995**, *117*, 9662; b) B. M. Trost, M. J. Krische, R. Radinov, G. Zanoni, *J. Am. Chem. Soc.* **1996**, *118*, 6297; c) B. M. Trost, N. R. Schmuff, *J. Am. Chem. Soc.* **1985**, *107*, 396; d) M. Ueda, J. F. Hartwig, *Org. Lett.* **2010**, *12*, 92; e) X.-S. Wu, Y. Chen, M.-B. Li, M.-G. Zhou, S.-K. Tian, *J. Am. Chem. Soc.* **2012**, *134*, 14694; f) K. Hiroi, K. Makino, *Chem. Lett.* **1986**, 617; g) K. Hirasawa, M. Kawamata, K. Hiroi, *Yakugaku Zasshi* **1994**, *114*, 111; h) H. Eicheimann, H.-J. Gais, *Tetrahedron: Asymmetry* **1995**, *6*, 643; i) B. M. Trost, M. L. Crawley, C. B. Lee, *J. Am. Chem. Soc.* **2000**, *122*, 6120; j) H.-J. Gais, N. Spalthoff, T. Jagusch, M. Frank, G. Raabe, *Tetrahedron Lett.* **2000**, *41*, 3809; k) H.-J. Gais, T. Jagusch, N. Spalthoff, F. Gerhards, M. Frank, G. Raabe, *Chem. Eur. J.* **2003**, *9*, 4202; l) T.-T. Wang, F.-X. Wang, F.-L. Yang, S.-K. Tian, *Chem. Commun.* **2014**, *50*, 3802.

In the same year, the Gias group showed that Pd-catalyzed asymmetric sulfonylation of allylic substrates in the presence of the Helmchen-Pfaltz-Williams ligands (*i.e.,* chiral phosphino-oxazoline ligand) gave the allylic sulfones in good yield and with moderate to high enantioselectivity (Scheme 5.3).[7h]
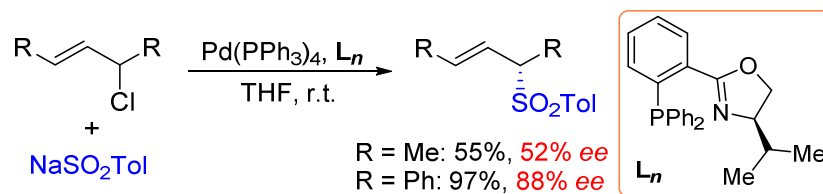
Scheme 5.3. Pd-catalyzed asymmetric allylic sulfonylation reported by Gias *et al.*

In 2000, the same group demonstrated that Pd-catalyzed kinetic resolution of racemic cyclic and acyclic carbonates with sulfur based nucleophiles (Scheme 5.4) can also be achieved.[7j,7k] A chiral Pd(0) complex bearing the Trost ligand **L1** (see Chapter 1) in combination with S-based nucleophiles promotes the kinetic resolution of allylic precursors with excellent levels of enantioselectivity to simultaneously give chiral allylic carbonates as well as allylic sulfones and sulfides. This kinetic resolution process allowed, at the time, for access to novel enantiopure cyclic alcohols.
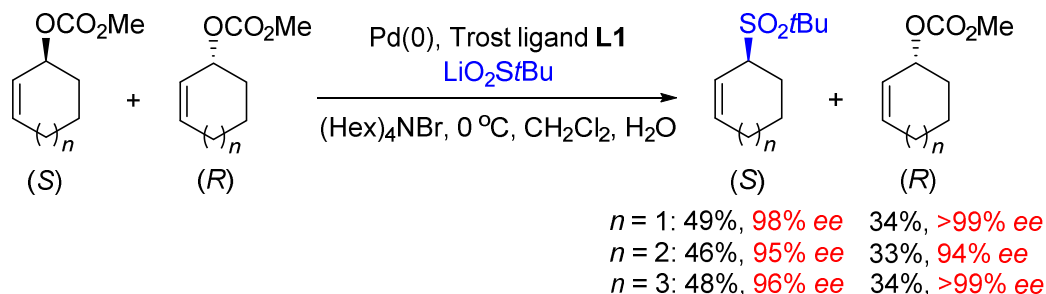
Scheme 5.4. Pd-catalyzed kinetic resolution of racemic allylic carbonates using sulfinate salts.

The Hartwig group developed in 2010 an Ir-catalyzed regio- and enantioselective allylic substitution process using aromatic and aliphatic sulfinates (Scheme 5.5).[7d] Notable features of this process include high regioselectivity of the allylic substitution reaction and having broad scope in allylic carbonate and sodium sulfonate reaction partners. A series of branched allylic sulfone products was obtained in good yield, with excellent selectivity towards the branched isomer, and high enantioselectivities of up to 98% *ee*.
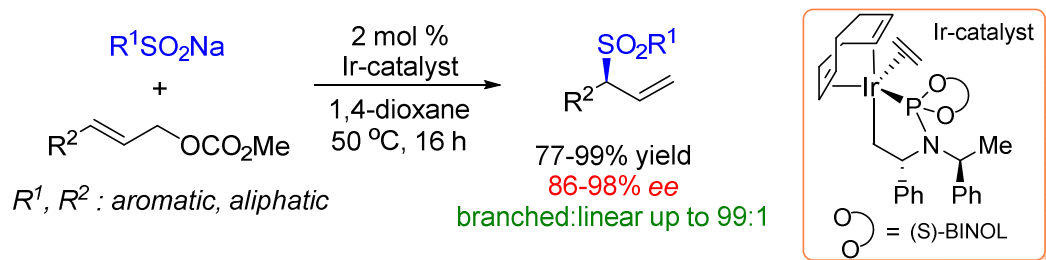
Scheme 5.5. Ir-catalyzed allylic substitution to afford α-mono-substituted allylic sulfones.

Subsequently, Tian and co-workers developed for the first time a highly efficient direct substitution reaction of primary allylic amines with sulfinate salts.[7e,71] In the presence of 0.1 mol % [PdCl(allyl)]$_2$, 0.4 mol % of dppb [1,4-bis(diphenylphosphino)butane], and excess of boric acid, a broad range of α-unbranched primary allylic amines could be smoothly substituted with sodium sulfinates in an α-selective fashion to give structurally diverse allylic sulfones in good yields with exclusive *E* selectivity. Replacing the dppb with 1,1′-bi-2-naphthol (BINOL) allowed unsymmetrical α-chiral, primary allylic amines to be transformed into the corresponding allylic sulfones in good to excellent yields with excellent retention of the chiral information. Importantly, the reaction complements known asymmetric methods in substrate scope via its unique ability to provide α-chiral allylic sulfones with high optical purity starting from unsymmetrical allylic electrophiles (Scheme 5.6).
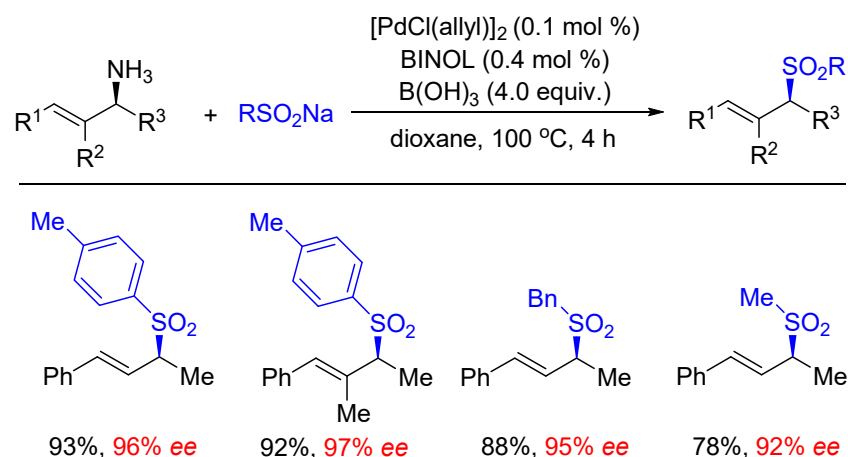
Scheme 5.6. Direct substitution of α-chiral primary allylic amines with sodium sulfonates under Pd-catalysis.

In 2015, Breit and co-worker developed a highly regio- and enantioselective hydrothiolation of terminal allenes which fulfills the criteria of an atom-economical reaction.[8] Through the application of two chiral rhodium catalyst systems, a wide variety of thiols and allenes could be coupled to first furnish chiral thioether intermediates. Subsequent oxidation gave access to the corresponding allylic sulfones in enantiomerically pure form. The reaction tolerates a variety of functional groups and labeling experiments provided insight into the reaction mechanism of the process (Scheme 5.7). Additionally, the same group reported the first rhodium-catalyzed atom-economic addition of free thiols to 1,3-disubstituted allenes.[9] By using dppb as a bidentate ligand and 30 mol % PTSA (*p*-toluenesulfonic acid) as an additive, the reaction led to the desired higher substituted allylic sulfones with excellent *Z*-selectivities and in high yields. The reaction tolerates a broad variety of aromatic and aliphatic thiols. Furthermore, a wide scope of different symmetrical and unsymmetrical acyclic and cyclic 1,3-disubstituted allenes proved to be efficient reaction partners. Starting from *racemic* allenes, a Rh(I)/(*S,S*)-Me-DuPhos catalyst was able to mediate a dynamic kinetic resolution, thus providing the corresponding *Z*-allylic thioethers and sulfones with high enantioselectivities (Scheme 5.8).
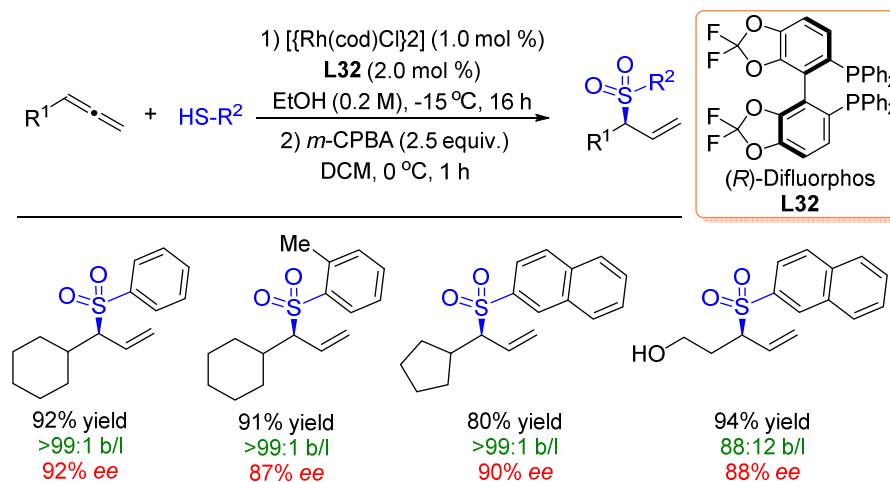
Scheme 5.7. Rh-catalyzed hydrothiolation of terminal allenes to provide chiral sulfones after oxidation.

(8) A. B. Pritzius, B. Breit, *Angew. Chem. Int. Ed.* **2015**, *54*, 3121.
(9) A. B. Pritzius, B. Breit, *Angew. Chem. Int. Ed.* **2015**, *54*, 15818.
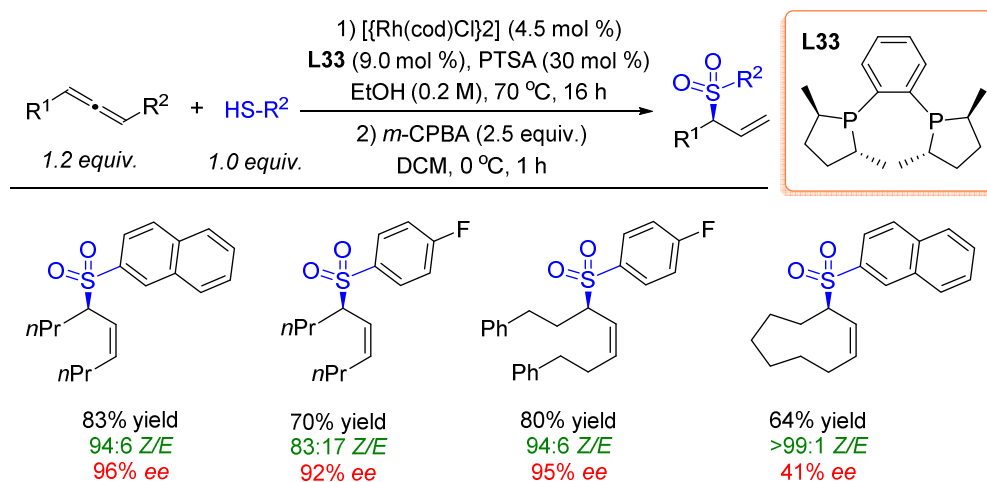
Scheme 5.8. Asymmetric hydrothiolation of 1,3-disubstituted allenes to afford chiral allylic sulfones after oxidation.
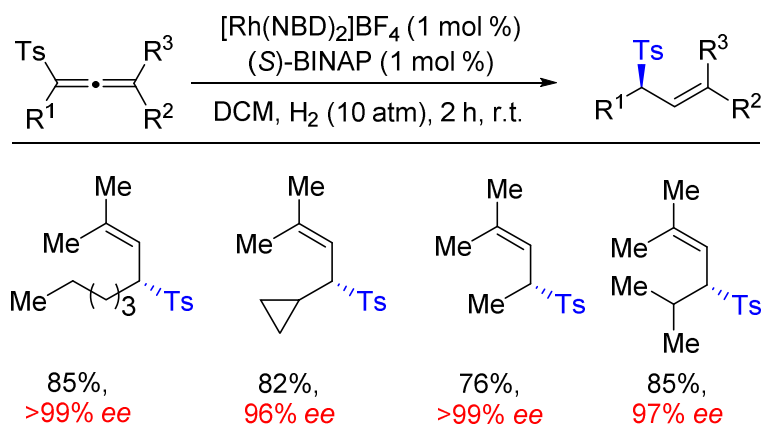
Scheme 5.9. Asymmetric semi-reduction of bulky tetrasubstituted allenes.

Recently, Zhang and co-workers reported a highly regio- and enantioselective hydrogenation of challenging tetrasubstituted allenyl sulfones affording chiral allylic sulfones in good yields (up to 99%) and with excellent regio- and enantioselectivities (99% ee).[10] The regio- and enantioselective hydrogenation of allenes has been rarely reported, despite the fact that the asymmetric semi-reduction of allenes provides an efficient access to chiral allylic compounds. The main reason could be due to the difficulty to simultaneously control the chemo-, regio-, and stereoselectivity of this reaction, and the asymmetric semi-reduction of more sterically hindered tetrasubstituted allenes has not been established yet. This method provides an efficient and concise route to chiral allylic

---

(10) J. Long, L. Shi, X. Li, H. Lv, X. Zhang, *Angew. Chem. Int. Ed.* **2018**, *57*, 13248.

sulfones, thus offering an atom-economic process with a wide range of potential applications in organic synthesis and medicinal chemistry (Scheme 5.9).

In spite of the significant progress in the area of asymmetric synthesis of allylic sulfones, the catalytic formation of sterically challenging, chiral α,α-disubstituted allylic sulfones incorporating tetrasubstituted tertiary carbons has proven to be elusive. Despite the availability of scarce example of such synthesis,[11] to the best of our knowledge a general asymmetric method for the regio- and enantioselective preparation of α,α-disubstituted allylic sulfones continues to be an unsolved, yet inspiring synthetic problem.

5.1.3 Aim of the Work presented in this Chapter

Forging chiral branched allylic derivatives from simple and readily available racemic starting materials continues to be an important task in synthetic chemistry, due to the potential of the allylic moiety for further elaboration and asymmetric synthesis.[12] In this respect, significant progress has been achieved by transition-metal mediated allylic substitution of primary and secondary allylic precursors, with Ir catalysis being prevalent.[13] However, the regio- and enantioselective synthesis of α,α-disubstituted allylic targets via substitution of tertiary allylic precursors by TM in general and for Pd in particular is rather rare and embodies a largely unexplored landscape in synthetic

(11) a) Y. Xiong, G. Zhang, *Org. Lett.* **2016**, *18*, 5094; b) J. E. Gomez, A. Cristofol, A. W. Kleij, *Angew. Chem. Int. Ed.* **2019**, *58*, 3903; c) X. H. Yang, R. T. Davison, S. Z. Nie, F. A. Cruz, T. M. McGinnis, V. M. Dong, *J. Am. Chem. Soc.* **2019**, *141*, 3006.

(12) For reviews on allylic substitution: a) B. M. Trost, D. L. Van Vranken, *Chem. Rev.* **1996**, *96*, 395; b) B. M. Trost, *Acc. Chem. Res.* **1996**, *29*, 355; c) B. M. Trost, M. L. Crawley, *Chem. Rev.* **2003**, *103*, 2921; d) H. Miyabe, Y. Takemoto, *Synlett* **2005**, 1641; e) B. M. Trost, M. R. Machacek, A. Aponick, *Acc. Chem. Res.* **2006,** *39*, 747; f) Z. Lu, S. Ma, *Angew. Chem. Int. Ed.* **2008**, *47*, 258; g) B. M. Trost, T. Zhang, J. D. Sieber, *Chem. Sci.* **2010**, *1*, 427; h) B. Sundararaju, M. Achard, C. Bruneau, *Chem. Soc. Rev.* **2012**, *41*, 4467.

(13) For representative reviews on iridium catalyzed asymmetric allylic substitution: a) G. Helmchen, A. Dahnz, P. Dübon, M. Schelwies, R. Weihofen, *Chem. Commun.* **2007**, 675; b) Y. Wu, D. Yang, Y. Long, *Chin. J. Org. Chem.* **2009**, *29*, 1522; c) J. F. Hartwig, L. M. Stanley, *Acc. Chem. Res.* **2010**, *43*, 1461; d) J. F. Hartwig, M. J. Pouy, *Top. Organomet. Chem.* **2011**, *34*, 169; e) W.-B. Liu, J.-B. Xia, S.-L. You, *Top. Organomet. Chem.* **2011**, *38*, 155; f) P. Tosatti, A. Nelson, S. P. Marsden, *Org. Biomol. Chem.* **2012**, *10*, 3147; g) J. C. Hethcox, S. E. Shockley, B. M. Stoltz, *ACS Catal.* **2016**, *6*, 6207; h) J. Qu, G. Helmchen, *Acc. Chem. Res.* **2017**, *50*, 2539; i) Q. Cheng, H.-F. Tu, C. Zheng, J.-P. Qu, G. Helmchen, S.-L. You, *Chem. Rev.* **2019**, *119*, 1855.

chemistry.[12,14] A major obstacle is the propensity of nucleophiles to attack at the less hindered terminus of the π-allyl-Pd intermediate, which leads to a linear allylic product.[15]
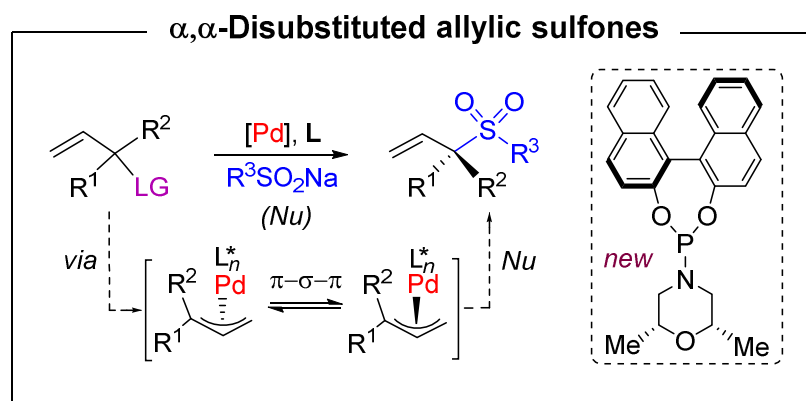
Scheme 5.10. Pd-catalyzed synthesis of α,α-disubstituted allylic sulfones using a newly developed phosphoramidite ligand.

A further requisite for the successful synthesis of chiral α,α-disubstituted allylic compounds is the ease of isomerization of the intermediate π-allyl-Pd species via π−σ−π interconversion (Scheme 5.10). When such isomerization is faster relative to subsequent nucleophilic attack, a dynamic kinetic resolution of the allyl palladium complex allows for kinetic discrimination of the two forward-going allylic substitution pathways, and thus efficient asymmetric induction.[12a,15a] In this context, we recently communicated a Pd-catalyzed allylic substitution process allowing for the preparation of enantioenriched α,α-disubstituted allylic amines and ethers, respectively.[16] Such an approach using more nucleophilic sulfur-centered species has intrinsically the challenge of being limited in scope and causing catalyst poisoning. In this chapter, we show that by careful ligand and process design, allylic sulfonylation of racemic tertiary allylic carbonates can be accomplished under Pd catalysis using sodium sulfinates as nucleophilic reaction partners.

(14) Selective examples for the asymmetric synthesis of α,α-disubstituted allylic compounds: a) B. M. Trost, R. C. Bunt, R. C. Lemoine, T. L. Calkins, *J. Am. Chem. Soc.* **2000**, *122*, 5968; b) P. Zhang, H. Le, R. E. Kyne, J. P. Morken, *J. Am. Chem. Soc.* **2011**, *133*, 9716; c) D. F. Fischer, Z. Xin, R. Peters, *Angew. Chem. Int. Ed*. **2007**, *46*, 7704; d) J. S. Arnold, H. M. Nguyen, *J. Am. Chem. Soc*. **2012**, *134*, 8380; e) A. Khan, S. Khan, I. Khan, C. Zhao, Y. Mao, Y. Chen, Y. J. Zhang, *J. Am. Chem. Soc.* **2017**, 139, 10733; f) B. W. H. Turnbull, P. A. Evans, *J. Org. Chem*. **2018**, *83*, 11463.

(15) a) S. A. Godleski, *Comprehensive Organic Synthesis*; B. M. Trost, I. Fleming, M. F. Semmelhack, Eds.; Pergamon Press: Oxford: Vol. 4, Chapter 3.3, pp 585-662; b) B. M. Trost, M.-H. Hung, *J. Am. Chem. Soc.* **1984**, *106*, 6837.

(16) a) A. Cai, W. Guo, L. Martínez-Rodríguez, A. W. Kleij, *J. Am. Chem. Soc.* **2016**, *138*, 14194; b) W. Guo, A. Cai, J. Xie, A. W. Kleij, *Angew. Chem. Int. Ed*. **2017**, *56*, 11797; c) J. Xie, W. Guo, A. Cai, E. C. Escudero-Adán, A. W. Kleij, *Org. Lett*. **2017**, *19*, 6388.

This process illustrates a combination of high regio- and enantiocontrol providing the first general route to elusive chiral, α,α-disubstituted branched allylic sulfones.

5.2 Results and Discussion

5.2.1 Optimization of the Reaction Conditions

Initially, the reaction of racemic tertiary allylic carbonate **1a** and sodium benzylsulfinate was selected as a model system, based on previous work in our group,[16] Various chiral phosphoramidite ligands were evaluated and the enantioinduction, rate and overall selectivity examined: these results are summarized in Table 5.1. In general, we found that the bulkiness of the nitrogen substituents of the phosphoramidite ligand exerts an important influence on the regio- and enantioselectivity in this benchmark allylic sulfonylation reaction (**L14–L33**). When using more bulky *N*-substituents, the starting material **1a** exclusively converted into linear allylic sulfone product (cf., for **L24** and **L33**). The rate of the reaction decreased significantly when using ligands containing substituents attached to the 3,3′-positions of the binaphthol backbone (**L15** and **L29**). Further to this, we found that the presence of *N*-heterocyclic groups in the phosphoramidite ligand such as in the case of **L20**, **L21** and **L31-L32** gave better enantioselectivity compared to others ligands under similar reaction conditions. Based on these results, we made a key observation in this preliminary evaluation of suitable P-ligands. Substituents at the binaphthol backbone and/or bulky groups present at the N-center of the phosphoramidite ligand decelerate the reaction progress and significantly affect the regio- and enantioselectivity of this reaction.

Table 5.1 Preliminary evaluation of suitable phosphoramidite ligands.
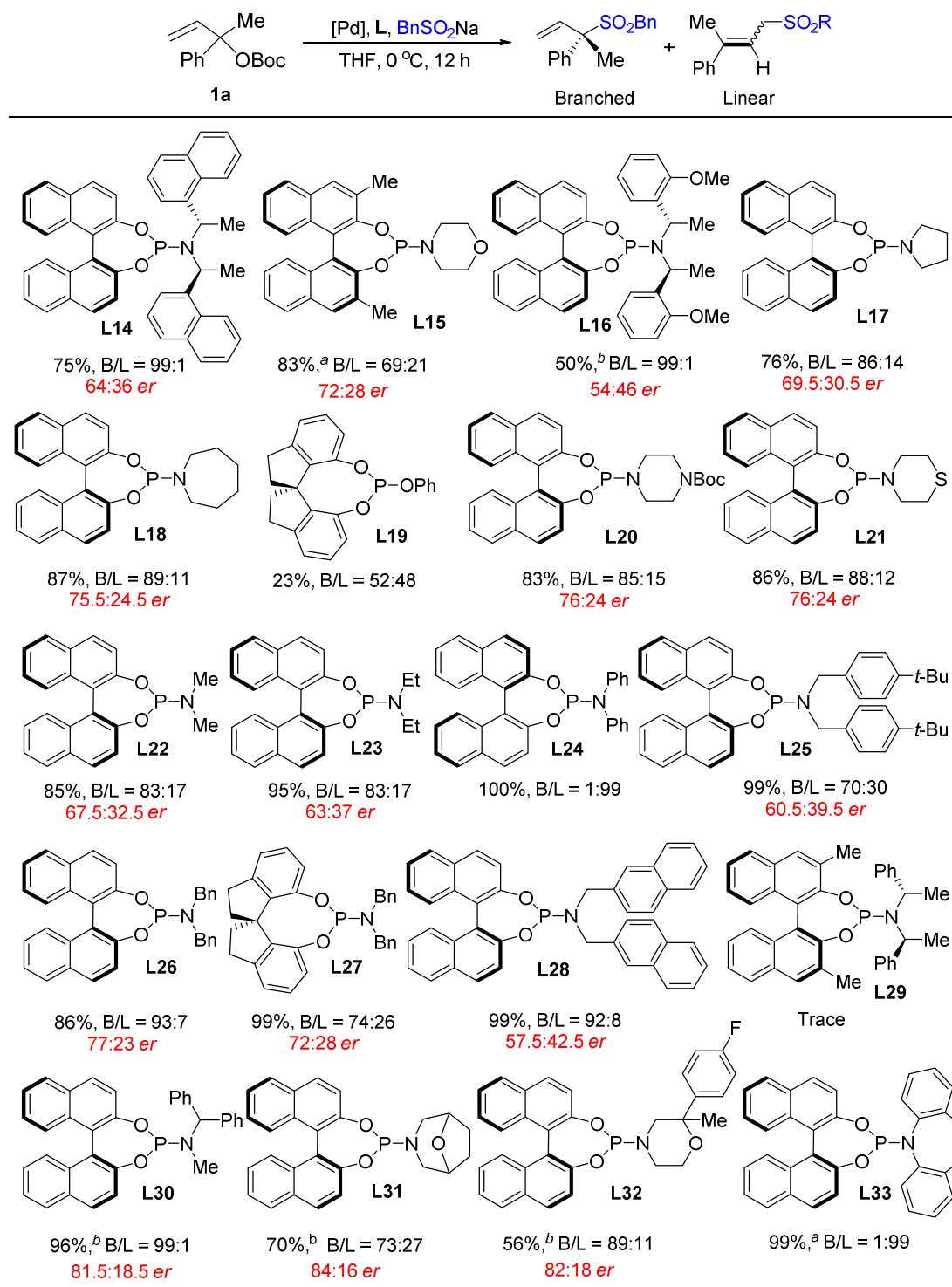
Reaction conditions: **1a** (0.15 mmol), BnSO$_2$Na (0.165 mmol, 1.1 equiv), THF (300 µL), Pd$_2$(dba)$_3$·CHCl$_3$ (2.5 mol %), **L** (10 mol %), 0 ºC, 12 h; the conversion and B/L ratio was determined by ^{1}H NMR analysis of the crude reaction mixture; the *er* values were determined by SFC (supercritical fluid chromatography). [a] Room temperature. [b] 2-Me-THF (300 µL).

Table 5.2 Selected data for the reactions employing phosphoramidite ligands **L1-10** in the optimization phase towards the formation of allylic sulfone product **2a**.[a]
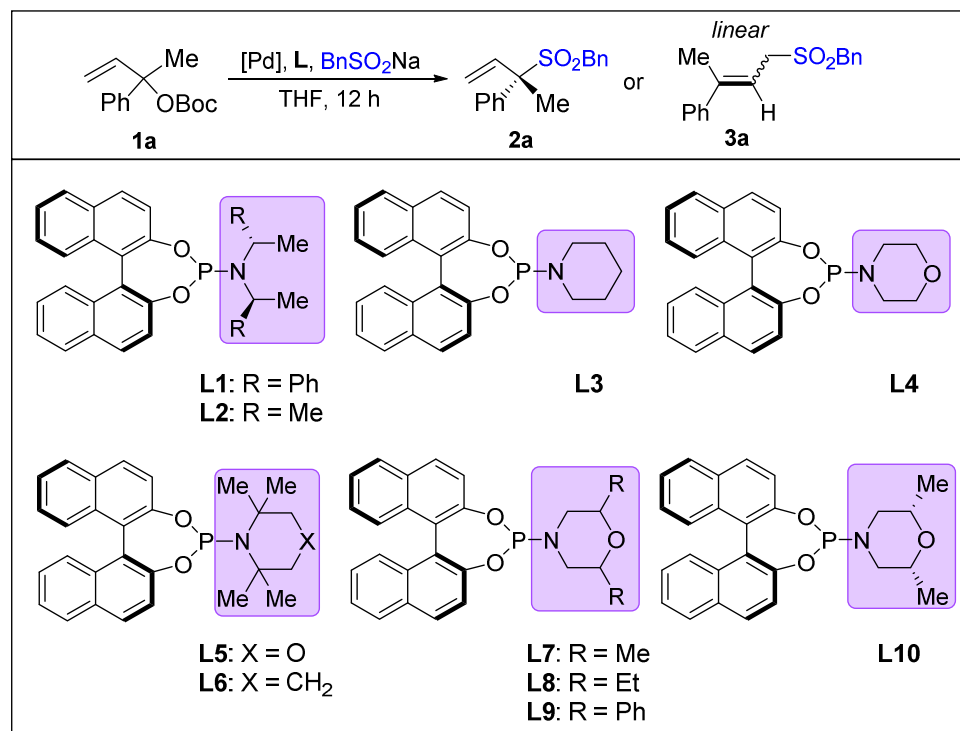
Entry	L	Solvent	T [°C]	2a/3a[b]	Yield 2a [%][b]	er[d]
1	**L1**	THF	0	99:1	67	76:24
2	**L2**	THF	0	96:4	83	67:33
3	**L3**	THF	0	35:65	27	32:68
4	**L4**	THF	0	88:12	78	70:30
5[e]	**L5**	THF	rt	99:1	71	59:41
6[e]	**L6**	THF	rt	99:1	36	60:40
7[f]	**L7**	THF	0	87:13	79	82.5:17.5
8	**L8**	THF	0	71:29	65	86:14
9	**L9**	THF	0	83:17	74	87:13
10[f]	**L10**	THF	0	87:13	80	85.5:14.5

[a] **1a** (0.15 mmol), BnSO$_2$Na (0.165 mmol, 1.1 equiv.), solvent (300 μL), Pd$_2$(dba)$_3$·CHCl$_3$ (2.5 mol %), **L** (10 mol %). [b] Determined by ^{1}H NMR analysis of the crude reaction mixture using toluene as internal standard. [c] Isolated yield. [d] *er* determined by SFC (supercritical fluid chromatography). [e] After 48 h. [f] After 8 h.

Based on the initial experiments reported in Table 1, we set out to first explore the effects of the chiral phosphoramidite ligands **L1–L4** (Table 5.2) on the regio- and enantioselectivity in this sulfonylation reaction. To our delight, the use of Feringa-type

ligand **L1**[17] (entry 1) and ligand **L2** (entry 2) provided good NMR yields of the branched allylic sulfone with excellent regiocontrol, though with low enantioinduction. Use of ligands **L3** and **L4** (entries 3 and 4) gave lower levels of regiocontrol and similar moderate enantioinduction. These results helped further to assess that the steric hindrance of the nitrogen substituent in the ligands affects the regio- and enantioselectivity in the allylic sulfonylation reaction.

Therefore, we next varied the steric nature of the substituents of the amine unit in the phosphoramidite ligand (Table 5.2; **L5–L10**). The presence of tetramethymorpholine- or piperidine-derived ligands **L5** and **L6** led to a decrease in the enantioselectivity, and importantly also a deceleration of the reaction progress was observed (entries 5 and 6; r.t. required). By switching the methyl substituents to the *β*-position in the amine moiety (**L7**), both the rate of the reaction and the enantioselectivity improved giving the branched allylic sulfone **2a** in 79% yield and 82.5:17.5 *er* (entry 7). Evaluation of other more bulky alkyl/aryl groups (ethyl and phenyl) at the same position of the phosphoramidite ligand (*i.e.,* **L8** and **L9**; entries 8 and 9) did not significantly change the reaction outcome. The presence of a chiral center in the amine module of the ligand **L10** slightly increased the enantioselectivity while maintaining the regioselectivity compared to **L7** utilized under similar conditions (entry 10).

Subsequently, the exploration of various solvents revealed that 2-Me-THF is the best medium for this reaction (Table 5.3; entries 1–4). Remarkably, complete linear regioselectivity was observed in DCM (entry 3). An increase in the amount of solvent (entries 5 and 6) and a decrease of the amount of nucleophile at lower reaction temperature (entries 7–9) significantly improved both regio- and enantioselectivity. The reaction was further optimized by changing the loading of the Pd precursor. These subtle changes finally furnished allylic sulfone **2a** in 82% isolated yield and with an 95:5 *er*, and with excellent regioselectivity (entry 20; **2a/3a** = 99:1). Notably, this synthetic method can be performed in the absence of additives and under air adding to the practicality of this asymmetric methodology.

(17) For a review: J. F. Teichert, B. L. Feringa, *Angew. Chem. Int. Ed.* **2010**, *49*, 2486.

Table 5.3 Effect of the solvent, temperature and other reaction parameters on the formation of allylic sulfone product **2a**.[a]

Entry	L	Solvent	T [ºC]	2a/3a[b]	Yield 2a [%][b]	er[d]
1	**L10**	CH$_3$CN	0	57:43	50	53.5:46.5
2	**L10**	2-Me-THF	0	88:12	82	86:14
3	**L10**	DCM	0	1:99	0	–
4	**L10**	Toluene	0	40:60	30	–
5[g]	**L10**	2-Me-THF	0	87:13	81	86.5:13.5
6[h]	**L10**	2-Me-THF	0	88:12	81	89.5:10.5
7[h,i]	**L10**	2-Me-THF	-10	88:12	79	90.5:9.5
8[e,h,i]	**L10**	2-Me-THF	-20	99:1	80[c]	93.5:6.5
9[e,h,i]	**L10**	THF	-20	91:9	78	92.5:7.5
10[e,h-j]	**L10**	2-Me-THF	-20	99:1	82[c]	95:5

[a] **1a** (0.15 mmol), BnSO$_2$Na (0.165 mmol, 1.1 equiv.), solvent (300 μL), Pd$_2$(dba)$_3$·CHCl$_3$ (2.5 mol %), **L** (10 mol %). [b] Determined by ^{1}H NMR analysis of the crude reaction mixture using toluene as internal standard. [c] Isolated yield. [d] *er* determined by SFC (supercritical fluid chromatography). [e] After 48 h. [f] After 8 h. [g] Solvent (500 μL). [h] Solvent (1.0 mL). [i] BnSO$_2$Na (0.10 mmol), **1a** (0.15 mmol, 1.5 equiv.). [j] Pd$_2$(dba)$_3$·CHCl$_3$ (3.5 mol %).

To further challenge this new asymmetric protocol, the preparation of α,α-disubstituted **aryl** allylic sulfones was then investigated (Table 5.4). Initially the reaction of racemic tertiary allylic carbonate **1a** and sodium benzenesulfinate was selected as a model system. The nucleophilic character of aromatic and aliphatic sulfinate salts is quite different, and to our delight the desired branched allylic sulfone products could be smoothly prepared in the presence Pd precursor and phosphoramidite ligand **L1** and **L2**, and THF as solvent, albeit with low enantioinduction (entries 1 and 2).

Then, a series of phosphoramidite ligands and solvents were screened, and the results are summarized in Table 5.4. The desired product could be generated in 80% ^{1}H NMR yield and with a 89:11 enantiomeric ratio when using **L4** (entry 4). By further optimization, the *er* value could be improved to 89.5:10.5 when the reaction was performed in THF and with a higher catalyst loading (Table 5.4; entry 21: 4 mol % [Pd] and 12 mol % **L4**). Subsequently, we attempted to further improve the results by changing

additives, scale and by using a N_2 atmosphere though without noticeable improvement (Table 5.4, entries 24-27).

Table 5.4 Screening of conditions towards formation of *N*-aryl allyl sulfones.

Entry	L	Solvent	T [°C]	B/L[b]	Yield **B** [%][b]	er[d]
1	**L1**	THF	0	99:1	86	68.5:31.5
2	**L2**	THF	0	89:11	82	62:38
3	**L3**	THF	0	79:21	65	78:22
4	**L4**	THF	0	85:15	80	89:11
5[e]	**L4′**	THF	0	74:26	68	67:33
6[e]	**L5**	THF	0	99:1	86	53:47
7[f]	**L6**	THF	0	99:1	88	54:46
8	**L7**	THF	0	96:4	82	81:19
9	**L8**	THF	0	59:41	52	52.5:47.5
10	**L9**	THF	0	83:17	75	87:13
11	**L10**	THF	0	68:3	60	55:45
12	**L11**	THF	0	55:45	45	54:46
13	**L12**	THF	0	-	trace	-
14[g]	**L4**	CH₃CN	0	74:26	50	62.5:37.5
15[e,g]	**L4**	2-Me-THF	0	84:16	76	88.5:11.5
16[e,g]	**L4**	EA	0	86:14	60	87:13
17[e,g]	**L4**	Et₂O	0	90:10	79	87.5:12.5
18[e,g]	**L4**	1,4-dioxane	0	95:5	85	86.5:13.5
19[e,g]	**L4**	CH₃NO₂	0	75:25	66	63.5:36.5
20[h]	**L4**	THF	0	85:15	79	89:11
21[i]	**L4**	**THF**	**0**	**87:13**	**84**[c]	**89.5:10.5**
22[j]	**L4**	THF	-20	95:5	48	90:10
23[k]	**L4**	THF	0	85:15	71	88:12

Table 5.4 - *continued*

24[l]	**L4**	THF	0	87:13	80	88.5:11.5
25[m]	**L4**	THF	0	85:15	79	84.5:15.5
26[n]	**L4**	THF	0	79:21	71	71:29
27[o]	**L4**	THF	0	85:15	79	87.5:12.5

[a]**1a** (0.15 mmol, 1.0 equiv.), PhSO$_2$Na (0.225 mmol, 1.5 equiv.), solvent (300 μL), Pd$_2$(dba)$_3$·CHCl$_3$ (2.5 mol %), **L** (10 mol %). [b]Determined by ^{1}H NMR analysis of the crude reaction mixture. [c]Isolated yield. [d]*er* determined by SFC. [e]24 h. [f]48 h. [g]PhSO$_2$Na (0.165 mmol, 1.1 equiv.). [h]BnSO$_2$Na (0.15 mmol, 1.0 equiv.), **1a** (0.3 mmol, 2.0 equiv), 36 h. [i]THF (400 μL). [j]Pd$_2$(dba)$_3$·CHCl$_3$ (4 mol %), **L** (12 mol %). [k]BnSO$_2$Na (0.45 mmol, 3.0 equiv.). [l]Additive: MgSO$_4$ (18 mg, 1.0 equiv.). [m]Additive: CsF (68.4 mg, 3.0 equiv.). [n]Additive: (C$_4$H$_9$)$_4$NCl (42 mg, 1.0 equiv.). [o]Reaction performed under a nitrogen atmosphere.

5.2.2 Scope of Sodium Alkylsulfinates

Having established these optimized conditions (Table 5.3, entry 10), the scope of the allylic substitution reaction was evaluated focusing first on the variation of the sodium alkylsulfinate nucleophile (Table 5.5, **1–17**). Various benzylsulfinates (**1–5**, **7** and **8**) were tolerated, giving rise to α,α-disubstituted allylic sulfones in good yields and with high enantioselectivity including those bearing aryl groups with *para* (**1–5**), *meta* (**7**) and *ortho* (**8**) substitutions. Importantly, various alkylsulfinate salts showed good reactivity and provided the desired branched allylic sulfone products with high *er* values (**6**, **9–17**) unlike in previous reports.[7] The allylic sulfone products containing ester and trifluoromethyl groups (**6** and **16**) were also obtained in good yields with 93.5:6.5 *er* and 92.8 *er*, respectively. Substrates with methyl (**10**), ethyl (**11**), *n*-butyl (**19**), isobutyl (**17**) and longer alkyl chains (**13**) were also productive reaction partners and afforded the chiral allylic sulfone products with high levels of enantioinduction. The installation of three-, five-, and six-membered rings (**12**, **14** and **15**) was easily accomplished without eroding the overall reactivity/enantioinduction. Notably, all the reactions proceeded with excellent regioselectivity typically being >95:5 in favor of the branched product.

Table 5.5 Scope of products by variation of the sodium alkylsulfinate reagent.

1: 56%, 94:6 er [a]

2: 63%, 94.5:5.5 er [a]

3: 77%, 94.5:5.5 er [a]

4: 83%, 93.5:6.5 er [c]

5: 76%, 93.5:6.5 er

6: 60%, 93.5:6.5 er [a]

7: 73%, 93:7 er

8: 72%, 93:7 er [b]

9: 56%, 95:5 er [d]

10: 67% [e] 92.5:7.5 er

11: 67% [a] 93:7 er

12: 64% 94.5:5.5 er

13: 55% [f] 94:6 er

14: 81% 93.5:6.5 er

15: 72% [a] 94:6 er

16: 89% 92:8 er

17: 75% 93.5:6.5 er
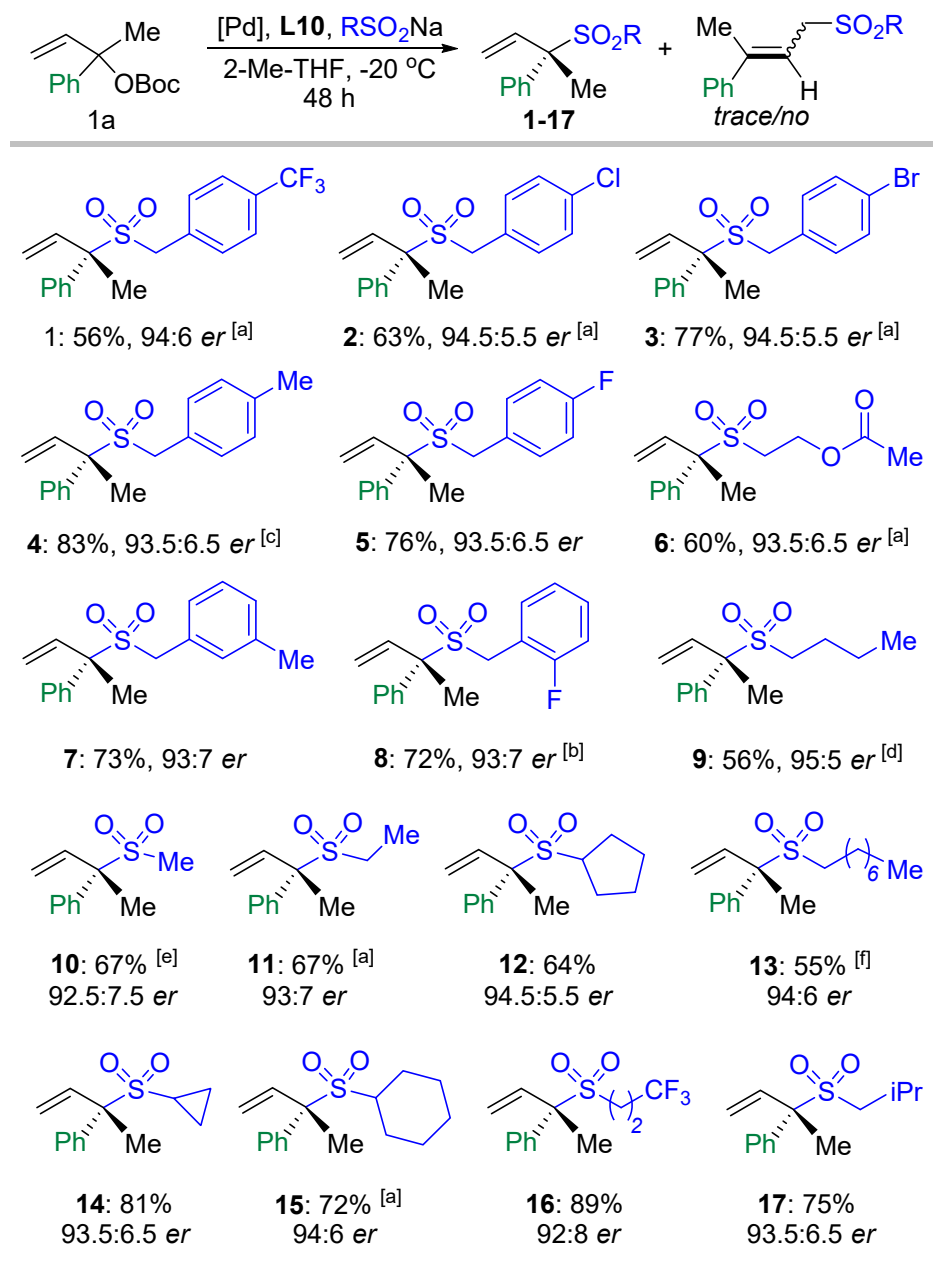
Reactions were performed under the optimized conditions (see **Table 5.3**, entry 10). Isolated yields are reported, and *er* values were determined by SFC (supercritical fluid chromatography). [a] After 72 h. [b] After 60 h. [c] [**Pd**] (2.5 mol %), **L10** (10 mol %), THF (1.0 mL). [d] After 96 h. [e] [**Pd**] (4 mol %), **L10** (12 mol %), 2-Me-THF (0.80 mL). [f] [**Pd**] (5.0 mol %), **L10** (20 mol %), 2-Me-THF (0.80 mL).

5.2.3 Scope of Racemic Tertiary Allylic Carbonates

We then focused on investigating the scope of the tertiary allylic precursors (Table 5.6). The absolute configuration of chiral allylic sulfone **2a** (*S*) was unambiguously confirmed by X-ray analysis (see insert). The reaction leading to product **2a** could be scaled up to 3.0 mmol without any significant erosion of the process outcome (647 mg, 75% yield, 95:5 *er*). The protocol proved to be rather efficient for various other reaction partners, and the use of a wide range of allylic carbonates was feasible providing access to enantioenriched α,α-disubstituted allylic sulfones **18–35** in moderate to good yields along with high levels of regio- and enantioselectivities. Substrates exerting different steric and electronic effects were tolerated with the use of *meta*-substituted α-aryl allylic precursors providing typically better enantiocontrol. The presence of a bulky naphthyl group did not reduce the efficiency of the catalytic protocol (**20**), while the installation of a 1,3-benzodioxole fragment (**22**: 85% yield, 93:7 *er*) of importance in pharmaceutical development[18] was also endorsed.

The developed method was unsatisfactory with tertiary allylic carbonates bearing *ortho*-substituents on the aryl group even at higher reaction temperatures, indicating some (steric) limitation of the present methodology. Alkyl substituted carbonates also seem to be suitable reaction partners as demonstrated by the preparation of **24** (67%) although with substantial lower enantioselectivity (64.5:35.5 *er*). When the Me substituent in the allylic precursor was replaced by an Et or *i*Pr group, exclusive formation of a linear allylic sulfone product was observed in 47% and 34% yield, respectively.

(18) a) J. D. Bloom, M. D. Dutia, B. D. Johnson, A. Wissner, M. G. Burns, E. E. Largis, J. A. Dolan, T. H. Claus, *J. Med. Chem.* **1992**, *35*, 3081; b) A. Ali, J. Wang, R. S. Nathans, H. Cao, N. Sharova, M. Stevenson, T. M. Rana, *ChemMedChem* **2012**, *7*, 1217.

Table 5.6 The scope of products attained by varying the tertiary allylic precursor.

2a: 82%, 95:5 *er*

18: 63%, 94:6 *er* [c]

19: 77%, 89:11 *er*

20: 80% 91:9 *er*

21: 76%[a] 93:7 *er*

22: 85%, 93:7 *er*

23: 80%, 93.5:6.5 *er*

24: 67% [a] 64.5:35.5 *er*

25: 71% [a] 94.5:5.5 *er*

26: 48% [a] 93:7 *er*

27: 80% [a] 94:6 *er*

28: 66% [b] 95:5 *er*

29: 45% [c] 93.5:6.5 *er*

30: 63% [a] 94:6 *er*

31: R = F; 63%, 88:12 er [a]
32: R = CF$_3$; 56%, 86:14 *er*

33: 69% 84:16 *er*

34: 52% [c] 93:7 *er*

35: 75% 91.5:8.5 *er*
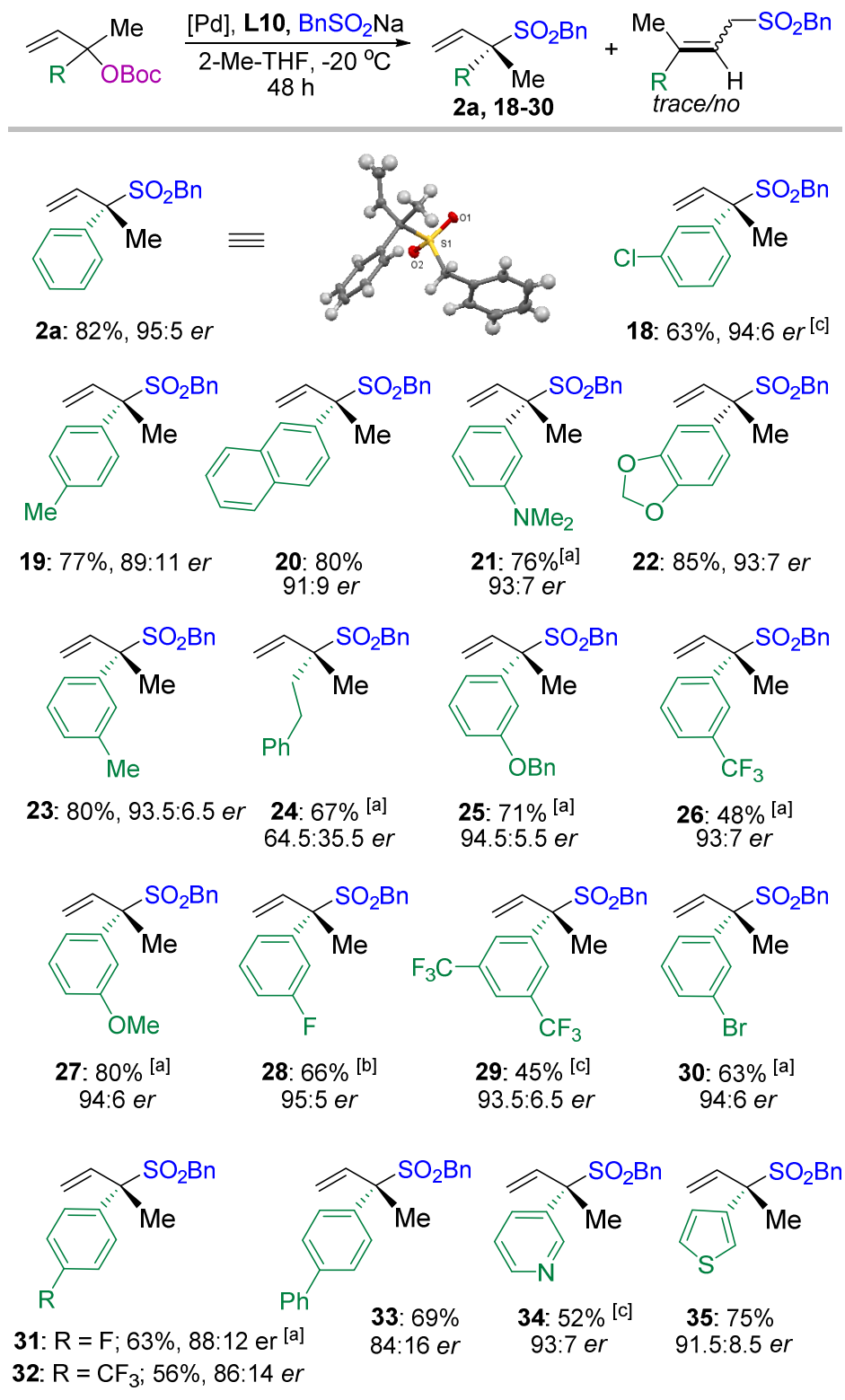
Reactions were performed under the optimized conditions (**Table 5.3**, entry 10). Isolated yields are reported, and *er* values were determined by SFC. [a] After 72 h. [b] After 60 h. [c] After 96 h.

5.2.4 Scope of Sodium Arylsulfinates

Table 5.7 Examination of various arylsulfinate reagents.
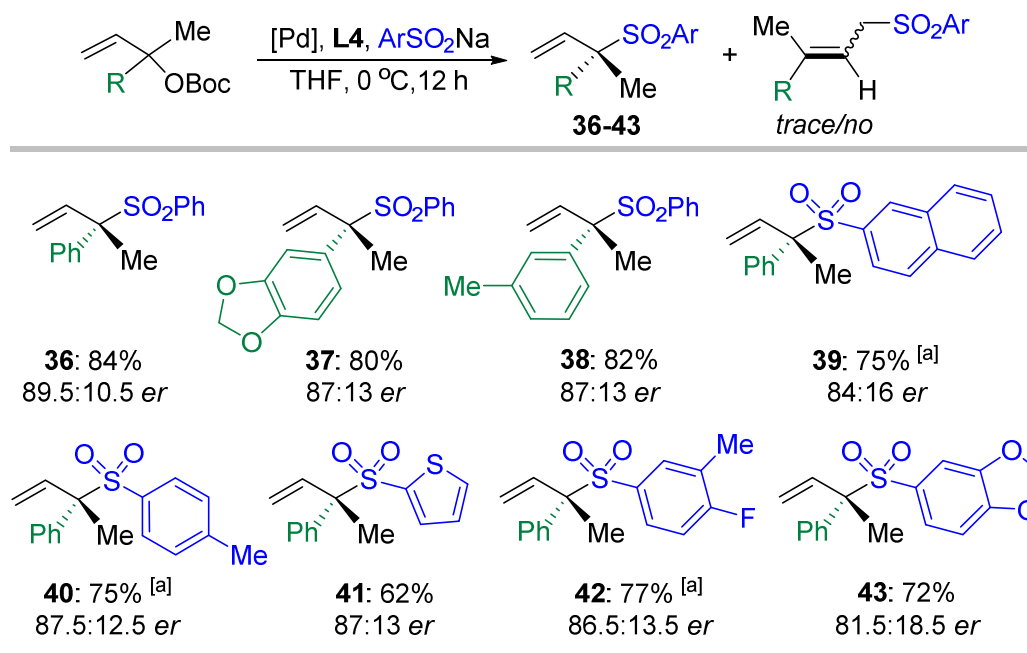
Reaction conditions: allylic precursor (0.15 mmol), arylsulfonate (0.18 mmol, 1.2 equiv.), [**Pd**] (2.5 mol %), **L4** (10 mol %), THF (0.4 mL), 0 ºC, open to air, 12 h. Isolated yields are reported, and *er* values were determined by SFC. [a] arylsulfinate (0.23 mmol, 1.5 equiv.), [**Pd**] (4 mol %), **L4** (16 mol %).

Encouraged by the asymmetric synthesis of various **alkyl** allylic sulfones, the regio- and enantioselective synthesis of α,α-disubstituted **aryl** allylic sulfones was then probed (Table 5.7). By re-optimization of the reaction conditions (see Table 5.4), a series of arylsulfonate nucleophiles and tertiary allylic carbonates were successfully employed in our process by using phosphoramidite ligand **L4**, giving access to allylic sulfones **36–43**. Notably, the introduction of bulky naphthyl and heteroaryl groups could be accomplished (**39**, **41** and **43**) and the chiral sulfones were isolated in good yields and with appreciable enantioselectivity.

5.2.5 Synthetic Transformations of Allylic Sulfone (2a)
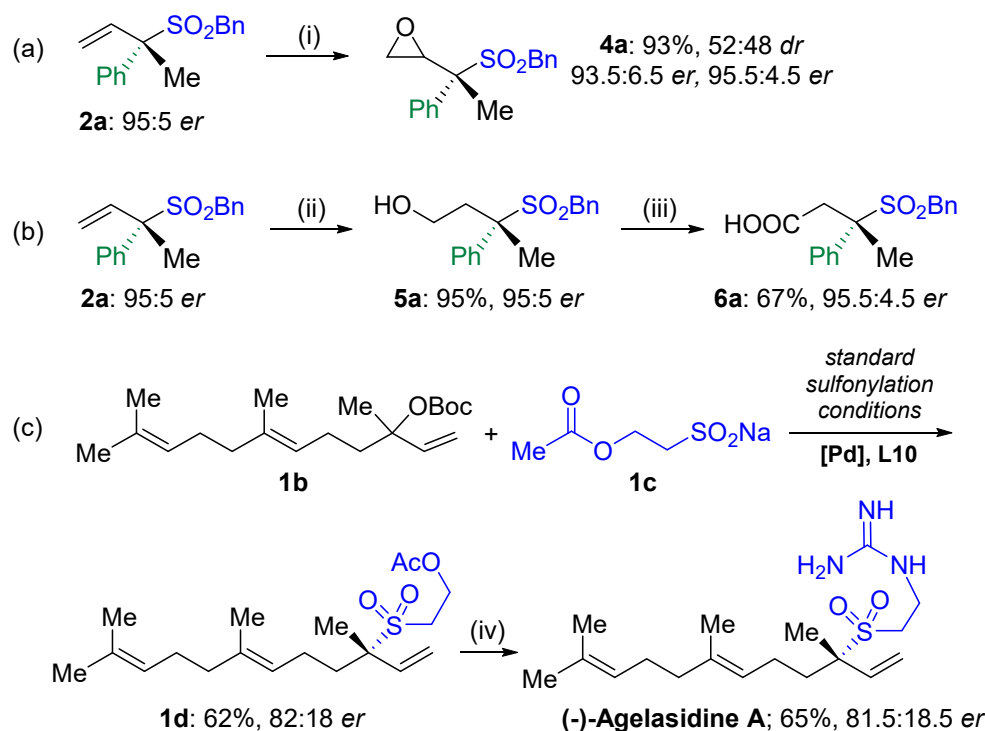
Reaction conditions: (i) m-CPBA (4.0 equiv.), DCM. (ii) 9-BBN (3.0 equiv.), THF, 60 ºC to r.t., then EtOH, NaOH, H_2O_2 (30%). (iii) PhI(OAc)$_2$ (2.0 equiv.), TEMPO (30 mol %), CH_3CN/H_2O (1:1). (iv) NaH, EtOH, NH$_2$C(=NH)NH$_2$·HCl, 1,4-dioxane, r.t.; see the Experimental Section for more details.

Scheme 5.11. Synthetic transformations carried out with allylic sulfone **2a** (a and b), and the formal synthesis of (−)-Agelasidine A (c).

Synthetic transformations of allylic sulfone **2a** were performed to demonstrate the utility of the newly developed building blocks. Oxidation of **2a** with 3-chloroperbenzoic acid smoothly led to epoxide **4a** in 93% yield while retaining the enantiopurity (Scheme 5.11a). Hydroboration of **2a** with 9-borabiclo-(3.3.1)nonane (9-BBN) and oxidative work-up furnished γ-sulfonyl alcohol **5a**, which upon oxidation by PhI(OAc)$_2$ and TEMPO gave γ-sulfonyl acid **6a** in 67% yield (Scheme 5.11b, 95.5:4.5 *er*). In addition, we focused on the formal synthesis of (-)-Agelasidine A, which is a natural sesquiterpene that was isolated from marine sponges of the genus *Agelas* and has antifungal and antimicrobial activity.[19] To achieve the synthesis of this target molecule using allylic sulfonylation as a key step, treatment of allylic carbonate **1b** with alkylsulfinate **1c** under

(19) H. Nakamura, H. Wu, J. Kobayashi, Y. Ohizumi, Y. Hirata, T. Higashijima, T. Miyazawa, *Tetrahedron Lett.* **1983**, *24*, 4105.

the optimized reaction conditions was performed. The enantioenriched allylic sulfone **1d** was isolated in 62% yield (82:12 *er*). Following a previous report,[20] (−)-Agelasidine A could be obtained in 65% yield from sulfone **1d** in the presence of excess guanidine.

5.3 Conclusions

In summary, we present herein the first general regio- and enantioselective synthesis of α,α-allylic sulfones featuring quaternary stereocenters based on Pd-catalyzed allylic sulfonylation. Crucial in the developed protocol is the presence of a new phosphoramidite ligand **L10** that is able to overcome simultaneously the intrinsic challenge of achieving both high regio- and enantio-control. The ligand optimization studies illustrate the delicate balance between the location of the steric impediment and its influence on the reaction outcome. Our methodology is characterized by a wide scope of chiral allylic sulfone scaffolds, excellent regio-selectivity and high enantio-induction, and user-friendly conditions. The formal synthesis of (−)-Agelasidine A supports the view that these chiral allylic sulfones hold great promise as synthetic building blocks, amplifying the repertoire of nucleophiles in challenging allylic substitution reactions.

---

(20) a) Y. Ichikawa, *Tetrahedron Lett.* **1988**, *29*, 4957; b) Y. Ichikawa, T. Kashiwagi, N. Urano, *J. Chem. Soc., Chem. Commun*. **1989**, 987; c) Y. Ichikawa, T. Kashiwagi, N. Urano, *A. J. Chem. Soc., Perkin Trans. 1* **1992**, *1*, 1497.

5.4 Experimental Section

5.4.1 General Considerations

Commercially available sulfonyl chlorides and solvents were purchased from Aldrich, TCI or Fluorochem, and used without further purification. The palladium precursors were purchased from Aldrich. Phosphoramidites **L1**, **L3** and **L22** were purchased from Aldrich; **L4**, **L16**, **L19**, **L23** and **L33** were purchased from Strem; **L2**,[21] **L11-L15**,[21] **L18**,[21] **L20-L21**,[21] **L24-L30**,[21] **L5-L10**,[22] **L17**[22] and **L31-L32**[22] were prepared according to previously reported protocols. ^{1}H NMR, ^{13}C NMR, ^{31}P NMR and ^{19}F NMR spectra were recorded at room temperature on a Bruker AV-400 or AV-500 spectrometer and referenced to the residual deuterated solvent signals. All reported NMR values are given in parts per million (ppm). FT-IR spectra were collected using a Bruker Optics FTIR Alpha spectrometer. Optical rotations were measured with a Jasco P-1030 Polarimeter. Mass spectrometric analyses, SFC (supercritical fluid chromatography) analyses, and X-ray diffraction studies were performed by the Research Support Area (RSA) at ICIQ.

5.4.2 General Procedure for the Preparation of Sodium Sulfinates

$$R\text{-}SO_2Cl \xrightarrow[\text{H}_2\text{O, 70-80 °C, 4 h}]{\text{Na}_2\text{SO}_3,\ \text{NaHCO}_3} R\text{-}SO_2Na$$
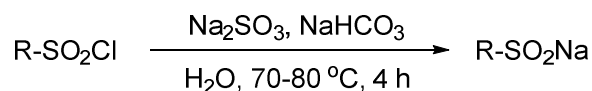
Sodium sulfinates were prepared according to a method reported in the literature.[23] Sodium sulfite (20 mmol), sodium bicarbonate (20 mmol) and the corresponding sulfonyl chloride (10 mmol) were dissolved in 10 mL of H_2O. After stirred at 70 °C or 80 °C for 4 h, the water was removed by a rotary evaporator. Then the remaining solid was extracted and recrystallized from ethanol to get the desired sodium sulfonate.

(21) A. Mercier, W. C. Yeo, J. Chou, P. D. Chaudhuri, G. Bernardinelli, E. P. Kündig, *Chem. Commun.* **2009**, 5227.
(22) B. Zhao, H. Du, R. Fu, Y. Shi, *Org. Synth.* **2010**, *87*, 263.
(23) B. Du, P. Qian, Y. Wang, H. Mei, J. Han, Y. Pan, *Org. Lett.* **2016**, *18*, 4144.

5.4.3 Procedure for the Synthesis of Phosphoramidite Ligands

Method A *(preparation of L2, L11-L15, L18, L20-L21, L24-L30):*
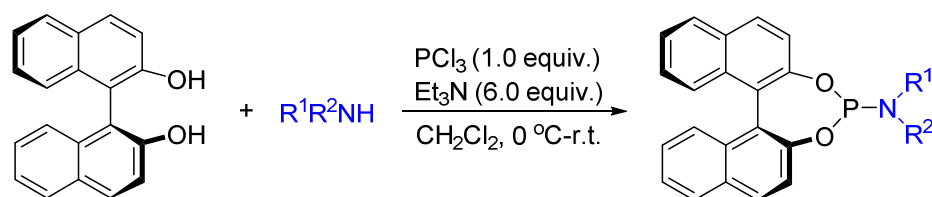
Distilled PCl$_3$ (90 µL, 1.03 mmol) was added to a solution of freshly distilled Et$_3$N (0.84 mL, 6.03 mmol) in CH$_2$Cl$_2$ (7.5 mL) at 0 °C and stirred for 0.5 h at this temperature. Then, the secondary amine (1 mmol) was added at 0 °C and stirred for 4 h at room temperature. (r.t.). The mixture was cooled to 0 °C, then (*S*)-BINOL (440 mg, 1 mmol) was added and the reaction was stirred overnight at r.t. The reaction mixture was diluted with CH$_2$Cl$_2$ (50 mL) and washed with H$_2$O. The organic layer was dried (Na$_2$SO$_4$) and concentrated. The residue was purified by flash chromatography on silica gel (CH$_2$Cl$_2$/hexane, 1:20) to afford ligand **L** as white foamy solid.

Method B *(preparation of L5-L10, L17 and L31-L32):*
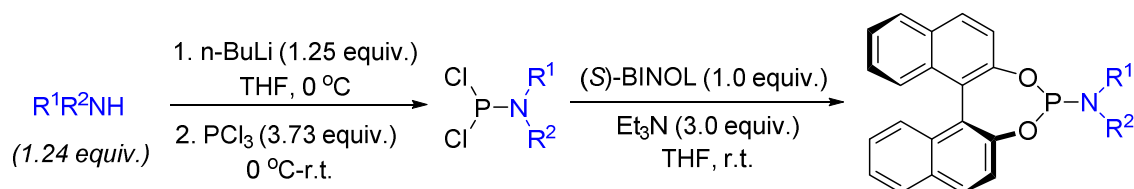
A 250-mL, two-necked, round-bottomed flask equipped with a Teflon-coated magnetic stir bar (length: 3.5 cm), internal thermometer, nitrogen inlet, and rubber septum is charged with secondary amine (29.5 mmol, 1.24 equiv.) and anhydrous THF (47.2 mL). The solution was cooled to 5 °C in an ice bath, treated with *n*-BuLi (19.5 mL, 29.8 mmol, 1.53 M in hexanes, 1.25 equiv.) using syringe addition over 5 min, and stirred at 0 °C for 30 min. To this solution was added phosphorus trichloride (PCl$_3$) (7.75 mL, 88.8 mmol, 3.73 equiv.) at such a rate as to keep the internal temperature below 10 °C (*ca.* 30 min.). After complete addition of PCl$_3$, the ice bath was removed, and the brown reaction mixture was stirred for 1 h and concentrated by rotary evaporation (25 °C, 55 mm Hg). The resulting residue was dissolved in THF (50.0 mL) and cooled to 5 °C in an ice bath. A solution of (*S*)-BINOL (7.08 g, 23.8 mmol, 1.00 equiv.) and Et$_3$N (10.1 mL, 71.4 mmol, 3.00 equiv.) in THF (17.8 mL) was added by a syringe pump over 15 min. The ice bath was subsequently removed. The reaction mixture was stirred for 20 h and concentrated

by rotary evaporation (25 °C, 18 mmHg). The resulting residue was dissolved in CH$_2$Cl$_2$ (60 mL) and the mixture was vacuum filtered. The solid was washed with CH$_2$Cl$_2$ (3 × 20 mL), the organic layer was dried (Na$_2$SO$_4$) and concentrated. The residue was purified by flash chromatography on silica gel (EA/hexane, 1:50) to afford ligand (S)-**L** as a white or pale yellow foamy solid.

5.4.4 Typical Procedure for the Synthesis of Allylic Sulfones
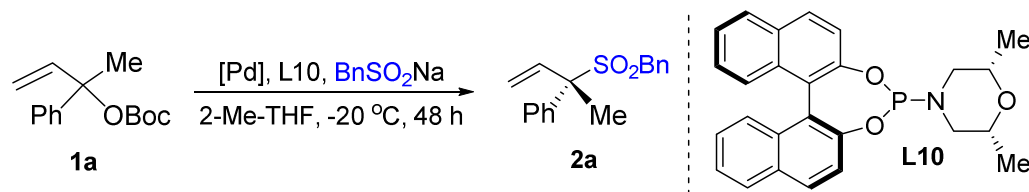
Representative case: To a screw-capped vial equipped with a magnetic stirring bar, Boc-protected allylic carbonate **1a** (0.15 mmol, 37 mg, 1.5 equiv.), Pd$_2$(dba)$_3$·CHCl$_3$ (3.64 mg, 3.5 mol %), **L10** (4.3 mg, 10.0 mol %), sodium benzylsulfinate (0.10 mmol, 17.8 mg, 1.0 equiv.) and 2-Me-THF (1.0 mL) were added. The resulting mixture was stirred at -20 °C for 48 h, and then the reaction mixture was warmed to room temperature, after which the product was purified by flash column chromatography on silica gel (hexane/ethyl acetate (EA) = 20:1) to afford the pure allylic sulfone **2a**. The enantiomeric excess of the product was determined by SFC equipped with a chiral column.

5.4.5 Procedures for Transformation of Chiral Allylic Sulfone (2a)
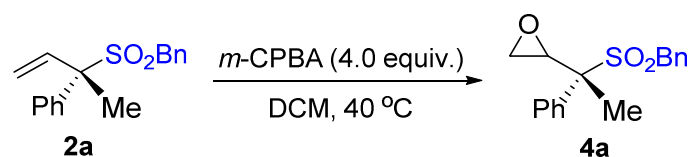
4a was prepared following a previously reported procedure:[24] To a vial equipped with a magnetic stirring bar, allylic sulfone **2a** (28.6 mg, 0.1 mmol) and *m*-CPBA (89 mg, 4.0 equiv., considering a 30% water content in the reagent) was added in dichloromethane (0.5 mL). The resulting reaction mixture was kept while stirring at 40 °C until the signal of the double bond in the ^{1}H NMR spectrum had disappeared (about 36 h, followed by NMR). The reaction mixture was then diluted with diethyl ether and water. The organic layer was separated and the aqueous layer was extracted by diethyl ether (3 × 5 mL). Then,

---

(24) G. Asensio, R. Mello, C. Boix-Bernardini, M. E. González-Núñez, G. Castellano, *J. Org. Chem.* **1995**, *60*, 3692.

the combined organic layers were dried over Na$_2$SO$_4$, filtered, and then concentrated under vacuum. The crude reaction mixture was purified by flash chromatography (hexane/EA = 15:1) to afford the pure epoxide **4a** (28 mg, 93%, 52:48 *dr*, 93.5:6.5 *er*, 95.5:4.5 *er*) as a white solid.
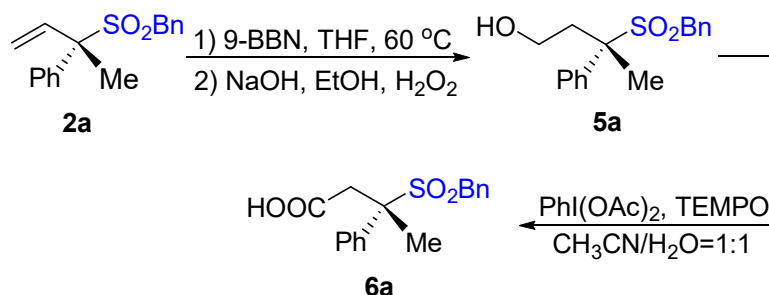
The synthesis of **5a** was performed according to a literature procedure[25] but with small modifications: to a solution of allylic sulfone **2a** (28.6 mg, 0.1 mmol) in THF (0.3 mL) was added 9-BBN (0.5 M in THF, 0.4 mL, 0.2 mol, 2.0 equiv.) at room temperature and the solution was stirred at 60 ºC for 5 h until no starting material (**1a**) was detected by ^{1}H NMR. Then the reaction mixture was warmed to room temperature, and aqueous NaOH solution (5.0 M, 0.5 mL, 2.5 mmol), EtOH (0.5 mL), and H$_2$O$_2$ (30% in H$_2$O, 0.5 mL) were added to the above-mentioned mixture, which was stirred at room temperature overnight, diluted with brine (5 mL) and extracted with ethyl acetate (3 × 5 mL). The combined organic phase was dried over Na$_2$SO$_4$, filtered, concentrated under vacuum and purified by flash chromatography (hexane/EA=2:1) to afford the pure *γ*-sulfonyl alcohol **5a** (29 mg, 95%, 95:5 *er*) as a white solid.

A mixture of **5a** (40 mg, 0.131 mmol), PhI(OAc)$_2$ (85 mg, 0.262 mmol, 2.0 equiv.), and TEMPO (6.11 mg, 0.0393 mmol, 0.3 equiv.) was stirred in CH$_3$CN/H$_2$O (1:1, 0.6 mL) at room temperature overnight. The solution was extracted with ethyl acetate, the organic phase was extracted with aq. NaHCO$_3$. The aqueous solution was acidified to pH 1 using 1 N HCl, and then extracted with ethyl acetate. The combined organic phases were dried over MgSO$_4$ and concentrated under vacuum. The crude product was purified by flash chromatography (hexane/EA=1:1) to afford the pure *γ*-sulfonyl acid **6a** (25 mg, 67%, 95.5:4.5 *er*) as a white solid.

---

(25) V. Khakyzadeh, Y. -H, Wang, B. Breit, *Chem. Commun.* **2017**, *53*, 4966.
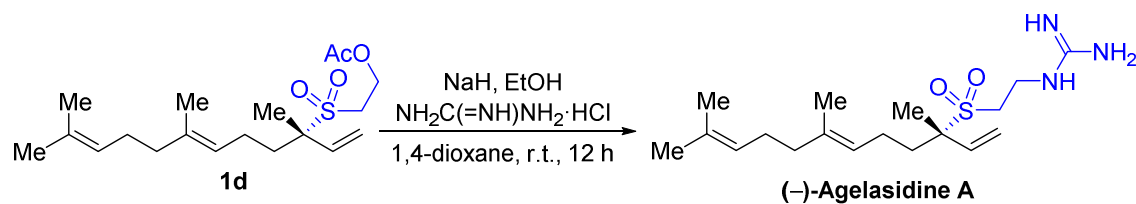
Synthesis of (–)-Agelasidine A: following a reported procedure,[26] sodium hydride (358 mg, 9.0 mmol, 60% dispersion in mineral oil) was treated with EtOH (6 ml) at 0 ºC under a nitrogen atmosphere. To this solution was added guanidine hydrochloride (856 mg, 9.0 mmol) at room temperature. After the mixture had been stirred for 1 h, a white precipitate was observed. The solution was filtered under a nitrogen atmosphere, and then concentrated under reduced pressure. The resulting guanidine-based product was dissolved in a mixture of 1,4-dioxane (3 mL) and water (3 mL). The solution was cooled to 0 ºC and a solution of compound **1d** (80 mg, 0.224 mmol) in 1,4-dioxane (3 mL) was added dropwise over the course of 1 h by a programmable syringe pump. The mixture was stirred overnight at room temperature, after which the 1,4-dioxane was evaporated off and water was added to the residual oil. The aqueous layer was neutralized with 6 N hydrochloric acid and then extracted with DCM. The combined organic phase was dried over Na_2SO_4 and concentrated under reduced pressure. The residual oil was purified by column chromatography (DCM/MeOH = 10:1) to obtain (–)-Agelasidine A (52 mg, 65%, 81.5:18.5 *er*) as a yellow oil.

(26) Y. Ichikawa, T. Kashiwagi, N. Urano, *J. Chem. Soc., Perkin Trans. 1*, **1992**, 1497.

5.4.6 Analytical Data for All Compounds

Characterization data for non-reported starting materials:
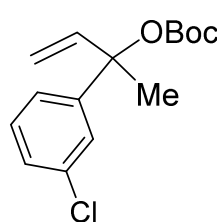
White oil; Column conditions: Hexane : EA = 100:1, R_f = 0.14. **^{1}H NMR** (500 MHz, CDCl$_3$): δ 7.38 (t, *J* = 2.1 Hz, 1H), 7.29–7.25 (m, 2H), 7.25–7.21 (m, 1H), 6.29 (dd, *J* = 17.5, 10.7 Hz, 1H), 5.32–5.27 (m, 2H), 1.85 (s, 3H), 1.43 (s, 9H) ppm. **^{13}C NMR** (126 MHz, CDCl$_3$): δ 151.47, 146.07, 140.48, 134.36, 129.64, 127.50, 125.58, 123.39, 115.74, 83.19, 82.14, 27.84, 25.79 ppm. **IR** (neat): ν = 2981, 1743, 1773, 1369, 1280, 1255, 1155, 786, 699 cm^{-1}. **HRMS** (ESI+, MeOH): *m/z* calcd. 305.0915 (M + Na)$^+$, found: 305.0925.
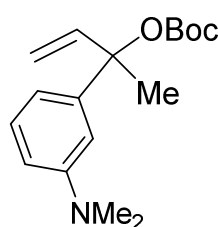
Yellow oil, Column conditions: Hexane : EA = 100:1, R_f = 0.1. **^{1}H NMR** (400 MHz, CDCl$_3$): δ 7.25 (t, *J* = 8.5 Hz, 1H), 6.82–6.76 (m, 2H), 6.69 (dd, *J* = 8.3, 2.4 Hz, 1H), 6.45 (dd, *J* = 17.5, 10.8 Hz, 1H), 5.40–5.28 (m, 2H), 2.98 (s, 6H), 1.92 (s, 3H), 1.48 (s, 9H) ppm. **^{13}C NMR** (101 MHz, CDCl$_3$): δ 151.48, 150.51, 144.67, 141.20, 128.88, 114.77, 113.36, 111.58, 109.11, 84.01, 81.40, 40.57, 27.80, 26.03 ppm. **IR** (neat): ν = 2983, 1737, 1586, 1368, 1280, 1254, 1159, 1103, 783, 694 cm^{-1}. **HRMS** (ESI+, MeOH): *m/z* calcd. 292.1907 (M + Na)$^+$, found: 292.1911.
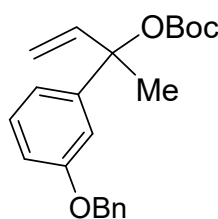
Pink solid, Column conditions: Hexane : EA = 100:1, R_f = 0.08. **^{1}H NMR** (500 MHz, CDCl$_3$): δ 7.51–7.46 (m, 2H), 7.45–7.40 (m, 2H), 7.36 (t, *J* = 7.3 Hz, 1H), 7.31 (t, *J* = 8.0 Hz, 1H), 7.13–7.09 (m, 1H), 7.08–7.04 (m, 1H), 6.92 (ddd, *J* = 8.2, 2.5, 0.8 Hz, 1H), 6.40 (dd, *J* = 17.4, 10.8 Hz, 1H), 5.38–5.30 (m, 2H), 5.08 (s, 2H), 1.92 (s, 3H), 1.49 (s, 9H) ppm. **^{13}C NMR** (126 MHz, CDCl$_3$): δ 158.81, 151.47, 145.56, 140.89, 136.96, 129.30, 128.53, 127.93, 127.55, 117.68, 115.07, 113.17, 112.29, 83.55, 81.63, 69.96, 27.78, 25.76 ppm. **IR** (neat): ν = 2978, 1744, 1582, 1368, 1277, 1253, 1153, 1075, 783, 698 cm^{-1}. **HRMS** (ESI+, MeOH): *m/z* calcd. 377.1723 (M + Na)$^+$, found: 377.1717.
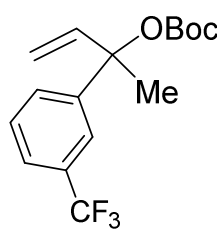
White oil; Column conditions: Hexane : EA = 100:1, R_f = 0.14. **^{1}H NMR** (400 MHz, CDCl$_3$): δ 7.64 (s, 1H), 7.55 (dd, J = 16.5, 7.7 Hz, 2H), 7.46 (t, J = 7.8 Hz, 1H), 6.38–6.28 (m, 1H), 5.36–5.28 (m, 2H), 1.88 (s, 3H), 1.42 (s, 9H) ppm. **^{19}F NMR** (376 MHz, CDCl$_3$): δ -62.71 ppm. **^{13}C NMR** (101 MHz, CDCl$_3$): δ 151.53, 145.17, 140.40, 130.84 (q, J = 32 Hz), 128.91, 128.63, 124.26 (q, J = 273 Hz), 124.24 (q, J = 4 Hz), 122.12 (q, J = 4 Hz), 116.11, 83.29, 82.36, 27.83, 25.99 ppm. **IR** (neat): ν = 2982, 1744, 1370, 1330, 1278, 1255, 1158, 1124, 857, 804, 704 cm^{-1}. **HRMS** (ESI+, MeOH): m/z calcd. 339.1178 (M + Na)$^+$, found: 339.1175.
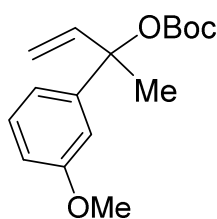
Yellow oil; Column conditions: Hexane : EA = 100:1, R_f = 0.15. **^{1}H NMR** (400 MHz, CDCl$_3$): δ 7.25 (t, J = 8.0 Hz, 1H), 7.00–6.92 (m, 2H), 6.80 (ddd, J = 8.2, 2.6, 0.8 Hz, 1H), 6.34 (dd, J = 17.5, 10.8 Hz, 1H), 5.32–5.24 (m, 2H), 3.79 (s, 3H), 1.86 (s, 3H), 1.42 (s, 9H) ppm. **^{13}C NMR** (101 MHz, CDCl$_3$): δ 159.63, 151.54, 145.58, 140.95, 129.34, 117.47, 115.17, 112.50, 111.20, 83.66, 81.77, 55.21, 27.85, 25.88 ppm. **IR** (neat): ν = 2977, 1740, 1582, 1368, 1268, 1156, 1096, 1046, 955, 873, 785, 704 cm^{-1}. **HRMS** (ESI+, MeOH): m/z calcd. 301.1410 (M + Na)$^+$, found: 301.1408.
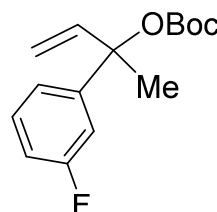
White solid; Column conditions: Hexane : EA = 100:1, R_f = 0.14. **^{1}H NMR** (400 MHz, CDCl$_3$): δ 7.30 (td, J = 8.0, 6.0 Hz, 1H), 7.16 (dd, J = 8.2, 1.3 Hz, 1H), 7.10 (dt, J = 10.4, 2.2 Hz, 1H), 6.99–6.91 (m, 1H), 6.31 (dd, J = 17.5, 10.8 Hz, 1H), 5.29 (m, 2H), 1.85 (s, 3H), 1.42 (s, 9H) ppm. **^{19}F NMR** (376 MHz, CDCl$_3$): δ -113.00 ppm. **^{13}C NMR** (101 MHz, CDCl$_3$): δ 162.93 (d, J = 246 Hz), 151.54, 146.69 (d, J = 7 Hz), 140.60, 129.89 (d, J = 8 Hz) 120.85 (d, J = 3 Hz), 115.67, 114.27 (d, J = 21 Hz), 112.59 (d, J = 23 Hz), 83.25, 82.15, 27.88, 25.84 ppm. **IR** (neat): ν = 2983, 1737, 1586, 1368, 1280, 1254, 1159, 1103, 1086, 829, 783, 694 cm^{-1}. **HRMS** (ESI+, MeOH): m/z calcd. 289.1210 (M + Na)+, found: 289.1202.
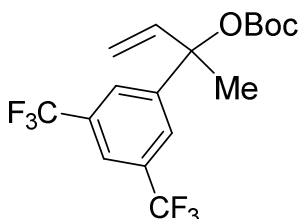
Yellow oil; Column conditions: Hexane : EA = 100:1, R_f = 0.14. **^{1}H NMR** (400 MHz, CDCl$_3$): δ 7.29 (d, J = 8.4 Hz, 1H), 7.23 (d, J = 2.2 Hz, 1H), 7.14 (dd, J = 8.4, 2.2 Hz, 1H), 6.30 (dd, J = 17.5, 10.7 Hz, 1H), 5.31–5.25 (m, 2H), 2.37 (s, 3H), 1.84 (s,

3H), 1.43 (s, 9H) ppm. ^{19}**F NMR** (376 MHz, CDCl$_3$): δ -63.05 ppm. ^{13}**C NMR** (101 MHz, CDCl$_3$): δ 151.46, 147.06, 139.61, 131.88 (q, J = 33 Hz), 125.59, 123.47 (q, J = 274 Hz), 121.43, 117.06, 82.84, 82.76, 27.75, 26.03 ppm. **IR** (neat): ν = 2985, 1745, 1372, 1275, 1130, 1002, 899, 792, 682 cm^{-1}. **HRMS** (ESI+, MeOH): m/z calcd. 407.1052 (M + Na)$^+$, found: 407.1049.
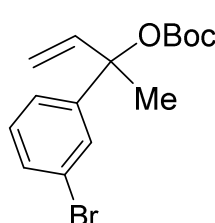
Yellow oil; Column conditions: Hexane : EA = 100:1, R_f = 0.1. ^{1}**H NMR** (400 MHz, CDCl$_3$): δ 7.53 (t, J = 1.9 Hz, 1H), 7.38 (d, J = 7.8 Hz, 1H), 7.30 (m, 1H), 7.22–7.17 (m, 1H), 6.29 (dd, J = 17.5, 10.8 Hz, 1H), 5.33–5.26 (m, 2H), 1.84 (s, 3H), 1.42 (s, 9H) ppm. ^{13}**C NMR** (101 MHz, CDCl$_3$): δ 151.44, 146.29, 140.44, 130.42, 129.91, 128.43, 123.84, 122.57, 115.75, 83.09, 82.10, 27.83, 25.80 ppm. **IR** (neat): ν = 2980, 1743, 1394, 1368, 1279, 1155, 1106, 852, 784, 699 cm^{-1}. **HRMS** (ESI+, MeOH): m/z calcd. 349.0410 (M + Na)$^+$, found: 349.0407.
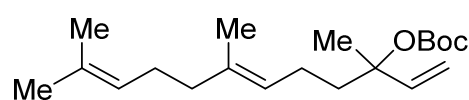
White oil; Column conditions: Hexane : EA = 100:1, R_f = 0.14. ^{1}**H NMR** (500 MHz, CDCl$_3$): δ 6.02 (dd, J = 17.6, 11.0 Hz, 1H), 5.19–5.12 (m, 2H), 5.11–5.05 (m, 2H), 2.06–1.94 (m, 6H), 1.83 (ddt, J = 8.8, 5.7, 2.6 Hz, 2H), 1.67 (s, 3H), 1.58 (d, J = 4.3 Hz, 6H), 1.53 (s, 3H), 1.46 (s, 9H) ppm. ^{13}**C NMR** (126 MHz, CDCl$_3$): δ 152.04, 141.82, 135.60, 131.43, 124.43, 123.72, 113.62, 83.67, 81.42, 39.79, 39.70, 27.98, 26.80, 25.80, 23.53, 22.39, 17.79, 16.05 ppm. **IR** (neat): ν = 2978, 2927, 1738, 1368, 1281, 1253, 1159, 1102, 854, 793 cm^{-1}. **HRMS** (ESI+, MeOH): m/z calcd. 345.2400 (M + Na)$^+$, found: 345.2399.
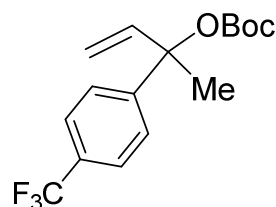
Yellow oil, Column conditions: Hexane : EA = 100:1, R_f = 0.16. ^{1}**H NMR** (400 MHz, CDCl$_3$): δ 7.60 (d, J = 8.3 Hz, 2H), 7.50 (d, J = 8.2 Hz, 2H), 6.37–6.28 (m, 1H), 5.34–5.28 (m, 2H), 1.87 (s, 3H), 1.42 (s, 9H) ppm. ^{19}**F NMR** (376 MHz, CDCl$_3$): δ -62.65 ppm. ^{13}**C NMR** (101 MHz, CDCl$_3$): δ 151.55, 148.01, 140.39, 129.62 (q, J = 32.3 Hz), 125.60, 125.44 (q, J = 3.0 Hz), 124.25 (q, J = 273.7 Hz), 116.05, 83.27, 82.37, 27.88, 25.91 ppm. **IR** (neat): ν = 2983, 1744, 1326, 1278, 1255, 1159, 1123, 1078, 1015, 838, 609 cm^{-1}. **HRMS** (ESI+, MeOH): m/z calcd. 339.1178 (M + Na)$^+$, found: 339.1165.
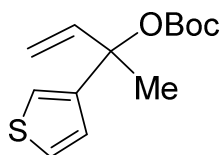
Yellow oil, Column conditions: Hexane : EA = 100:1, R_f = 0.13. **¹H NMR** (500 MHz, CDCl₃): δ 7.24 (dd, J = 5.0, 3.0 Hz, 1H), 7.17 (dd, J = 3.0, 1.4 Hz, 1H), 7.04 (dd, J = 5.1, 1.4 Hz, 1H), 6.30 (dd, J = 17.5, 10.7 Hz, 1H), 5.23–5.19 (m, 2H), 1.88 (s, 3H), 1.40 (s, 9H) ppm. **¹³C NMR** (126 MHz, CDCl₃): δ 151.56, 144.89, 141.06, 126.01, 125.75, 121.04, 114.63, 82.02, 81.78, 27.86, 25.71 ppm. **IR** (neat): ν = 2979, 1742, 1368, 1276, 1252, 1152, 1095, 841, 789, 649 cm⁻¹. **HRMS** (ESI+, MeOH): m/z calcd. 277.0869 (M + Na)⁺, found: 277.0860.
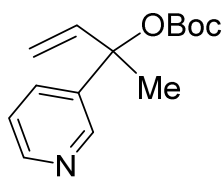
Brown oil, Column conditions: Hexane : EA = 100:1, R_f = 0.15. **¹H NMR** (500 MHz, CDCl₃): δ 8.56 (d, J = 2.4 Hz, 1H), 8.42 (dd, J = 4.8, 1.5 Hz, 1H), 7.60 (dt, J = 8.0, 2.0 Hz, 1H), 7.17 (dd, J = 8.0, 4.8 Hz, 1H), 6.22 (dd, J = 17.4, 10.9 Hz, 1H), 5.24–5.18 (m, 2H), 1.80 (s, 3H), 1.32 (s, 9H) ppm. **¹³C NMR** (126 MHz, CDCl₃): δ 151.31, 148.51, 147.10, 140.13, 139.13, 132.86, 122.95, 115.89, 82.17, 82.15, 27.70, 25.56 ppm. **IR** (neat): ν = 2978, 1744, 1582, 1368, 1277, 1253, 1153, 1075, 948, 783, 698 cm⁻¹. **HRMS** (ESI+, MeOH): m/z calcd. 250.1438 (M + Na)⁺, found: 250.1435.
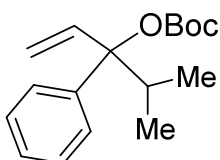
White solid; Column conditions: Hexane : EA = 100:1, R_f = 0.10. **¹H NMR** (400 MHz, CDCl₃): δ 7.42–7.33 (m, 4H), 7.31–7.25 (m, 1H), 6.48 (dd, J = 17.5, 11.2 Hz, 1H), 5.50–5.34 (m, 2H), 2.53 (p, J = 6.8 Hz, 1H), 1.40 (s, 9H), 0.94 (d, J = 6.7 Hz, 3H), 0.80 (d, J = 6.9 Hz, 3H) ppm. **¹³C NMR** (101 MHz, CDCl₃): δ 151.38, 141.30, 136.03, 127.74, 127.10, 126.45, 116.58, 88.05, 81.46, 37.71, 27.78, 17.57 ppm. **IR** (neat): ν = 2982, 1744, 1330, 1278, 1158, 1124, 1072, 857, 804, 704 cm⁻¹. **HRMS** (ESI+, MeOH): m/z calcd. 299.1618 (M + Na)⁺, found: 299.1617.

Characterization data for non-reported phosphoramidite ligands:
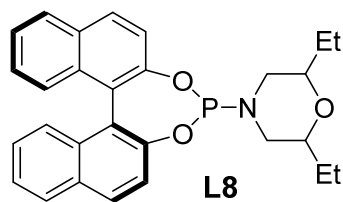
White solid; Column conditions: Hexane : EA = 50:1, R_f = 0.19, $[\alpha]_D^{25}$ = 45.8 (c = 0.1, CHCl$_3$). **^{1}H NMR** (500 MHz, CDCl$_3$): δ 7.98 (d, J = 8.8 Hz, 1H), 7.92 (m, 3H), 7.52 (d, J = 8.8 Hz, 1H), 7.42 (m, 4H), 7.34 (d, J = 8.5 Hz, 1H), 7.29–7.24 (m, 2H), 3.32–3.12 (m, 4H), 2.54–2.44 (m, 1H), 2.35 (dd, J = 22.9, 5.2 Hz, 1H), 1.46–1.34 (m, 2H), 1.24 (dq, J = 13.9, 6.7, 6.2 Hz, 2H), 0.82 (t, J = 7.6 Hz, 3H), 0.76 (t, J = 7.5 Hz, 3H) ppm. **^{31}P NMR** (202 MHz, CDCl$_3$): δ 147.65 ppm. **^{13}C NMR** (126 MHz, CDCl$_3$): δ 149.59, 149.55, 149.45, 132.93, 132.70, 131.53, 130.90, 130.46, 130.03, 128.47, 128.35, 127.09, 127.00, 126.26, 124.96, 124.79, 124.04, 122.84, 122.12, 122.02, 78.35, 78.19, 48.84, 48.70, 26.32, 26.31, 9.71, 9.69 ppm. **IR** (neat): ν = 2932, 1462, 1327, 1236, 1033, 942, 820, 747, 626, 598 cm^{-1}. **HRMS** (ESI+, MeOH): *m/z* calcd. 458.1880 (M + H)$^+$, found: 458.1864.
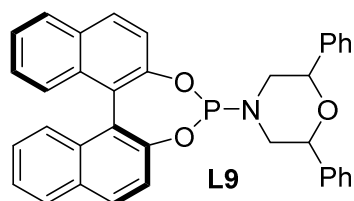
White solid; Column conditions: Hexane : EA = 50:1, R_f = 0.16, $[\alpha]_D^{25}$ = 344.4 (c = 0.11, CHCl$_3$). **^{1}H NMR** (500 MHz, CDCl$_3$): δ 8.01 (dd, J = 8.7, 2.7 Hz, 2H), 7.95 (t, J = 7.2 Hz, 2H), 7.57 (t, J = 9.1 Hz, 2H), 7.48–7.42 (m, 3H), 7.41–7.38 (m, 3H), 7.35–7.26 (m, 5H), 7.25–7.19 (m, 3H), 7.16–7.10 (m, 2H), 4.72 (dd, J = 10.4, 2.1 Hz, 1H), 4.64 (dd, J = 10.5, 2.4 Hz, 1H), 3.61 (t, J = 10.9 Hz, 1H), 3.34 (dd, J = 13.0, 5.5 Hz, 1H), 2.85 (ddd, J = 13.0, 10.6, 6.5 Hz, 1H), 2.74 (ddd, J = 13.9, 10.7, 4.2 Hz, 1H) ppm. **^{31}P NMR** (202 MHz, CDCl$_3$): δ 147.26 ppm. **^{13}C NMR** (126 MHz, CDCl$_3$): δ 149.41, 149.18, 139.62, 139.60, 132.92, 132.84, 131.58, 131.05, 130.60, 130.27, 128.51, 128.48, 128.35, 128.32, 127.99, 127.74, 127.09, 127.07, 126.47, 126.35, 126.19, 125.79, 125.05, 125.00, 123.92, 123.06, 122.04, 121.92, 79.35, 78.74, 50.95, 50.40 ppm. **IR** (neat): ν = 2838, 1589, 1463, 1326, 1229, 1203, 1069, 997, 945, 820, 695, 556 cm^{-1}. **HRMS** (ESI+, MeOH): *m/z* calcd. 554.1880 (M + H)$^+$, found: 554.1880.
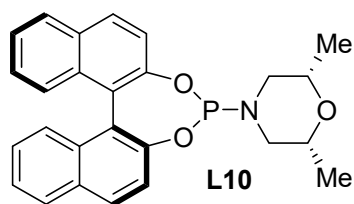
White solid; Column conditions: Hexane : EA = 50:1, R_f = 0.1, $[\alpha]_D^{25}$ = 478.7 (c = 0.1, CHCl$_3$). **^{1}H NMR** (500 MHz, CDCl$_3$): δ 7.97 (d, J = 8.8 Hz, 1H), 7.92 (d, J = 8.5 Hz, 3H), 7.51 (d, J = 8.7 Hz, 1H), 7.46–7.37 (m, 4H), 7.34 (d, J = 8.5 Hz, 1H), 7.31–7.23 (m, 2H), 3.60–3.44 (m, 2H), 3.16–3.11 (m, 2H), 2.52 (ddd, J = 13.9, 10.3, 4.3 Hz, 1H), 2.30 (ddd, J = 13.0, 10.4, 4.9 Hz, 1H), 1.02 (d, J = 6.3 Hz, 3H), 0.97 (d, J = 6.2 Hz, 3H) ppm. **^{31}P NMR** (202 MHz, CDCl$_3$): δ 146.58 ppm. **^{13}C NMR** (126 MHz, CDCl$_3$): δ 149.64, 149.60, 149.37, 132.90, 132.67, 131.53, 130.88, 130.48, 129.98, 128.46, 128.42, 127.10, 127.03, 126.26, 124.99, 124.78, 124.05, 124.01, 122.82, 122.00, 73.04, 72.99, 50.21, 49.63, 18.77, 18.68 ppm. **IR** (neat): ν = 2970, 2840, 1589, 1462, 1323, 1230, 1137, 1086, 1022, 937, 819, 747, 626, 558 cm^{-1}. **HRMS** (ESI+, MeOH): m/z calcd. 430.1567 (M + H)$^+$, found: 430.1562.
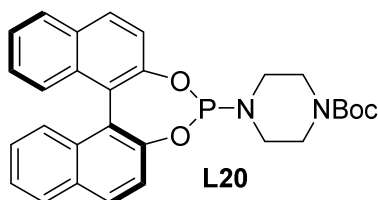
White solid; Column conditions: Hexane : EA = 50:1, R_f = 0.1, $[\alpha]_D^{25}$ = 410.7 (c = 0.12, CHCl$_3$). **^{1}H NMR** (500 MHz, CDCl$_3$): δ 7.98 (d, J = 8.8 Hz, 1H), 7.97–7.92 (m, 2.4 Hz, 3H), 7.52 (d, J = 8.1 Hz, 1H), 7.46–7.37 (m, 4H), 7.34 (d, J = 8.1 Hz, 1H), 7.31–7.23 (m, 2H), 3.28 (s, 4H), 2.97 (d, J = 43.6 Hz, 4H), 1.44 (s, 9H) ppm. **^{31}P NMR** (202 MHz, CDCl$_3$): δ 147.77 ppm. **^{13}C NMR** (126 MHz, CDCl$_3$): δ 154.78, 149.59, 149.55, 149.36, 132.90, 132.69, 131.56, 130.93, 130.51, 130.25, 128.48, 127.08, 127.04, 126.33, 126.30, 125.01, 124.88, 123.99, 123.95, 122.92, 121.95, 80.00, 44.35, 44.20, 28.53, 27.06 ppm. **IR** (neat): ν = 2923, 1692, 1416, 1364, 1231, 1129, 936, 820, 748, 686, 557 cm^{-1}. **HRMS** (ESI+, MeOH): m/z calcd. 523.1757 (M + Na)$^+$, found: 523.1772.
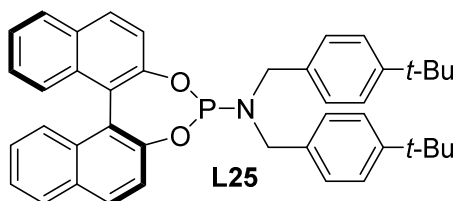
White solid; Column conditions: Hexane : EA = 50:1, R_f = 0.3, $[\alpha]_D^{25}$ = 143.2 (c = 0.11, CHCl$_3$). **^{1}H NMR** (500 MHz, CDCl$_3$): δ 8.05 (d, J = 8.8 Hz, 1H), 7.97 (d, J = 8.1 Hz, 1H), 7.84 (d, J = 8.1 Hz, 1H), 7.79 (d, J = 8.8 Hz, 1H), 7.69 (d, J = 8.7 Hz, 1H), 7.47–7.45 (m, 1H), 7.44 (d, J = 8.2 Hz, 4H), 7.41 (d, J = 4.1 Hz, 1H), 7.40 (d, J = 3.7 Hz, 1H), 7.38–7.35 (m, 1H), 7.32–7.22 (m, 6H), 7.13 (d, J = 8.8 Hz, 1H), 4.22 (dd, J = 14.9, 7.6 Hz, 2H), 3.52 (t, J = 14.0 Hz, 2H), 1.40 (s, 18H) ppm. **^{31}P NMR** (202 MHz, CDCl$_3$): δ 148.37 ppm. **^{13}C NMR** (126

MHz, CDCl$_3$): δ 150.34, 149.90, 149.86, 149.54, 135.08, 133.01, 132.64, 131.56, 130.79, 130.36, 130.15, 128.66, 128.46, 128.25, 127.18, 127.04, 126.18, 125.37, 124.92, 124.70, 124.21, 124.18, 122.33, 121.71, 47.98, 47.82, 34.67, 31.58 ppm. **IR** (neat): ν = 2959, 1950, 1509, 1462, 1361, 1328, 1229, 1068, 947, 819, 747, 556 cm^{-1}. **HRMS** (ESI+, MeOH): *m/z* calcd. 646.2845 (M + Na)$^+$, found: 646.2841.
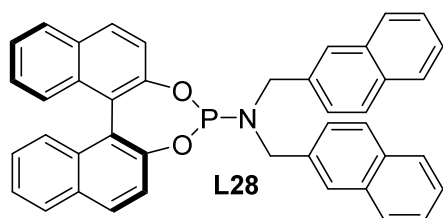
White solid; Column conditions: Hexane : EA = 50:1, R_f = 0.2, $[\alpha]_D^{25}$ = -28.3 (*c* = 0.11, CHCl$_3$). **¹H NMR** (500 MHz, CDCl$_3$): δ 8.09 (d, *J* = 8.8 Hz, 1H), 8.00 (d, *J* = 8.1 Hz, 1H), 7.96–7.90 (m, 4H), 7.88–7.81 (m, 3H), 7.77 (dd, *J* = 8.8, 3.3 Hz, 2H), 7.67–7.62 (m, 4H), 7.57–7.51 (m, 4H), 7.48 (t, *J* = 7.4 Hz, 1H), 7.43 (d, *J* = 8.6 Hz, 2H), 7.37 (t, *J* = 7.4 Hz, 1H), 7.33–7.28 (m, 2H), 7.26–7.21 (m, 1H), 4.45 (dd, *J* = 14.9, 7.7 Hz, 2H), 3.75–3.64 (m, 2H) ppm. **³¹P NMR** (202 MHz, CDCl$_3$): δ 147.88 ppm. **¹³C NMR** (126 MHz, CDCl$_3$): δ 149.85, 149.81, 149.45, 135.35, 133.38, 133.00, 132.62, 131.63, 130.81, 130.50, 130.35, 129.65, 129.22, 129.10, 129.06, 128.50, 128.45, 128.35, 127.89, 127.86, 127.20, 127.05, 126.85, 126.66, 126.60, 126.30, 126.27, 126.22, 125.99, 125.70, 125.63, 125.02, 124.75, 124.24, 124.20, 122.96, 122.31, 121.63, 48.69, 48.53 ppm. **IR** (neat): ν = 3015, 2906, 1693, 1589, 1462, 1327, 1229, 1069, 926, 816, 747 cm^{-1}. **HRMS** (ESI+, MeOH): *m/z* calcd. 634.1906 (M + Na)$^+$, found: 634.1915.
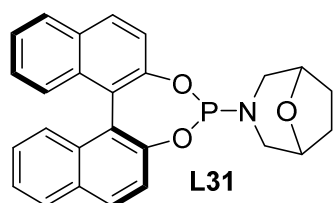
White solid; Column conditions: Hexane : EA = 50:1, R_f = 0.1, $[\alpha]_D^{25}$ = 608.4 (*c* = 0.09, CHCl$_3$). **¹H NMR** (500 MHz, CDCl$_3$): δ 7.98 (d, *J* = 8.8 Hz, 1H), 7.92 (d, *J* = 8.7 Hz, 3H), 7.53 (d, *J* = 8.8 Hz, 1H), 7.47–7.37 (m, 4H), 7.33 (d, *J* = 8.3 Hz, 1H), 7.30–7.23 (m, 2H), 4.29 (s, 1H), 3.93 (d, *J* = 6.9 Hz, 1H), 3.38–3.34 (m, 1H), 3.18 (t, *J* = 12.1 Hz, 1H), 2.79 (d, *J* = 12.9 Hz, 1H), 2.59 (d, *J* = 12.6 Hz, 1H), 1.95–1.84 (m, 3H), 1.80–1.71 (m, 1H) ppm. **³¹P NMR** (202 MHz, CDCl$_3$): δ 149.60 ppm. **¹³C NMR** (126 MHz, CDCl$_3$): δ 149.94, 149.90, 149.34, 132.94, 132.63, 131.53, 130.95, 130.41, 130.31, 128.49, 128.46, 127.09, 126.97, 126.28, 124.98, 124.80, 123.99, 123.02, 122.11, 122.07, 74.91, 74.74, 51.20, 48.19, 27.82, 27.32 ppm. **IR** (neat): ν = 2938, 1589, 1462, 1326, 1229, 1069, 998, 939, 820, 756, 624, 550 cm^{-1}. **HRMS** (ESI+, MeOH): *m/z* calcd. 450.1230 (M + Na)$^+$, found: 450.1230.
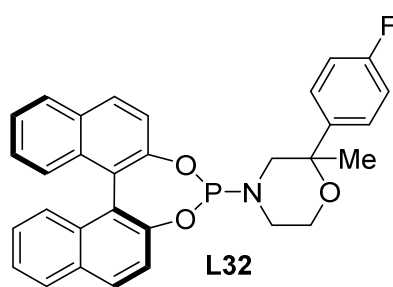
White solid; Column conditions: Hexane : EA = 50:1, R_f = 0.1, $[\alpha]_D^{25}$ = 442.8 (c = 0.09, CHCl$_3$). **^{1}H NMR** (400 MHz, CDCl$_3$): δ 8.04–7.81 (m, 4H), 7.60–7.40 (m, 6H), 7.34 (ddd, J = 29.5, 11.9, 6.4 Hz, 4H), 7.15 (dt, J = 33.6, 8.7 Hz, 2H), 3.89–3.68 (m, 1H), 3.55–3.41 (m, 2H), 3.27 (ddd, J = 52.1, 13.5, 8.1 Hz, 1H), 2.99–2.68 (m, 2H), 1.46 (d, J = 27.7 Hz, 3H) ppm. **^{19}F NMR** (376 MHz, CDCl$_3$): δ -115.97 ppm. **^{31}P NMR** (202 MHz, CDCl$_3$): δ 147.79 ppm. **^{13}C NMR** (101 MHz, CDCl$_3$): δ 163.23, 160.79, 149.80, 149.19, 139.62, 132.86, 132.64, 131.55, 130.90, 130.51, 130.31, 130.00, 128.42, 128.17, 127.69, 126.98, 126.30, 125.02, 124.86, 123.91, 122.94, 121.94, 121.83, 115.55, 74.57, 61.71, 52.89, 43.32, 27.87 ppm. **IR** (neat): ν = 2846, 1589, 1507, 1229, 1070, 1015, 937, 820, 799, 748, 697, 556 cm^{-1}. **HRMS** (ESI+, MeOH): m/z calcd. 532.1448 (M + Na)$^+$, found: 532.1442.

*Characterization data of allylic sulfones **1-43, 2a, 4a, 5a, 6a**, and **(–)-Aglasidine A***:
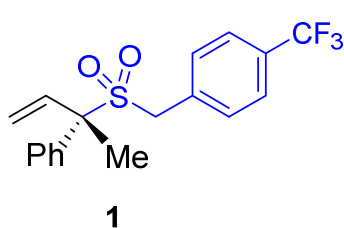
Scale: 0.10 mmol, (56% yield, 94:6 er), white solid, Hexane : EA = 10 : 1, R_f = 0.13. **^{1}H NMR** (400 MHz, CDCl$_3$): δ 7.72–7.66 (m, 2H), 7.57 (d, J = 8.1 Hz, 2H), 7.45–7.39 (m, 3H), 7.36 (d, J = 8.1 Hz, 2H), 6.66 (dd, J = 17.3, 10.9 Hz, 1H), 5.66–5.49 (m, 2H), 4.09–3.96 (m, 2H), 1.98 (s, 3H) ppm. **^{19}F NMR** (376 MHz, CDCl$_3$): δ -62.89 ppm. **^{13}C NMR** (101 MHz, CDCl$_3$): δ 136.08, 135.33, 131.73, 131.21, 131.01 (q, J = 32.3 Hz), 129.14, 128.86, 128.75, 125.62 (q, J = 4 Hz), 124.04 (q, J = 273.7 Hz), 120.64, 71.91, 53.74, 19.82 ppm. **IR** (neat): ν = 2947, 1629, 1321, 1289, 1165, 1124, 1065, 1020, 701, 653 cm^{-1}. **HRMS** (ESI+, MeOH): m/z calcd. 377.0794 (M + Na)$^+$, found: 377.0805. **SFC** conditions: Chiralpak OJSFC (150 x 3.1 mm, 3 μm), Mobile phase: CO$_2$/IPA 90:10, Flow: 2 mL/min, ABPR: 2000 psi, Inj volume: 2 μL; 94:6 er; $[\alpha]_D^{25}$ = 27.9 (c = 0.09, CHCl$_3$).
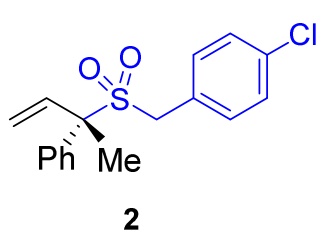
Scale: 0.10 mmol, (63% yield, 94.5:5.5 er), light yellow oil, Hexane : EA = 10 : 1, R_f = 0.16. **^{1}H NMR** (400 MHz, CDCl$_3$): δ 7.72–7.66 (m, 2H), 7.46–7.36 (m, 3H), 7.32–7.27 (m, 2H), 7.20–7.14 (m, 2H), 6.64 (dd, J = 17.3, 10.9 Hz, 1H), 5.65–5.46 (m, 2H), 4.03–3.87 (m, 2H), 1.95 (s, 3H) ppm. **^{13}C NMR** (126 MHz, CDCl$_3$): δ 136.27, 135.51, 135.14, 132.64, 129.04, 128.99, 128.82, 128.75, 125.58,

120.44, 71.77, 53.61, 19.84 ppm. **IR** (neat): ν = 2947, 1619, 1418, 1321, 1124, 1065, 1020, 701 cm^{-1}. **HRMS** (ESI+, MeOH): *m/z* calcd. 343.0530 $(M + Na)^+$, found: 343.0527. **SFC** conditions: Chiralpak IG (150 x 4.6 mm, 3μm), Mobile phase: CO_2/EtOH 70:30, Flow: 2 mL/min, ABPR: 2000 psi; 94.5:5.5 *er*; $[\alpha]_D^{25}$ = 27.9 (*c* = 0.09, CHCl$_3$).
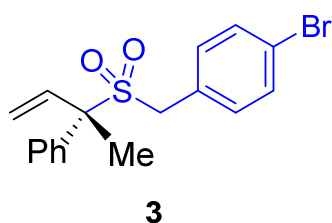
Scale: 0.10 mmol, (77% yield, 94.5:5.5 *er*), white solid, Hexane : EA = 10 : 1, R_f = 0.14. **^{1}H NMR** (500 MHz, CDCl$_3$): δ 7.71–7.66 (m, 2H), 7.47–7.37 (m, 5H), 7.14–7.08 (m, 2H), 6.64 (dd, *J* = 17.3, 10.9 Hz, 1H), 5.61 (d, *J* = 10.9 Hz, 1H), 5.51 (d, *J* = 17.3 Hz, 1H), 3.99–3.86 (m, 2H), 1.95 (s, 3H) ppm. **^{13}C NMR** (126 MHz, CDCl$_3$): δ 136.23, 135.47, 132.92, 131.92, 129.03, 128.80, 128.74, 126.10, 123.33, 120.44, 71.76, 53.65, 19.82 ppm. **IR** (neat): ν = 2945, 1486, 1291, 1275, 1127, 1069, 1012, 928, 699, 647 ppm. **HRMS** (ESI+, MeOH): *m/z* calcd. 387.0025 $(M + Na)^+$, found: 387.0010. **SFC** conditions: Chiralcel OJ-SFC (150 x 3 mm, 3μm), Mobile phase: CO_2/MeOH 80:20, Flow: 2 mL/min, ABPR: 2000 psi; 94.5:5.5 *er*; $[\alpha]_D^{25}$ = 17.7 (*c* = 0.11, CHCl$_3$).
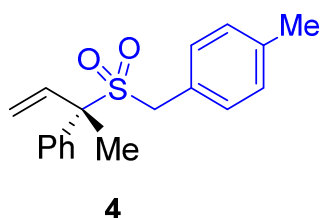
Scale: 0.10 mmol, (83% yield, 93.5:6.5 *er*), light yellow solid, Hexane : EA = 10 : 1, R_f = 0.12. **^{1}H NMR** (400 MHz, CDCl$_3$) δ 7.73–7.67 (m, 2H), 7.45–7.35 (m, 3H), 7.13 (s, 4H), 6.64 (dd, *J* = 17.3, 10.9 Hz, 1H), 5.59 (d, *J* = 10.9 Hz, 1H), 5.49 (d, *J* = 17.3 Hz, 1H), 4.01–3.89 (m, 2H), 2.33 (s, 3H), 1.93 (s, 3H) ppm. **^{13}C NMR** (126 MHz, CDCl$_3$): δ 138.78, 136.58, 135.80, 131.23, 129.50, 128.89, 128.79, 128.74, 123.90, 120.14, 71.62, 54.16, 21.36, 19.86 ppm. **IR** (neat): ν = 2918, 1572, 1283, 1128, 1065, 930, 812, 699, 635, 484 cm^{-1}. **HRMS** (ESI+, MeOH): *m/z* calcd. 323.1076 $(M + Na)^+$, found: 323.1078. **SFC** conditions: Chiralcel OJSFC (150 x 3 mm, 3 μm), Mobile phase; CO_2/MeOH 80:20, Flow: 2 mL/min, ABPR: 2000 psi; 93.5:6.5 *er*; $[\alpha]_D^{25}$ = 12.6 (*c* = 0.1, CHCl$_3$).
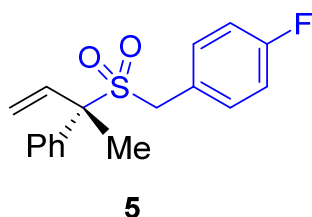
Scale: 0.10 mmol, (76% yield, 93.5:6.5 *er*), yellow solid, Hexane : EA = 10 : 1, R_f = 0.14. **^{1}H NMR** (500 MHz, CDCl$_3$): δ 7.70–7.66 (m, 2H), 7.44–7.35 (m, 3H), 7.22–7.17 (m, 2H), 7.02–6.97 (m, 2H), 6.63 (dd, *J* = 17.3, 10.9 Hz, 1H), 5.59 (d, *J*

= 10.9, 1H), 5.49 (d, J = 17.3 Hz, 1H), 4.00–3.89 (m, 2H), 1.94 (s, 3H) ppm. **^{19}F NMR** (376 MHz, CDCl$_3$): δ -112.94 ppm. **^{13}C NMR** (126 MHz, CDCl$_3$): δ 163.23 (d, J = 248.2 Hz), 136.33, 135.56, 133.14, 133.07, 129.00, 128.77 (d, J = 3.8 Hz), 122.81 (d, J = 2.5 Hz), 120.33, 115.80 (d, J = 21.4 Hz), 71.62, 53.44, 19.82 ppm. **IR** (neat): ν = 2945, 1604, 1509, 1415, 1284, 1225, 1065, 729, 698, 579 cm^{-1}. **HRMS** (ESI+, MeOH): m/z calcd. 327.0825 (M + Na)$^+$, found: 327.0824. **SFC conditions**: chiralpak IG (150 x 4.6 mm, 3 μm), Mobile phase: CO$_2$/MeOH 60:40, Flow: 2 mL/min, ABPR: 2000 psi; 93.5:6.5 er; $[α]_D^{25}$ = 20.7 (c = 0.1, CHCl$_3$).
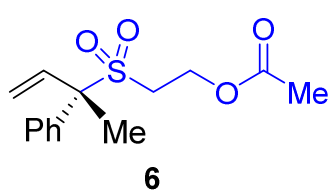
Scale: 0.10 mmol, (60% yield, 93.5:6.5 er), yellow oil, Hexane : EA = 10 : 1, R_f = 0.14. **^{1}H NMR** (400 MHz, CDCl$_3$): δ 7.69–7.63 (m, 2H), 7.44–7.37 (m, 3H), 6.64 (dd, J = 17.4, 10.9 Hz, 1H), 5.62 (d, J = 10.9 Hz, 1H), 5.52 (d, J = 17.4 Hz, 1H), 4.35 (td, J = 6.5, 3.3 Hz, 2H), 3.20–3.06 (m, 2H), 2.03 (s, 3H), 1.97 (s, 3H) ppm. **^{13}C NMR** (101 MHz, CDCl$_3$): δ 170.67, 135.66, 135.15, 129.10, 128.82, 128.75, 120.65, 71.47, 57.06, 46.97, 20.87, 19.42 ppm. **IR** (neat): ν = 2975, 1745, 1417, 1302, 1282, 1222, 1134, 1042, 945, 699, 654, 592 cm^{-1}. **HRMS** (ESI+, MeOH): m/z calcd. 305.0818 (M + Na)$^+$, found: 305.0816. **SFC conditions**: Column ChiralPak IG (150 x 4.6 mm, 3 μm), Isocratic CO$_2$/MeOH 60:40, 2 mL/min, 2000 psi; 93.5:6.5 er; $[α]_D^{25}$ = 48.6 (c = 0.1, CHCl$_3$).
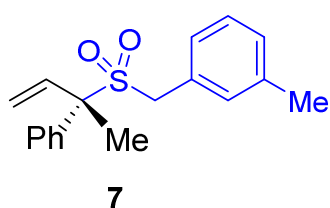
Scale: 0.10 mmol, (73% yield, 93:7 er), yellow solid, Hexane : EA = 10 : 1, R_f = 0.12. **^{1}H NMR** (500 MHz, CDCl$_3$): δ 7.73–7.69 (m, 2H), 7.46–7.37 (m, 3H), 7.26–7.19 (m, 1H), 7.14 (d, J = 7.6 Hz, 1H), 7.05 (d, J = 5.7 Hz, 2H), 6.65 (dd, J = 17.3, 10.9 Hz, 1H), 5.60 (d, J = 10.9 Hz, 1H), 5.50 (d, J = 17.3 Hz, 1H), 4.01–3.91 (m, 2H), 2.32 (s, 3H), 1.95 (s, 3H) ppm. **^{13}C NMR** (126 MHz, CDCl$_3$): δ 138.37, 136.48, 135.72, 132.04, 129.59, 128.88, 128.76, 128.69, 128.55, 128.42, 126.82, 120.14, 71.61, 54.30, 21.38, 19.80 ppm. **IR** (neat): ν = 2944, 1605, 1288, 1141, 1125, 1065, 929, 695, 517 cm^{-1}. **HRMS** (ESI+, MeOH): m/z calcd. 323.1076 (M + Na)$^+$, found: 323.1081. **SFC conditions**: Colum: Chiralcel OJSFC (150 x 3 mm, 3 μm), Mobile phase; CO$_2$/MeOH 80:20, Flow: 2 mL/min, ABPR: 2000 psi; 93:7 er; $[α]_D^{25}$ = 17.2 (c = 0.1, CHCl$_3$).
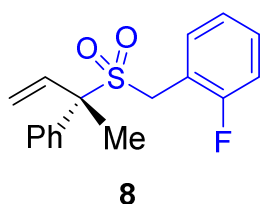
Scale: 0.10 mmol, (72% yield, 93:7 *er*), yellow solid, Hexane : EA = 10 : 1, R_f = 0.12. **^{1}H NMR** (400 MHz, CDCl$_3$): δ 7.74–7.68 (m, 2H), 7.43–7.37 (m, 3H), 7.36–7.28 (m, 2H), 7.11 (td, *J* = 7.6, 1.1 Hz, 1H), 7.04 (t, *J* = 9.0 Hz, 1H), 6.69 (dd, *J* = 17.4, 10.9 Hz, 1H), 5.61 (d, *J* = 10.9 Hz, 1H), 5.54 (d, *J* = 17.4 Hz, 1H), 4.18–4.04 (m, 2H), 2.02 (s, 3H) ppm. **^{19}F NMR** (376 MHz, CDCl$_3$): δ -116.25 ppm. **^{13}C NMR** (101 MHz, CDCl$_3$): δ 161.52 (d, *J* = 249.5 Hz), 136.12, 135.44, 133.05 (d, *J* = 3.0 Hz), 130.88 (d, *J* = 8.0 Hz), 128.94, 128.79, 128.69, 124.39 (d, *J* = 4.0 Hz), 120.35, 115.70 (d, *J* = 22.2 Hz), 114.94 (d, *J* = 15.2 Hz), 71.69, 47.39, 19.70 ppm. **IR** (neat): ν = 2974, 1495, 1445, 1295, 1233, 1136, 940, 766, 698, 640 cm^{-1}. **HRMS** (ESI+, MeOH): *m/z* calcd. 327.0825 (M + Na)$^+$, found: 327.0818. **SFC** conditions: Column: Chiralpak IG (150 x 4.6 mm, 3 μm), Mobile phase: CO$_2$/EtOH 65:35, Flow: 2 mL/min, ABPR: 2000 psi; 93:7 *er*; $[α]_D^{25}$ = 17.8 (c = 0.11, CHCl$_3$).
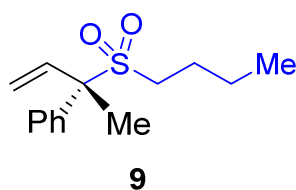
Scale: 0.10 mmol, (56% yield, 95:5 *er*), yellow oil, Hexane : EA = 10 : 1, R_f = 0.14. **^{1}H NMR** (400 MHz, CDCl$_3$): δ 7.71–7.65 (m, 2H), 7.46–7.36 (m, 3H), 6.68 (dd, *J* = 17.4, 10.9 Hz, 1H), 5.61 (d, *J* = 10.9 Hz, 1H), 5.51 (d, *J* = 17.4 Hz, 1H), 2.85–2.67 (m, 2H), 1.98 (s, 3H), 1.79–1.69 (m, 2H), 1.38 (h, *J* = 7.4 Hz, 2H), 0.89 (t, *J* = 7.4 Hz, 3H) ppm. **^{13}C NMR** (101 MHz, CDCl$_3$): δ 136.42, 135.76, 128.79, 128.72, 128.66, 120.02, 70.73, 47.35, 22.98, 22.05, 19.58, 13.68 ppm. **IR** (neat): ν = 2960, 1447, 1291, 1271, 1132, 1095, 697, 596 cm^{-1}. **HRMS** (ESI+, MeOH): *m/z* calcd. 275.1076 (M + Na)$^+$, found: 275.1080. **SFC** conditions: Column: IG Column, Isocratic CO$_2$/MeOH 75:25, 2 mL/min, 2000 psi; 95:5 *er*; $[α]_D^{25}$ = -9.6 (c = 0.1, CHCl$_3$).

Scale: 0.10 mmol, (67% yield, 92.5:7.5 *er*), white solid, Hexane : EA = 10 : 1, R_f = 0.1. **^{1}H NMR** (500 MHz, CDCl$_3$): δ 7.69–7.64 (m, 2H), 7.43–7.35 (m, 3H), 6.67 (dd, *J* = 17.4, 10.9 Hz, 1H), 5.61 (d, *J* = 10.9 Hz, 1H), 5.52 (d, *J* = 17.4 Hz, 1H), 2.66 (s, 3H), 1.97 (s, 3H) ppm. **^{13}C NMR** (126 MHz, CDCl$_3$): δ 136.17, 135.60, 128.93, 128.74, 128.68, 120.26, 70.54, 35.84, 19.63 ppm. **IR** (neat): ν = 2932, 1495, 1286, 1135, 1068, 953, 732, 699, 526 cm^{-1}. **HRMS** (ESI+, MeOH): *m/z* calcd. 233.0607 (M + Na)$^+$, found: 233.0599. **SFC** conditions: Column:

chiralpak IG (150 x 4.6 mm, 3 μm), Mobile phase: CO_2/MeOH 85:15, Flow: 2 mL/min, ABPR: 2000 psi; 95:5 *er*; $[\alpha]_D^{25} = 41.4$ (c = 0.1, CHCl$_3$).
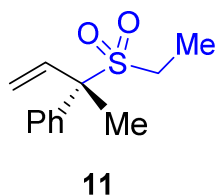
Scale: 0.10 mmol, (67% yield, 93:7 *er*), yellow oil, Hexane : EA = 10 : 1, R_f = 0.1. **^{1}H NMR** (500 MHz, CDCl$_3$): δ 7.68–7.65 (m, 2H), 7.42–7.34 (m, 3H), 6.66 (dd, *J* = 17.4, 10.9 Hz, 1H), 5.59 (d, *J* = 10.9 Hz, 1H), 5.49 (d, *J* = 17.4 Hz, 1H), 2.82 (dq, *J* = 13.5, 7.5 Hz, 1H), 2.74 (dq, *J* = 13.3, 7.5 Hz, 1H), 1.96 (s, 3H), 1.26 (t, *J* = 7.5 Hz, 3H) ppm. **^{13}C NMR** (126 MHz, CDCl$_3$): δ 136.43, 135.72, 128.80, 128.71, 128.68, 120.03, 70.57, 42.15, 19.63, 5.57 ppm. **IR** (neat): ν = 2944, 1447, 1292, 1132, 1067, 934, 697, 587 cm^{-1}. **HRMS** (ESI+, MeOH): *m/z* calcd. 247.0763 (M + Na)$^+$, found: 247.0755. **SFC** conditions: Column: ChiralPak IG (4.6 mm x 150 mm, 3 μm), Isocratic CO_2/MeOH 75:25, 2000 psi, Flow: 2 mL/min; 93:7 *er*; $[\alpha]_D^{25} = 40.0$ (c = 0.12, CHCl$_3$).
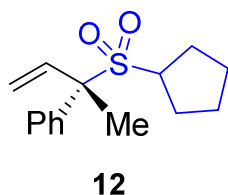
Scale: 0.10 mmol, (64% yield, 94.5:5.5 *er*), white solid, Hexane : EA = 10 : 1, R_f = 0.2. **^{1}H NMR** (500 MHz, CDCl$_3$): δ 7.69–7.64 (m, 2H), 7.41–7.33 (m, 3H), 6.69 (dd, *J* = 17.4, 10.9 Hz, 1H), 5.55 (d, *J* = 10.9 Hz, 1H), 5.44 (d, *J* = 17.4 Hz, 1H), 3.33 (p, *J* = 8.1 Hz, 1H), 1.95 (s, 5H), 1.74–1.62 (m, 4H), 1.52–1.42 (m, 2H) ppm. **^{13}C NMR** (126 MHz, CDCl$_3$): δ 136.78, 136.21, 128.79, 128.71, 128.55, 119.50, 71.27, 58.82, 28.37, 28.17, 25.90, 25.83, 19.93 ppm. **IR** (neat): ν = 2945, 1447, 1281, 1123, 1060, 930, 706, 559 cm^{-1}. **HRMS** (ESI+, MeOH): *m/z* calcd. 287.1076 (M + Na)$^+$, found: 287.1077. **SFC** conditions: Column: chiralpak IG (150 x 4.6 mm, 3 μm), Mobile phase: CO_2/MeOH 65:35, Flow: 2 mL/min, ABPR: 2000 psi; 94.5:5.5 *er*; $[\alpha]_D^{25} = 35.9$ (c = 0.11, CHCl$_3$).
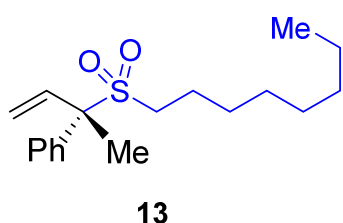
Scale: 0.10 mmol, (55% yield, 94:6 *er*), yellow oil, Hexane : EA = 10 : 1, R_f = 0.2. **^{1}H NMR** (400 MHz, CDCl$_3$): δ 7.69–7.63 (m, 2H), 7.43–7.35 (m, 3H), 6.66 (dd, *J* = 17.4, 10.9 Hz, 1H), 5.58 (d, *J* = 10.9 Hz, 1H), 5.48 (d, *J* = 17.4 Hz, 1H), 2.82–2.64 (m, 2H), 1.95 (s, 3H), 1.79–1.67 (m, 2H), 1.33–1.19 (m, 10H), 0.86 (t, *J* = 6.9 Hz, 3H) ppm. **^{13}C NMR** (101 MHz, CDCl$_3$): δ 136.43, 135.77, 128.79, 128.72, 128.67, 120.02, 70.72, 47.65, 31.80, 29.16, 29.02, 28.81, 22.71, 21.03, 19.59, 14.19 ppm. **IR** (neat): ν = 2924, 2855, 1447, 1288, 1133, 1066, 929, 697,

598 cm^{-1}. **HRMS** (ESI+, MeOH): *m/z* calcd. 331.1702 (M + Na)$^+$, found: 331.1702. **SFC** conditions: OJ Column (0.3 cm x 15 cm, 3 μm SFC), Isocratic CO$_2$/MeOH 90:10, 2 mL/min, 2000 psi; 94:6 *er*; $[\alpha]_D^{25}$ = 27.1 (c = 0.11, CHCl$_3$).

14

Scale: 0.10 mmol, (81% yield, 93.5:6.5 *er*), white solid, Hexane : EA = 10 : 1, R_f = 0.1. **^{1}H NMR** (500 MHz, CDCl$_3$): δ 7.69–7.66 (m, 2H), 7.42–7.34 (m, 3H), 6.72 (dd, *J* = 17.4, 10.9 Hz, 1H), 5.57 (d, *J* = 10.9 Hz, 1H), 5.49 (d, *J* = 17.4 Hz, 1H), 2.15 (tt, *J* = 8.0, 4.9 Hz, 1H), 1.99 (s, 3H), 1.11–0.99 (m, 2H), 0.89–0.84 (m, 2H) ppm. **^{13}C NMR** (126 MHz, CDCl$_3$): δ 136.66, 135.95, 128.87, 128.70, 128.48, 119.68, 71.04, 25.81, 19.69, 5.18, 4.84 ppm. **IR** (neat): ν = 3060, 1446, 1306, 1282, 1133, 1068, 879, 698, 676 cm^{-1}. **HRMS** (ESI+, MeOH): *m/z* calcd. 259.0763 (M + Na)$^+$, found: 259.0761. **SFC** conditions: Column: ChiralPak IG (4.6 mm x 150 mm, 3 μm), Isocratic CO$_2$/MeOH 70:30, 2000 psi, Flow: 2 mL/min; 93.5:6.5 *er*; $[\alpha]_D^{25}$ = 34.2 (c = 0.09, CHCl$_3$).
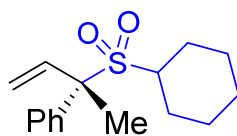
15

Scale: 0.10 mmol, (72% yield, 94:6 *er*), yellow solid, Hexane : EA = 10 : 1, R_f = 0.18. **^{1}H NMR** (400 MHz, CDCl$_3$): δ 7.69–7.63 (m, 2H), 7.41–7.32 (m, 3H), 6.68 (dd, *J* = 17.4, 10.9 Hz, 1H), 5.54 (d, *J* = 10.9 Hz, 1H), 5.42 (d, *J* = 17.4 Hz, 1H), 2.94 (tt, *J* = 12.1, 3.4 Hz, 1H), 1.96 (s, 3H), 1.87–1.73 (m, 4H), 1.60–1.39 (m, 3H), 1.15–1.07 (q, *J* = 11.5, 9.3 Hz, 3H) ppm. **^{13}C NMR** (101 MHz, CDCl$_3$): δ 136.85, 136.46, 128.73, 128.70, 128.53, 119.36, 71.87, 59.20, 26.91, 26.87, 25.62, 25.09, 20.23 ppm. **IR** (neat): ν =2834, 2855, 1446, 1273, 1133, 1062, 930, 700, 642 cm^{-1}. **HRMS** (ESI+, MeOH): *m/z* calcd. 301.1233 (M + Na)$^+$, found: 301.1232. **SFC** conditions: Column: ChiralPak IG (4.6 mm x 150 mm, 3 μm), Isocratic CO$_2$/MeOH 65:35, 2000 psi, Flow: 2 mL/min; 94:6 *er*; $[\alpha]_D^{25}$ = 45.3 (c = 0.1, CHCl$_3$).
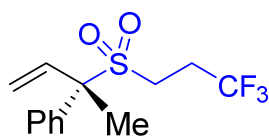
16

Scale: 0.10 mmol, (89% yield, 92:8 *er*), yellow oil, Hexane : EA = 10 : 1, R_f = 0.2. **^{1}H NMR** (400 MHz, CDCl$_3$): δ 7.66 (dd, *J* = 8.0, 1.8 Hz, 2H), 7.46–7.39 (m, 3H), 6.65 (dd, *J* = 17.4, 10.9 Hz, 1H), 5.65 (d, *J* = 10.9 Hz, 1H), 5.55 (d, *J* = 17.4 Hz, 1H), 3.07–2.88 (m, 2H), 2.58–2.35 (m, 2H), 1.99 (s, 3H) ppm. **^{19}F NMR** (376 MHz, CDCl$_3$): δ -65.76 ppm. **^{13}C NMR** (101 MHz, CDCl$_3$): δ 135.31, 134.85, 129.30, 128.92, 128.72,

125.83 (q, J = 277.8 Hz), 120.98, 71.33, 41.11, 26.83 (q, J = 31.3 Hz), 19.55 ppm. **IR** (neat): ν = 1446, 1381, 1291, 1270, 1245, 1136, 1086, 697, 584 cm^{-1}. **HRMS** (ESI+, MeOH): *m/z* calcd. 315.0637 (M + Na)$^+$, found: 315.0632. **SFC** conditions: Column: chiralpak IG (150 x 4.6 mm, 3 μm), Mobile phase: CO_2/MeOH 90:10, Flow: 2 mL/min, ABPR: 2000 psi; 92:8 *er*; $[\alpha]_D^{25}$ = 37.2 (c = 0.1, CHCl$_3$).

17
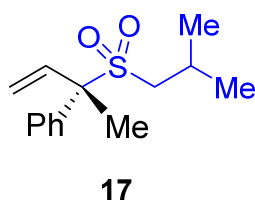
Scale: 0.10 mmol, (75% yield, 93.5:6.5 *er*), yellow solid, Hexane : EA = 10 : 1, R_f = 0.14. **¹H NMR** (400 MHz, CDCl$_3$): δ 7.69–7.62 (m, 2H), 7.43–7.34 (m, 3H), 6.65 (dd, J = 17.4, 10.9 Hz, 1H), 5.58 (d, J = 10.9 Hz, 1H), 5.48 (d, J = 17.4 Hz, 1H), 2.68 (dd, J = 13.2, 6.5 Hz, 1H), 2.57 (dd, J = 13.2, 6.6 Hz, 1H), 2.31 (hept, J = 6.8 Hz, 1H), 1.94 (s, 3H), 1.03 (dd, J = 6.7, 1.0 Hz, 6H) ppm. **¹³C NMR** (101 MHz, CDCl$_3$): δ 136.35, 135.81, 128.74, 128.72, 128.62, 119.99, 71.05, 54.57, 23.40, 23.06, 19.47 ppm. **IR** (neat): ν = 2960, 1449, 1282, 1132, 1064, 931, 700, 576 cm^{-1}. **HRMS** (ESI+, MeOH): *m/z* calcd. 275.1076 (M + Na)$^+$, found: 275.1072. **SFC** conditions: Column: chiralpak IG (150 x 4.6 mm, 3 μm), Mobile phase: CO_2/MeOH 80:20, Flow: 2 mL/min, ABPR: 2000 psi; 93.5:6.5 *er*; $[\alpha]_D^{25}$ = 31.1 (c = 0.11, CHCl$_3$).

2a
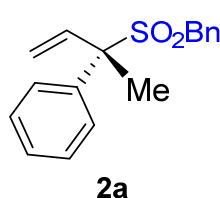
Scale: 0.10 mmol, (82% yield, 95:5 *er*), yellow solid, Hexane : EA = 10 : 1, R_f = 0.12. **¹H NMR** (500 MHz, CDCl$_3$): δ 7.71 (dd, J = 8.3, 1.4 Hz, 2H), 7.45–7.38 (m, 3H), 7.33 (dd, J = 5.0, 2.0 Hz, 3H), 7.27–7.23 (m, 2H), 6.65 (dd, J = 17.3, 10.9 Hz, 1H), 5.60 (d, J = 10.9 Hz, 1H), 5.50 (d, J = 17.3 Hz, 1H), 4.05–3.95 (m, 2H), 1.95 (s, 3H) ppm. **¹³C NMR** (126 MHz, CDCl$_3$): δ 136.45, 135.69, 131.36, 128.92, 128.81, 128.77, 128.73, 128.71, 127.09, 120.20, 71.67, 54.36, 19.80 cm^{-1}. **IR** (neat): ν = 2942, 1449, 1286, 1124, 1065, 928, 751, 693, 641, 523 cm^{-1}. **HRMS** (ESI+, MeOH): *m/z* calcd. 309.0920 (M + Na)$^+$, found: 309.0905. **SFC** conditions: IG Column, Isocratic CO_2/MeOH/DEA 65:35:0.1, 2 mL/min, 2000 psi; 95:5 *er*; $[\alpha]_D^{25}$ = 16.2 (c = 0.11, CHCl$_3$).
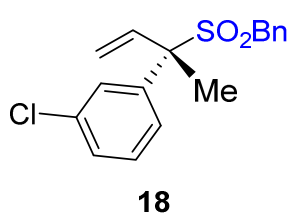
18

Scale: 0.10 mmol, (63% yield, 94:6 *er*), yellow oil, Hexane : EA = 10 : 1, R_f = 0.15. **¹H NMR** (500 MHz, CDCl$_3$): δ 7.65–7.59 (m, 2H), 7.38–7.31 (m, 5H), 7.29–7.25 (m, 2H), 6.60 (dd, J = 17.3, 10.9 Hz, 1H), 5.63 (d, J = 10.9 Hz, 1H), 5.51 (d, J = 17.3 Hz,

1H), 4.10–4.01 (m, 2H), 1.92 (s, 3H) ppm. **^{13}C NMR** (126 MHz, CDCl$_3$): δ 138.52, 135.23, 134.72, 131.34, 129.88, 129.11, 128.98, 128.98, 128.79, 127.10, 126.87, 120.75, 71.30, 54.68, 19.89 ppm. **IR** (neat): ν = 2990, 1570, 1456, 1413, 1297, 1133, 938, 695, 641 cm^{-1}. **HRMS** (ESI+, MeOH): *m/z* calcd. 343.0530 (M + Na)$^+$, found: 343.0517. **SFC** conditions: ID Column, Isocratic CO$_2$/MeOH 85:15, 3 mL/min, 1500 psi; 94:6 *er*; $[\alpha]_D^{25}$ = 20.5 (c = 0.13, CHCl$_3$).
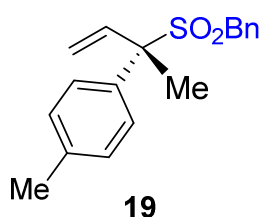
Scale: 0.10 mmol, (77% yield, 88.5:11.5 *er*), yellow solid, Hexane : EA = 10 : 1, R_f = 0.15. **^{1}H NMR** (500 MHz, CDCl$_3$): δ 7.56 (d, *J* = 8.4 Hz, 2H), 7.31 (dd, *J* = 5.0, 1.9 Hz, 3H), 7.25–7.19 (m, 4H), 6.62 (dd, *J* = 17.3, 10.9 Hz, 1H), 5.56 (d, *J* = 10.9 Hz, 1H), 5.47 (d, *J* = 17.4 Hz, 1H), 4.02–3.93 (m, 2H), 2.36 (s, 3H), 1.91 (s, 3H) ppm. **^{13}C NMR** (126 MHz, CDCl$_3$): δ 138.89, 135.82, 133.39, 131.37, 129.46, 128.75, 128.69, 128.65, 127.23, 119.98, 71.52, 54.27, 21.18, 19.80 ppm. **IR** (neat): ν = 3032, 1496, 1455, 1296, 1133, 1066, 966, 695, 635, 513 cm^{-1}. **HRMS** (ESI+, MeOH): *m/z* calcd. 323.1076 (M + Na)$^+$, found: 323.1083. **SFC** conditions: Column ChiralPak ID (100 x 4.6 mm, 3 μm, Isocratic CO$_2$/MeOH 85:15, 3 mL/min, 1500 psi; 88.5:11.5 *er*; $[\alpha]_D^{25}$ = 25.9 (c = 0.11, CHCl$_3$).
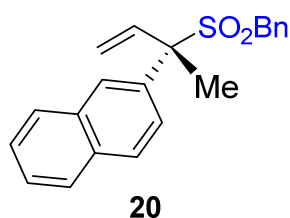
Scale: 0.10 mmol, (80% yield, 91:9 *er*), yellow solid, Hexane : EA = 10 : 1, R_f = 0.11, **^{1}H NMR** (500 MHz, CDCl$_3$): δ 8.09 (s, 1H), 7.93–7.85 (m, 4H), 7.57–7.51 (m, 2H), 7.33–7.27 (m, 3H), 7.23 (dd, *J* = 7.7, 1.8 Hz, 2H), 6.76 (dd, *J* = 17.3, 10.9 Hz, 1H), 5.65 (d, *J* = 10.9 Hz, 1H), 5.53 (d, *J* = 17.3 Hz, 1H), 4.08–3.96 (m, 2H), 2.05 (s, 3H) ppm. **^{13}C NMR** (126 MHz, CDCl$_3$): δ 135.68, 133.98, 133.17, 133.07, 131.35, 128.79, 128.67, 128.61, 128.41, 128.38, 127.62, 127.13, 127.05, 126.62, 126.08, 120.39, 72.00, 54.60, 20.09 ppm. **IR** (neat): ν = 3055, 2953, 1454, 1292, 1273, 1130, 943, 695, 645, 473 cm^{-1}. **HRMS** (ESI+, MeOH): *m/z* calcd. 359.1076 (M + Na)$^+$, found: 359.1084. **SFC** conditions: Column ChiralPak IC (100 x 4.6 mm, 3 μm, Isocratic CO$_2$/MeOH 75:25, 3 ml/min, 1500 psi; 91:9 *er*; $[\alpha]_D^{25}$ = 55.2 (c = 0.12, CHCl$_3$).
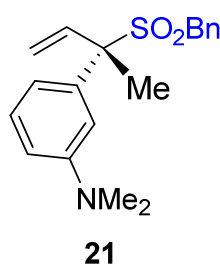
Scale: 0.10 mmol, (76% yield, 94.5:5.5 *er*), yellow oil, Hexane : EA = 10 : 1, R_f = 0.08. **¹H NMR** (500 MHz, CDCl₃): δ 7.31–7.27 (m, 3H), 7.27–7.20 (m, 3H), 7.08 (t, *J* = 2.1 Hz, 1H), 6.99 (d, *J* = 7.8 Hz, 1H), 6.74 (dd, *J* = 8.3, 2.4 Hz, 1H), 6.58 (dd, *J* = 17.3, 10.9 Hz, 1H), 5.55 (d, *J* = 10.9 Hz, 1H), 5.48 (d, *J* = 17.3 Hz, 1H), 4.05–3.93 (m, 2H), 2.96 (s, 6H), 1.91 (s, 3H) ppm. **¹³C NMR** (126 MHz, CDCl₃): δ 150.70, 137.47, 135.92, 131.40, 129.30, 128.69, 128.64, 127.42, 119.87, 16.54, 113.03, 113.02, 72.12, 54.48, 40.72, 19.93 ppm. **IR** (neat): ν = 2985, 1599, 1495, 1433, 1295, 1132, 1065, 933, 771, 695, 641, 515 cm⁻¹. **HRMS** (ESI+, MeOH): *m/z* calcd. 330.1522 (M + H)⁺, found: 330.1512. **SFC** conditions: Column: Chiralpak IC (100 x 4.6 mm, 3 μm), Mobile phase: CO₂/IPA 60:40, Flow: 3 mL/min, ABPR: 1500 psi; 94.5:5.5 *er*; $[\alpha]_D^{25}$ = 29.7 (c = 0.11, CHCl₃).
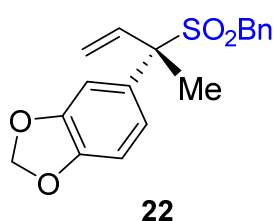
Scale: 0.10 mmol, (85% yield, 93:7 *er*), yellow solid, Hexane : EA = 10 : 1, R_f = 0.17. **¹H NMR** (400 MHz, CDCl₃): δ 7.36–7.31 (m, 3H), 7.30–7.26 (m, 2H), 7.22 (d, *J* = 2.0 Hz, 1H), 7.12 (dd, *J* = 8.3, 2.0 Hz, 1H), 6.83 (d, *J* = 8.3 Hz, 1H), 6.58 (dd, *J* = 17.3, 10.9 Hz, 1H), 5.99 (s, 2H), 5.57 (d, *J* = 10.9 Hz, 1H), 5.48 (d, *J* = 17.3 Hz, 1H), 4.08–3.97 (m, 2H), 1.89 (s, 3H) ppm. **¹³C NMR** (101 MHz, CDCl₃): δ 148.16, 148.07, 135.78, 131.34, 129.93, 128.80, 128.72, 127.21, 122.62, 120.08, 109.55, 108.19, 101.59, 71.57, 54.36, 20.16 ppm. **IR** (neat): ν = 2985, 1509, 1488, 1284, 1242, 1125, 1042, 942, 778, 706, 645 cm⁻¹. **HRMS** (ESI+, MeOH): *m/z* calcd. 353.0818 (M + Na)⁺, found: 353.0823. **SFC** conditions: Column: chiralpak IE 150 x 3 mm, 3 μm, Mobile phase: CO₂/EtOH 70:30, Flow: 2 mL/min, ABPR: 2000 psi; 93:7 *er*; $[\alpha]_D^{25}$ = 35.6 (c = 0.09, CHCl₃).
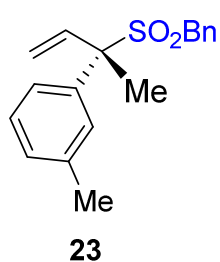
Scale: 0.10 mmol, (80% yield, 93.5:6.5 *er*), yellow solid, Hexane : EA = 10 : 1, R_f = 0.17. **¹H NMR** (500 MHz, CDCl₃): δ 7.50–7.46 (m, 2H), 7.33–7.27 (m, 4H), 7.25–7.21 (m, 2H), 7.18 (d, *J* = 7.5 Hz, 1H), 6.62 (dd, *J* = 17.4, 10.9 Hz, 1H), 5.57 (d, *J* = 10.9 Hz, 1H), 5.48 (d, *J* = 17.4 Hz, 1H), 3.99 (q, *J* = 13.3 Hz, 2H), 2.37 (s, 3H), 1.91 (s, 3H) ppm. **¹³C NMR** (126 MHz, CDCl₃): δ 138.38, 136.40, 135.84, 131.37, 129.69, 129.43, 128.80, 128.70, 128.59, 127.21, 125.81, 120.05, 71.67, 54.44, 21.79, 19.82 ppm. **IR** (neat): ν =

2938, 1602, 1493, 1291, 1124, 1063, 951, 761, 693, 650, 521 cm^{-1}. **HRMS** (ESI+, MeOH): m/z calcd. 323.1076 (M + Na)$^+$, found: 323.1085. **SFC conditions:** Column ChiralPak IG, Isocratic CO_2/ACN 60:40, 2 mL/min, 2000 psi; 93.5:6.5 er; $[\alpha]_D^{25}$ = 24.1 (c = 0.10, CHCl$_3$).
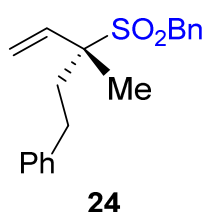
Scale: 0.10 mmol, (67% yield, 64.5:35.5 er), white solid, Hexane : EA = 10 : 1, R_f = 0.14. **^{1}H NMR** (400 MHz, CDCl$_3$): δ 7.44–7.37 (m, 5H), 7.32 (t, J = 7.3 Hz, 2H), 7.25–7.17 (m, 3H), 6.19 (dd, J = 17.5, 10.8 Hz, 1H), 5.62 (d, J = 10.8 Hz, 1H), 5.51 (d, J = 17.5 Hz, 1H), 4.20 (s, 2H), 2.72–2.55 (m, 2H), 2.33–2.25 (m, 2H), 1.62 (s, 3H) ppm. **^{13}C NMR** (101 MHz, CDCl$_3$): δ 141.05, 136.04, 131.46, 128.83, 128.80, 128.65, 128.47, 126.98, 126.34, 120.69, 68.30, 53.16, 34.59, 30.02, 16.56 ppm. **IR** (neat): ν = 2940, 1494, 1455, 1290, 1136, 1085, 950, 765, 697, 646, 513ppm. **HRMS** (ESI+, MeOH): m/z calcd. 337.1233 (M + Na)$^+$, found: 337.1237. **SFC conditions:** IG Column, Isocratic CO_2/EtOH 65:35, 2000 psi, 2 mL/min; 64.5:35.5 er; $[\alpha]_D^{25}$ = 54.1 (c = 0.09, CHCl$_3$).
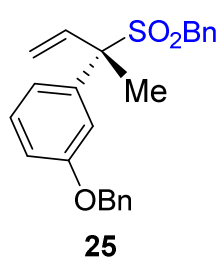
Scale: 0.10 mmol, (71% yield, 94.5:5.5 er), yellow oil, Hexane : EA = 10 : 1, R_f = 0.11. **^{1}H NMR** (500 MHz, CDCl$_3$): δ 7.45 (d, J = 7.4 Hz, 2H), 7.39 (t, J = 7.5 Hz, 2H), 7.34–7.27 (m, 7H), 7.23 (dd, J = 7.4, 2.2 Hz, 2H), 7.03–6.98 (m, 1H), 6.58 (dd, J = 17.3, 10.9 Hz, 1H), 5.58 (d, J = 10.9 Hz, 1H), 5.48 (d, J = 17.3 Hz, 1H), 5.08 (s, 2H), 4.02–3.92 (m, 2H), 1.91 (s, 3H) ppm. **^{13}C NMR** (126 MHz, CDCl$_3$): δ 158.87, 138.11, 136.84, 135.56, 131.38, 129.71, 128.80, 128.75, 128.70, 128.21, 127.74, 127.13, 121.29, 120.26, 115.93, 115.23, 71.71, 70.25, 54.47, 19.91 ppm. **IR** (neat): ν = 3032, 1580, 1455, 1295, 1252, 1133, 1024, 736, 695, 642. **HRMS** (ESI+, MeOH): m/z calcd. 415.1338 (M + Na)$^+$, found: 415.1335. **SFC conditions:** ID Column, Isocratic CO_2/MeOH 80:20, 3 mL/min, 1500 psi; 94.5:5.5 er; $[\alpha]_D^{25}$ = 44.7 (c = 0.09, CHCl$_3$).
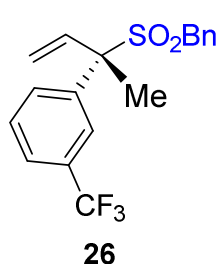
Scale: 0.10 mmol, (48% yield, 93:7 er), yellow solid, Hexane : EA = 10 : 1, R_f = 0.11. **^{1}H NMR** (400 MHz, CDCl$_3$): δ 7.97–7.84 (m, 2H), 7.64 (d, J = 7.8 Hz, 1H), 7.53 (t, J = 7.9 Hz, 1H), 7.35–7.30 (m, 3H), 7.29–7.24 (m, 2H), 6.66 (dd, J = 17.4, 10.9 Hz, 1H), 5.67 (d, J = 10.9 Hz, 1H), 5.53 (d, J = 17.4 Hz, 1H), 4.08 (d, J = 3.3 Hz, 2H), 1.96 (s,

3H) ppm. ^{19}**F NMR** (376 MHz, CDCl$_3$): δ -62.24 ppm. ^{13}**C NMR** (101 MHz, CDCl$_3$): δ 137.51, 135.14, 132.42, 131.30, 131.00 (q, J = 33.3 Hz), 129.18, 129.01, 128.81, 126.77, 125.73 (q, J = 4.0 Hz), 125.43 (q, J = 4.0 Hz), 124.01 (q, J = 273.7 Hz), 121.01, 71.23, 54.74, 19.90 ppm. **IR** (neat): ν = 2940, 1494, 1455, 1290, 1136, 1085, 1000, 950, 756, 697, 646, 513 cm^{-1}. **HRMS** (ESI+, MeOH): *m/z* calcd. 377.0794 (M + Na)$^+$, found: 377.0806. **SFC** conditions: Column: Chiralpak IG (150 x 4.6 mm, 3 μm), Mobile phase: CO$_2$/EtOH 85:15, Flow: 2 mL/min, ABPR: 2000 psi; 93:7 *er*; [α]$_D^{25}$ = 15.6 (c = 0.11, CHCl$_3$).

27
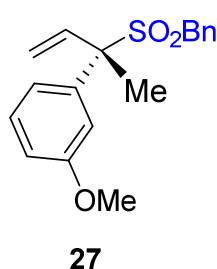
Scale: 0.10 mmol, (80% yield, 94:6 *er*), yellow solid, Hexane : EA = 10 : 1, R_f = 0.11. ^{1}**H NMR** (500 MHz, CDCl$_3$): δ 7.35–7.28 (m, 4H), 7.29–7.22 (m, 4H), 6.94–6.89 (m, 1H), 6.59 (dd, J = 17.3, 10.9 Hz, 1H), 5.57 (d, J = 10.9 Hz, 1H), 5.48 (d, J = 17.3 Hz, 1H), 4.05–3.94 (m, 2H), 3.81 (s, 3H), 1.91 (s, 3H) ppm. ^{13}**C NMR** (126 MHz, CDCl$_3$): δ 159.73, 138.09, 135.59, 131.36, 129.66, 128.80, 128.70, 127.13, 120.98, 120.23, 115.00, 114.14, 71.69, 55.46, 54.46, 19.90 ppm. **IR** (neat): ν = 2937, 1580, 1492, 1433, 1284, 1256, 1133, 1040, 951, 770, 698, 644, 516 cm^{-1}. **HRMS** (ESI+, MeOH): *m/z* calcd. 339.1025 (M + Na)$^+$, found: 339.1012. **SFC** conditions: Column: Chiralpak IA (100 x 4.6 mm, 3μm), Mobile phase: CO$_2$/MeOH 70:30, Flow: 3 mL/min, ABPR: 1500 psi; 94:6 *er*; [α]$_D^{25}$ = 29.4 (c = 0.11, CHCl$_3$).

28
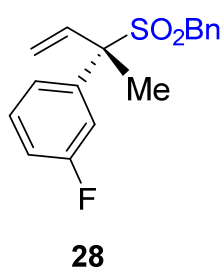
Scale: 0.10 mmol, (66% yield, 95:5 *er*), white solid, Hexane : EA = 10 : 1, R_f = 0.11. ^{1}**H NMR** (400 MHz, CDCl$_3$): δ 7.49 (ddd, J = 8.0, 1.8, 0.9 Hz, 1H), 7.43–7.36 (m, 2H), 7.36–7.31 (m, 3H), 7.27 (dt, J = 7.7, 2.5 Hz, 2H), 7.09 (tdd, J = 8.2, 2.5, 0.9 Hz, 1H), 6.60 (dd, J = 17.3, 10.9 Hz, 1H), 5.63 (d, J = 10.9 Hz, 1H), 5.51 (d, J = 17.3 Hz, 1H), 4.10–3.99 (m, 2H), 1.93 (s, 3H) ppm. ^{19}**F NMR** (376 MHz, CDCl$_3$): δ -111.68 ppm. ^{13}**C NMR** (101 MHz, CDCl3): δ 162.77 (q, J = 247.5 Hz), 138.97 (q, J = 8.1 Hz), 135.28, 131.36, 130.18, 130.14 (q, J = 8.1 Hz), 130.10, 128.96, 128.80, 126.88, 124.50 (q, J = 3.0 Hz), 120.68, 116.19 (q, J = 27.3 Hz), 115.97 (q, J = 25.3 Hz), 115.84, 71.32, 54.59, 19.92. ppm **IR** (neat): ν = 2989, 1584, 1489, 1295, 1245, 1131, 1080, 925, 778, 694, 646, 513 cm^{-1}. **HRMS** (ESI+, MeOH): *m/z* calcd. 327.0825 (M + Na)$^+$, found: 327.0822. **SFC** conditions: Column: cel2 (150 x 3 mm, 2.5 μm), Mobile

phase: CO_2/ACN 90:10, Flow: 2 mL/min, ABPR: 2000 psi; 95:5 *er*; $[\alpha]_D^{25}$ = 29.4 (c = 0.11, $CHCl_3$).
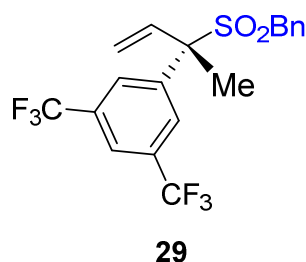
Scale: 0.10 mmol, (45% yield, 93.5:6.5 *er*), yellow solid, Hexane : EA = 10 : 1, R_f = 0.2. **¹H NMR** (400 MHz, $CDCl_3$): δ 8.09 (s, 2H), 7.86 (s, 1H), 7.36–7.27 (m, 5H), 6.69 (dd, *J* = 17.4, 10.9 Hz, 1H), 5.75 (d, *J* = 10.9 Hz, 1H), 5.59 (d, *J* = 17.4 Hz, 1H), 4.18 (s, 2H), 1.99 (s, 3H) ppm. **¹⁹F NMR** (376 MHz, $CDCl_3$): δ -62.89 ppm. **¹³C NMR** (101 MHz, $CDCl_3$): δ 139.12, 134.58, 131.91 (q, *J* = 33.3 Hz), 131.25, 129.23, 129.12, 128.95, 126.50, 123.22 (q, *J* = 273.7 Hz), 122.85, 121.92, 70.85, 55.17, 20.04 ppm. **IR** (neat): ν = 2946, 1469, 1365, 1275, 1128, 1077, 948, 902, 682, 639, 504 ppm. **HRMS** (ESI+, MeOH): *m/z* calcd. 445.0667 (M + Na)⁺, found: 445.0670. **SFC conditions**: Column ChiralPak IG (150 x 4.6 mm, 3 μm), Isocratic CO_2/IPA 95:5, 2 mL/min, 2000 psi; 93.5:6.5 *er*; $[\alpha]_D^{25}$ = 10.6 (c = 0.12, $CHCl_3$).
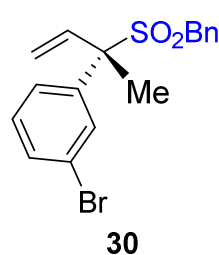
Scale: 0.10 mmol, (63% yield, 94:6 *er*), yellow oil, Hexane : EA = 10 : 1, R_f = 0.14. **¹H NMR** (400 MHz, $CDCl_3$): δ 7.79 (t, *J* = 1.9 Hz, 1H), 7.68 (ddd, *J* = 8.0, 1.9, 0.9 Hz, 1H), 7.53 (ddd, *J* = 8.0, 1.8, 0.9 Hz, 1H), 7.38–7.33 (m, 3H), 7.31–7.25 (m, 3H), 6.62 (dd, *J* = 17.3, 10.9 Hz, 1H), 5.68–5.49 (m, 2H), 4.13–4.02 (m, 2H), 1.93 (s, 3H) ppm. **¹³C NMR** (101 MHz, $CDCl_3$): δ 138.73, 135.16, 132.02, 131.76, 131.32, 130.14, 128.96, 128.77, 127.57, 126.83, 122.83, 120.77, 71.22, 54.66, 19.85 ppm. **IR** (neat): ν = 2989, 1563, 1455, 1296, 1133, 769, 695, 641, 515 cm⁻¹. **HRMS** (ESI+, MeOH): *m/z* calcd. 387.0025 (M + Na)⁺, found: 387.0012. **SFC conditions**: Column: Chiralpak IA (100 x 4.6 mm, 3μm), Mobile phase: CO_2/MeOH 80:20, Flow: 3 mL/min, ABPR: 1500 psi; 94:6 *er*; $[\alpha]_D^{25}$ = 22.4 (c = 0.11, $CHCl_3$).
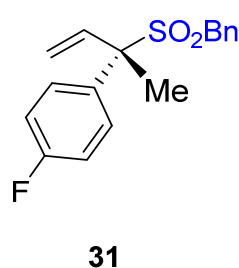
Scale: 0.10 mmol, (63% yield, 88:12 *er*), white solid, Hexane : EA = 10 : 1, R_f = 0.10. **¹H NMR** (400 MHz, $CDCl_3$): δ 7.70–7.63 (m, 2H), 7.33 (dd, *J* = 5.0, 1.9 Hz, 3H), 7.28–7.24 (m, 2H), 7.13–7.06 (m, 2H), 6.63 (dd, *J* = 17.3, 10.9 Hz, 1H), 5.64–5.45 (m, 2H), 4.08–3.98 (m, 2H), 1.93 (s, 3H) ppm. **¹⁹F NMR** (376 MHz, $CDCl_3$): δ -112.93 ppm. **¹³C NMR** (101 MHz, $CDCl_3$): δ 163.02 (d, *J* = 250.5 Hz),

135.63, 132.13 (d, J = 3.0 Hz), 131.33, 130.79 (d, J = 4.0 Hz), 128.90, 128.78, 127.00, 120.38, 115.64 (d, J = 21.2 Hz), 71.14, 54.42, 20.06 ppm. **IR** (neat): ν = 2947, 1601, 1508, 1295, 1234, 1135, 1121, 1063, 950, 772, 698, 637, 518 cm-1. **HRMS** (ESI+, MeOH): m/z calcd. 327.0825 (M + Na)$^+$, found: 327.0827. **SFC conditions**: Column: Chiralpak IE-3 150x3mm, 3μm, Mobile Phase: CO_2/MeOH 80:20, Flow: 2mL/min, ABPR: 2000psi; 88:12 er; $[\alpha]_D^{25}$ = -17.8 (c = 0.11, CHCl$_3$).
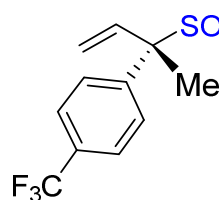
Scale: 0.10 mmol, (56% yield, 86:14 er), white solid, Hexane : EA = 10 : 1, R_f = 0.10. **^{1}H NMR** (400 MHz, CDCl$_3$): δ 7.81 (d, J = 8.3 Hz, 2H), 7.65 (d, J = 8.4 Hz, 2H), 7.35–7.30 (m, 3H), 7.29–7.24 (m, 2H), 6.67 (dd, J = 17.4, 10.9 Hz, 1H), 5.69–5.48 (m, 2H), 4.13–4.04 (m, 2H), 1.96 (s, 3H) ppm. **^{19}F NMR** (376 MHz, CDCl$_3$): δ -62.93 ppm. **^{13}C NMR** (101 MHz, CDCl$_3$): δ 140.44, 135.21, 131.31, 130.96 (q, J = 33.3 Hz), 129.29, 129.01, 128.82, 126.78, 125.52 (q, J = 4.0 Hz), 123.98 (q, J = 273.7 Hz), 71.35, 54.76, 19.95 ppm. **IR** (neat): ν = 2969, 1614, 1412, 1321, 1296, 1163, 1114, 1071, 1010, 848, 700, 645, 512 cm^{-1}. **HRMS** (ESI+, MeOH): m/z calcd. 377.0794 (M + Na)+, found: 377.0796. **SFC conditions**: IG Column, Isocratic CO_2/MeOH 60:40, 2 ml/min, 2000 psi; 86:14 er; $[\alpha]_D^{25}$ = -11.7 (c = 0.09, CHCl$_3$).
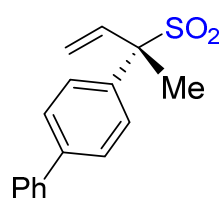
Scale: 0.10 mmol, (69% yield, 84:16 er), white solid, Hexane : EA = 10 : 1, R_f = 0.10. **^{1}H NMR** (500 MHz, CDCl$_3$): δ 7.78–7.74 (m, 2H), 7.66–7.60 (m, 4H), 7.46 (t, J = 7.6 Hz, 2H), 7.40–7.36 (m, 1H), 7.33 (dd, J = 5.0, 2.0 Hz, 3H), 7.30–7.26 (m, 2H), 6.70 (dd, J = 17.3, 10.9 Hz, 1H), 5.65–5.51 (m, 2H), 4.06 (q, J = 13.3 Hz, 2H), 1.98 (s, 3H) ppm. **^{13}C NMR** (126 MHz, CDCl$_3$): δ 141.68, 140.25, 135.68, 135.32, 131.37, 129.23, 129.02, 128.83, 128.75, 127.86, 127.34, 127.26, 127.15, 120.29, 71.58, 54.50, 19.85 ppm. **IR** (neat): ν = 2971, 1486, 1302, 1286, 1135, 1067, 942, 763, 730, 695, 640, 513 cm^{-1}. **HRMS** (ESI+, MeOH): m/z calcd. 385.1233 (M + Na)$^+$, found: 385.1237. **SFC conditions**: Column ChiralPak ID (100x4.6mm, 3μm), Isocratic CO_2/IPA 75:25, 3 ml/min, 1500 psi; 84:16 er; $[\alpha]_D^{25}$ = 7.5 (c = 0.10, CHCl$_3$).

Scale: 0.10 mmol, (52% yield, 93:7 *er*), yellow solid, Hexane : EA = 2 : 1, R_f = 0.15. **^{1}H NMR** (500 MHz, CDCl$_3$): δ 8.80 (d, *J* = 2.5 Hz, 1H), 8.58 (dd, *J* = 4.7, 1.5 Hz, 1H), 8.03 (ddd, *J* = 8.2, 2.5, 1.6 Hz, 1H), 7.32–7.24 (m, 6H), 6.65 (dd, *J* = 17.4, 10.9 Hz, 1H), 5.64 (d, *J* = 10.9 Hz, 1H), 5.50 (d, *J* = 17.4 Hz, 1H), 4.11–4.04 (m, 2H), 1.94 (s, 3H) ppm. **^{13}C NMR** (126 MHz, CDCl$_3$): δ 149.89, 149.51, 136.70, 134.72, 132.28, 131.28, 128.97, 128.80, 126.62, 123.30, 121.06, 70.12, 54.50, 19.53 ppm. **IR** (neat): ν = 2918, 1454, 1295, 1283, 1136, 1070, 946, 715, 696, 644, 518 cm^{-1}. **HRMS** (ESI+, MeOH): *m/z* calcd. 288.1053 (M + Na)$^+$, found: 288.1046. **SFC** conditions: Column: Chiralpak IC (100x4.6mm, 3μm), Mobile phase: CO$_2$/EtOH 65:35, Flow: 3mL/min, ABPR: 1500psi; 93:7 *er*; $[\alpha]_D^{25}$ = 22.3 (c = 0.11, CHCl$_3$).

Scale: 0.10 mmol, (75% yield, 91.5:8.5 *er*), yellow oil, Hexane : EA = 10 : 1, R_f = 0.10. **^{1}H NMR** (400 MHz, CDCl$_3$): δ 7.44 (dd, *J* = 2.5, 1.9 Hz, 1H), 7.41–7.37 (m, 2H), 7.36–7.31 (m, 3H), 7.29–7.25 (m, 2H), 6.55 (dd, *J* = 17.3, 10.8 Hz, 1H), 5.59–5.43 (m, 2H), 4.01 (q, *J* = 13.2 Hz, 2H), 1.91 (s, 3H) ppm. **^{13}C NMR** (101 MHz, CDCl$_3$): δ 137.41, 135.03, 131.31, 128.83, 128.74, 127.95, 127.09, 126.33, 125.23, 120.21, 69.80, 54.18, 20.00 ppm. **IR** (neat): ν = 3002, 1601, 1493, 1410, 1282, 1121, 1068, 996, 947, 770, 695, 642, 518 cm^{-1}. **HRMS** (ESI+, MeOH): *m/z* calcd. 315.0484 (M + Na)$^+$, found: 315.0478. **SFC** conditions: Column: OJ-3 (150x3.1mm, 3μm), Mobile phase: CO$_2$/EtOH 75:25, Flow: 2mL/min, ABPR: 2000 psi; 91.5:8.5 *er*; $[\alpha]_D^{25}$ = 1.6 (c = 0.11, CHCl$_3$).
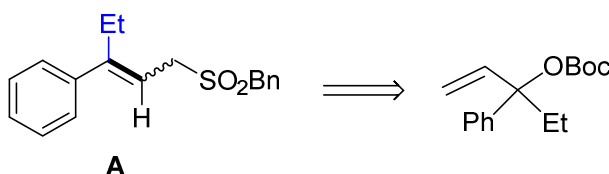
(Precursor to **A** is known, see: *Angew. Chem. Int. Ed.* **2017**, *56*, 11797-11801), Yellow oil (47%, *Z/E* = 72:28), Hexane : EA = 10 : 1, R_f = 0.10. **^{1}H NMR** (400 MHz, CDCl$_3$): δ 7.47–7.41 (m, 4H), 7.41–7.30 (m, 5H), 7.21–7.16 (m, 1H), 5.68 (dt, *J* = 27.7, 7.7 Hz, 1H), 4.18 (d, *J* = 72.8 Hz, 2H), 3.82 (d, *J* = 7.8 Hz, 1H), 3.61 (d, *J* = 7.5 Hz, 1H), 2.55–2.46 (m, 2H), 1.01 (dt, *J* = 25.1, 7.5 Hz, 3H) ppm. **^{13}C NMR** (101 MHz, CDCl$_3$): δ 151.17, 141.16, 130.81, 129.13, 128.68, 128.54, 128.03, 127.77, 126.64, 112.33, 58.69, 51.99, 23.69, 13.27 ppm. **IR** (neat): ν = 2969, 1494, 1455, 1305,

1116, 973, 764, 697 cm^{-1}. **HRMS** (ESI+, MeOH): *m/z* calcd. 323.1076 (M + Na)$^{+}$, found: 323.1068.
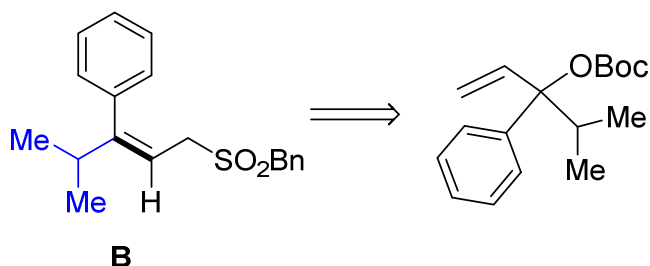
B: White solid (34%, *Z/E* >99:1), Hexane : EA = 10 : 1, R_f = 0.12. **^{1}H NMR** (400 MHz, CDCl$_3$): δ 7.37– 7.27 (m, 6H), 7.23–7.19 (m, 2H), 7.12–7.06 (m, 2H), 5.59 (td, *J* = 7.5, 1.1 Hz, 1H), 4.05 (s, 2H), 3.51 (d, *J* = 7.5 Hz, 2H), 2.68 (p, *J* = 6.7 Hz, 1H), 1.06 (d, *J* = 6.8 Hz, 6H) ppm. **^{13}C NMR** (101 MHz, CDCl$_3$): δ 157.04, 139.04, 130.78, 128.97, 128.96, 128.51, 127.73, 127.61, 110.47, 58.52, 52.70, 36.52, 21.58 ppm. **IR** (neat): ν = 2964, 1456, 1306, 1118, 1031, 881, 787, 695, 500 cm^{-1}. **HRMS** (ESI+, MeOH): *m/z* calcd. 337.1233 (M + Na)$^{+}$, found: 337.1234.

Note below the **2D NMR** spectra for compound **B**.

2D ^{1}H-^{1}H COSY NMR spectrum (CDCl$_3$)
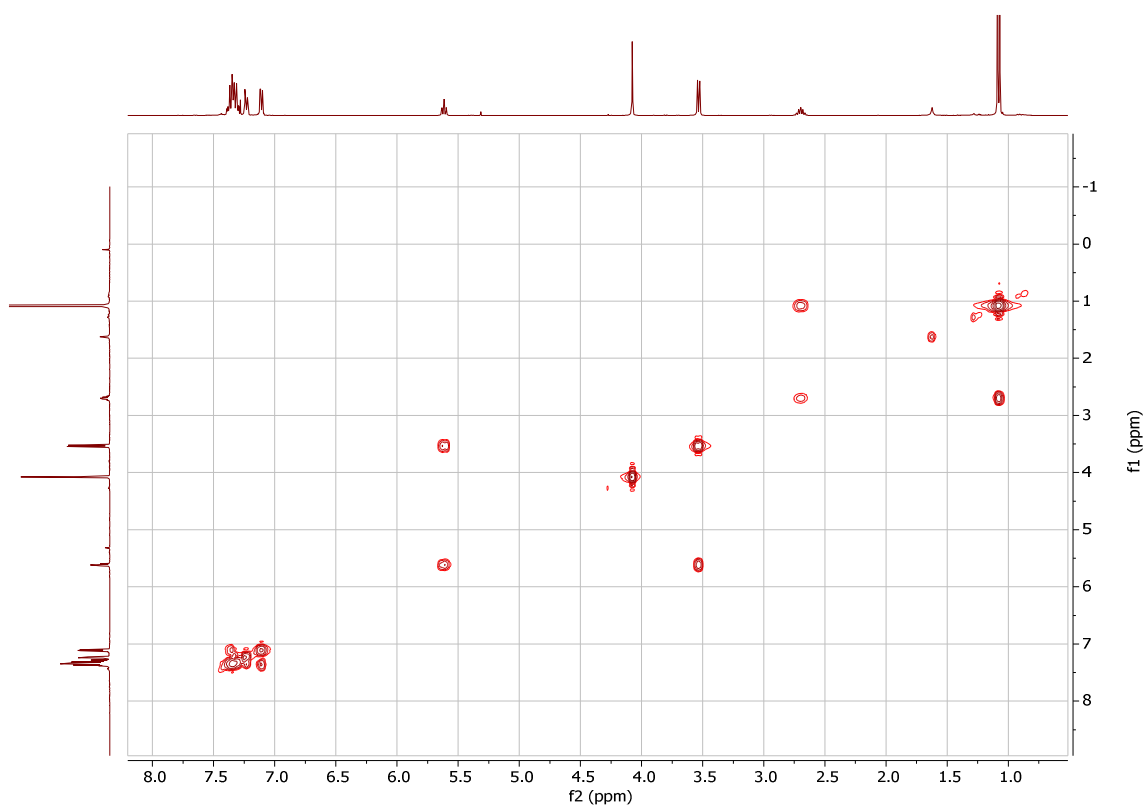
2D ^{1}H-^{13}C HSQC NMR spectrum (CDCl$_3$)
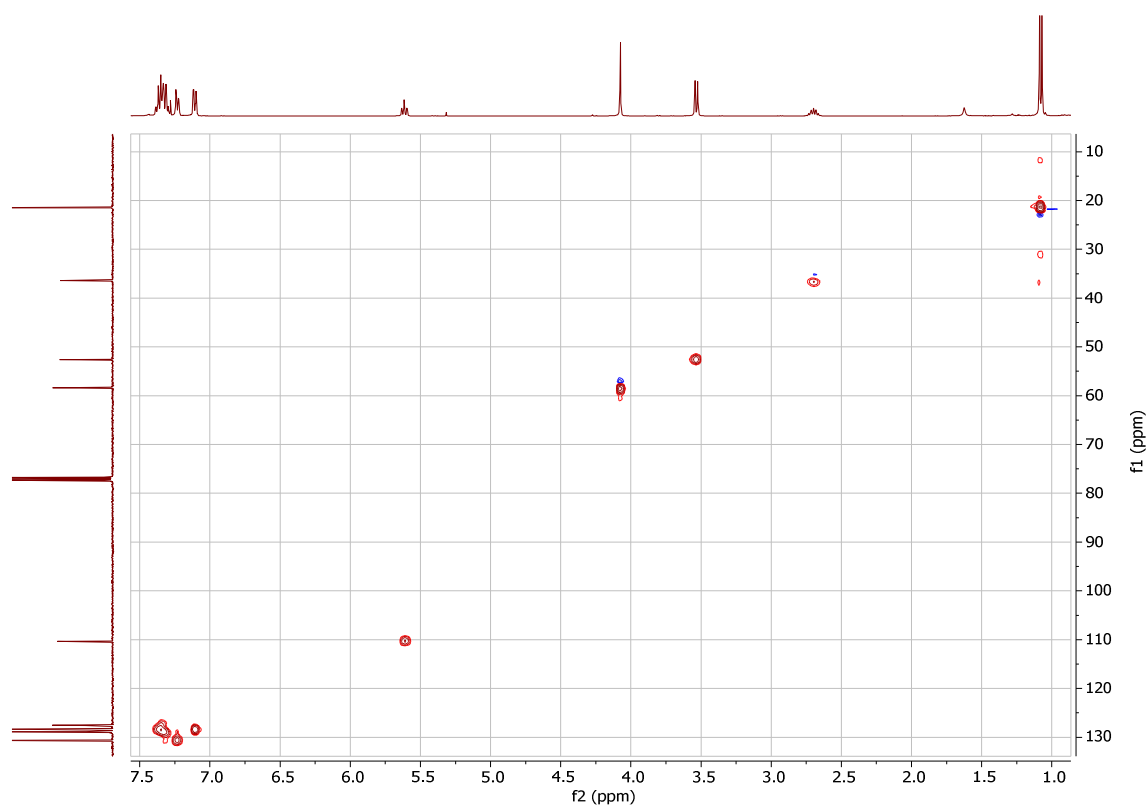
2D ^{1}H-^{1}H NOESY NMR spectrum (CDCl$_3$)

36
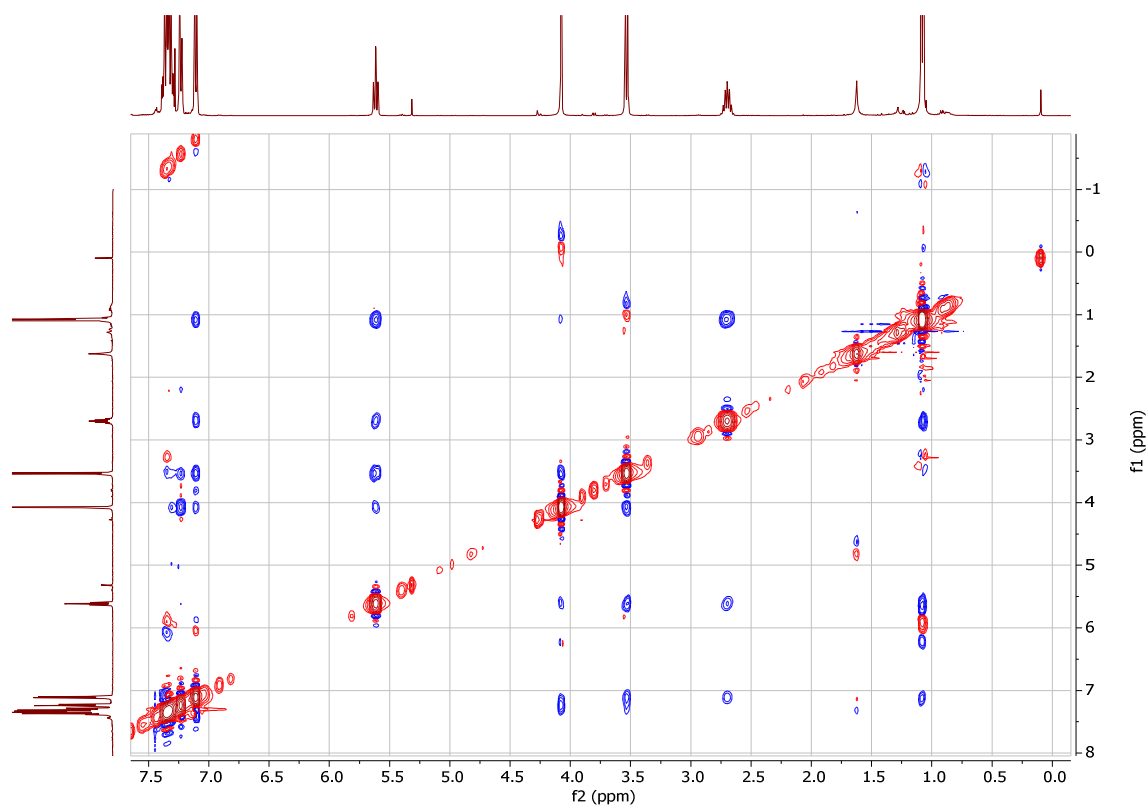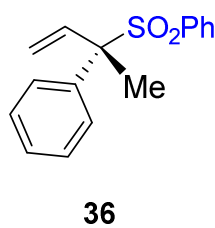
Scale: 0.15 mmol, (84% yield, 89.5:10.5 *er*), yellow solid, Hexane : EA = 10 : 1, R_f = 0.22. **^{1}H NMR** (400 MHz, CDCl$_3$): δ 7.57–7.46 (m, 5H), 7.39–7.28 (m, 5H), 6.71 (dd, J = 17.3, 10.9 Hz, 1H), 5.50 (d, J = 10.9 Hz, 1H), 5.35 (d, J = 17.3 Hz, 1H), 1.86 (s, 3H) ppm. **^{13}C NMR** (101 MHz, CDCl$_3$): δ 136.08, 135.69, 135.35, 133.61, 130.58, 129.07, 128.69, 128.28, 128.20, 120.03, 71.51, 19.38 ppm. **IR** (neat): ν = 3057, 1444, 1415, 1292, 1140, 1066, 943, 755, 715, 686, 595 cm^{-1}. **HRMS** (ESI+, MeOH): *m/z* calcd. 295.0763 (M + Na)$^+$, found: 295.0750. **SFC conditions**: ID Column, Isocratic CO$_2$/MeOH 90:10, 3 mL/min, 1500 psi; 89.5:10.5 *er*; $[\alpha]_D^{25}$ = 22.4 (c = 0.11, CHCl$_3$).

37
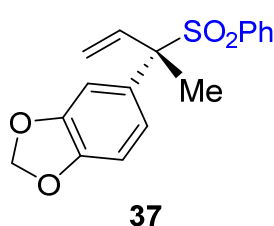
Scale: 0.15 mmol, (80% yield, 87:13 *er*), yellow oil, Hexane : EA = 10 : 1, R_f = 0.11. **^{1}H NMR** (500 MHz, CDCl$_3$): δ 7.59–7.54 (m, 3H), 7.43–7.37 (m, 2H), 7.07 (d, J = 2.0 Hz, 1H), 6.88 (dd, J = 8.3, 2.0 Hz, 1H), 6.71 (d, J = 8.3 Hz, 1H), 6.62 (dd, J = 17.3, 10.9 Hz, 1H), 5.99–5.95 (m, 2H), 5.46 (d, J = 10.9 Hz, 1H), 5.30 (d, J = 17.3 Hz, 1H), 1.79 (s, 3H) ppm. **^{13}C NMR** (126 MHz, CDCl$_3$): δ 147.96, 147.67, 135.75, 135.50, 133.67, 130.61, 129.56, 128.34, 122.98, 119.90, 109.88, 107.78, 101.46, 71.39, 19.81 ppm. **IR** (neat): ν = 2916, 1487, 1433, 1285, 1243, 1137, 1118, 1028, 921, 807, 685, 613, 534 cm^{-1}. **HRMS** (ESI+, MeOH): *m/z* calcd. 339.0662 (M + Na)$^+$, found: 339.0670. **SFC conditions**: ID Column, Isocractic CO$_2$/MeOH/DEA 80:20:1, 1500 psi, 3 mL/min; 87:13 *er*; $[\alpha]_D^{25}$ = -29.5 (c = 0.1, CHCl$_3$).

38
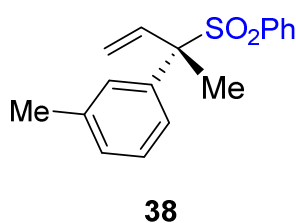
Scale: 0.15 mmol, (82% yield, 87:13 *er*), yellow solid, Hexane : EA = 10 : 1, R_f = 0.24. **^{1}H NMR** (500 MHz, CDCl$_3$): δ 7.56–7.51 (m, 1H), 7.51–7.47 (m, 2H), 7.39–7.33 (m, 2H), 7.25 (d, J = 6.2 Hz, 2H), 7.20–7.15 (m, 1H), 7.12 (d, J = 7.7 Hz, 1H), 6.69 (dd, J = 17.4, 10.9 Hz, 1H), 5.47 (d, J = 10.9 Hz, 1H), 5.32 (d, J = 17.4 Hz, 1H), 2.29 (s, 3H), 1.83 (s, 3H) ppm. **^{13}C NMR** (101 MHz, CDCl$_3$): δ 145.95, 143.23, 142.47, 136.37, 129.36, 128.72, 126.30, 117.40, 115.88, 113.74, 60.19, 29.32, 21.13 ppm. **IR** (neat): ν = 2920, 1446, 1297, 1142, 1063, 932, 717, 690, 603, 541 cm^{-1}. **HRMS** (ESI+, MeOH): *m/z* calcd. 309.0920 (M + Na)$^+$, found: 309.0915. **SFC conditions**: IG column, Isocratic CO$_2$/MeOH/DEA 60:40:0.1, 2 mL/min, 2000 psi; 87:13 *er*; $[\alpha]_D^{25}$ = -26.7 (c = 0.1, CHCl$_3$).
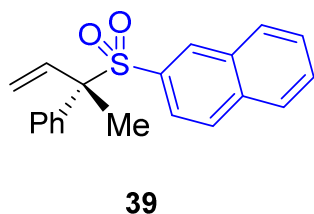
Scale: 0.15 mmol, (75% yield, 84:16 *er*), yellow solid, Hexane : EA = 10 : 1, R_f = 0.22. **^{1}H NMR** (500 MHz, CDCl$_3$): δ 8.08–8.05 (m, 1H), 7.85 (dd, *J* = 15.4, 8.2 Hz, 2H), 7.77 (d, *J* = 8.7 Hz, 1H), 7.64 (ddd, *J* = 8.2, 6.9, 1.3 Hz, 1H), 7.58 (ddd, *J* = 8.1, 7.0, 1.2 Hz, 1H), 7.52–7.47 (m, 2H), 7.41 (dd, *J* = 8.6, 1.8 Hz, 1H), 7.37–7.32 (m, 1H), 7.32–7.27 (m, 2H), 6.76 (dd, *J* = 17.3, 10.9 Hz, 1H), 5.52 (d, *J* = 10.9 Hz, 1H), 5.37 (d, *J* = 17.3 Hz, 1H), 1.91 (s, 3H) ppm. **^{13}C NMR** (126 MHz, CDCl$_3$): δ 136.20, 135.38, 135.28, 132.79, 132.60, 131.77, 129.54, 129.31, 129.19, 128.75, 128.24, 128.14, 127.92, 127.47, 125.29, 120.14, 71.78, 19.46 ppm. **IR** (neat): ν = 3055, 1625, 1444, 1293, 1141, 1127, 1059, 939, 747, 660, 572 cm^{-1}. **HRMS** (ESI+, MeOH): *m/z* calcd. 345.0920 (M + Na)$^+$, found: 345.0904. **SFC** conditions: Column: Chiralcel OJ-SFC (150 x 3.1 mm, 3μm), Mobile phase: CO$_2$/IPA 75:25, Flow: 2 mL/min, ABPR: 2000 psi; 84:16 *er*; $[\alpha]_D^{25}$ = -50.7 (c = 0.11, CHCl$_3$).
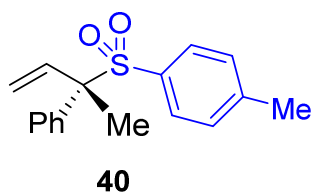
Scale: 0.15 mmol, (75% yield, 87.5:12.5 *er*), yellow solid, Hexane : EA = 10 : 1, R_f = 0.22. **^{1}H NMR** (500 MHz, CDCl$_3$): δ 7.51–7.47 (m, 2H), 7.36 (d, *J* = 8.3 Hz, 2H), 7.34–7.28 (m, 3H), 7.15 (d, *J* = 7.9 Hz, 2H), 6.70 (dd, *J* = 17.3, 10.9 Hz, 1H), 5.49 (d, *J* = 10.9 Hz, 1H), 5.34 (d, *J* = 17.3 Hz, 1H), 2.38 (s, 3H), 1.85 (s, 3H) ppm. **^{13}C NMR** (126 MHz, CDCl$_3$): δ 144.58, 136.28, 135.56, 132.76, 130.62, 129.11, 128.96, 128.62, 128.18, 119.86, 71.41, 21.71, 19.41 ppm. **IR** (neat): ν = 2950, 1595, 1285, 1062, 945, 822, 692, 655, 579, 522 cm^{-1}. **HRMS** (ESI+, MeOH): *m/z* calcd. 309.0920 (M + Na)$^+$, found: 309.0931. **SFC** conditions: Column: Chiralcel OJ-SFC (150 x 3.1 mm, 3μm), Mobile phase: CO$_2$/IPA 85:15, Flow: 2 mL/min, ABPR: 2000 psi; 87.5:12.5 *er*; $[\alpha]_D^{25}$ = -39.4 (c = 0.09, CHCl$_3$).
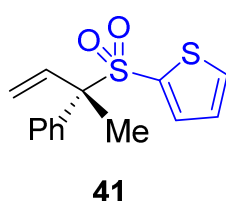
Scale: 0.15 mmol, (62% yield, 87:13 *er*), yellow oil, Hexane : EA = 10 : 1, R_f = 0.19. **^{1}H NMR** (500 MHz, CDCl$_3$): δ 7.61 (dd, *J* = 5.0, 1.3 Hz, 1H), 7.56–7.52 (m, 2H), 7.35–7.32 (m, 3H), 7.28–7.25 (m, 1H), 7.01 (dd, *J* = 5.0, 3.8 Hz, 1H), 6.72 (dd, *J* = 17.3, 10.9 Hz, 1H), 5.55 (d, *J* = 10.9 Hz, 1H), 5.41 (d, *J* = 17.3 Hz, 1H), 1.94 (s, 3H) ppm. **^{13}C NMR** (126 MHz, CDCl$_3$): δ 136.23, 135.20, 134.76, 129.06, 128.83, 128.53, 128.34, 127.21, 126.04, 120.36, 72.18, 19.53 ppm. **IR** (neat): ν = 3094, 1496, 1446, 1400, 1299, 1137, 1061, 1011,

936, 726, 695, 599 cm^{-1}. **HRMS** (ESI+, MeOH): *m/z* calcd. 301.0327 (M + Na)$^+$, found: 301.0314. **SFC** conditions: Column: Chiralpak OJSFC (150 x 3.1 mm, 3 μm), Mobile phase: CO_2/IPA 80:20, Flow: 2 mL/min, ABPR: 2000 psi, Inj volume: 2 μL; 87:13 *er*; $[\alpha]_D^{25}$ = -32.1 (c = 0.12, CHCl$_3$).
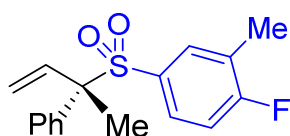
42

Scale: 0.15 mmol, (77% yield, 86.5:13.5 *er*), yellow solid, Hexane : EA = 10 : 1, R_f = 0.27. **^{1}H NMR** (400 MHz, CDCl$_3$): δ 7.49–7.44 (m, 2H), 7.35–7.27 (m, 4H), 7.25–7.20 (m, 1H), 6.97 (t, *J* = 8.8 Hz, 1H), 6.67 (dd, *J* = 17.3, 10.9 Hz, 1H), 5.52 (d, *J* = 10.9 Hz, 1H), 5.38 (d, *J* = 17.3 Hz, 1H), 2.19 (s, 3H), 1.85 (s, 3H) ppm. **^{19}F NMR** (376 MHz, CDCl$_3$): δ -108.14 ppm. **^{13}C NMR** (101 MHz, CDCl$_3$): δ 164.47 (d, *J* = 154.5 Hz), 136.15, 135.21, 134.33 (d, *J* = 7.1 Hz), 131.09 (d, *J* = 4.0 Hz), 130.54 (d, *J* = 9.1 Hz), 129.14, 128.77, 128.23, 125.64 (d, *J* = 18.2 Hz), 120.19, 115.16 (d, *J* = 23.2 Hz), 71.65, 19.38, 14.41 ppm. **IR** (neat): ν = 2985, 1581, 1488, 1447, 1293, 1242, 1137, 1119, 1059, 895, 799, 695 cm^{-1}. **HRMS** (ESI+, MeOH): *m/z* calcd. 327.0825 (M + Na)$^+$, found: 327.0841. **SFC** conditions: Chiralcel OJ-SFC (150 x 3.1 mm, 3 μm), Mobile phase: CO_2/MeOH 90:10, Flow: 2 mL/min, ABPR: 2000 psi; 86.5:13.5 *er*; $[\alpha]_D^{25}$ = -29.9 (c = 0.11, CHCl$_3$).
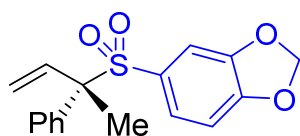
43

Scale: 0.15 mmol, (72% yield, 81.5:18.5 *er*), yellow solid, Hexane : EA = 10 : 1, R_f = 0.14. **^{1}H NMR** (500 MHz, CDCl$_3$): δ 7.53–7.47 (m, 2H), 7.35–7.29 (m, 3H), 7.04 (dd, *J* = 8.2, 1.8 Hz, 1H), 6.88 (d, *J* = 1.8 Hz, 1H), 6.74 (d, *J* = 8.2 Hz, 1H), 6.69 (dd, *J* = 17.3, 10.9 Hz, 1H), 6.04 (s, 2H), 5.50 (d, *J* = 10.9 Hz, 1H), 5.36 (d, *J* = 17.3 Hz, 1H), 1.86 (s, 3H) ppm. **^{13}C NMR** (126 MHz, CDCl$_3$): δ 152.21, 147.65, 136.28, 135.53, 129.08, 128.96, 128.72, 128.22, 126.72, 119.92, 110.56, 107.74, 102.41, 71.70, 19.46 ppm. **IR** (neat): ν = 3055, 1599, 1499, 1478, 1291, 1249, 1132, 1113, 1049, 1033, 930, 896, 692, 639 cm^{-1}. **HRMS** (ESI+, MeOH): *m/z* calcd. 339.0662 (M + Na)$^+$, found: 339.0651. **SFC** conditions: Chiralpak OJSFC (150 x 3.1 mm, 3 μm), Mobile phase: CO_2/IPA 80:20, Flow: 2 mL/min, ABPR: 2000 psi, Inj volume: 2 μL; 81.5:18.5 *er*; $[\alpha]_D^{25}$ = -29.5 (c = 0.11, CHCl$_3$).
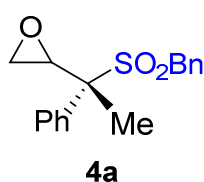
Scale: 0.10 mmol, (93% yield, 52:48 *dr*, 93.5:6.5 *er* and 95.5:4.5 *er*), white solid, Hexane : EA = 10 : 1, R_f = 0.15. **¹H NMR** (500 MHz, CDCl₃): δ 7.82–7.64 (m, 2H), 7.48–7.30 (m, 7H), 7.18 (dd, *J* = 7.8, 1.7 Hz, 1H), 4.33–4.23 (m, 1H), 4.02–3.92 (m, 1H), 3.67 (dd, *J* = 4.0, 2.6 Hz, 1H), 2.93 (dt, *J* = 44.5, 4.3 Hz, 1H), 2.83 (ddd, *J* = 29.9, 4.6, 2.7 Hz, 1H), 1.67 (d, *J* = 1.0 Hz, 3H) ppm. **¹³C NMR** (126 MHz, CDCl₃): δ 134.49, 134.39, 131.61, 131.37, 129.39, 129.34, 129.01, 128.88, 128.75, 128.74, 128.72, 126.89, 126.61, 69.24, 68.46, 56.36, 55.94, 53.45, 53.25, 44.64, 44.19, 15.88, 14.10 ppm. **IR** (neat): ν = 2941, 1495, 1450, 1291, 1126, 1073, 860, 693, 618, 525 cm⁻¹. **HRMS** (ESI+, MeOH): *m/z* calcd. 325.0869 (M + Na)⁺, found: 325.0861. **SFC conditions**: Column: Chiralcel OJSFC (150 x 3.1 mm, 3 μm), Mobile phase: CO₂/ACN 80:20, Flow: 2 mL/min, ABPR: 2000 psi; 93.5:6.5 *er,* 95.5:4.5 *er*; $[\alpha]_D^{25}$ = -14.4 (c = 0.1, CHCl₃).
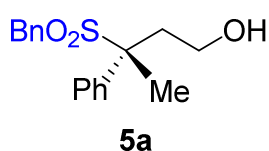
Scale: 0.10 mmol, (95% yield, 95:5 *er*), yellow solid, Hexane : EA = 2 : 1, R_f = 0.1. **¹H NMR** (500 MHz, CDCl₃): δ 7.71–7.66 (m, 2H), 7.44 (dt, *J* = 13.0, 6.9 Hz, 3H), 7.34–7.27 (m, 3H), 7.16 (dd, *J* = 7.6, 1.9 Hz, 2H), 3.89 (d, *J* = 13.2 Hz, 1H), 3.72–3.55 (m, 3H), 2.73 (ddd, *J* = 13.5, 7.4, 5.8 Hz, 1H), 2.52 (ddd, *J* = 14.2, 7.6, 6.8 Hz, 1H), 3.04 (s, 3H) ppm. **¹³C NMR** (126 MHz, CDCl₃): δ 135.90, 131.33, 129.06, 129.03, 128.81, 128.70, 128.54, 126.78, 68.38, 58.71, 53.21, 36.95, 19.86 ppm. **IR** (neat): ν = 3512, 2929, 1447, 1275, 1111, 1065, 1040, 927, 774, 699, 613, 520 cm⁻¹. **HRMS** (ESI+, MeOH): *m/z* calcd. 327.1025 (M + Na)⁺, found: 327.1021. **SFC conditions**: Column: Chiralpak OJSFC (150 x 3.1 mm, 3 μm), Mobile phase: CO₂/MeOH 90:10, Flow: 2 mL/min, ABPR: 2000 psi; 95:5 *er*; $[\alpha]_D^{25}$ = -10.3 (c = 0.12, CHCl₃).
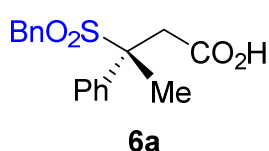
Scale: 0.10 mmol, (67% yield, 95.5:4.5 *er*), yellow solid, Hexane : EA = 1 : 1, R_f = 0.1. **¹H NMR** (400 MHz, CDCl₃): δ 7.65–7.60 (m, 2H), 7.47–7.39 (m, 3H), 7.34–7.27 (m, 3H), 7.18–7.13 (m, 2H), 3.88 (d, *J* = 13.2 Hz, 1H), 3.68–3.57 (m, 2H), 3.11 (d, *J* = 16.2 Hz, 1H), 2.04 (s, 3H) ppm. **¹³C NMR** (101 MHz, CDCl₃): δ 173.90, 134.92, 131.32, 129.23, 129.00, 128.97, 128.80, 128.38, 126.39, 67.55, 53.13, 38.18, 19.87 ppm. **IR** (neat): ν = 2925, 1708, 1418, 1286, 1227, 1124, 1067, 767, 693, 615, 497 cm⁻¹. **HRMS** (ESI–, MeOH): *m/z* calcd. 317.0853 (M - H)⁻, found: 317.0856. **SFC conditions**: ID Column

(150 x 4.6 mm, 5μm), Isocratic CO_2/MeOH 75:25, 3 mL/min, 1500 psi; 95.5:4.5 *er*; $[\alpha]_D^{25} = -12.2$ (c = 0.12, CHCl$_3$).

1d
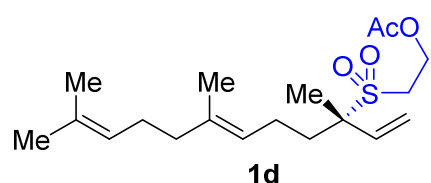
Scale: 0.50 mmol, (62% yield, 82:18 *er*), colorless oil, Hexane : EA = 10 : 1, R_f = 0.12. **^{1}H NMR** (500 MHz, CDCl$_3$): δ 5.99 (dd, *J* = 17.5, 10.8 Hz, 1H), 5.51 (d, *J* = 10.8 Hz, 1H), 5.39 (d, *J* = 17.5 Hz, 1H), 5.11–5.03 (m, 2H), 4.49 (t, *J* = 6.6 Hz, 2H), 3.24 (t, *J* = 6.6 Hz, 2H), 2.07–2.01 (m, 5H), 1.93 (dt, *J* = 24.2, 7.7 Hz, 6H), 1.66 (s, 3H), 1.57 (d, *J* = 9.6 Hz, 6H), 1.49 (s, 3H) ppm. **^{13}C NMR** (126 MHz, CDCl$_3$): δ 170.71, 136.57, 135.65, 131.60, 124.22, 122.73, 120.77, 68.26, 57.04, 45.73, 39.69, 31.73, 26.68, 25.78, 22.12, 20.86, 17.78, 16.12, 16.01 ppm. **IR** (neat): ν = 2967, 2916, 1736, 1369, 1269, 1138, 1059, 955, 628, 573 cm^{-1}. **HRMS** (ESI+, MeOH): *m/z* calcd. 319.1914 (M + Na)$^+$, found: 319.1900. **SFC** conditions: Column: chiralpak IB (100 x 4.6 mm, 3 μm), Mobile phase: CO_2/IPA 70:30, ABPR: 1500 psi, Flow: 3 mL/min; 82:18 *er*; $[\alpha]_D^{25} = 21.0$ (c = 0.1, CHCl$_3$).

(-)-Agelasidine A
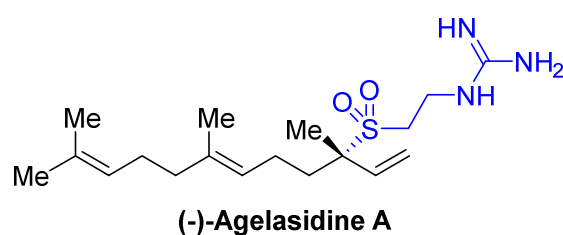
Scale: 0.15 mmol, (65% yield, 81.5:18.5 *er*), colorless oil, DCM : MeOH = 10 : 1, R_f = 0.1. **^{1}H NMR** (500 MHz, CDCl$_3$): δ 5.93 (dd, *J* = 17.5, 10.8 Hz, 1H), 5.55 (d, *J* = 10.8 Hz, 1H), 5.42 (d, *J* = 17.4 Hz, 1H), 5.11–5.02 (m, 2H), 3.83–3.71 (m, 2H), 3.28 (tt, *J* = 13.5, 6.9 Hz, 2H), 2.06–2.00 (m, 2H), 1.98–1.81 (m, 6H), 1.65 (s, 3H), 1.56 (d, *J* = 10.4 Hz, 6H), 1.48 (s, 3H) ppm. **^{13}C NMR** (126 MHz, CDCl$_3$): δ 157.68, 136.60, 134.76, 131.53, 124.25, 122.67, 121.88, 68.35, 46.01, 39.76, 35.00, 31.58, 26.74, 25.79, 22.09, 17.79, 16.17, 16.05 ppm. **IR** (neat): ν = 3417, 2923, 1671, 1644, 1447, 1277, 1126, 1082, 936, 722, 628 cm^{-1}. **HRMS** (ESI+, MeOH): *m/z* calcd. 356.2366 (M + H)$^+$, found: 356.2355. **SFC** conditions: IE Column, Isocratic CO_2/MeOH/DEA 75:25:0.1, 2 mL/min, 2000; 81.5:18.5 *er*; $[\alpha]_D^{25} = 16.7$ (c = 0.12, CHCl$_3$).

5.4.7 X-ray Crystallographic Data for Compound (2a)

Table 5.8. Crystal data and structure refinement for allylic sulfone **2a** (CCDC 1923367).

Empirical formula	$C_{17}H_{18}O_2S$
Formula weight	286.37
Temperature	100(2) K
Wavelength	0.71073 Å
Crystal system	Orthorhombic
Space group	$P2(1)2(1)2(1)$
Unit cell dimensions	a = 8.8376(2)Å $\alpha = 90°$.
	b = 10.8241(2)Å $\beta = 90°$.
	c = 15.8808(3)Å $\gamma = 90°$.
Volume	1519.14(5) $Å^3$
Z	4
Density (calculated)	1.252 mg/m^3
Absorption coefficient	0.212 mm^{-1}
F(000)	608
Crystal size	$0.3 \times 0.3 \times 0.15$ mm^3
Theta range for data collection	2.277 to 32.223°.
Index ranges	-12<=h<=13,-15<=k<=16,-23<=l<=23
Reflections collected	27620
Independent reflections	5053[R(int) = 0.0345]
Completeness to theta =32.223°	95.8%
Absorption correction	Multi-scan
Max. and min. transmission	0.969 and 0.745
Refinement method	Full-matrix least-squares on F^2
Data / restraints / parameters	5053/ 0/ 182
Goodness-of-fit on F^2	1.035
Final R indices [I>2sigma(I)]	$R_1 = 0.0340$, w$R_2 = 0.0952$
R indices (all data)	$R_1 = 0.0351$, w$R_2 = 0.0958$
Flack parameter	$x = -0.014(13)$
Largest diff. peak and hole	0.827 and -0.429 e·$Å^{-3}$
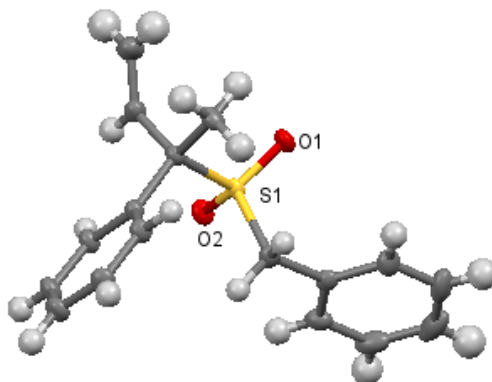
ORTEP view of the molecular structure of **2a** with the adopted numbering scheme. Note that the structure was measured using the same experimental method as described in chapter 2.

General Conclusions

To conclude this doctoral dissertation, I have been fortunate to have worked on several challenging projects during my PhD, regarding the design and development of ligands and transition metal complexes that can be used to promote allylic substitution reactions with high regio- and enantioselectivity. Accordingly, I was able to develop a Pd-catalyzed regio- and enantioselective synthesis of α,α-disubstituted branched allylic **aryl** amines. This user-friendly and efficient method marks a significant step forward in the challenging synthesis of this important class of molecules, and shows that a proper ligand design is required to stir both regio- and enantiocontrol in this allylic chemistry. Furthermore, it also marks phosphoramidites as privileged ligand scaffolds in this type of chemistry.
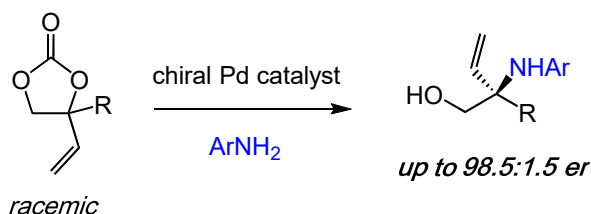
The use of a vinyl cyclic carbonate substrate limited the above-mentioned process to the use of **aryl** amines only since aliphatic amines rapidly ring-open cyclic carbonates to afford carbamate products. With an alternative linear tertiary allylic carbonate as substrate, under otherwise the same conditions, we were able to obtain the desired α,α-disubstituted *N*-**alkyl** allylic amines with good to excellent regio- and enantioselectivity. Our protocol marks the first transition metal mediated formation of these elusive allylic amine products using key chiral phosphoramidite ligands.

In terms of mechanistic insight, we established a collaboration with the group of Prof. G. Huang at Tianjin University (China). On the basis of carefully designed control experiments and density functional theory (DFT) studies, we were able to elucidate in detail the origin of regio- and enantioselectivity in the formation of α,α-disubstituted *N*-**aryl** allylic amines reported in Chapter 2 of this thesis. Specifically, we established that after oxidative addition of the vinyl cyclic carbonate to a Pd(0) complex, nucleophilic attack through an outer-sphere pathway gives the *opposite* regio-isomer (linear) compared to what is experimentally (branched) observed. We found that nucleophilic attack of the

amine reagent occurs by a unique type of chelation–assisted, inner-sphere pathway (see Figure below). Importantly, the combination of theoretical and experimental analyses allowed us to propose a reasonable explanation for the regio- and enantiocontrol exerted by the optimized Pd/phosphoramidite catalyst, with value for future developments in this area.
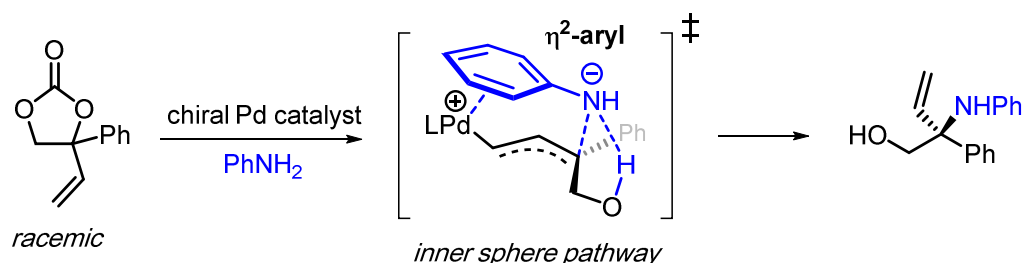
More recently, I focused on the regio- and enantioselective construction of allylic sulfones featuring elusive quaternary carbon stereogenic centers. The strategy involving relatively nucleophilic S-centered reagents typically suffers from limited scope and catalyst poisoning. Chiral allylic sulfones are important motifs serving, inter alia, as anticancer agents and antibacterial agents. Approximately 20% of all FDA approved drugs are organosulfur compounds, and their preparation is thus of high significance. To address the shortcoming mentioned above, I prepared and screened various ligand candidates, allowing to finally identifying a highly efficient and new phosphoramidite ligand (i.e., in-house developed). We thus succeeded in

developing a general enantioselective Pd-catalyzed method for the synthesis of sterically encumbered α,α-disubstituted allylic sulfones. Crucial in this respect was to optimize the steric impediment present in the *N*-alkyl substituent of the phosphoramidite ligand, hence permitting to obtain excellent chemo-selectivity, high regio-selectivity and good levels of enantio-induction.

UNIVERSITAT
ROVIRA i VIRGILI

ICIQ [R]

Institut
Català
d'Investigació
Química